Modulation of Aryl Hydrocarbon Receptor (AHR)-Regulated Metabolic Enzymes by Arsenic Trioxide and its Thioarsenical Metabolite

by

Mahmoud Abdelraouf Abdelkader Elghiaty

A thesis submitted in partial fulfillment of the requirements for the degree of

Doctor of Philosophy

in

Pharmaceutical Sciences

Faculty of Pharmacy and Pharmaceutical Sciences

University of Alberta

ABSTRACT

Arsenic trioxide (ATO^{III}) has evolved into a successful therapy for acute promyelocytic leukemia (APL), however, being an arsenical, it retains at its core the hypertoxic characteristics of that notorious metalloid. Such inherent toxicity causes a constellation of complications in APL patients, including hepatotoxicity, and may also limit expanding clinical ATO^{III} applications. In humans, ATO^{III} undergoes progressive metabolism into diverse methylated intermediates/products, which can, at least partly, be responsible for the overall toxic outcome of ATO^{III}. The thio-methylated $MMMTA^{V}$ is one of these metabolites that have been identified in ATO^{III}-treated APL patients. Arsenicals are well-known modulators of cytochrome P450 (CYP) enzymes, most notably the aryl hydrocarbon receptor (AHR)-regulated CYP1A1/1A2. These enzymes are pivotal for metabolism of endobiotics and commercial drugs, therefore, modifying their activity can entail a disease state or clinical drug-drug interactions, respectively. Additionally, altering CYP1A1/1A2 can aggravate environmental toxicants impact through their activation or diminished elimination. Therefore, this work aimed to determine the possible effects of ATO^{III} and $MMMTA^{V}$ on constitutive and TCDD-inducible levels of hepatic CYP1A1/1A2 using *in vivo* and *in vitro* models. We also aimed to investigate *in vivo* effects of ATO^{III} on hepatic non-AHR-regulated CYP enzymes with the associated perturbations in arachidonic acid (AA) metabolism. Finally, we explored *in vivo* effects of ATO^{III} on drug transporters. For this purpose, C57BL/6 mice were intraperitoneally injected with 8 mg/kg ATO^{III} (or 12.5 mg/kg $MMMTA^{V}$) with or without 15 μg/kg TCDD for 6 and 24 h. Furthermore, HepG2 and Hepa1c1c7 cell lines were treated with varying concentrations of ATO^{III} (or $MMMTA^{V}$) with or without 1 nM TCDD for 6 and 24 h. In C57BL/6 mice, ATO^{III} inhibited TCDD-mediated induction of hepatic CYP1A1/1A2 mRNA, proteins, and activities. Significant reductions in CYP1A2, but not CYP1A1, protein and activity were observed at basal levels. In

HepG2 cells, a similar inhibitory effect was observed in inducible CYP1A1/1A2 at all expression levels. Such inhibition was transcriptionally regulated by interfering with AHR-mediated activation of the xenobiotic response element (XRE). Also, post-translational modification through up-regulated heme oxygenase 1 (HMOX1) might be, at least partially, implicated in reducing enzyme activity. In Hepa1c1c7 cells, TCDD-inducible CYP1A1/1A2 expressions were increased at all expression levels, while only basal levels of mRNA transcripts, in addition to protein in case of CYP1A2, were up-regulated. Such contradiction with the *in vivo* murine model was attributed to transcriptional regulation related to AHR nuclear accumulation as well as XRE activation. Moreover, post-transcriptional and post-translational mechanisms caused increased production and decreased degradation of CYP gene products. $MMMTA^{V}$ ultimately increased CYP1A1/1A2 inducible activities in C57BL/6 mice. The same pattern of effect was also observed in Hepa1c1c7 cells. At early stage of CYP1A1 gene expression, i.e., mRNA transcripts formation, a significant decrease was obtained in both models. Such effect was only explained by transcriptional regulation mediated by interference with AHR-mediated XRE activation. As opposed to these murine models, the effect on inducible CYP1A1 in HepG2 cells was consistently inhibitory across all expression levels. Similarly, this inhibition was attributed to transcriptional regulation at the level of XRE activation. We also showed that *in vivo* alteration of CYP enzymes by ATO^{III} goes beyond AHR-regulated CYP1A subfamily to include other CYP families (CYP2, CYP3, and CYP4). ATO^{III} altered hepatic AA metabolism in C57BL/6 mice through modulating the underlying network of enzymes. Such modulation impacts AA biotransformation pathway from its beginning at the step of AA liberation and extends through the eicosanoids (e.g., hydroxyeicosatetraenoic acids (HETEs))-generating cyclooxygenases, lipoxygenases, and CYP enzymes routes. ATO^{III} suppressed *Cyp2e1*, while induced *Cyp2j9* and most of *Cyp4a* and *Cyp4f*, causing 17(S)-HETE and 18(R)-HETE increase, and 18(S)-HETE decrease. ATO^{III} also induced *Cyp4a10*, *Cyp4a14*,

Cyp4f13, *Cyp4f16*, and *Cyp4f18*, causing 20-HETE elevation. In conclusion, modulating CYP1A enzymes by ATO^{III} and $MMMTA^{V}$ implies their possible involvement in clearance-related consequences for the substrates of these enzymes such as interactions with co-administered drugs, like granisetron which is widely used anti-emetic for chemotherapy-induced nausea and vomiting, or suboptimal environmental toxicants elimination. Also, Modifying the homeostatic production of bioactive AA metabolites can entail toxic events that compromise overall body tolerability to ATO^{III} treatment. Additionally, this situation may be aggravated by unfavorable changes in the expression of ATO^{III} transport systems, such as increased expression of influx aquaporin channels, with ensuing enhancement of its toxicity.

PREFACE

This thesis is an original work by Mahmoud Abdelraouf Abdelkader Elghiaty. All experimental procedures involving animals received approval from the University of Alberta Health Sciences Animal Policy and Welfare Committee.

Section 1.1.1 of this thesis has been published in: **El-Ghiaty MA**, El-Kadi AOS. The Duality of Arsenic Metabolism: Impact on Human Health. *Annu Rev Pharmacol Toxicol*. 2023 Jan 20;63:341-358. doi: 10.1146/annurev-pharmtox-051921-020936. I was responsible for reviewing literature, summarizing data, writing the manuscript, drawing the figures, and responding to reviewers' comments. Ayman O.S. El-Kadi was the principal investigator and the supervisory author who was involved in concept formation and manuscript reviewing.

Sections 1.1.2, 1.1.3, 1.2, 1.3, and 1.4.1 of this thesis have been published in: **El-Ghiaty MA**, El-Kadi AOS. Arsenic: Various species with different effects on cytochrome P450 regulation in humans. *EXCLI J*. 2021 Jul 12;20:1184-1242. doi: 10.17179/excli2021-3890. I was responsible for reviewing literature, summarizing data, writing the manuscript, designing the tables, drawing the figures, and responding to reviewers' comments. Ayman O.S. El-Kadi was the principal investigator and the supervisory author who was involved in concept formation and manuscript reviewing.

Parts of section 1.2 of this thesis have been published in: **El-Ghiaty MA**, Shoieb SM, El-Kadi AOS. Cytochrome P450-mediated drug interactions in COVID-19 patients: Current findings and possible mechanisms. *Med Hypotheses*. 2020 Nov;144:110033. doi: 10.1016/j.mehy.2020.110033. I was responsible for reviewing literature, summarizing data, writing the manuscript, and responding to reviewers' comments. Sherif M. Shoieb was responsible for manuscript reviewing. Ayman O.S. El-Kadi was the principal investigator and the supervisory author who was involved in concept formation and manuscript reviewing.

Section 1.4.2 of this thesis has been published in: **El-Ghiaty MA**, El-Mahrouk SR, Alqahtani MA, El-Kadi AOS. Differential modulation of cytochrome P450 enzymes by arsenicals in non-human experimental models. *Drug Metab Rev*. 2023 Nov;55(4):405-427. doi: 10.1080/03602532.2023.2254525. I was responsible for reviewing literature, summarizing data, reviewing the manuscript, designing the tables, drawing the figures, and responding to reviewers'

comments. Sara R. El-Mahrouk was responsible for writing the manuscript. Mohammed A. Alqahtani contributed to writing the introduction section of the manuscript. Ayman O.S. El-Kadi was the principal investigator and the supervisory author who was involved in concept formation and manuscript reviewing.

Sections 3.1 and 3.2.2, as well as parts of section 4.1 of this thesis have been published in: **El-Ghiaty MA**, Alqahtani MA, El-Kadi AOS. Down-regulation of hepatic cytochromes P450 1A1 and 1A2 by arsenic trioxide (ATO) in vivo and in vitro: A role of heme oxygenase 1. *Chem Biol Interact*. 2022 Sep 1;364:110049. doi: 10.1016/j.cbi.2022.110049. I was responsible for designing the research, conducting the experiments, performing data analysis, writing the manuscript, and responding to reviewers' comments. Mohammed A. Alqahtani assisted in experimental optimization and method development. Ayman O.S. El-Kadi was the principal investigator and the supervisory author who was involved in concept formation and manuscript reviewing.

Section 3.2.1 and parts of section 4.1 of this thesis have been published in: **El-Ghiaty MA**, Alqahtani MA, El-Kadi AOS. Arsenic trioxide (ATO) up-regulates cytochrome P450 1A (CYP1A) enzymes in murine hepatoma Hepa-1c1c7 cell line. *Environ Toxicol Pharmacol*. 2023 Aug;101:104214. doi: 10.1016/j.etap.2023.104214. I was responsible for designing the research, conducting the experiments, performing data analysis, writing the manuscript, and responding to reviewers' comments. Mohammed A. Alqahtani assisted in experimental optimization and method development. Ayman O.S. El-Kadi was the principal investigator and the supervisory author who was involved in concept formation and manuscript reviewing.

Sections 3.3, 3.4, and 4.2 of this thesis have been published in: **El-Ghiaty MA**, Alqahtani MA, El-Kadi AOS. Modulation of cytochrome P450 1A (CYP1A) enzymes by monomethylmonothioarsonic acid (MMMTAV) in vivo and in vitro. *Chem Biol Interact*. 2023 May 1;376:110447. doi: 10.1016/j.cbi.2023.110447. I was responsible for designing the research, conducting the experiments, performing data analysis, writing the manuscript, and responding to reviewers' comments. Mohammed A. Alqahtani assisted in experimental optimization and method development. Ayman O.S. El-Kadi was the principal investigator and the supervisory author who was involved in concept formation and manuscript reviewing.

Sections 3.5 and 4.3, as well as parts of section 1.2 of this thesis have been published in: **El-Ghiaty MA**, Alqahtani MA, El-Mahrouk SR, Isse FA, Alammari AH, El-Kadi AOS. Alteration of hepatic

cytochrome P450 expression and arachidonic acid metabolism by arsenic trioxide (ATO) in C57BL/6 mice. *Biol Trace Elem Res*. 2024. doi: 10.1007/s12011-024-04225-1. (in press). I was responsible for designing the research, conducting the experiments, performing data analysis, writing the manuscript, and responding to reviewers' comments. Mohammed A. Alqahtani assisted in experimental optimization and method development. Sara R. El-Mahrouk contributed significantly to writing the manuscript and participated in the microsomal incubation of arachidonic acid and extraction of its metabolites. Fadumo A. Isse performed the separation and quantification of arachidonic acid metabolites. Ahmad H. Alammari participated in the microsomal incubation of arachidonic acid and extraction of its metabolites. Ayman O.S. El-Kadi was the principal investigator and the supervisory author who was involved in concept formation and manuscript reviewing.

This work is dedicated with love and gratitude to

my parents, brother, and sister.

Thank you for being a continuing source of love and support.

ACKNOWLEDGEMENTS

I would like to express my deepest appreciation and gratitude to my supervisor and mentor, *Dr. Ayman O.S. El-Kadi*, for giving me the opportunity to be a part of his research group and for conceptualizing the research project presented in this thesis. I am also thankful for his guidance, encouragement, and support throughout my PhD program.

I sincerely acknowledge the members of my supervisory committee, *Dr. Dion R. Brocks* and *Dr. Tony K.L. Kiang*, for their valuable suggestions and constructive feedback.

My appreciation is extended to my former and current colleagues in Dr. El-Kadi's research group for their cooperation and support, with special thanks to *Dr. Sherif M. Shoieb*, *Mohammed A. Alqahtani*, *Sara R. El-Mahrouk*, *Rahmat Hidayat*, and *Mohammed A.W. ElKhatib*.

I am grateful to the late *Dr. Michael S. Denison* (University of California, Davis, CA, USA), who passed away on March 22nd, 2022, for providing us with the HepG2 and Hepa1c1c7 cell lines stably transfected with the XRE-luciferase reporter gene plasmid (pGudLuc7.5).

Many thanks to the academic, administrative, and support staff at the Faculty of Pharmacy and Pharmaceutical Sciences for their assistance, with special thanks to *Ms. Diseray Schamehorn*, the Graduate Studies Coordinator.

I am thankful for the generous financial support provided by the University of Alberta, the Faculty of Pharmacy and Pharmaceutical Sciences, and the Cancer Research Institute of Northern Alberta in the form of several scholarships and awards including Alberta Innovates Graduate Student Scholarship, Rachel Mandel Scholarship in Lymphoma and Other Blood Cancers, and others. I would also like to thank the Natural Sciences and Engineering Research Council of Canada (NSERC) for funding this research project (Discovery Grant 250139).

Finally, I am indebted to my wonderful family for making this journey possible.

TABLE OF CONTENTS

LIST OF TABLES

LIST OF FIGURES

LIST OF ABBREVIATIONS

3-MC	3-Methylcholanthrene
9cRA	9-Cis-retinoic acid
βNF	Beta-naphthoflavone
AA	Arachidonic acid
ABH	4-Aminobiphenyl N-hydroxylation
Act-D	Actinomycin-D
AHR	Aryl hydrocarbon receptor
ANDM	Aminopyrine N-demethylation
APH	Aniline p-hydroxylation
APL	Acute promyelocytic leukemia
AQPs	Aquaporin channels
ARNT	Aryl hydrocarbon receptor nuclear translocator
AS3MT	Arsenic (+3 oxidation state) methyltransferase
As^{III}-GS_3	Arsenic triglutathione
AsB	Arsenobetaine
AsC	Arsenocholine
AsLipids	Arsenolipids
AsSugars	Arsenosugars
ABCs	ATP-binding cassette proteins
ATO^{III}	Arsenic trioxide
ATP	Adenosine triphosphate
ATSDR	Agency for Toxic Substances and Disease Registry
B[a]A	Benzo[a]anthracene
B[a]P	Benzo[a]pyrene
B[b]F	Benzo[b]fluoranthene
bHLH	Basic helix-loop-helix
B[k]F	Benzo[k]fluoranthene
BPDE	Benzo(a)pyrene-7,8-dihydrodiol-9,10-epoxide
BROD	Benzyloxyresorufin O-dealkylation

BZND	Benzphetamine N-demethylation
CAT-Tox (L)iver	Human hepatoma (HepG2) cells-derived recombinant cell lines each containing a gene promoter/response element fused to the chloramphenicol acetyl transferase (CAT) reporter gene
CCA	Chromated copper arsenate
CEPA	Canadian Environmental Protection Act
CHX	Cycloheximide
CML	Chronic myelogenous leukemia
COH	Coumarin 7-hydroxylation
CRC	Colorectal cancer
CYP	Cytochrome P450
Cys	Cysteine
DB[ah]A	Dibenzo[a,h]anthracene
DEX	Dexamethasone
DFB	3-[(3,4-Difluorobenzyl)oxy]-5,5-dimethyl-4-[4-(methylsulfonyl)phenyl]furan-2(5H)-one
DHETs	Dihydroxyeicosatrienoic acids
DMA^{III}	Dimethylarsinous acid
DMA^{III}-GS	Dimethylarsinous acid glutathione
DMA^{V}	Dimethylarsinic acid
DMAA	Dimethylarsenoacetate
DMAB	Dimethylarsenobutanoic acid
DMAE	Dimethylarsenoethanol
DMAPr	Dimethylarsenopropanoic acid
$DMDTA^{V}$	Dimethyldithioarsinic acid
$DMMTA^{V}$	Dimethylmonothioarsinic acid
$DMMTA^{V}$-GS	Dimethylmonothioarsinic acid glutathione
DRE	Dioxin response element
ECOD	7-Ethoxycoumarin O-deethylation
EETs	Epoxyeicosatrienoic acids
EGF	Epidermal growth factor

ERND	Erythromycin N-demethylation
EROD	7-Ethoxyresorufin O-deethylation
e-waste	Electronic waste
GLUT4	Glucose transporter type 4
GR	Glutathione reductase
GSH	Reduced glutathione
GSSG	Oxidized glutathione
GSTO1	Glutathione S-transferase omega-1
GTP	Guanosine triphosphate
HAHs	Halogenated aromatic hydrocarbons
HETEs	Hydroxyeicosatetraenoic acids
HIF	Hypoxia-inducible factor
HSP90	Heat shock protein 90
HXs	Hepoxilins
IARC	International Agency for Research on Cancer
iAs	Inorganic arsenic
iAs^{III}	Arsenite
iAs^{V}	Arsenate
KGDH	α-Ketoglutarate dehydrogenase
LEL	Lowest effects levels
LTs	Leukotrienes
LXs	Lipoxins
MAC	Maximum acceptable concentration
MMA^{III}	Monomethylarsonous acid
MMA^{III}-GS_2	Monomethylarsonous acid diglutathione
MMA^{V}	Monomethylarsonic acid
$MMMTA^{V}$	Monomethylmonothioarsonic acid
MROD	7-Methoxyresorufin O-demethylation
NAC	N-acetylcysteine
NAPS	Canadian National Air Pollution Surveillance
NLS	Nuclear localization sequence

oAs	Organic arsenic
p23	Prostaglandin E synthase 3
PAHs	Polycyclic aromatic hydrocarbons
PARP-1	Poly(ADP-ribose) polymerase-1
PB	Phenobarbital
PDH	Pyruvate dehydrogenase
Pi	Inorganic phosphate
PKB/Akt	Protein kinase B
PROD	7-Pentoxyresorufin O-dealkylation
PSL	Priority Substances List
PXR	Pregnane X receptor
RARE	Retinoic acid response element
RXRα	Retinoid X receptor alpha
SAM	S-adenosylmethionine
Si	Silicon
Sp1	Transcription factor Sp1
SPL	Substance Priority List
TCDD	2,3,7,8-Tetrachlorodibenzo-p-dioxin
TETRA	Tetramethylarsonium ion
Thio-DMAA	Thio-dimethylarsenoacetate
Thio-DMAB	Thio-dimethylarsenobutanoic acid
Thio-DMAE	Thio-dimethylarsenoethanol
Thio-DMAPr	Thio-dimethylarsenopropanoic acid
$TMAO^V$	Trimethylarsine oxide
TrxR	Thioredoxin reductase
$Trx\text{-}S_2$	Oxidized thioredoxin
$Trx\text{-}SH_2$	Reduced thioredoxin
UROX	Uroporphyrinogen oxidation
VEGF	Vascular endothelial growth factor
XAP-2	Hepatitis B Virus X-associated protein 2
XPA	Human xeroderma pigmentosum group A

XRE	Xenobiotic response element
ZnF	Zinc-finger

CHAPTER 1.

INTRODUCTION

Portions of this chapter have been published in:

1. **El-Ghiaty MA**, El-Kadi AOS. The Duality of Arsenic Metabolism: Impact on Human Health. *Annu Rev Pharmacol Toxicol*. 2023 Jan 20;63:341-358. doi: 10.1146/annurev-pharmtox-051921-020936.

2. **El-Ghiaty MA**, El-Kadi AOS. Arsenic: Various species with different effects on cytochrome P450 regulation in humans. *EXCLI J*. 2021 Jul 12;20:1184-1242. doi: 10.17179/excli2021-3890.

3. **El-Ghiaty MA**, El-Mahrouk SR, Alqahtani MA, El-Kadi AOS. Differential modulation of cytochrome P450 enzymes by arsenicals in non-human experimental models. *Drug Metab Rev*. 2023 Nov;55(4):405-427. doi: 10.1080/03602532.2023.2254525.

4. **El-Ghiaty MA**, Shoieb SM, El-Kadi AOS. Cytochrome P450-mediated drug interactions in COVID-19 patients: Current findings and possible mechanisms. *Med Hypotheses*. 2020 Nov;144:110033. doi: 10.1016/j.mehy.2020.110033.

1.1. Arsenic

Arsenic is a naturally occurring element that is widely distributed in the environmental media. The toxic nature of arsenic was recognized from early times, long before the documented recovery of its elemental form by Albertus Magnus amid the 13th century (1). Historically, arsenic was known as the "king of poisons" because of its wide use as a murder weapon. It was notorious for being specifically a "poison of kings" that was commonly used to assassinate rulers and nobility. This was attributed to the fact that arsenic compounds are usually tasteless and odorless and are also lethal in small amounts. Moreover, poisoning is also masked by non-specific symptoms that mimic those of food poisoning (2). Being almost untraceable in the body, arsenic was frequently used as a poison till the 19th century when a sensitive detection method was developed and published by James Marsh (3).

The first documentation of arsenic implication in cancer dates to early 1800s when John Paris noticed high rate of scrotal skin cancer among workers in copper smelting in Cornwall and Wales. These observations also included farm animals near the smelters. He speculated that exposure to arsenic fumes, associated with the metals, is the reason behind these findings (4).

Because of its deleterious effects, arsenic is recognized as an environmental toxicant and carcinogen by regulatory agencies. Arsenic ranks first on the Substance Priority List (SPL) established by the Agency for Toxic Substances and Disease Registry (ATSDR) (5). Under the Canadian Environmental Protection Act (CEPA), arsenic and its compounds were included in the first Priority Substances List (PSL1) published in 1989 by Environment Canada and Health Canada. In 1993, environmental and human health assessment reports of the substances on this list revealed that arsenic and its inorganic compounds are toxic and pose a risk to the health of humans and to the environment (6). The Monographs Program of the International Agency for Research on Cancer (IARC), which identifies carcinogenic hazards to humans, has classified arsenic and its inorganic compounds as a Group 1 human carcinogen (7).

Because of its omnipresence, life forms are vulnerable to inevitable arsenic exposure. Arsenic threatens hundreds of millions of people globally with potentially unsafe exposure levels (8). While some heavy metals are indispensable trace elements required for certain biological processes, these micronutrients become hazardous toxicants if exceeded their optimal concentrations. In this regard, scarce studies have postulated the possible physiological functions of arsenic (9); however, this

metalloid is generally regarded as a toxicant with no essential role in living organisms. That is probably why arsenic does not have a specific cellular uptake system, and it enters the cell adventitiously via transporters that are physiologically meant for certain nutrients. For instance, trivalent form of arsenic can cross the plasma membrane through aquaglyceroporin channels as a molecular mimic of glycerol (10), while, in its pentavalent state, it imitates inorganic phosphate and shares its transporters (11).

1.1.1. Arsenic biotransformation and speciation

Arsenic has a wide range of compounds that are classified as either inorganic (iAs) or organic (oAs) arsenicals (Figure 1.1). Depending on the source of exposure, human body may encounter different iAs and/or oAs species, each of which can behave differently inside the body and have different metabolic fate. It should be noted that, because of inter-species variation in arsenic metabolic handling, we focus here on the metabolites identified in humans.

1.1.1.1. Biotransformation of inorganic arsenic (iAs)

The biogeochemical cycle of arsenic starts with the mobilization from its oxidized minerals, arsenites (iAs^{III}) and arsenates (iAs^{V}), as water-soluble trivalent arsenious acid (H_3AsO_3) and pentavalent arsenic acid (H_3AsO_4) along with their dissociated derivatives. Through hydrothermal fluids, these species can end up in ground and surface water bodies which represent a portal to all life forms. That is why drinking water is considered the major source of human arsenic exposure, especially in highly contaminated regions where threatening exposure levels exist. Also, because aqueous arsenic is almost exclusively iAs, with evident toxicity, unmonitored drinking water sources are considered the greatest menace to human health (12). Besides water, plant-based diet, as rice and its products, is another source of human exposure to iAs because of the absence of arsenic methylation ability in plants (13). Other iAs sources include industrially polluted air and arsenic-based medications as the anticancer arsenic trioxide (ATO^{III}) (14).

Once inside a biosystem, iAs undergoes biotransformation, via methylation, into more complex oAs (15-17). The main methylated products generated in iAs metabolism are well-defined; however, the exact reaction sequence and enzymes involved are still debated. As analytical techniques advance, more intermediates are identified, and new pathways are suggested.

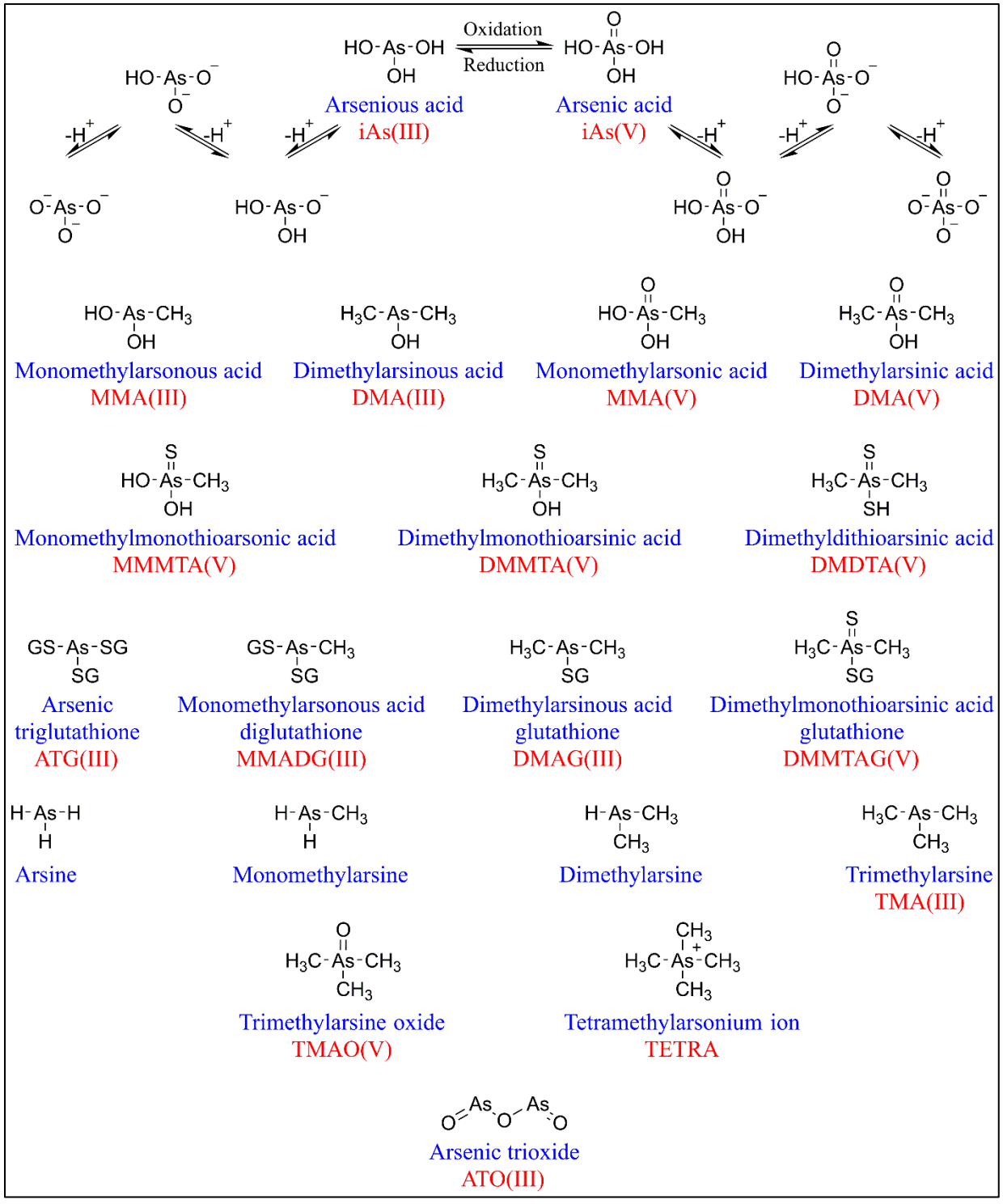

Figure 1.1. Chemical structures, names, and abbreviations of some arsenic compounds. Arsenious and arsenic acids are interconverted under oxidizing and reducing conditions with subsequent dissociation of each acid to its respective oxo-anions by further increase in pH. **Figure adapted from (14).**

In mid-20th century, Frederick Challenger proposed a pathway based on two alternating steps of reduction, catalyzed by glutathione S-transferase omega-1 (GSTO1) using glutathione (GSH) as a reducing agent, and oxidation coupled with methylation, catalyzed by arsenic (+3 oxidation state) methyltransferase (AS3MT) using S-adenosylmethionine (SAM) as a methyl donor, resulting in sequential methylation to mono-, di-, and ultimately tri-methylated species with interconversion of oxidized and reduced forms (Figure 1.2) (15).

Through its main source of exposure, i.e., drinking water, arsenic mostly exists in its pentavalent form (iAs^{V}); however, iAs^{III} predominates under anaerobic conditions (14). After oral ingestion, both iAs^{III} and iAs^{V} are highly absorbed, then extensively metabolized, and finally excreted primarily in urine (18). Most of the absorbed iAs^{V} is rapidly reduced to iAs^{III} in the blood, then the latter can be easily taken up via simple diffusion (as opposed to iAs^{V} which relies on energy-dependent transport system similar to inorganic phosphate) (19; 20) by hepatocytes where it proceeds to methylation (21). Since AS3MT activity is not induced by iAs^{V}, the non-reduced fraction of iAs^{V} taken up by hepatocytes must undergo reduction as a prerequisite step for methylation (20). In humans, a relatively small fraction of ingested iAs is excreted unchanged in urine ($iAs^{III} > iAs^{V}$) (22), while the main portion is mono-methylated into monomethylarsonous acid (MMA^{III}) and monomethylarsonic acid (MMA^{V}), which can be either excreted directly or, mostly, further methylated into their dimethylated counterparts, dimethylarsinous acid (DMA^{III}) and dimethylarsinic acid (DMA^{V}), resulting ultimately in more urinary DMA than MMA (23; 24).

In fact, formation of the dimethylated species can be used as a marker of arsenic methylation, and subsequently clearance, efficiency. Generally, the lower the methylation capacity to form DMA, the lower the urinary excretion rate of arsenic. For instance, mice have very fast urinary arsenic elimination because of their efficient methylation that results in a high fraction of DMA with minimal MMA in urine, while humans have relatively higher urinary MMA. Interestingly, some mammalian species, as marmoset monkeys, show no methylated arsenicals in urine after iAs treatment because of lacking the ability to produce functional AS3MT. In such case, iAs becomes strongly bound to different tissues and gets excreted unmodified in urine at a relatively lower rate, resulting in longer arsenic retention time in the body (14). It should be noted that elevated iAs levels in arsenic methylators, as humans, may not indicate inefficient methylation but rather reflect recent excessive arsenic exposure (22) that results in surpassing the hepatic methylation capacity

(25; 26). That is probably why higher arsenic exposure in drinking water is associated with higher urinary iAs fraction and lower DMA^V/MMA^V ratio (27).

AS3MT, a key player that catalyzes trivalent species methylation, exhibits genetic polymorphisms that highly influence arsenic methylation efficiency and the ensuing health effects. The importance of AS3MT activity in detoxifying arsenic through methylation can be demonstrated by the regions with heavy arsenic exposure where arsenic burden is believed to drive positive selection of *AS3MT* variants capable of efficient methylation (producing a lower percentage of MMA^V), thus enabling adaptation to these challenging environments (28). Certain AS3MT variants have relatively compromised catalytic activity, which can be attributed to diminished enzyme affinity for its cofactor SAM or its substrate as well as to structural instability of the enzyme itself (29).

In acute promyelocytic leukemia patients receiving ATO^{III} treatment, urinary DMA^V fraction and secondary arsenic methylation index (SMI = DMA^V/MMA^V) have been reported to be negatively associated with serum levels of alanine aminotransferase (ALT) and aspartate aminotransferase (AST). The elevated markers of liver injury, typified by ALT and AST, in some patients indicate a high risk for developing hepatotoxicity in response to ATO^{III} administration. In these patients, a significantly lower percentage of DMA^V and lower SMI imply inefficient arsenic methylation, which in turn is associated with certain AS3MT genotypes (30).

Several studies from Taiwan have previously pointed out the association between low arsenic methylation capacity (with an unfavorable urinary arsenic profile, i.e., higher percentage of MMA^V, lower percentage of DMA^V, higher PMI (primary arsenic methylation index = MMA^V/iAs), and lower SMI) and the incidence of bladder cancer (specifically urothelial carcinoma) (31). The risk of developing bladder cancer in Taiwanese people chronically exposed to iAs in drinking water was later ascribed to specific genetic variants of AS3MT that were associated with a higher percentage of MMA^V and a lower percentage of DMA^V in urine (32).

AS3MT Met287Thr (T→C; rs11191439) is a relatively high-frequency exonic single-nucleotide polymorphism (SNP) that results in replacing the methionyl residue at position 287 of the protein by a threonyl residue (33). Studies from different populations have reported abnormal urinary patterns of arsenic metabolites in iAs-exposed carriers of the Met287Thr variant compared with the wild genotype, which is indicative of inefficient methylation. Moreover, these carriers have shown significant signs of arsenic-related toxicities.

A study conducted in a central European population has demonstrated that, compared to the wild type (TT), both heterozygous (TC) and homozygous (CC) genotypes of this SNP had a significantly lower percentage of DMA^V in urine, while MMA^V fraction was significantly higher (34). In a Vietnamese population, heterozygous Met287Thr individuals (TC) have demonstrated significantly higher PMI relative to the wild type (TT) (35). Hernández *et al*. (33) have reported a higher MMA^V fraction in the urine of Chilean individuals carrying one Met287Thr variant allele than in that of wild-genotype individuals, and the increment was much higher in those carrying both variant alleles. Later, the same research group reported a positive association between the Met287Thr polymorphism and micronucleus frequency found in peripheral blood lymphocytes, a marker for genotoxicity, from copper-mining workers who were chronically exposed to high arsenic levels (36).

In another population from Mexico, it has also been reported that children with the AS3MT Met287Thr SNP present with significantly higher levels of DNA damage, as measured by the comet assay, in response to medium or high arsenic exposures in drinking water (37). In a study by Valenzuela *et al*. (38) conducted in an iAs-endemic area in Mexico, a significantly higher percentage of MMA^{III} in urine was detected in mutant homozygous (CC) and heterozygous (TC) individuals compared with the wild-type homozygotes (TT). Additionally, the Met287Thr variant was found to be marginally linked to the risk of arsenic-induced premalignant skin lesions, with the frequency of the C allele being higher among the individuals with lesions as opposed to those without lesions. Besides MMA^{III}, higher fractions of DMA^{III} have been observed in the urine of Mexican individuals with the Met287Thr variant, who were also found to be more frequently classified as diabetic by common clinical criteria than were respective wild-type carriers. Therefore, such a genotype puts its carriers at higher risk for developing diabetes upon iAs exposure in drinking water, possibly because of the enhanced production of its toxic trivalent metabolites (39). In a US population with low to moderate iAs exposure in drinking water, an elevated risk of bladder cancer has been observed in individuals with at least one copy of the C allele of the Met287Thr polymorphism compared with the TT homozygotes (wild type) (40).

Pentavalent methylated species, specifically the dimethylated DMA^V, are the dominant excretory forms of arsenic and more prevalent than trivalent ones in human urine. This can be attributed to their relatively lower reactivity to tissue components with subsequent easier and quicker excretion

(24; 41), as opposed to trivalent forms which are mainly bound to intracellular thiols of vital molecules as the tripeptide GSH (16) and proteins (17). Additionally, improper sampling and analytical techniques, especially in early studies, that result in oxidation of trivalent forms to their pentavalent counterparts may account for the absence of detectable MMA^{III} and DMA^{III} levels (20; 22). Therefore, in contrast to Challenger's classical pathway in which pentavalent arsenicals have to be reduced to trivalent ones to accept a methyl group, the trivalent forms are considered transient intermediates in arsenic biomethylation which eventually get oxidized to the more stable pentavalent end-products, as proposed by Hayakawa's (16) and Naranmandura's (17) methylation pathways (42) (Figure 1.2).

The prevalent and more stable pentavalent methylated forms were more commonly and readily detected in urine, and because of their relatively lower toxicity, compared with their iAs precursors, biomethylation was historically thought of as an exclusively detoxifying mechanism. However, with modern methodology, detection of the less stable trivalent methylated intermediates, which are relatively more toxic, has changed that view (19; 43-45).

The end-product of human arsenic biomethylation is considered to be DMA^{V} because of its rapid urinary clearance, thus leaving almost no chance for the methylation pathway to proceed towards further metabolism into a trimethylarsinic form (19).

The methylated oxo-arsenicals can get sulfur incorporated into their chemical structure replacing the oxygen bonded to arsenic atom, thus forming a family of thioarsenicals. These sulfur-containing derivatives have been identified in humans upon exposure to iAs (26; 46-48). The synthetic pathway of thioarsenicals is yet to be fully understood; however, the fact that oral administration was the route of arsenic exposure in almost all studies, in both humans and animals, has strongly suggested the involvement of pre-systemic gut metabolism via H_2S-producing anaerobic microflora (49).

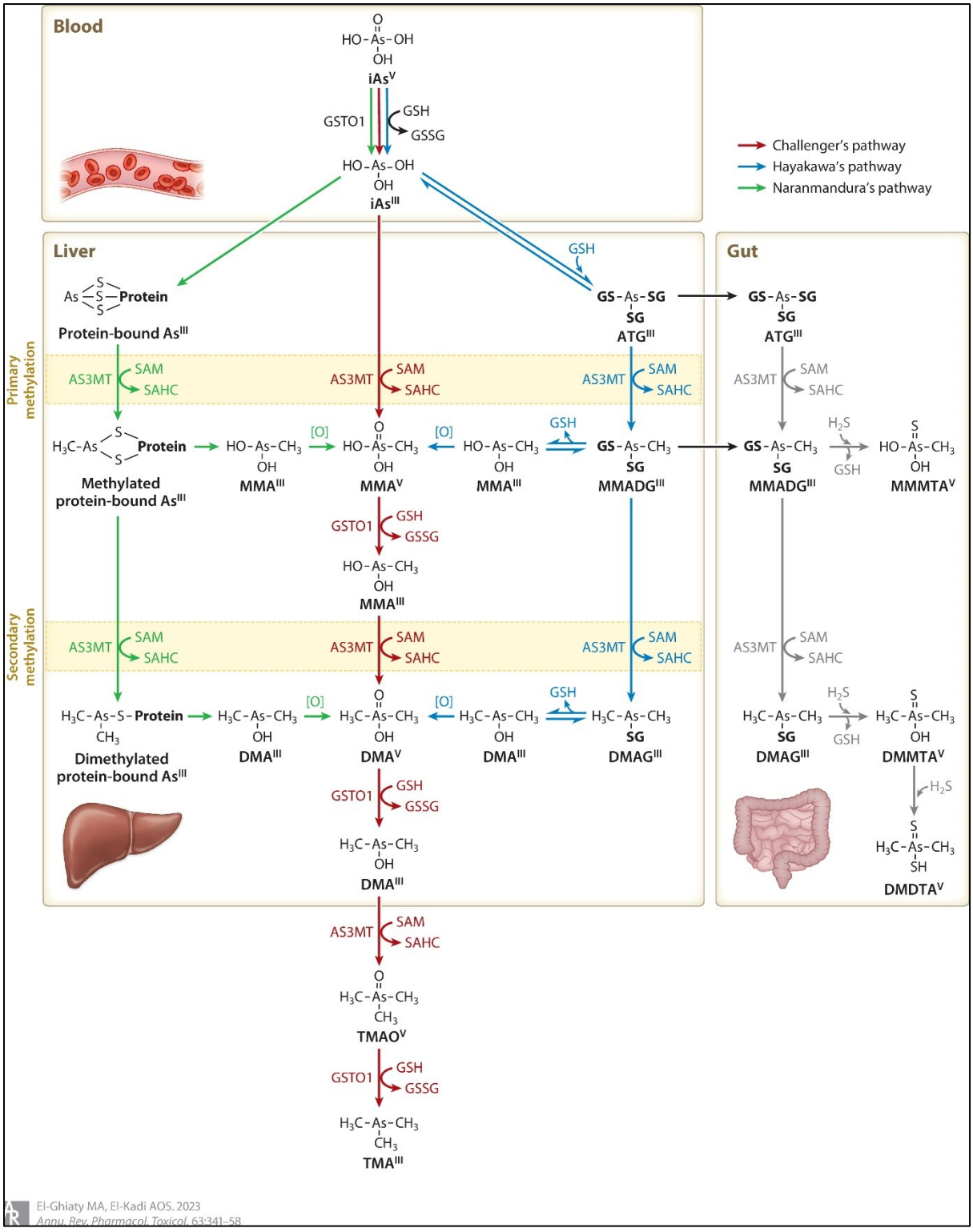

Figure 1.2. Arsenic methylation and thiolation pathways.
iAs undergoes hepatic methylation via Challenger's (red arrows), Hayakawa's (blue arrows), or Naranmandura's (green arrows) pathways. Thiolation of some glutathione complexes is mediated by gut microbiota (gray arrows). **Figure adapted from (50).**

Interestingly, some studies have reported thioarsenicals formation after intravenous arsenic exposure (26; 48; 51). This can be explained by enterohepatic recycling where hepatically synthesized methylated species are excreted in bile as GSH complexes, specifically arsenic triglutathione (As^{III}-GS_3) and monomethylarsonous acid diglutathione (MMA^{III}-GS_2) but not dimethylarsinous acid glutathione (DMA^{III}-GS) which has slower formation and less stability (18), converted into thiolated forms by gut microbiota, then reabsorbed into blood to be finally excreted in urine (16; 52) (Figure 1.2). The identified thiolated metabolites are exclusively pentavalent (trivalent ones are hypothesized to be transient intermediates) and include monomethylmonothioarsonic acid ($MMMTA^{V}$), dimethylmonothioarsinic acid ($DMMTA^{V}$), and dimethyldithioarsinic acid ($DMDTA^{V}$). Of note, sulfur-containing glutathione-conjugated trivalent arsenic complexes; as As^{III}-GS_3, MMA^{III}-GS_2, and DMA^{III}-GS; are not considered thioarsenicals. Interestingly, $DMMTA^{V}$ was the only pentavalent arsenic form to be detected in a complex with glutathione ($DMMTA^{V}$-GS) (14).

The family of volatile arsenicals includes the inorganic arsine (AsH_3) along with its methylated derivatives; mono-, di-, and tri-methylarsine ($(CH_3)AsH_2$, $(CH_3)_2AsH$, and $(CH_3)_3As$). Human exposure to arsine is usually occupational and its poisoning cases are mainly reported among workers in industrial fields. Limited studies have investigated the metabolic behavior of arsine in humans; however, it is believed that it transforms into iAs which then follows the methylation pathway towards MMA^{V} and DMA^{V} formation (53).

1.1.1.2. Biotransformation of organic arsenic (oAs)

The wide human exposure to arsenic takes place orally via ingesting arsenic-contaminated water or food. When arsenic levels in drinking water are controlled, food becomes the major source of exposure (54). While arsenic in drinking water is predominantly iAs, varying amounts of both iAs and oAs can be found in different types of food. For instance, almost 90% of dietary arsenic exposure in the U.S. is ascribed to seafood consumption, in which arsenic is primarily in the form of complex organoarsenicals. Meat food products usually contain more methylated organic arsenic forms (MMA^{V} and DMA^{V}) than iAs (14). In an inorganic form, arsenic is minimally excreted in cattle milk (55). In plant food products, iAs is prevalent as we mentioned earlier; however, methylated species may be also detected in these products. In this case, methylated forms are believed to be directly taken up by the plant from the soil after being originally produced by soil

microorganisms (13). While the inorganic fraction of dietary arsenic undergoes extensive biotransformation through methylation, dietary organoarsenicals are usually excreted unchanged with no evidence for demethylation into iAs in mammals (19; 56).

Because of the ubiquity of iAs in seawater, marine creatures have developed the ability to tolerate its presence by converting it into a wide range of organoarsenicals, while retaining minimal amount of iAs. Marine oAs range from the simple methylated compounds, which represent a minor fraction, as MMA^V, DMA^V, trimethylarsine oxide ($TMAO^V$), and tetramethylarsonium ion (TETRA) to the more sophisticated arsenobetaine (AsB) and its metabolic precursor arsenocholine (AsC), along with arsenosugars (AsSugars) and arsenolipids (AsLipids). The presence of these compounds varies among different marine species and types of seafood products (14; 44). Interestingly, it has been reported that post-mortem degradation of $TMAO^V$ results in its lower levels in stored/frozen than fresh fish. On the other hand, TETRA has been found to be enriched to detectable levels in seafood products by dry cooking owing to thermal decarboxylation of AsB (57). Because of co-exposure to multiple marine arsenicals upon consuming a seafood meal, predicting urinary metabolites and their levels is complex and depends on the collective metabolic fates of ingested species and their relative abundance in meal components.

The dominant form in marine life is AsB which is rapidly excreted unchanged in urine upon human consumption. Interestingly, Harrington *et al.* have demonstrated that AsB can undergo aerobic, but not anaerobic, *in vitro* degradation into DMA^V, $TMAO^V$, and dimethylarsenoacetate (DMAA) after 7-day incubation with human gut microflora. However, the reported incubation time is irrelevant to the realistic gut retention time, which is far less than 7 days, beside the fact that microbial gut populations are mainly anaerobic (58; 59). Compared to AsB, AsSugars are substantially more prone to biodegradation through liver enzymatic and/or gut microbial activities, with only little amount being excreted unchanged. DMA^V is the major AsSugars metabolite in human urine, in addition to dimethylarsenoethanol (DMAE), DMAA, and $TMAO^V$. Interestingly, it has been reported that AsSugars metabolism also yields thiolated analogues of these oxo-metabolites including $DMMTA^V$ and the more complex thio-dimethylarsenoethanol (thio-DMAE), thio-dimethylarsenoacetate (thio-DMAA), and thio-arsenosugar (59). AsLipids undergo extensive metabolic breakdown in humans, yielding mainly DMA^V, with no detectable intact AsLipids molecules being excreted in urine. Additionally, a minor fraction is excreted as

dimethylarsenopropanoic acid (DMAPr) and dimethylarsenobutanoic acid (DMAB) as well as their thiolated analogues (thio-DMAPr and thio-DMAB) (57).

MMA and DMA are commonly encountered in food products in their prevalent and stable pentavalent state. When these compounds are ingested by humans, they are essentially excreted unchanged in urine, but also may undergo limited metabolism. Because they are products of iAs metabolism too, the presence of these species in urine is a non-specific marker for iAs exposure and/or direct dietary intake (56). That is why food restrictions should be implemented in designing studies of arsenic metabolism, otherwise results from these studies should be interpreted with caution due to such interference (14).

Unlike iAs, only limited early studies were conducted to assess the metabolic fate of ingested methylated arsenicals in humans. After administering a single oral dose of MMA^V to volunteering laboratory members, Buchet *et al.* have reported urinary excretion of unmodified MMA^V with only 13% of excreted species being further methylated into DMA^V. In this study, volunteers who ingested a dose of DMA^V showed only unchanged DMA^V in their urine and there was no evidence for further metabolism (60). Interestingly, a study by Marafante *et al.* has reported $TMAO^V$ detection in urine after exposure of a healthy human subject to a high oral dose of ^{74}As-labelled DMA^V. Only 4% of the dose was excreted as $TMAO^V$ while the rest was in the form of DMA^V. With the exception of the studies involving seafood, this is the only report about human urinary $TMAO^V$ (61). Because it is unlikely for the human hepatic methylation to go beyond DMA^V, and because animal studies, in addition to Marafante's study in a human, reporting urinary $TMAO^V$ as a methylation product of other simpler arsenicals were based only on oral exposure, with no $TMAO^V$ being formed after intravenous administration, it is believed that $TMAO^V$ is a product of extrahepatic methylation mediated by intestinal microbial activity (14; 19).

1.1.1.3. Toxicological implications of arsenic methylation

Arsenic has a diverse assortment of compounds with varying levels of toxic implications. The toxicity of an arsenical can be generally predicted by its oxidation state and degree of methylation. Comparative *in vitro* studies, using human cell lines with different arsenic metabolites, have revealed that lower oxidation number implies higher toxicity, while higher methylation state suggests lower toxicity. Therefore, the trivalent species ($MMA^{III} > DMA^{III} > iAs^{III}$) (43) are much more cytotoxic than their pentavalent counterparts ($iAs^V > MMA^V \approx DMA^V$) (45). The cytotoxicity

of thioarsenicals, including the pentavalent $MMMTA^{V}$ and $DMDTA^{V}$, has been found to be comparable to the pentavalent methylated forms; however, the reports about $DMMTA^{V}$ have shown striking toxicity that exceeds that of iAs^{III} (43; 45). Other organoarsenicals as $TMAO^{V}$, TETRA, AsB, AsC, AsSugars, and AsLipids have not exhibited tangible toxicity. The toxicity of such marine forms might originate from their metabolic conversion to the more toxic arsenic forms; however, based on their exposure estimates and expected metabolic yield, these forms are deemed non-toxic (57).

Mechanistically, Toxic interactions of trivalent, both inorganic and organic, species can be generally ascribed to their affinity to sulfhydryl-containing biomolecules especially peptides and proteins. Covalent binding of neutral trivalent arsenicals to free cysteine (Cys) thiols can trigger conformational alterations and functional aberrations of the target protein. That is why arsenic is implicated in inactivating about 200 enzymes (62). On the other hand, the relatively lower toxicity of pentavalent arsenicals can be attributed not only to their lower reactivity towards biomolecules, but also to their nature of being negatively charged at physiological pH with lower degree of cellular uptake as opposed to trivalent forms which are neutral and more membrane permeable (63). However, once inside the cell, pentavalent forms can get reduced to their trivalent partners which by turn exert bioreactivity (64; 65). That is probably why DMA^{V} requires reduction by GSH (66) to elicit cytolethality (67). Aside from low protein reactivity, inorganic, but not methylated, pentavalent arsenic imitates inorganic phosphate and, if accumulated intracellularly at significant levels without being reduced to iAs^{III}, can interfere with several biochemical processes by replacing it (68). The exceptionally high toxicity of $DMMTA^{V}$ compared to other pentavalent forms has been linked to its thiol reactivity, because of its non-anionic hydroxyl group (18), that specifically causes GSH depletion by forming $DMMTA^{V}$-GS complexes, resulting in profound oxidative stress higher than that of iAs^{III} (69). Furthermore, $DMMTA^{V}$-GS is suggested to be converted into thiolated DMA^{III} by excess GSH, which by turn is oxidized to the more toxic DMA^{III} (65), and this may explain why GSH enhances $DMMTA^{V}$ cytotoxicity (70).

Besides direct protein interactions, inhibiting various biological processes by arsenic is usually attributed to inducing oxidative stress which itself can result from direct interaction with antioxidant systems of the thiol-based electron donors; GSH and thioredoxin ($Trx\text{-}SH_2$) which, during their defensive activity, get oxidized to the disulfide forms; GSSG and $Trx\text{-}S_2$, respectively.

Regeneration of the functioning reduced state of GSH and Trx-SH_2 relies on glutathione reductase (GR) and thioredoxin reductase (TrxR), respectively, which also depend on thiols at their redox active site. The function of both glutathione (GSH/GR) and thioredoxin (Trx/TrxR) systems is not limited to fueling the antioxidant defense to keep redox homeostasis, but it also includes regulating DNA synthesis for replication or repair, transcription factors activity and gene expression, and protein synthesis and folding (71).

The reliance of these systems on thiols renders them an ideal target for trivalent arsenicals that result in denaturing the reducing cellular environment and several biochemical derangements. It has been reported that all trivalent forms can bind directly to the free vicinal thiols of Trx, with MMA^{III} having higher affinity and forming more stable complexes than iAs^{III} and DMA^{III}. Pentavalent iAs^{V}, MMA^{V}, and DMA^{V} did not elicit any effect; however, at human body temperature (37°C), as the Trx concentration increases, more pentavalent species are reduced to their trivalent counterparts, which by turn can bind to Trx (72). Also, MMA^{III} has shown more potent concentration-dependent reduction in TrxR activity compared to iAs^{III}, while no change in activity was observed after DMA^{III} treatment (73). Interestingly, disrupting Trx/TrxR system by irreversible inactivation of TrxR has been linked to ATO^{III} mechanism of cytotoxic activity (74). Similarly, trivalent methylated arsenicals have exhibited more potent GR inhibition than iAs^{III}, while their pentavalent analogs could not affect GR activity (75).

Pyruvate dehydrogenase (PDH) multi-enzyme complex is a critical system that bridges the first and second stages of aerobic cellular respiration for the ultimate production of adenosine triphosphate (ATP). It has been reported that trivalent arsenicals can inhibit PDH complex through direct binding to vicinal dithiols of the reduced lipoic acid moiety, a cofactor for one of its subunits, with MMA^{III} being more potent inhibitor, through more stable binary binding, than iAs^{III}. DMA^{III} also inhibited the complex but after longer incubation time, probably because of either its instability towards oxidation to DMA^{V} or its limited ability to bind only monothiols as its extra methyl group hinders chelated binding. On the other hand, none of the pentavalent counterparts were able to inhibit the complex. Inhibiting such complex not only reduces cellular ATP production but also leads to oxidative stress through depleting reducing equivalents pool. In addition to PDH complex, α-ketoglutarate dehydrogenase (KGDH) enzyme complex is affected in a similar way (76).

In addition to PDH inhibition, glucose homeostasis can be also disrupted through suppressing insulin-stimulated glucose uptake that is mediated by protein kinase B (PKB/Akt) phosphorylation with its ensuing glucose transporter type 4 (GLUT4) translocation to the plasma membrane. Only trivalent species have shown significant inhibition with the following order of potency (MMA^{III} > DMA^{III} > iAs^{III}). Later, this inhibition was attributed to the binding affinity, which was the highest for MMA^{III}, to closely spaced cysteines of 3-phosphoinositide-dependent kinase-1 (PDK-1). Interestingly, DMA^{III} has lost its inhibitory effect at longer incubation time, probably because of being oxidized to the non-active DMA^{V} (77). Similarly, trivalent arsenicals (MMA^{III} > DMA^{III} > iAs^{III}) have demonstrated significant inhibition of glucose-stimulated insulin secretion. Such diabetogenic effect is mediated by inhibiting Ca^{2+} influx, probably through interfering with disulfide linkage formation between α2 and δ subunits of $Ca_v1.2$ channels (78).

Compromised cellular DNA repair machinery can result in progressive accumulation of mutations, which by turn can initiate carcinogenesis. Arsenic is not directly DNA reactive, and its carcinogenicity is more likely based on epigenetic and indirect genotoxic mechanisms as interfering with DNA repair. In this regard, arsenic targets zinc-finger (ZnF) proteins involved in DNA repair and/or DNA damage signaling. Generally, ZnF is a protein domain containing multiple motifs of finger-like protrusions of Zn^{2+} coordinated to cysteine thiolates and/or histidine imidazole groups, and this domain is responsible for the contact of its proteins with different target molecules as DNA, RNAs, and proteins in a variety of biological processes. The mechanistic explanation of arsenicals inhibition of these proteins is the direct interaction with Cys thiol at the ZnF with subsequent displacement of Zn^{2+}, thus halting recognition and binding to damaged DNA (79). It has been demonstrated that methylating iAs^{III} to MMA^{III} increases its binding ability to more configurations of ZnF peptides (80).

At 10 times lower concentrations than iAs^{III}, both MMA^{III} and DMA^{III} have significantly reduced the extent of poly(ADP-ribosyl)ation stimulated by H_2O_2 in mammalian cells. MMA^{V} and DMA^{V} have not altered poly(ADP-ribose) polymerase-1 (PARP-1) activity, even at cytotoxic concentrations. Of note, PARP-1 gene expression, assessed by real-time PCR, was not altered by trivalent species (81).

Preincubation of human cells with iAs^{III} or MMA^{III} has significantly enhanced (+)-Benzo(a)pyrene-7,8-dihydrodiol-9,10-epoxide (BPDE)-induced DNA adducts formation in a

concentration-dependent manner, with MMA^{III} being more potent at 10 times lower concentrations. In contrast, DMA^{III}, MMA^{V}, and DMA^{V} have not affected adduct formation. After additional post-incubation with respective arsenical, all tested compounds have demonstrated significant concentration-dependent reduction in cellular ability to repair BPDE-induced adducts. Both MMA^{III} and DMA^{III} were the most potent inhibitors, followed by iAs^{III}, and finally MMA^{V} and DMA^{V} which required 100 times higher concentrations than MMA^{III} to give comparable effect. Additionally, only trivalent arsenicals (MMA^{III} > DMA^{III} > iAs^{III}) were able to release Zn^{2+} from a synthesized ZnF domain of the human xeroderma pigmentosum group A (XPA) repair protein, while pentavalent methylated forms exhibited little or no effect, even at much higher concentrations (82; 83).

Besides DNA repair proteins, other ZnF proteins, as the glucocorticoid receptor, can be also targeted by iAs^{III} and MMA^{III}, where only the latter has shown the ability to displace Zn^{2+} at the DNA-binding domain of the receptor (84).

In addition to their clastogenicity, trivalent, especially the methylated, forms have demonstrated the most potent aneugenic effect which was suggested to be mediated by tubulin polymerization blocking via crosslinking pairs of vicinal cysteine residues near the guanosine triphosphate (GTP)-binding site (85).

The negative impact of arsenic methylation is not limited to the production of bioreactive metabolites, several cofactors, as GSH and SAM, are also consumed in the process resulting in potential homeostatic perturbations. It should be noted that these cofactors have high cellular reserve, moreover, intracellular iAs is usually present at too low concentration to allow stoichiometric depletion of them. However, high iAs load, as in chronic exposure, can cause them to be heavily exhausted. For instance, SAM consumption by arsenic methylation, especially with deficient dietary replenishment, has been implicated in carcinogenesis through genomic hypomethylation (86).

1.1.2. Environment arsenic sources (with examples from the Canadian environment)

Arsenic is a natural component of the earth's crust, with varying amounts depending on the local geological history of the geographic region. From its natural repositories, arsenic is released and dispersed into the pedosphere, hydrosphere, and atmosphere (Figure 1.3).

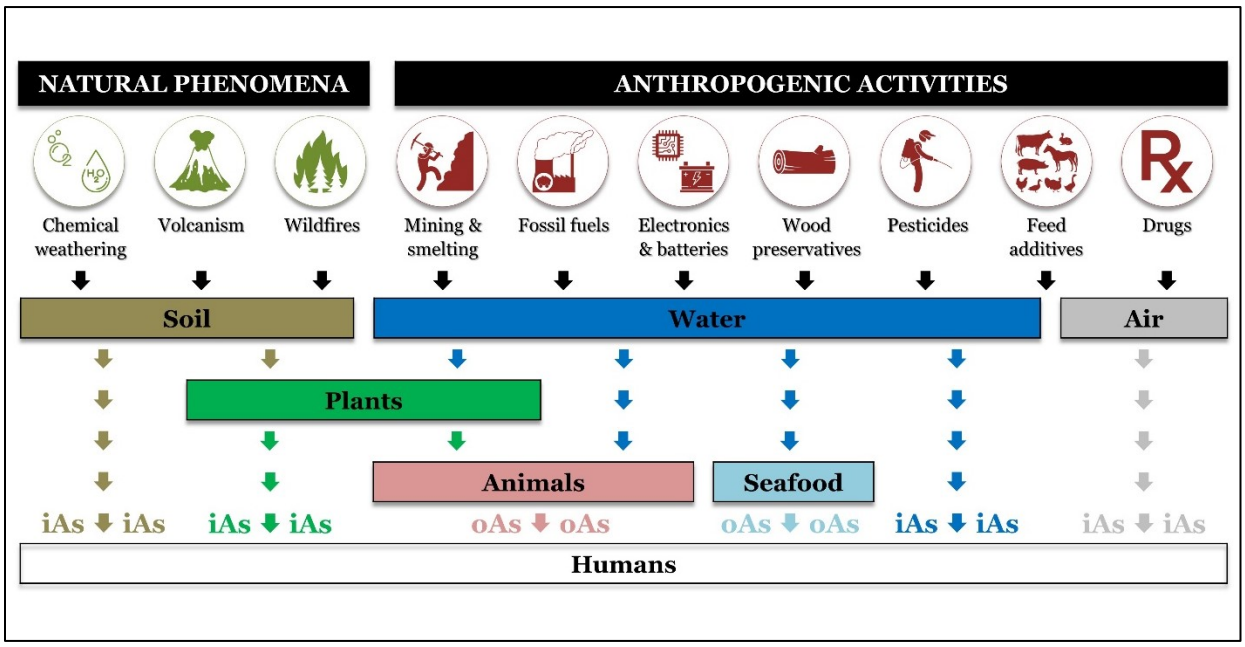

Figure 1.3. Pictorial depiction of various natural phenomena and anthropogenic activities that contribute to arsenic release from its natural repositories to the environment. Subsequently, human exposure to the released arsenic can take place either directly through soil, water, or air, or indirectly through different food products. The main arsenic form, inorganic (iAs) or organic (oAs), is shown for each route of exposure. **Figure adapted from (14).**

Natural geogenic processes including weathering and volcanism achieve arsenic release slowly. However, greatly enhanced release results from anthropogenic activities that involve arsenic-containing products or wastes. For instance, the global anthropogenic contribution to atmospheric emissions of arsenic is estimated to be about three times higher than that from natural sources (87). It is of grave importance to understand how arsenic is introduced to the biosphere to characterize its environmental levels and subsequently assess the risk of human exposure.

1.1.2.1. Natural arsenic sources

1.1.2.1.1. Chemical weathering

Chemical weathering in the presence of oxygen and water is the main natural mechanism of arsenic mobilization from its minerals. Arsenic-bearing minerals such as arsenopyrite, realgar, and orpiment, represent the starting point for oxidation and hydrolysis, and from which arsenic is subsequently released resulting in enrichment of the surrounding soil with highly soluble species (88). The global average natural arsenic level released into uncontaminated soil is 5 mg/kg, with much higher levels being detected near high geological deposits of arsenic-rich minerals, or in human-impacted spots as mining areas (5).

In Canadian uncontaminated soil, arsenic can be found naturally at levels of 4.8-13.6 mg/kg (89). Pyrite oxidation, upon exposure to the air, in acid sulfate soils located in northwestern Alberta results in arsenic enrichment up to 37.9 mg/kg (90). In British Columbia, Warren *et al.* have detected extremely high arsenic concentrations of 4600 mg/kg in A_2 soil horizon in the neighborhood of some mineralized veins (91).

1.1.2.1.2. Volcanism

Volcanism is another significant natural arsenic-releasing mechanism. Large amounts of arsenic are mobilized, especially to the atmosphere, by volcanic activity through volcanic emissions including ash and gases (92-94). In addition to ground water contamination by volcanic eruptions, surface water can be also affected by deposition and dissolution of volcanic ash (95; 96).

1.1.2.1.3. Wildfires

Wildfires represent an increasingly important global phenomenon, particularly tied to hot and dry weather, and their risk is expected to increase as a result of climate change (97). They contribute to releasing large quantities of toxic pollutants including arsenic (98; 99). The inability of plants to metabolize arsenic in addition to its inadvertent uptake and accumulation in different parts of the

shoot system render these plants a threatening source of iAs which can be released in wildfires. Significantly higher levels of arsenic are detected in wildfire-impacted areas, especially in urban residential areas, because of burning buildings and other urban elements, compared to open wildlands (100; 101).

In Canada, wildfire has been a major environmental concern for a long time, burning approximately 2 million hectares of forest annually (in some years, more than 7 million hectares) (102). For instance, in 2003, British Columbia had catastrophic wildfires where nearly 2,500 fires burnt more than 265,000 hectares (103). The costliest natural disaster in the history of Canada was the 2016 Horse River wildfire in Alberta. Because of the toxic fire ashes containing arsenic, the re-entry of Fort McMurray residents, who were evacuated from the wildfire-ravaged area, was delayed for five months. Fourteen months later, samples of ground ashes from wildland-urban interface fires in Fort McMurray have shown residual arsenic pollution originating, most probably, from burning local buildings rather than forests (104).

1.1.2.2. Anthropogenic arsenic sources

In addition to these natural processes, a wide range of human activities has also been implicated in arsenic mobilization. These activities, because of environmental awareness, have become historical and do not exist anymore, or, because of technological improvement and remediation, still exist but are well-regulated under rigorous restrictions for arsenic release. However, the old practices have resulted in the release of massive amounts of arsenic that have impacted the environment till today, because once released, arsenic cannot be destroyed but can only be converted into different forms thus spreading its toxic effects throughout the ecosystem (105).

1.1.2.2.1. Mining and smelting

The significant natural occurrence of arsenic in sulfide-bearing ore deposits of metals such as lead, copper, zinc, gold and silver, poses high risk of arsenic liberation upon extraction of such metals (106). Mining and metallurgical processing operations represent a significant source of heavy metals pollution including arsenic (107). Mining can accelerate the weathering process via oxidation of arsenic-bearing minerals, mainly sulfides, resulting in the formation of sulfuric acid. The outflow of such acidic water, namely acid mine drainage, with its elevated levels of heavy metals facilitates arsenic release to the soil in the vicinity of mines (108). High concentrations of arsenic have been detected in the blood (109), urine (110), and hair (111) of miners.

In smelters, the pyrometallurgical treatment of metal ores, such as copper, results in removal of arsenic, a common impurity in copper ores, by oxidation into ATO^{III}. Subsequently, under high temperatures, ATO^{III} volatilizes and escapes in the generated flue gases, and ultimately, as the gases cool down, condenses on particulate matter, and is captured by the flue dust as white powder. Such dust not only affects the atmosphere, but also can deposit to contaminate soil and water (112). ATO^{III} can be found naturally as two dimorphs of trivalent arsenic oxide minerals (arsenites), namely; arsenolite and claudetite, but its common source is oxidation through roasting of arsenic-bearing ore minerals or coal. The gaseous emissions from copper smelters account for about half of the annual anthropogenic arsenic emissions to the atmosphere (113). Additionally, wastewater from these smelters also contains considerable amounts of arsenic and must be treated before disposal (114). Exposure of smelter workers to arsenic results in high urinary concentrations of its metabolites (115) and it has been tied to peripheral neuropathy (116; 117), Raynaud's phenomenon (118), cancer (119), and other disorders (120). Arsenic-mediated lung cancer is identified as the major cause of mortality among smelter workers (121; 122), as suggested by high arsenic concentrations detected in autopsy samples of lung tissue from dead workers (123). The carcinogenic effect also extends to those who are living in the vicinity of smelters (124).

A few kilometers away from Yellowknife (Northwest Territories), Giant Mine was a gold mine that operated for over five decades, until it became officially abandoned in 2005. Arsenopyrite-bearing gold ore mining operations, especially roasting, have swamped the surrounding environment with massive amounts of ATO^{III} dust from stack emissions. Moreover, thousands of tons of ATO^{III} were stored in underground chambers and are currently an ongoing source of arsenic to groundwater. A costly remediation plan to permanently freeze these chambers, to keep groundwater seepage out, was approved by the Canadian federal government in 2014 (125).

Another example of legacy arsenic contamination is located in Cobalt town (Ontario) where historical silver and cobalt mining activity took place. The mineralogical association of arsenic with silver and cobalt ores resulted in tons of arsenic-rich tailings and wastes that were disposed into nearby depressions (often lakes). Almost a century after ending the operations there, wastes are still lingering in both aquatic and terrestrial environments till today (126). In northern Saskatchewan, high levels of arsenic have been detected in Rabbit Lake uranium mine tailings

(127). Historical gold mining in Nova Scotia has left many arsenic-rich tailings deposits in different areas across the province (128).

Athabasca oil sands (Alberta) are large deposits of bitumen that are considered the largest known reservoir of crude bitumen in the world. Surface mining operations in these bituminous sands result in generating massive volumes of wastes in which arsenic is present in significant levels, thus posing ecological risks. The development of mining operations in that area has been accompanied with increased arsenic concentrations in Athabasca River (129).

Smelters across Canada pose a great threat to the environment through arsenic release. Examples include base-metal smelting complex in Flin Flon (Manitoba) and Creighton (Saskatchewan) (130), lead smelter in Belledune (New Brunswick) (131), copper smelter in Rouyn-Noranda (Québec) (132), and lead-zinc processing facility, formerly a gold smelter, in Trail (British Columbia) (133).

1.1.2.2.2. Fossil fuels

As a fossil fuel, coal is combusted to produce very high temperatures used in several applications, notably generating electricity, through steam, in coal power stations. Coal is a natural source of arsenic and primarily responsible for its release in different forms. During combustion, only minor part remains in bottom ash, while the rest volatilizes and either escapes in gaseous phase or, mainly, deposits on fly ash (134). Because it occurs as a surface precipitate, arsenic in fly ash is highly leachable, thus ending up in soil or water (135). Through technologies as electrostatic precipitators, more than 95% of fly ash is collected before being released from smoke stacks, thus decreasing atmospheric emissions, however its subsequent disposal remains a threat to soil and water (136). Metabolites of arsenic were detected in the urine of power plants' workers (137). Moreover, arsenic release associated with coal combustion is strongly correlated to the incidence of cancer among these workers (138; 139). Combustion of fuels in automotive engines can also contribute to arsenic emissions (140; 141).

Establishment of coal-fired power plants has resulted in enrichment of arsenic in Wabamun Lake (Alberta) sediments to concentrations beyond the lowest effects levels (LEL) for toxicity to benthic organisms (142). Compared to background areas, statistically significant higher concentrations of arsenic have been detected in Grand Lake (New Brunswick) sediments because of coal-combustion ash discharges (143).

1.1.2.2.3. Electronics and batteries

Arsenic is an important element in various industrial applications. It is a common n-type dopant in manufacturing semiconductors, with gallium arsenide (GaAs) being the second, after doped silicon, most commonly used semiconductor material in electronics industry such as integrated circuits, light emitting diodes, laser diodes, and solar cells (144). GaAs and other arsenic-based III-V semiconductors, such as indium arsenide (InAs), may impose serious toxic and carcinogenic pulmonary effects on workers in the semiconductor industry (145) who are at high risk of exposure to significant levels of arsenic especially through inhalation (146; 147). High levels of urinary arsenic metabolites have been reported in workers from a manufacturing plant (148), and were correlated to oxidative injury (149). Because of highly contaminated industrial waste effluents from manufacturing plants (150), arsenic threat is not limited to occupational exposure and can affect the surrounding environment through water (151) and air (152).

On the other hand, the rapid expansion of technology with rising demand for consumer electronics has resulted in the creation of staggering quantities of electronic waste (e-waste) around the globe. The total e-waste generated worldwide was estimated at approximately 53.6 million tons in 2019, where the contribution of Canada was about 757000 tons (153). About 60 chemical elements can be found in various disposed electronics, and some of which is hazardous such as arsenic (154; 155). The environmental threats of e-waste necessitate efficient recycling, however, in 2019, only 17.4% of it was officially documented as properly collected and recycled (153). Additionally, improper handling of such waste through informal recycling can aggravate the situation and increase the release of toxic substances (156). In Canada, several organizations are currently working on e-waste recycling through collection, dismantling, hazardous material removal, and recovering of valuable elements (157; 158).

Another industrial application of arsenic is alloying with lead in the manufacturing of lead-acid batteries, which are mostly used as car batteries. Secondary lead smelters produce lead by recovering it from lead-bearing scrap materials (most of which are scrap automobile batteries). Arsenic, among other metals, is typically detected in the area surrounding the recycling facilities (159-161). Interestingly, arsenic was detected in shed deciduous teeth of children who are living near a lead-acid battery smelter (162). An early study in southern Ontario, has reported high levels

of arsenic contamination in soil and vegetation from different locations in the vicinity of two secondary lead smelters (163).

1.1.2.2.4. Wood preservatives

Arsenic-based wood preservatives, such as chromated copper arsenate (CCA), were developed to prevent its deterioration, especially for outdoor use, by microorganisms or insects. The preservative is applied by pressure treatment and, typically, 1 m^3 of CCA-treated wood contains about 1.41 kg of arsenic (164). From CCA-treated wood, arsenic can leach through weathering during normal use (165), or through disposal via landfilling (166; 167) or incineration (168).

Zagury *et al.* have reported high arsenic concentrations in samples from the soil adjacent to the CCA-treated utility poles in Montréal (Québec) (169). Similarly, significant levels of arsenic leaching from CCA-treated utility poles have been detected in in western Newfoundland and Labrador (170). In Edmonton (Alberta), the average arsenic level on the hands of children playing in playgrounds with CCA-treated wood structures (0.5 μg) was significantly higher than that from playgrounds not constructed with CCA-treated wood (0.095 μg) (171). Of note, the maximum amount of arsenic detected on children hands in that study (<4 μg) was lower than the reported children average daily intake of total arsenic from food in Canada (14.9 μg) (172). As of December 31, 2003, CCA was phased out of residential applications in Canada, and its use is currently restricted to industrial wood products (89).

1.1.2.2.5. Pesticides

The inherent toxicity of arsenic has led to its use in wood preservatives as well as agricultural pesticides. Both organic and inorganic arsenic-based compounds were developed and used as insecticides, rodenticides, and herbicides (173). Arsenical pesticides have a negative impact on the cultivated plants (174), groundwater and surface water (175; 176), as well as applicators and farmers (177; 178). Additionally, arsenic contamination, because of spills and releases, has been also reported at manufacturing sites (179; 180). The threat of arsenic-bearing pesticides still exists despite being banned and phased out because of environmental persistence of arsenic residues that resulted from extensive long-term application of these pesticides (181; 182).

In southern Ontario, using lead arsenate in apple orchards for over 70 years resulted in more than 10 folds elevation (from 7.4 ppm to 121 ppm) in arsenic level in soil samples (183). Similar observations were reported in Annapolis Valley apple orchards (Nova Scotia) (184). In addition to

high arsenic concentrations in soil samples, significant levels were reported in plant tissue from apple orchards and potato fields in the same province (185). In Niagara (Ontario), elevated arsenic was detected in samples from trees of different fruits, that had received repeated applications of lead arsenate (186).

1.1.2.2.6. Feed additives

In animal husbandry, especially poultry, phenylarsonic compounds, most notably of which are roxarsone and nitarsone, have been used as feed additives for improving feed efficiency and protection against parasitic infections. These compounds were originally approved on the basis of being harmless organoarsenicals, however, it has been found that they get converted into inorganic arsenic within the chicken (187; 188). Consequently, their U.S. Food and Drug Administration (FDA) approvals were withdrawn (189). The presence of these compounds in poultry litter, which is commonly used as an organic fertilizer, results in soil contamination, where they can undergo biotic (190-192) or abiotic (193) conversion into more toxic inorganic species. Eventually, arsenic in the soil may end up in ground water (194) or the cultivated plants (195; 196).

1.1.2.2.7. Drugs

Arsenic is regarded as a double-edged sword, which, despite its toxic nature, has proven therapeutic benefits that date back to the days of Hippocrates who used arsenic sulfides (realgar and orpiment) to treat ulcers and abscesses. Arsenic-based pharmaceuticals have been employed in various disorders throughout history (197), however, a detailed description of these agents started in late 18^{th} century, by the discovery of Thomas Fowler's solution (1% potassium arsenite solution formed by dissolving ATO^{III} in potassium bicarbonate) that was used for a variety of systemic illnesses. In 1878, it was first reported that Fowler's solution can lower the white blood cell counts in leukemia patients, and subsequently, it became the mainstay for the treatment of chronic myelogenous leukemia (CML) until the advent of, the safer, radiation and chemotherapy by the beginning of the 20^{th} century (198).

In the early 20^{th} century, the sodium salt of arsanilic acid, a compound that was discovered 40 years earlier by reacting arsenic acid with aniline, was introduced as the first organoarsenical medicine. This compound was found to be 40 times less toxic than the inorganic Fowler's solution, hence named atoxyl, and was used for the treatment of trypanosomiasis (199). Additional experimentations on atoxyl led Paul Ehrlich, the founder of chemotherapy, to the discovery of

arsphenamine, marketed as salvarsan, in 1910. Salvarsan was the "magic bullet" for treating syphilis. Generally, the clinical applications of arsenicals gradually declined because of posing greater health threats than the diseases that they were supposedly curing. Eventually, arsenic medicines have been largely replaced by less toxic compounds. For instance, salvarsan was replaced by penicillin for syphilis treatment (200).

However, some arsenicals are still used, despite their severe toxicity, for treating diseases that typically result in death if untreated, such as the antitrypanosomal melarsoprol (atoxyl was the first effective treatment but blindness was a serious side effect) (201; 202).

The rebirth of ATO^{III} therapy occurred in the 1970s as a treatment for acute promyelocytic leukemia (APL), and in 2000, it was approved by FDA as a frontline therapy for this disease (203). ATO^{III} exerts its anticancer activity in its hydrolyzed form, iAs^{III}, which is subsequently metabolized into different methylated metabolites. These metabolites may ultimately contribute to the overall pharmacological activity of ATO^{III}, however their anticancer activity is yet to be proven (204).

About 90% of APL cases are associated with a t(15; 17) chromosomal rearrangement which is a reciprocal translocation of the retinoic acid receptor alpha (*RARA*) gene on chromosome 17 with the promyelocytic leukemia gene (*PML*) on chromosome 15 (205). The vitamin A derivative, retinoic acid, interacts with the RARα nuclear receptor, the protein product of *RARA* gene, which by turn acts as a differentiating agent of normal myeloid hematopoietic cells. The *PML-RARA* fusion gene results in the production of a hybrid protein with oncogenic activity. That fusion protein causes progressive accumulation of promyelocytes in the bone marrow through blocking myeloid differentiation at the promyelocytic stage with added proliferative advantage to leukemic cells (206).

The mainstay for APL treatment is the all-trans retinoic acid (ATRA) which effectively induces terminal differentiation of the leukemic promyelocytes through dissociating co-repressor complexes from PML-RARα and triggering proteasome-dependent PML-RARα degradation (207). In combination with conventional chemotherapy, ATRA produces about 70% cure for APL. Interestingly, almost 90% of APL patients can be cured by ATRA when combined with ATO^{III}, while ATO^{III} monotherapy can achieve a cure rate of ≈70% among these patients (207). While ATO^{III} cytotoxic effect is widely attributed to reactive oxygen species (ROS)-induced

depolarization of mitochondrial membrane with subsequent activation of the downstream apoptotic pathways, this mechanism can only partially decipher ATO^{III}-induced malignant cell death. Many studies have revealed that ATO^{III} additionally interacts with PML-RARα and induces different modifications, at the PML B-domain, that initiate ubiquitination and proteasomal degradation of that oncogenic product (203).

Because of its success in APL, ATO^{III} is currently being investigated for the treatment of other types of cancer (208-211). However, being one of arsenic compounds, ATO^{III} retains at its core the hypertoxic characteristics of that notorious heavy metalloid. The innate toxicity of ATO^{III} results in a constellation of side effects and complications in APL patients (212) including hepatotoxicity (213) which can be severe enough to result in treatment discontinuation (214). Moreover, these toxicities may stand as a major hurdle against employing ATO^{III} in the treatment of other types of cancer especially solid tumors, where a worse toxicity profile is expected, because much higher ATO^{III} doses, than those used in APL, are required to compensate for the rapid ATO^{III} renal clearance and allow sufficient uptake of it by the tumor mass (215; 216).

1.1.3. Routes of human exposure to arsenic

Humans are exposed to arsenic via several pathways including ingestion of food, drinking water, inhalation of air, or dermal contact (Figure 1.3). Arsenic exposure is a multifactorial process depending on local geochemistry (i.e., natural presence), environmental pollution, and lifestyles of the population. For instance, occupational exposure in industrial environments occurs primarily through inhalation (12).

1.1.3.1. Drinking water

For the general population, exposure is mostly oral via ingesting arsenic-contaminated food or water. Drinking water is widely regarded as the major source of exposure especially in areas with arsenic concentrations exceeding the World Health Organization (WHO) guidelines value (10 μg/L) e.g. by living near either a natural geological source or a contaminated site (217). However, in the presence of water with safe arsenic levels below that limit, food may become a greater contributor to total arsenic intake than drinking water. Assessment of health risks is based on a general understanding that inorganic forms of arsenic are more harmful than organic ones, and that most cases of arsenic-induced toxicity in humans are associated with inorganic arsenic exposure. There is no evidence for the demethylation of organoarsenicals into inorganic forms in mammals

(218). Since aqueous arsenic species are almost exclusively inorganic, compared to only 10% iAs in food, drinking water is usually considered the greatest menace to human health (12).

Various sources of drinking water fall into two main categories: surface water and groundwater. The risk of arsenic exposure may vary depending on the source of water. In anthropogenically impacted areas, all water sources, especially surface water, become vulnerable to contamination. However, naturally, groundwater usually poses higher risk for exposure (219). Extremely high arsenic levels in groundwater may result from its presence at depths where it is exposed to more naturally occurring arsenic sediments. Moreover, drinking water supplied from groundwater is extracted by pumping wells, and such pumping activity causes disruption of soil sediments and facilitates arsenic mobilization to the groundwater (220). Additionally, groundwater from wells is often not treated before human consumption, because it is generally less accessible to treatment methods than surface water, and its treatment is usually more difficult and expensive (221).

In 1980s, the Canadian drinking water guidelines recommended a maximum acceptable concentration (MAC) for arsenic of 50 μg/L (222). However, with the growing knowledge about arsenic-mediated harmful effects as well as the development of more sensitive laboratory methods for detection, that limit was later changed to 25 μg/L (223), and currently a limit matching the published WHO guidelines (10 μg/L) is set by Health Canada (224). It is worth mentioning that this limit doesn't warrant protection against arsenic harm (225), and a limit of 0.3 μg/L would be ideal for achieving an "essentially negligible" lifetime risk of cancer, but 10 μg/L is the lowest concentration that is technically achievable in the Canadian drinking water systems. Generally, arsenic levels in drinking water are less than 5 μg/L in most locations across Canada (172).

However, the natural occurrence of arsenic at high levels in certain locations (226) has created "hotspots" for arsenic exposure through drinking water beyond 10 μg/L (Figure 1.4). This may be a major concern especially in provinces and territories that depend partially (as Alberta) or completely (as Prince Edward Island) on ground water which represent more than 30% of the population (227). It would be safer to rely on the controlled municipal drinking water supplies, but approximately 4 million Canadians obtain their water as groundwater through privately-owned domestic wells (228), and in such case, water is not subject to regulated testing and therefore may contain unknown and possibly unsafe arsenic concentrations as reported in several studies (229-232).

1.1.3.2. Food

Food is another major source of both organic and inorganic arsenic for typical individuals. Arsenic can be found in most diets with varying amounts and forms, i.e., organic or inorganic, depending on the type of food (233). For instance, seafood represents about 90% of dietary arsenic exposure in the U.S., of which the vast majority is in complex organic forms. As mentioned earlier, arsenobetaine is the predominant species in marine food, which was found to be not cytotoxic, mutagenic, immunotoxic, or embryotoxic (44; 234). Comprehensive lists showing the levels of different arsenic species in various food products from different countries can be found in several good review articles (56; 235).

Livestock are exposed to arsenic in contaminated environment through water, plants, incidental soil ingestion, or feed additives. Eventually, inevitable human exposure to arsenic can occur via consuming such animal food products. Studies have reported arsenic exposure through different types of meat (236; 237) as well as milk (238) and eggs (239). Because of their arsenic methylation ability, organoarsenicals are the main form in animal food products besides an inorganic fraction (187; 188; 240). Interestingly, arsenic excreted in milk was found to be entirely inorganic (55).

In addition to water, plants are regarded as an important gate for arsenic entry to the food chain when cultivated in arsenic-rich soil or irrigated with arsenic-contaminated water. Therefore, plants are mostly exposed to inorganic forms of arsenic (241). Arsenic is considered non-essential for plants, and it has no specific uptake system, therefore, it relies on adventitious uptake pathways via various transporters that are naturally intended for minerals and nutrients. For example, iAs^{V} is quite similar to inorganic phosphate (Pi) and can compete with it for the uptake via phosphate transporters. Similarly, the uptake of iAs^{III}, which is the dominant species in anaerobic environments, can be achieved by silicon (Si) transporters due to structural similarity between arsenious acid and silicic acid which both exist as neutral species in such environments (242). Because of the competition of iAs^{V} and iAs^{III} with these structurally similar species, plants can be protected from arsenic by using phosphate and silicon supplements, respectively (243).

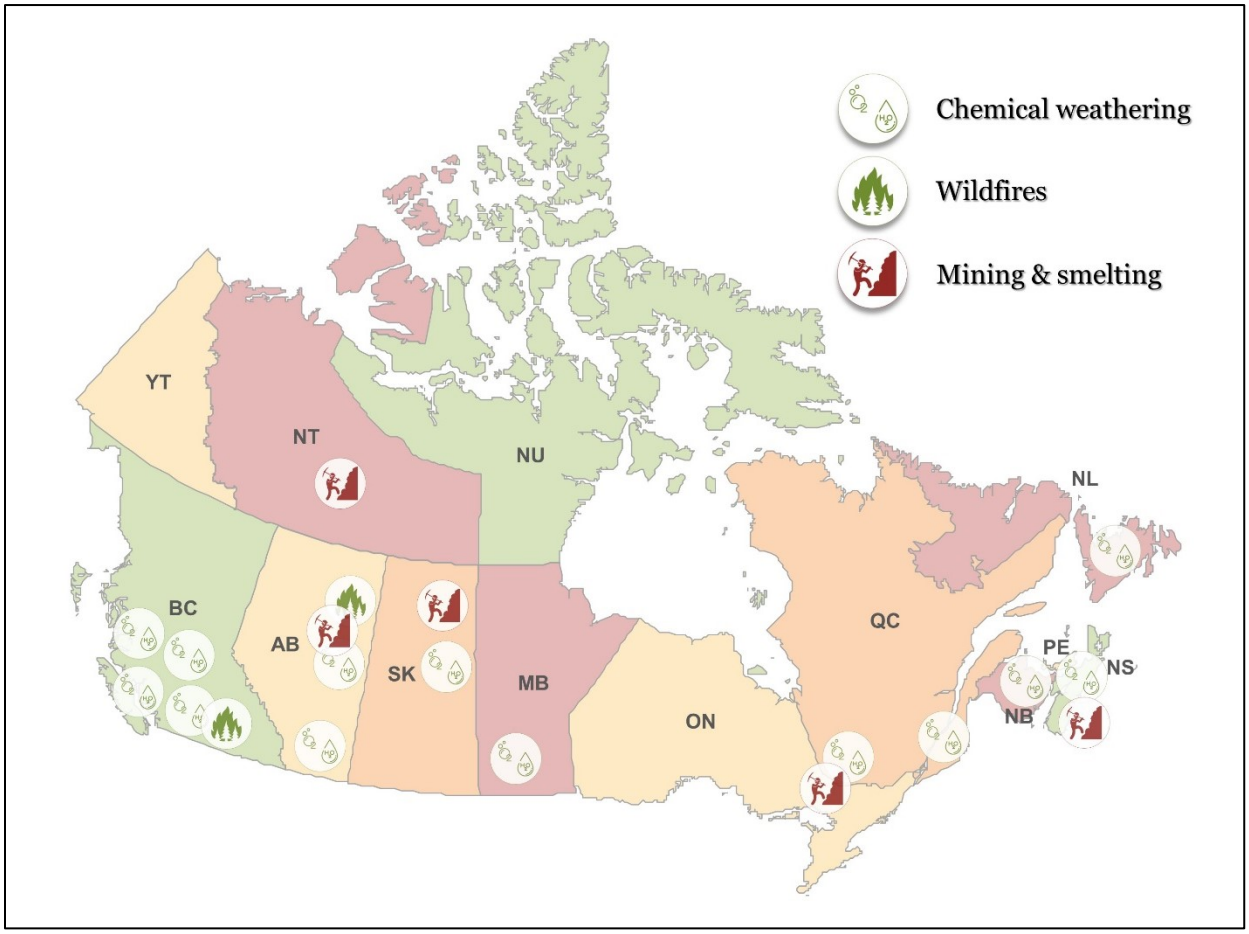

Figure 1.4. Map of Canada showing notable examples of arsenic sources in different provinces and territories.
Natural weathering in specific areas has resulted in hotspots (> 10 µg/L arsenic in water) for arsenic exposure in drinking water. Wildfires such as; 2003 wildfires (Okanagan Mountain Park, BC) and 2016 wildfires (Fort McMurray, AB). Mining & smelting operations in Athabasca oil sands (AB), Giant Mine (Yellowknife, NT), Uranium mine (Rabbit Lake, SK), Silver & cobalt mines (Cobalt town, ON), and Gold mines (NS). **Figure adapted from (14).**

In contaminated environments, the overwhelmingly high arsenic concentrations result in extensive uptake and accumulation in their edible parts. Additionally, while animals can metabolize and excrete excess iAs resulting in low iAs quantities in their food products (217), higher plants have no methylation ability for iAs because of lacking the required genes (244). Therefore, consumption of plant-derived food products, such as fruits and vegetables, may result in exposure to high levels of iAs (217).

Rice is one of the most severely arsenic-affected plants because of its special cultivation method in flooded paddy soils that creates an ideal anaerobic environment for iAs^{III}. Since it requires large amounts of Si for its optimal growth, rice is a very efficient plant in accumulating Si (making up to 10% of the shoot biomass) (245). Subsequently, excessive inadvertent uptake of iAs^{III} takes place, which is then translocated to rice grains resulting in about 10 folds of the iAs accumulated in other grains such as wheat and barley (246). The fact that rice is a globally important food crop and a primary daily source of calories for more than half the world's population, renders it a potential source of human exposure to iAs (247). Additionally, high concentrations of iAs can be also found in rice-based products including baby rice, rice cereals and rice crackers consumed by infants and young children who are especially vulnerable to the adverse health effects (248; 249).

In addition to food products, the presence of arsenic in other plant-based products such as tobacco leaves imply a significant exposure through cigarette smoke (250; 251). Arsenic has been found to act synergistically with other carcinogens in cigarette smoke in the induction of lung cancer (252).

1.1.3.3. Air

A relatively much lower arsenic exposure can result from inhalation of polluted air in which arsenic is mostly present in an inorganic form adsorbed onto particulate matter. This kind of exposure is commonly related to emissions in industrial environments where significant arsenic levels are released to the atmosphere (253). Exposure to volatile arsines may happen especially in the vicinity of their, previously mentioned, releasing sources (254).

In remote areas away from anthropogenic releases, the average atmospheric level of arsenic is 0.02-4 ng/m^3, while in urban areas may reach 200 ng/m^3. Concentrations of several hundred nanograms per cubic meter have been reported in some cities especially in industrially impacted areas (255). In Canada, a significant decline in the levels of major air pollutants, including arsenic, have been observed over the past four decades (256). The mean airborne concentration of arsenic in 11

Canadian cities and one rural site monitored from 1985 to 1990 was 0.001 μg/m^3 (6). According to the Canadian National Air Pollution Surveillance (NAPS) monitoring system, the average concentration of arsenic measured in outdoor air in 2011 was 0.00043 μg/m^3 (257). Much higher arsenic concentrations have been recorded in industrial zones (89).

1.1.3.4. Dermal exposure

Dermal contact is another route of arsenic exposure associated with relatively low risk of poisoning. Exposure may happen through water (258; 259), soil (260), and arsenic-preserved wood structures (261; 262). Individuals suffering from blackfoot disease, a severe vascular disease associated with long-term arsenic exposure via drinking water, usually have concurrent occupational dermal exposure to arsenic-contaminated water and soil through farming, fishery, or salt production (263; 264). Arsenic in soil occurs primarily in inorganic forms (89), and, besides dermal exposure, incidental ingestion can be a significant exposure pathway for soil especially among children while playing (265; 266).

1.2. Cytochrome P450 (CYP) enzymes

Metabolic biotransformation in biological systems aims at maintaining physiological homeostasis by generating energy and building functional and structural molecules (such as proteins and lipids) from consumed food, as well as eliminating catabolic wastes. This process comprises a wide range of enzyme-catalyzed reactions arranged in well-defined metabolic pathways in which a substrate is sequentially converted to the desired end-product. Human body may encounter a non-nutritious foreign substance that is not expected to be naturally present within the system (such as environmental pollutants and drugs), namely a xenobiotic. In this case, the metabolic machinery acts as a defense system that attempts to detoxify the foreign compound by modifying its chemical structure to deactivate it and facilitate its excretion. However, sometimes, xenobiotic metabolism backfires by producing more active intermediates with subsequent detrimental effects. In mammals, different organs (such as lung, kidney, heart, brain, skin, and intestine) contribute to metabolism (including xenobiotic biotransformation) in the body; however, the liver is considered the major contributor through its diverse arsenal of enzymes (267).

Cytochrome P450 (CYP) enzymes constitute a superfamily of heme-containing monooxygenase enzymes, a part of which represents a major class of xenobiotic-metabolizing enzymes involved in the oxidative biotransformation of most drugs and other lipophilic xenobiotics (268). These

enzymes are ubiquitous and have been identified in all kingdoms of life (269). CYP enzymes are prominent metabolic enzymes that are found primarily in hepatic microsomes in addition to other extrahepatic tissues (270). In humans, there are 57 members in CYP superfamily that are grouped into 18 families and 44 subfamilies based on their sequence homology. Most of these enzymes have specific endogenous metabolic functions including the metabolism of fatty acids (such as arachidonic acid), cholesterol, bile-acids, steroid hormones, vitamin D, and others (271). Being physiologically involved in metabolizing endogenous substrates, derangements in CYP function have been implicated in several disease states. In this case, CYP can be reversely exploited as a target for treating such pathological conditions (272-274).

Besides endogenous substrates, members belonging to the CYP1, CYP2, and CYP3 families are collectively involved in the xenobiotic metabolism of the majority of drugs and other foreign chemicals (275). For instance, it is estimated that about 75% of marketed drugs undergo CYP-mediated hepatic elimination, mostly through metabolic pathways involving CYP3A4/5, CYP2C9, CYP2D6, CYP2C19, and CYP1A2 (268; 276). Because of such deep involvement in xenobiotic biotransformation, CYP can significantly modulate the overall body exposure to foreign chemicals through either detoxification or bioactivation. Therefore, CYP enzymes mediating such biotransformation have been widely studied for their toxicological implications (268).

CYP activity may reduce the efficacy and/or toxicity of a drug by accelerating the elimination of its active form. In other circumstances, such metabolic activity may enhance the efficacy or toxicity of a drug by activating its inert prodrug or generating toxic metabolites, respectively (277). Consequently, alteration of CYP activity in relation to certain drug can result in crucial modification in its behavior inside the body and the ultimate outcome of its exposure. That is why induction or inhibition of CYP activity by concomitant medications can result in clinically relevant drug interactions (278), that may necessitate revising and updating safety profiles of pharmaceutical products (279).

The impact of CYP activity, and the possible alteration of such activity, is not limited to drugs but extends to include all foreign chemicals undergoing CYP-mediated biotransformation that may be altered by co-exposure to other xenobiotics capable of modulating CYP metabolizing activity. Environmental contaminants form a major cluster of xenobiotics that are hazardous to humans. Additionally, they may accumulate in the environment, due to their recalcitrant properties and long

degradation periods, thus aggravating their threat to human health (280). Polycyclic aromatic hydrocarbons (PAHs) represent a notable family of these pollutants, which are well-known for their toxic and carcinogenic properties. These compounds are mainly produced in the environment as airborne contaminants resulting from incomplete combustion of organic matter such as fossil fuels (281). Benzo[a]pyrene (B[a]P) is a widely studied member of this family which is a potent lung carcinogen found at high levels in cigarette smoke (282). B[a]P is a procarcinogen whose bioactivation into a mutagenic intermediate is based on its capacity to stimulate its own metabolism. As a PAH, B[a]P induces the production of its metabolizing enzymes, most notably CYP1A1, via activating its master regulator; the aryl hydrocarbon receptor (AHR). Through its diol epoxide metabolite, B[a]P form covalent DNA adducts by interacting with N^2-position of guanine in critical genes such as the p53 tumor suppressor, as commonly seen in lung cancer smokers, resulting in initiation of tumorigenesis (283; 284).

In this case, cancer risk evaluation might be underestimated if based only on the sole exposure to such CYP-dependent carcinogen, because human body is exposed daily to various pollutants and co-exposure to complex mixtures of contaminants is inevitable. These co-contaminants can enhance the bioactivation of other contaminants through manipulating their activating enzymes. These co-contaminants include heavy metals such as arsenic (285). Several epidemiological studies have reported significantly high incidence of lung cancer among cigarette smokers who are concurrently exposed to arsenic (252; 286-291). Studies on animals have also revealed that tumorigenic potential of B[a]P in the respiratory tract can be significantly enhanced by arsenic co-exposure (292; 293). Considering that arsenic is a well-established carcinogen (294), the potentiated B[a]P effect may be regarded as synergistic co-carcinogenesis caused by both of them as shown by rat lung cell transformation rate that has increased beyond 500- and 200-folds compared with arsenic alone or B[a]P alone, respectively (295). It has been also reported that arsenic enhances the benzo[a]pyrene diol epoxide (BPDE)-DNA adduct-induced mutagenesis in the lung (296; 297). Interestingly, CYP1A1, the key activator of B[a]P, was found to be induced in the lung by arsenic exposure at the levels of mRNA, protein, and/or catalytic activity in both *in vivo* and *in vitro* studies (218; 298-303). Although some studies do not support this effect (298; 302; 304; 305), arsenic-mediated positive modulation of CYP1A1 remains a potential clue to the high incidence of lung cancer among cigarette smokers.

When it comes to endogenous substrates, the alteration in CYP activity can inevitably result in physiologic perturbations that entail toxic manifestations. Generally, studies of CYP modulation focus mainly on their involvement in xenobiotic metabolic transformations, especially those with ensuing drug interactions, with relatively smaller interest in the CYP-mediated endobiotic metabolism alteration. The metabolism of arachidonic acid (AA), a polyunsaturated omega-6 fatty acid, leads to the production of bioactive lipid mediators, called eicosanoids, that have physiological functions as well as significant roles in the pathophysiological progression or regression of multiple ailments such as liver diseases (306).

Aside from the cyclooxygenases and lipoxygenases pathways, CYP enzymes catalyze the third major eicosanoids-generating pathway that produces two main families of AA metabolites, the CYP epoxygenases-derived epoxyeicosatrienoic and dihydroxyeicosatrienoic acids (EETs + DHETs) and the CYP ω-hydroxylases-derived hydroxyeicosatetraenoic acids (HETEs). Of note, some CYP isoforms function as both epoxygenases and hydroxylases (307). Additionally, lipoxygenases also contribute to the production of some HETEs (306). Depending on the stereochemistry of the epoxygenation or hydroxylation reaction, different stereoisomers of each EET or HETE is obtained, respectively, where each isomer may have distinct biological activity (308; 309). According to the way of epoxide function group insertion, each of the EETs regioisomers (5,6-, 8,9-, 11,12-, and 14,15-EET) can have one of two isomeric forms, either R,S or S,R (310). For the HETEs, hydroxylation creates a chiral center, thus forming R and S enantiomers, in the midchain (5-, 8-, 9-, 11-, 12-, and 15-HETE) and subterminal (16-, 17-, 18-, and 19-HETE) metabolites, but not in the terminal 20-HETE (311).

These eicosanoids are currently under investigations for being involved in different pathologies such as metabolic (312; 313), immune (314; 315), inflammatory (316), pulmonary (317; 318), hepatic (306; 319), renal (320), and cardiovascular (321; 322) diseases as well as cancer (309; 323). While these studies have reported how hepatic and extra-hepatic AA metabolism, especially the CYP-mediated pathway, is modulated in various pathological conditions, only few studies have examined the effect of arsenicals exposure on such metabolism which may be a key for understanding arsenic-related adverse events.

1.3. Aryl hydrocarbon receptor (AHR) and CYP regulation

The expression of different CYP isoforms is subject to the control of an intricate network of various transcription factors (275; 324), one of which is the AHR which has gained its importance from the significant clinical impacts of its associated CYP enzymes.

AHR is a ligand-activated bHLH/Per-ARNT-Sim transcription factor which is retained in the cytoplasm as an inactive complex with a dimer of the chaperone heat shock protein 90 (HSP90), the co-chaperone prostaglandin E synthase 3 (p23), and a molecule of hepatitis B Virus X-associated protein 2 (XAP-2) (Figure 1.5). Upon binding to one of its agonists, such as PAHs or halogenated aromatic hydrocarbons (HAHs), AHR molecule undergoes a conformational change exposing its nuclear localization sequence (NLS). Eventually, the activated AHR translocates into the nucleus where it dissociates from its cytoplasmic complex and dimerizes with the aryl hydrocarbon receptor nuclear translocator (ARNT) to form a heterodimer that binds to the xenobiotic response element (XRE), also known as dioxin response element (DRE), found in the promoter regions of AHR-regulated genes (325-327).

The name of AHR was originally based on the assumption that it functions primarily as a sensor for xenobiotic chemicals, the most notable of which are aromatic (aryl) hydrocarbons such as PAHs (e.g. benzo[a]pyrene, 3-methylcholanthrene, and beta-naphthoflavone) and HAHs (e.g. 2,3,7,8-tetrachlorodibenzo-*p*-dioxin). However, extensive studying of the AHR has revealed its promiscuous ligand specificity that allows binding to a large number of structurally diverse chemicals. Besides PAHs and HAHs, some natural exogenous compounds such as flavonoids (e.g. quercetin, kaempferol (328), and resveratrol (329)) and indoles (e.g. indole-3-carbinol (330)) have been found to act as AHR ligands. Additionally, several endogenously formed molecules have been identified as AHR ligands, such as the indole amino acid (tryptophan) and its catabolites (e.g. tryptamine, indole acetic acid (331; 332), and kynurenic acid (333)), as well as other indoles (e.g. indirubin and indigo) (334). Other endogenous ligands include tetrapyrroles (e.g. bilirubin (335) and biliverdin (336)) and arachidonic acid metabolites (e.g. lipoxin A4 (337) and some prostaglandins (338)).

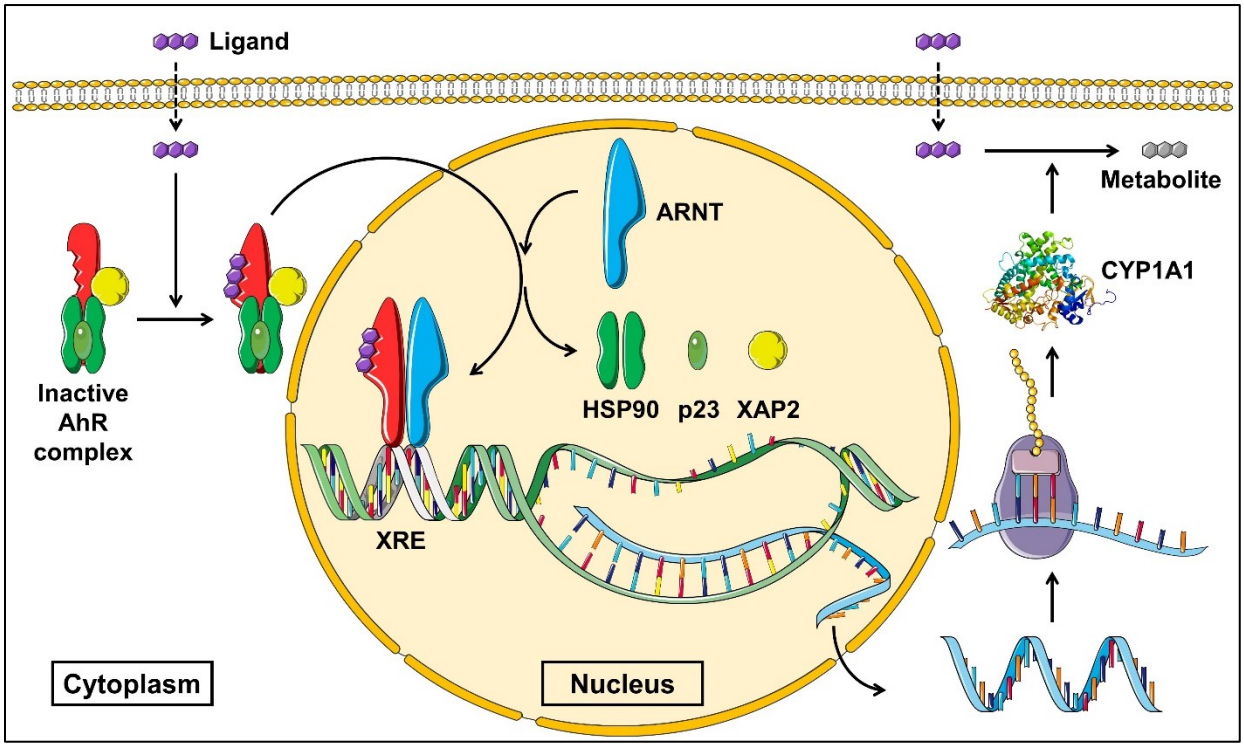

Figure 1.5. AHR signaling pathway.
The unliganded AHR resides in the cytoplasm, complexed with a dimer of the chaperone heat shock protein 90 (HSP90), the co-chaperone prostaglandin E synthase 3 (p23), and a molecule of hepatitis B Virus X-associated protein 2 (XAP-2). Ligand-mediated activation of the AHR results in its nuclear translocation where it dissociates from its complex and forms a heterodimer with the aryl hydrocarbon receptor nuclear translocator (ARNT) that binds to the xenobiotic response element (XRE) found in the promoter regions of AHR-regulated genes such as CYP1A1. **Figure adapted from (14).**

AHR is a gene battery that regulates a group of phase I as well as phase II enzymes (285). The expression of CYP1A1, CYP1A2, CYP1B1, and CYP2S1 genes, which represent phase I group, is regulated by AHR response elements found in their promoters, therefore they are highly inducible by AHR ligands (339-342). In humans, CYP1A1, CYP1A2, and CYP1B1 are constitutively expressed in the liver; however, only CYP1A2 is detected at much higher levels. CYP1A1 and CYP1B1 are primarily extrahepatic enzymes and their hepatic levels are very low or undetectable (275). Human CYP2S1 levels are generally low across the different organs in the body (including the liver) (343). AHR-regulated CYP1A1, 1A2, and 1B1 have gained significant attention because of their ability to activate the procarcinogenic AHR ligands (344; 345).

1.4. Modulation of CYP enzymatic machinery by arsenic

1.4.1. Alteration of CYP expression in human experimental models

For years, different arsenic species have been studied for their modulatory effects on different CYP enzymes, and have shown species-, tissue-, and/or enzyme-specific effects. Identifying these effects is highly important in understanding how these compounds affect different tissues in the human body, and this can be exploited in either establishing preventive measures for arsenic toxicity or developing therapeutic strategies for treating certain diseases. Arsenic-mediated alteration of the CYP enzymes has been reported at multiple levels of their expression including mRNA, protein, and catalytic activity. Some studies have also investigated the influence of arsenic on the transcriptional regulators of these enzymes. These CYP-regulating transcription factors act downstream of signaling cascades related to biological/environmental stimuli.

Experimental animal models represent a major avenue of research, especially in the field of toxicology, where using human subjects is, obviously, impossible. However, extrapolating experimental data from animals to humans can be very complex and may result in poor prediction of human reactions to different xenobiotics. That is why bridging studies using human *in vitro* models constitute an indispensable tool for elucidating human responses (346). For instance, difference in metabolic behavior, resulting from species-specific enzyme expression or activity, is a hallmark of inter-species variability in xenobiotic handling that eventually complicates the translation of exposure outcomes in animals to humans (347). Being at the core of the metabolic system, CYP enzymes are no exception. Species-related disparity in catalytic activity/specificity of some CYP isoforms may produce different induction/inhibition patterns for the enzymes.

Additionally, inter-species differences can also originate from varying expression of specific isoforms among species (348). Accurate prediction of human metabolic response can be achieved by using human-based *in vitro* models, especially for the liver which is the major metabolic organ, such as cellular systems (e.g. primary liver cells and derived cell lines), as well as enzymes preparations (e.g. tissue homogenates, subcellular fractions, and purified enzymes) (346; 349; 350). Because of the reliable *in vitro-in vivo* correlation provided by these human *in vitro* models, FDA can waive clinical drug-drug interaction studies when a drug candidate is tested negative in human *in vitro* CYP induction studies (350).

Throughout reviewing the literature, we have come across a plethora of studies investigating arsenic-related effects on different members of CYP superfamily using various animal models, but here we shed light on studies based on human *in vitro* models (Table 1.1). These studies should, to a great extent, depict what would happen inside the human body upon exposure to this toxicant.

The most commonly used experimental model in these studies was liver cells especially human hepatoma (HepG2) cells and primary human hepatocytes. Out of all arsenic species, the trivalent inorganic arsenite has drawn most attention from researchers who assessed its effect specifically on AHR-regulated CYP1 family as well as pregnane X receptor (PXR)-regulated CYP3A4.

In liver cells, inorganic arsenic species and organoarsenicals have opposite effects on CYP1A1 mRNA and protein levels. On one hand; arsenite (351) and ATO^{III} (352) cause reduction in CYP1A1 mRNA transcripts and protein produced constitutively and/or induced by well-known inducers as TCDD (2,3,7,8-tetrachlorodibenzo-*p*-dioxin), B[k]F (Benzo[k]fluoranthene), and 3-MC (3-methylcholanthrene), but on the other hand; monomethylarsonic acid, dimethylarsinic acid, and trimethylarsine oxide (353) cause significant increase at both mRNA and protein levels. Interestingly, monomethylarsonous acid is the only organic species which has effects matching these of arsenite and ATO^{III} (351).

Actinomycin D chase studies assessing CYP1A1 mRNA stability have revealed no effect exerted by either arsenite (354) or monomethylarsonous acid (351). However, monomethylarsonous acid, but not arsenite, decreases the protein stability of CYP1A1 as shown by cycloheximide chase experiments (351).

The effect of the mentioned arsenicals on EROD (7-ethoxyresorufin O-deethylation) activity of CYP1A1 follows the same pattern as what has been observed with mRNA and protein. Additionally, incubation of arsenite with human recombinant CYP1A1 (supersomes) results in a significant decrease in its 17β-estradiol 2-hydroxylation activity (355). Also, monomethylarsonous acid has a direct inhibitory effect on EROD activity of TCDD-induced CYP1A1 (351).

Arsenite has organ-specific effects on CYP1A1 as shown from studies on the cells derived from extrahepatic tissues. For instance, arsenite potentiates CYP1A1 mRNA basal level in human lung adenocarcinoma (H1355) cells (300), but has no effect on its basal or inducible protein levels in human lung adenocarcinoma (CL3) cells (305). In human breast cancer (T-47D) cells, arsenite doesn't alter B[a]P-induced CYP1A1 mRNA but causes significant reduction in its inducible protein levels as well as 17β-estradiol 2-hydroxylation activity (355; 356).

Because of being subjected to the same transcriptional regulation via AHR, it is not surprising that CYP1A2 is similarly affected by arsenicals as CYP1A1. Arsenite causes significant reduction in inducible CYP1A2 mRNA, protein, as well as EROD (357) and MROD (7-methoxyresorufin O-demethylation) (354) activities. Besides decreasing the inducible level of CYP1A protein, monomethylarsonous acid reduces its stability as well (351). CYP1B1 is another AHR-regulated enzyme whose basal protein level, in human breast epithelial (MCF10A) cells (358), and induced 17β-estradiol 4-hydroxylation activity, in T-47D cells (355), significantly decrease in response to ATO^{III} and arsenite treatments, respectively. Also, incubation of arsenite with human recombinant CYP1B1 (supersomes) causes significant reduction in its 17β-estradiol 4-hydroxylation activity (355).

The above-mentioned findings about CYP1A1, CYP1A2, and CYP1B1 have been further elucidated by studies investigating their upstream transcriptional control by the AHR. Immunocytochemical analysis of AHR localization have revealed significant reduction in TCDD-stimulated nuclear localization of the AHR in HepG2 cells co-treated with either arsenite or monomethylarsonous acid (351). On the other hand, the methylated arsenicals; monomethylarsonic acid, dimethylarsinic acid, and trimethylarsine oxide cause significant increase in AHR nuclear accumulation (353). AHR transcriptional activity has been assessed through luciferase-based reporter assays. HepG2 cells and human hepatoma (Hep3B) cells transfected with reporter constructs, carrying CYP1A1 gene promoter sequence located upstream of the firefly luciferase

reporter gene, have shown AHR-dependent induction of firefly luciferase activity (normalized using *Renilla* luciferase activity in a dual-luciferase reporter assay) after being treated with B[k]F and 3-MC, respectively. However, arsenite (359) and ATO^{III} (352) significantly decrease B[k]F and 3-MC-induced activity, respectively. Arsenite and monomethylarsonous acid (351), but not ATO^{III} (352), reduce both basal and inducible AHR-dependent XRE-driven firefly luciferase reporter activity. In case of monomethylarsonic acid, dimethylarsinic acid, and trimethylarsine oxide; an opposite effect on XRE-mediated luciferase activity has been observed in both absence and presence of TCDD (353).

H1355 cells transfected with XRE-luciferase genetic construct have shown significant increase in reporter activity in response to arsenite treatment, i.e., opposing its effect in liver cells (300). Also, contrary to what has been observed with inorganic arsenic species, Tully *et al.* have reported that arsenate causes increase in AHR-dependent reporter signal (360). This study used CAT-Tox (L)iver assay system which is a recombinant cell line derived from HepG2 cells and contains either CYP1A1 gene promoter or XRE fused to the chloramphenicol acetyl transferase (CAT) reporter gene (361).

Table 1.1. The effect of different arsenic species on the expression of different CYP enzymes in human experimental models.

CYP	LEVEL	EFFECT	EXPERIMENTAL MODEL	REFERENCE
ARSENITE				
CYP1A1	mRNA	↔ CYP1A1 mRNA	Human hepatoma (HepG2) cells	(359)
		↓ CYP1A1 mRNA	Human hepatoma (HepG2) cells	(351)
		↑ CYP1A1 mRNA (concentration- and time-dependent effect)	Human lung adenocarcinoma (H1355) cells	(300)
		↔ CYP1A1 mRNA stability	Human hepatoma (HepG2) cells	(359)
		↓ CYP1A1 mRNA induced by TCDD (concentration- and time-dependent effect)	Human hepatoma (HepG2) cells	(351; 354; 362)

		↔ CYP1A1 mRNA induced by TCDD stability	Human hepatoma (HepG2) cells	(351; 354)
		↔ CYP1A1 mRNA induced by B[k]F	Human hepatocytes, human hepatoma (HepG2) cells	(357; 363)
		↓ CYP1A1 mRNA induced by B[k]F	Human hepatoma (HepG2) cells	(359)
		↔ CYP1A1 mRNA induced by B[k]F stability	Human hepatoma (HepG2) cells	(359)
		↔ CYP1A1 mRNA induced by B[a]P	Human breast cancer (T-47D) cells	(355; 356)
	Protein	↓ CYP1A protein	Human hepatoma (HepG2) cells	(351)
		↔ CYP1A1 protein	Human lung adenocarcinoma (CL3) cells	(305)
		↓ CYP1A protein induced by TCDD	Human hepatoma (HepG2) cells	(351)
		↓ CYP1A1 protein induced by TCDD (concentration-dependent effect)	Human hepatoma (HepG2) cells	(354; 362)
		↔ CYP1A protein induced by TCDD stability	Human hepatoma (HepG2) cells	(351)
		↓ CYP1A1 protein induced by B[k]F (concentration-dependent effect)	Human hepatocytes, human hepatoma (HepG2) cells	(357; 363; 364)
		↔ CYP1A1 protein induced by B[a]P	Human lung adenocarcinoma (CL3) cells	(305)
		↓ CYP1A1 protein induced by B[a]P	Human breast cancer (T-47D) cells	(355; 356)
	Activity	↔ CYP1A1 (EROD) activity	Human hepatoma (HepG2) cells, human hepatoma (Huh7) cells	(364; 365)
		↓ CYP1A1 (EROD) activity	Human hepatoma (HepG2) cells	(351)
		↓ CYP1A1 (17β-estradiol 2-hydroxylation) activity	CYP1A1 supersomes	(355)
		↓ CYP1A1 (EROD) activity induced by	Human hepatoma (HepG2) cells,	(351; 354; 362; 365)

		TCDD (concentration-dependent effect)	human hepatoma (Huh7) cells	
		↓ CYP1A1 (17β-estradiol 2-hydroxylation) activity induced by TCDD (in enzyme induction phase)	Human breast cancer (T-47D) cells	(355; 356)
		↔ CYP1A1 (17β-estradiol 2-hydroxylation) activity induced by TCDD (in metabolism phase)	Human breast cancer (T-47D) cells	(355; 356)
		↔ CYP1A1 (EROD) activity induced by TCDD (direct effect)	Human hepatoma (HepG2) cells	(351)
		↓ CYP1A1 (EROD) activity induced by B[k]F	Human hepatocytes, human hepatoma (HepG2) cells	(357; 363; 364)
		↓ CYP1A1 (EROD) activity induced by B[a]P	Human hepatocytes, human hepatoma (HepG2) cells	(357; 363)
		↓ CYP1A1 (17β-estradiol 2-hydroxylation) activity induced by B[a]P (concentration-dependent effect)	Human breast cancer (T-47D) cells	(355; 356)
		↓ CYP1A1 (EROD) activity induced by B[a]A	Human hepatocytes, human hepatoma (HepG2) cells	(357; 363)
		↓ CYP1A1 (EROD) activity induced by B[b]F	Human hepatocytes, human hepatoma (HepG2) cells	(357; 363)
		↓ CYP1A1 (EROD) activity induced by DB[ah]A	Human hepatocytes, human hepatoma (HepG2) cells	(357; 363)
CYP1A2	mRNA	↓ CYP1A2 mRNA induced by B[k]F	Human hepatocytes	(357)
	Protein	↓ CYP1A protein	Human hepatoma (HepG2) cells	(351)
		↓ CYP1A protein induced by TCDD	Human hepatoma (HepG2) cells	(351)
		↔ CYP1A protein induced by TCDD stability	Human hepatoma (HepG2) cells	(351)
		↓ CYP1A2 protein induced by B[k]F	Human hepatocytes	(357)

		(concentration-dependent effect)		
	Activity	↓ CYP1A2 (MROD) activity induced by TCDD	Human hepatoma (HepG2) cells	(354)
		↓ CYP1A2 (EROD) activity induced by B[k]F	Human hepatocytes	(357)
		↓ CYP1A2 (EROD) activity induced by B[a]P	Human hepatocytes	(357)
		↓ CYP1A2 (EROD) activity induced by B[a]A	Human hepatocytes	(357)
		↓ CYP1A2 (EROD) activity induced by B[b]F	Human hepatocytes	(357)
		↓ CYP1A2 (EROD) activity induced by DB[ah]A	Human hepatocytes	(357)
CYP1B1	mRNA	↔ CYP1B1 mRNA induced by B[a]P	Human breast cancer (T-47D) cells	(355; 356)
	Activity	↓ CYP1B1 (17β-estradiol 4-hydroxylation) activity	CYP1B1 supersomes	(355)
		↓ CYP1B1 (17β-estradiol 4-hydroxylation) activity induced by TCDD (in enzyme induction phase)	Human breast cancer (T-47D) cells	(355; 356)
		↔ CYP1B1 (17β-estradiol 4-hydroxylation) activity induced by TCDD (in metabolism phase)	Human breast cancer (T-47D) cells	(355; 356)
		↓ CYP1B1 (17β-estradiol 4-hydroxylation) activity induced by B[a]P (concentration-dependent effect)	Human breast cancer (T-47D) cells	(355; 356)
CYP3A4	mRNA	↓ CYP3A4 mRNA (concentration-dependent effect)	Human hepatocytes	(366; 367)
		↓ CYP3A4 mRNA induced by rifampicin (concentration-dependent effect)	Human hepatocytes	(366; 367)
		↓ CYP3A4 mRNA induced by PB	Human hepatocytes	(366)
	Protein	↓ CYP3A4 protein	Human hepatocytes	(366)
		↓ CYP3A4 protein induced by rifampicin	Human hepatocytes	(366)

		↓ CYP3A4 protein induced by PB	Human hepatocytes	(366)
	Activity	↓ CYP3A4 (testosterone 6β-hydroxylation) activity	Human hepatocytes	(366)
		↓ CYP3A4 (testosterone 6β-hydroxylation) activity induced by rifampicin	Human hepatocytes	(366)
		↓ CYP3A4 (testosterone 6β-hydroxylation) activity induced by PB	Human hepatocytes	(366)
---	---	↔ AHR mRNA	Human lung adenocarcinoma (H1355) cells	(300)
		↔ AHR nuclear accumulation	Human hepatoma (HepG2) cells	(351)
		↔ AHR nuclear accumulation induced by TCDD	Human hepatoma (HepG2) cells	(362)
		↓ AHR nuclear accumulation induced by TCDD	Human hepatoma (HepG2) cells	(351)
		↔ AHR-dependent CYP1A1-luciferase activity induced by TCDD	Human hepatoma (HepG2) cells	(362)
		↓ AHR-dependent CYP1A1-luciferase activity induced by B[k]F	Human hepatoma (HepG2) cells	(359)
		↔ AHR-dependent XRE-luciferase activity	Human hepatoma (HepG2) cells	(359)
		↓ AHR-dependent XRE-luciferase activity	Human hepatoma (HepG2) cells	(351; 354)
		↑ AHR-dependent XRE-luciferase activity (time-dependent effect)	Human lung adenocarcinoma (H1355) cells	(300)
		↓ AHR-dependent XRE-luciferase activity induced by TCDD (concentration-dependent effect)	Human hepatoma (HepG2) cells, human hepatoma (Huh7) cells	(351; 354; 365)
		↔ AHR-dependent XRE-luciferase activity induced by B[k]F	Human hepatoma (HepG2) cells	(359)

		↔ PXR mRNA induced by rifampicin	Human hepatocytes	(366)
		↔ PXR protein	Human hepatocytes	(366)
		↔ PXR protein induced by rifampicin	Human hepatocytes	(366)
		↓ Ectopic human PXR-dependent rat CYP3A23-luciferase activity induced by rifampicin	Human hepatoma (HepG2) cells	(367)
		↓ RXRα mRNA	Human hepatocytes	(366)
		↓ RXRα mRNA induced by rifampicin	Human hepatocytes	(366)
		↓ RXRα protein	Human hepatocytes	(366)
		↓ RXRα protein induced by rifampicin	Human hepatocytes	(366)
		↓ Ectopic human RXRα-dependent mouse RARE-luciferase activity induced by 9cRA	Human hepatoma (HepG2) cells	(367)
		↔ Sp1 mRNA induced by rifampicin	Human hepatocytes	(366)
		↔ Sp1 protein induced by rifampicin	Human hepatocytes	(366)
ARSENIC TRIOXIDE				
CYP1A1	mRNA	↓ CYP1A1 mRNA induced by 3-MC (concentration-dependent effect)	Human hepatoma (Hep3B) cells	(352)
	Protein	↓ CYP1A1 protein induced by 3-MC (concentration-dependent effect)	Human hepatoma (Hep3B) cells	(352)
	Activity	↓ CYP1A1 (EROD) activity induced by TCDD (concentration-dependent effect)	Human hepatoma (Hep3B) cells	(352)
		↓ CYP1A1 (EROD) activity induced by 3-MC (concentration-dependent effect)	Human hepatocytes, human hepatoma (HepG2) cells, human hepatoma (Hep3B) cells	(352)
		↔ CYP1A1 (EROD) activity induced by 3-MC (direct effect)	Human hepatoma (Hep3B) cells	(352)
		↓ CYP1A1 (EROD) activity induced by B[a]P	Human hepatoma (Hep3B) cells	(352)

		(concentration-dependent effect)		
CYP1A2	Activity	↔ CYP1A2 (EROD) activity	Human hepatocytes	(352)
CYP1B1	Protein	↓ CYP1B1 protein (concentration-dependent effect)	Human breast epithelial (MCF10A) cells	(358)
---	---	↔ AHR-dependent CYP1A1-luciferase activity	Human hepatoma (Hep3B) cells	(352)
		↓ AHR-dependent CYP1A1-luciferase activity induced by 3-MC (concentration-dependent effect)	Human hepatoma (Hep3B) cells	(352)
		↔ AHR-dependent XRE-luciferase activity	Human hepatoma (Hep3B) cells	(352)
		↔ AHR-dependent XRE-luciferase activity induced by 3-MC	Human hepatoma (Hep3B) cells	(352)
ARSENATE				
---	---	↑ AHR-dependent CYP1A1-CAT expression (concentration-dependent effect)	Human hepatoma (HepG2) cells (CAT-Tox (L)iver assay system)	(360)
		↑ AHR-dependent XRE-CAT expression (concentration-dependent effect)	Human hepatoma (HepG2) cells (CAT-Tox (L)iver assay system)	(360)
MONOMETHYLARSONOUS ACID				
CYP1A1	mRNA	↓ CYP1A1 mRNA (concentration-dependent effect)	Human hepatoma (HepG2) cells	(351)
		↓ CYP1A1 mRNA induced by TCDD (concentration- and time-dependent effect)	Human hepatoma (HepG2) cells	(351)
		↔ CYP1A1 mRNA induced by TCDD stability	Human hepatoma (HepG2) cells	(351)
	Protein	↓ CYP1A protein (concentration-dependent effect)	Human hepatoma (HepG2) cells	(351)
		↓ CYP1A protein induced by TCDD (concentration-dependent effect)	Human hepatoma (HepG2) cells	(351)

		↓ CYP1A protein induced by TCDD stability	Human hepatoma (HepG2) cells	(351)
	Activity	↓ CYP1A1 (EROD) activity	Human hepatoma (HepG2) cells	(351)
		↓ CYP1A1 (EROD) activity induced by TCDD (concentration-dependent effect)	Human hepatoma (HepG2) cells	(351)
		↓ CYP1A1 (EROD) activity induced by TCDD (concentration-dependent direct effect)	Human hepatoma (HepG2) cells	(351)
CYP1A2	Protein	↓ CYP1A protein (concentration-dependent effect)	Human hepatoma (HepG2) cells	(351)
		↓ CYP1A protein induced by TCDD (concentration-dependent effect)	Human hepatoma (HepG2) cells	(351)
		↓ CYP1A protein induced by TCDD stability	Human hepatoma (HepG2) cells	(351)
---	---	↔ AHR nuclear accumulation	Human hepatoma (HepG2) cells	(351)
		↓ AHR nuclear accumulation induced by TCDD	Human hepatoma (HepG2) cells	(351)
		↓ AHR-dependent XRE-luciferase activity	Human hepatoma (HepG2) cells	(351)
		↓ AHR-dependent XRE-luciferase activity induced by TCDD	Human hepatoma (HepG2) cells	(351)
MONOMETHYLARSONIC ACID				
CYP1A1	mRNA	↑ CYP1A1 mRNA	Human hepatoma (HepG2) cells	(353)
		↑ CYP1A1 mRNA induced by TCDD	Human hepatoma (HepG2) cells	(353)
	Protein	↑ CYP1A1 protein	Human hepatoma (HepG2) cells	(353)
		↑ CYP1A1 protein induced by TCDD	Human hepatoma (HepG2) cells	(353)
	Activity	↑ CYP1A1 (EROD) activity	Human hepatoma (HepG2) cells	(353)
		↑ CYP1A1 (EROD) activity induced by TCDD	Human hepatoma (HepG2) cells	(353)
---	---	↓ AHR protein stability	Human hepatoma (HepG2) cells	(353)

		↑ AHR nuclear accumulation	Human hepatoma (HepG2) cells	(353)
		↑ AHR-dependent XRE-luciferase activity	Human hepatoma (HepG2) cells	(353)
		↑ AHR-dependent XRE-luciferase activity induced by TCDD	Human hepatoma (HepG2) cells	(353)
DIMETHYLARSINIC ACID				
CYP1A1	mRNA	↑ CYP1A1 mRNA	Human hepatoma (HepG2) cells	(353)
		↑ CYP1A1 mRNA induced by TCDD	Human hepatoma (HepG2) cells	(353)
	Protein	↑ CYP1A1 protein	Human hepatoma (HepG2) cells	(353)
		↑ CYP1A1 protein induced by TCDD	Human hepatoma (HepG2) cells	(353)
	Activity	↑ CYP1A1 (EROD) activity	Human hepatoma (HepG2) cells	(353)
		↑ CYP1A1 (EROD) activity induced by TCDD	Human hepatoma (HepG2) cells	(353)
---	---	↓ AHR protein stability	Human hepatoma (HepG2) cells	(353)
		↑ AHR nuclear accumulation	Human hepatoma (HepG2) cells	(353)
		↑ AHR-dependent XRE-luciferase activity	Human hepatoma (HepG2) cells	(353)
		↑ AHR-dependent XRE-luciferase activity induced by TCDD	Human hepatoma (HepG2) cells	(353)
TRIMETHYLARSINE OXIDE				
CYP1A1	mRNA	↑ CYP1A1 mRNA	Human hepatoma (HepG2) cells	(353)
		↑ CYP1A1 mRNA induced by TCDD	Human hepatoma (HepG2) cells	(353)
	Protein	↑ CYP1A1 protein	Human hepatoma (HepG2) cells	(353)
		↑ CYP1A1 protein induced by TCDD	Human hepatoma (HepG2) cells	(353)
	Activity	↑ CYP1A1 (EROD) activity	Human hepatoma (HepG2) cells	(353)
		↑ CYP1A1 (EROD) activity induced by TCDD	Human hepatoma (HepG2) cells	(353)
---	---	↓ AHR protein stability	Human hepatoma (HepG2) cells	(353)

		↑ AHR nuclear accumulation	Human hepatoma (HepG2) cells	(353)
		↑ AHR-dependent XRE-luciferase activity	Human hepatoma (HepG2) cells	(353)
		↑ AHR-dependent XRE-luciferase activity induced by TCDD	Human hepatoma (HepG2) cells	(353)

1.4.2. Alteration of CYP expression in non-human experimental models

1.4.2.1. The effect of arsenite on the expression of CYP enzymes in different species

1.4.2.1.1. CYP1 family

As shown in (Table 1.2), iAs^{III} differentially modulates both constitutive and inducible expressions of CYP enzymes in a species-, tissue-, time-, and enzyme-specific manner. In general, iAs^{III} down-regulates both basal and inducible levels of total CYP content in different tissues in mouse, rat, and guinea pig (298; 299; 304; 368-375). Additionally, total CYP enzyme activity; measured by different assays, such as aminopyrine N-demethylation (ANDM), 7-ethoxycoumarin O-deethylation (ECOD), 7-ethoxyresorufin O-deethylation (EROD), benzphetamine N-demethylation (BZND), and 7-pentoxyresorufin O-dealkylation (PROD); has been also reported to decrease in the liver of Wistar albino rats (371; 375).

Regarding CYP1A1, several studies have shown that iAs^{III} increases basal CYP1A1 mRNA level in both *in vivo* and *in vitro* models, such as mouse lung and mouse hepatoma (Hepa1c1c7) cells, respectively (Table 1.3). This has been attributed to iAs^{III} ability to enhance AHR nuclear recruitment, and increase AHR binding to its regulatory element, the xenobiotic response element (XRE), with subsequent increase in XRE activation as demonstrated by the luciferase reporter gene activity in Hepa1c1c7 cells (376; 377).

On the contrary, iAs^{III} treatment significantly decreased the constitutive CYP1A1 mRNA in the brain of C57BL/6 mice and liver of common carp. Moreover, iAs^{III} decreased the catalytic activity of hepatic, pulmonary, and renal CYP1A1 in C57BL/6 mice (301; 304; 378).

Several AHR activators such as 3-MC, beta-naphthoflavone (βNF), B[a]P) and TCDD have been employed in the studies investigating the effect of iAs^{III} on the inducible CYP1A1 expression. Using Hepa1c1c7 cells, iAs^{III} significantly potentiated 3-MC-, βNF-, B[a]P-, and TCDD-mediated induction of CYP1A1 mRNA, and such effect was inverted into a significant decrease in the

catalytic activity. Interestingly, there was no change at protein level for the aforementioned inducers except for a significant increase in case of βNF (376; 377; 379-381). In C57BL/6 mouse primary hepatocytes, iAs^{III} significantly reduced TCDD inducible CYP1A1 mRNA and activity (380).

In vivo experiments, using C57BL/6 mice, have shown that iAs^{III} significantly increases (24 h exposure) hepatic and extrahepatic CYP1A1 mRNA induced by TCDD after an initial decrease (6 h exposure), with no effect on its protein expression. Interestingly, the TCDD inducible CYP1A1 activity was increased in all investigated organs except the kidney, in which it was decreased. At transcriptional level, iAs^{III} down-regulated the TCDD-induced AHR-dependent XRE-luciferase activity in mouse hepatocytes (Table 1.4) (301; 380; 381).

Anwar-Mohamed *et al.* have justified the difference between 6 h and 24 h responses to iAs^{III} and TCDD co-treatment at mRNA level by the direct effect of non-metabolized iAs^{III} in the form of sodium arsenite at 6 h treatment whereas the effect after 24 h is believed to be an indirect effect that may be due to metabolic and other kinetic factors (380).

In Sprague-Dawley rats, iAs^{III} increased basal CYP1A1 mRNA and protein levels in lung tissue (299), while decreased the 3-MC inducible CYP1A1 mRNA and protein content in Fischer 344 rat hepatocytes (382). Both constitutive and inducible activities of CYP1A1 have been reported to decrease by iAs^{III} with the exception of the basal pulmonary CYP1A1 activity in Sprague-Dawley rats (299; 303; 372; 383). In Hartley guinea pig, both basal and βNF-induced CYP1A1 activities have been decreased in all organs by iAs^{III} except the lung (298).

Similar to CYP1A1, iAs^{III} has differential effect on CYP1A2 mRNA, protein and activity. It has been found that iAs^{III} decreases basal mRNA in the liver of C3H mice and brain of C57BL/6 mice (384; 385). Additionally, it inhibited TCDD- mediated induction of hepatic, renal, and cardiac CYP1A2 mRNA in C57BL/6 mice after 6 h treatment. Interestingly, after 24 h treatment, iAs^{III} enhanced TCDD-mediated induction of CYP1A2 mRNA in the kidney, but not the liver, lung, or heart (301; 380). Of note, the reduction seen at the level of mRNA was accompanied by subsequent decrease in CYP1A2 catalytic activity in C57BL/6 mouse kidney, and Hepa1c1c7 cells. Interestingly, iAs^{III} potentiated both basal and TCDD-mediated induction of activity in C57BL/6 mouse lung (301; 304; 379; 380). In rat models, significant decrease was observed in CYP1A2 catalytic activity, *in vivo* and *in vitro* (299; 383).

Table 1.2. The effect of arsenite on the expression of total CYP enzymes in different species.

SPECIES	LEVEL	EFFECT	EXPERIMENTAL MODEL	REFERENCE
ARSENITE				
TOTAL CYP				
Mouse	---	↓ CYP content	C57BL/6 mice (liver)	(304)
Rat	---	↑ CYP content	Wistar albino rats (liver)	(386)
		↓ CYP content	Sprague-Dawley rats (liver)	(299; 368)
			Wistar albino rats (liver)	(369-375)
			Wistar albino rats (kidney)	(373)
		↓ CYP content induced by isosafrole	Wistar albino rats (liver)	(371)
		↓ CYP content induced by PB	Wistar albino rats (liver)	(371)
		↔ CYP content induced by 3-MC	Wistar albino rats (liver)	(371)
	Activity	↓ ANDM activity	Wistar albino rats (liver)	(375)
		↓ ECOD activity	Wistar albino rats (liver)	(371)
		↓ EROD activity	Wistar albino rats (liver)	(371)
		↔ BZND activity	Wistar albino rats (liver)	(371)
		↔ PROD activity	Wistar albino rats (liver)	(371)
		↓ BZND activity induced by isosafrole	Wistar albino rats (liver)	(371)
		↓ BZND activity induced by PB	Wistar albino rats (liver)	(371)
		↓ EROD activity induced by isosafrole	Wistar albino rats (liver)	(371)
		↓ EROD activity induced by PB	Wistar albino rats (liver)	(371)
		↓ PROD activity induced by PB	Wistar albino rats (liver)	(371)
		↔ BZND activity induced by 3-MC	Wistar albino rats (liver)	(371)
		↔ ECOD activity induced by 3-MC	Wistar albino rats (liver)	(371)

		↔ ECOD activity induced by isosafrole	Wistar albino rats (liver)	(371)
		↔ ECOD activity induced by PB	Wistar albino rats (liver)	(371)
		↔ EROD activity induced by 3-MC	Wistar albino rats (liver)	(371)
Guinea pig	---	↓ CYP content	Hartley guinea pigs (liver)	(298)
			Hartley guinea pigs (kidney)	(298)
		↔ CYP content	Hartley guinea pigs (lung)	(298)

Table 1.3. The effect of arsenite on the expression of CYP1A subfamily in different species.

SPECIES	LEVEL	EFFECT	EXPERIMENTAL MODEL	REFERENCE
ARSENITE				
CYP1A1				
Mouse	mRNA	↑ CYP1A1 mRNA	C57BL/6 mice (lung)	(301)
			ICR mice (lung)	(300)
			Mouse hepatoma (Hepa1c1c7) cells	(376; 377; 379)
		↓ CYP1A1 mRNA	C57BL/6 mice (brain)	(385)
		↔ CYP1A1 mRNA	129/Sv mice (liver)	(387)
			C57BL/6 mice (liver)	(304; 375)
			C57BL/6 mice (lung)	(304)
			C57BL/6 mice (kidney)	(301; 304)
			C57BL/6 mice (heart)	(301)
		↑ CYP1A1 mRNA induced by 3-MC	Mouse hepatoma (Hepa1c1c7) cells	(379)
		↑ CYP1A1 mRNA induced by βNF	Mouse hepatoma (Hepa1c1c7) cells	(379)
		↑ CYP1A1 mRNA induced by B[a]P	Mouse hepatoma (Hepa1c1c7) cells	(379)
		↑ CYP1A1 mRNA induced by TCDD	C57BL/6 mice (liver)	(380)
			C57BL/6 mice (lung)	(301)
			C57BL/6 mice (kidney)	(301)
			Mouse hepatoma (Hepa1c1c7) cells	(376; 379)
		↓ CYP1A1 mRNA induced by TCDD	C57BL/6 mice (liver)	(380)
			C57BL/6 mice (kidney)	(301)

			C57BL/6 mice (heart)	(301)
			C57BL/6 mouse hepatocytes	(380)
		↔ CYP1A1 mRNA induced by B[a]P	Mouse hepatoma (Hepa1c1c7) cells	(376)
		↔ CYP1A1 mRNA induced by TCDD	C57BL/6 mice (heart)	(301)
			Mouse hepatoma (Hepa1c1c7) cells	(381)
		↑ CYP1A1 mRNA induced by TCDD stability	Mouse hepatoma (Hepa1c1c7) cells	(377)
	Protein	↑ CYP1A1 protein	ICR mice (lung)	(300)
		↔ CYP1A1 protein	Mouse hepatoma (Hepa1c1c7) cells	(379)
		↑ CYP1A1 protein induced by βNF	Mouse hepatoma (Hepa1c1c7) cells	(379)
		↔ CYP1A1 protein induced by 3-MC	Mouse hepatoma (Hepa1c1c7) cells	(379)
		↔ CYP1A1 protein induced by B[a]P	Mouse hepatoma (Hepa1c1c7) cells	(379)
		↔ CYP1A1 protein induced by TCDD	Mouse hepatoma (Hepa1c1c7) cells	(379)
		↔ CYP1A1 protein induced by TCDD stability	Mouse hepatoma (Hepa1c1c7) cells	(377)
	Activity	↑ CYP1A1 (EROD) activity	C57BL/6 mice (lung)	(301)
			ICR mice (lung)	(300)
		↓ CYP1A1 (EROD) activity	C57BL/6 mice (lung)	(304)
			C57BL/6 mice (kidney)	(301)
		↓ CYP1A1/2 (EROD) activity	C57BL/6 mice (liver)	(304)
		↔ CYP1A1 (EROD) activity	C57BL/6 mice (liver)	(380)
			C57BL/6 mice (kidney)	(304)
			Mouse hepatoma (Hepa1c1c7) cells	(377; 379)
		↑ CYP1A1 (EROD) activity induced by TCDD	C57BL/6 mice (liver)	(380)
			C57BL/6 mice (lung)	(301)
		↓ CYP1A1 (EROD) activity induced by 3-MC	Mouse hepatoma (Hepa1c1c7) cells	(379)
		↓ CYP1A1 (EROD) activity induced by βNF	Mouse hepatoma (Hepa1c1c7) cells	(379)

		↓ CYP1A1 (EROD) activity induced by B[a]P	Mouse hepatoma (Hepa1c1c7) cells	(379)
		↓ CYP1A1 (EROD) activity induced by TCDD	C57BL/6 mice (kidney)	(301)
			C57BL/6 mouse hepatocytes	(380)
			Mouse hepatoma (Hepa1c1c7) cells	(377; 379)
		↔ CYP1A1 (B[a]P 3-hydroxylation) activity induced by B[a]P	Mouse hepatoma (Hepa1c1c7) cells	(388)
Rat	mRNA	↑ CYP1A1 mRNA	Sprague-Dawley rats (lung)	(299)
		↔ CYP1A1 mRNA	Sprague-Dawley rats (liver)	(299)
			Sprague-Dawley rats (kidney)	(299)
		↓ CYP1A1 mRNA induced by 3-MC	Fischer 344 rat hepatocytes	(382)
	Protein	↑ CYP1A1 protein	Sprague-Dawley rats (lung)	(299)
		↓ CYP1A1 protein induced by 3-MC	Fischer 344 rat hepatocytes	(382)
	Activity	↑ CYP1A1 (EROD) activity	Sprague-Dawley rats (lung)	(299; 303)
		↓ CYP1A1 (EROD) activity	Sprague-Dawley rats (liver)	(303)
			Sprague-Dawley rats (kidney)	(303)
			Wistar albino rats (liver)	(372)
		↓ CYP1A1/2 (EROD) activity	Sprague-Dawley rats (liver)	(299)
		↓ CYP1A1 (EROD) activity (direct effect)	Sprague-Dawley rats (lung)	(303)
		↓ CYP1A1 (EROD) activity induced by 3-MC	Fischer 344 rat hepatocytes	(382)
		↓ CYP1A1 (EROD) activity induced by TCDD	Sprague-Dawley rat hepatocytes	(383)
Guinea pig	Activity	↓ CYP1A1 (EROD) activity	Hartley guinea pigs (liver)	(298)
			Hartley guinea pigs (lung)	(298)

			Hartley guinea pigs (kidney)	(298)
		↓ CYP1A1 (EROD) activity (direct effect)	Hartley guinea pigs (liver)	(298)
		↑ CYP1A1 (EROD) activity induced by βNF	Hartley guinea pigs (lung)	(298)
		↓ CYP1A1 (EROD) activity induced by βNF	Hartley guinea pigs (liver)	(298)
			Hartley guinea pigs (kidney)	(298)
Fish	mRNA	↓ CYP1A1 mRNA	Common carp (liver)	(378)
		↓ CYP1A1 mRNA induced by B[a]P	Zebrafish (liver)	(389)
	Protein	↔ CYP1A1 protein induced by B[a]P	Zebrafish (liver)	(389)
	Activity	↓ CYP1A1 (EROD) activity	Common carp (liver)	(378)
		↓ CYP1A1 (EROD) activity induced by B[a]P	Zebrafish (liver)	(389)
CYP1A2				
Mouse	mRNA	↓ CYP1A2 mRNA	C3H mice (liver)	(384)
			C57BL/6 mice (brain)	(385)
		↔ CYP1A2 mRNA	C57BL/6 mice (liver)	(380)
			C57BL/6 mice (lung)	(301)
			C57BL/6 mice (kidney)	(301)
			C57BL/6 mice (heart)	(301)
		↑ CYP1A2 mRNA induced by TCDD	C57BL/6 mice (kidney)	(301)
		↓ CYP1A2 mRNA induced by TCDD	C57BL/6 mice (liver)	(380)
			C57BL/6 mice (kidney)	(301)
			C57BL/6 mice (heart)	(301)
		↔ CYP1A2 mRNA induced by TCDD	C57BL/6 mice (liver)	(380)
			C57BL/6 mice (lung)	(301)
			C57BL/6 mice (heart)	(301)
	Activity	↑ CYP1A2 (MROD) activity	C57BL/6 mice (lung)	(301)
		↓ CYP1A2 (MROD) activity	C57BL/6 mice (kidney)	(301)
		↓ CYP1A1/2 (EROD) activity	C57BL/6 mice (liver)	(304)
		↔ CYP1A2 (MROD) activity	C57BL/6 mice (liver)	(380)
			Mouse hepatoma (Hepa1c1c7) cells	(379)

		↑ CYP1A2 (MROD) activity induced by TCDD	C57BL/6 mice (liver)	(380)
			C57BL/6 mice (lung)	(301)
		↓ CYP1A2 (MROD) activity induced by 3-MC	Mouse hepatoma (Hepa1c1c7) cells	(379)
		↓ CYP1A2 (MROD) activity induced by βNF	Mouse hepatoma (Hepa1c1c7) cells	(379)
		↓ CYP1A2 (MROD) activity induced by B[a]P	Mouse hepatoma (Hepa1c1c7) cells	(379)
		↓ CYP1A2 (MROD) activity induced by TCDD	C57BL/6 mice (kidney)	(301)
			Mouse hepatoma (Hepa1c1c7) cells	(379)
Rat	Activity	↓ CYP1A1/2 (EROD) activity	Sprague-Dawley rats (liver)	(299)
		↓ CYP1A2 (MROD) activity induced by TCDD	Sprague-Dawley rat hepatocytes	(383)
CYP1A4				
Chicken	mRNA	↓ CYP1A4 mRNA induced by 3-MC	Chick embryo hepatocytes	(390)
		↔ CYP1A4 mRNA induced by 3-MC with superinduction by CHX	Chick embryo hepatocytes	(390)
		↔ CYP1A4 mRNA induced by 3-MC stability	Chick embryo hepatocytes	(390)
	Protein	↓ CYP1A4/5 protein induced by 3-MC	Chick embryo hepatocytes	(391; 392)
	Activity	↓ CYP1A4 (EROD) activity induced by 3-MC	Chick embryo hepatocytes	(390)
		↓ CYP1A4/5 (EROD) activity induced by 3-MC	Chick embryo hepatocytes	(391; 392)
CYP1A5				
Chicken	mRNA	↓ CYP1A5 mRNA induced by 3-MC	Chick embryo hepatocytes	(390)
		↔ CYP1A5 mRNA induced by 3-MC with superinduction by CHX	Chick embryo hepatocytes	(390)
		↔ CYP1A5 mRNA induced by 3-MC stability	Chick embryo hepatocytes	(390)

	Protein	↓ CYP1A4/5 protein induced by 3-MC	Chick embryo hepatocytes	(391; 392)
	Activity	↓ CYP1A5 (UROX) activity induced by 3-MC	Chick embryo hepatocytes	(390)
		↓ CYP1A4/5 (EROD) activity induced by 3-MC	Chick embryo hepatocytes	(391; 392)
CYP1A				
Mouse	Protein	↑ CYP1A protein	C57BL/6 mice (lung)	(301)
		↔ CYP1A protein	C57BL/6 mice (liver)	(380)
			C57BL/6 mice (kidney)	(301)
		↑ CYP1A protein induced by TCDD	C57BL/6 mice (liver)	(380)
			C57BL/6 mice (lung)	(301)
		↓ CYP1A protein induced by TCDD	C57BL/6 mice (kidney)	(301)
			C57BL/6 mouse hepatocytes	(380)
Rat	mRNA	↓ CYP1A mRNA induced by TCDD	Sprague-Dawley rat hepatocytes	(383)
	Protein	↓ CYP1A protein induced by TCDD	Sprague-Dawley rat hepatocytes	(383)

Table 1.4. The effect of arsenite on the expression of CYP regulators in different species.

SPECIES	LEVEL	EFFECT	EXPERIMENTAL MODEL	REFERENCE
ARSENITE				
CYP REGULATION: AHR				
Mouse	Activity	↑ AHR-dependent XRE-luciferase activity	Mouse hepatoma (Hepa1c1c7) cells	(377)
		↔ AHR-dependent XRE-luciferase activity	C57BL/6 mouse hepatocytes	(380)
		↓ AHR-dependent XRE-luciferase activity induced by TCDD	C57BL/6 mouse hepatocytes	(380)
		↓ AHR-dependent CYP1A1-luciferase activity induced by TCDD	Mouse hepatoma (Hepa1c1c7) cells	(381)
	---	↑ AHR nuclear accumulation	Mouse hepatoma (Hepa1c1c7) cells	(376)
	---	↑ AHR-XRE binding	Mouse hepatoma (Hepa1c1c7) cells	(376)

		↔ AHR-XRE binding induced by TCDD	Mouse hepatoma (Hepa1c1c7) cells	(362)
Rat	Protein	↔ AHR protein stability	Sprague-Dawley rat hepatocytes	(383)
		↔ AHR protein induced by TCDD stability	Sprague-Dawley rat hepatocytes	(383)
	---	↔ AHR nuclear accumulation	Sprague-Dawley rat hepatocytes	(383)
		↓ AHR nuclear accumulation induced by TCDD	Sprague-Dawley rat hepatocytes	(383)
	---	↔ AHR-XRE binding	Sprague-Dawley rat hepatocytes	(383)
		↓ AHR-XRE binding induced by TCDD	Sprague-Dawley rat hepatocytes	(383)
CYP REGULATION: PXR				
Mouse	mRNA	↑ PXR mRNA	Transgenic-CYP3A4 mice (small intestine)	(393)
		↑ RXRα mRNA	Transgenic-CYP3A4 mice (small intestine)	(393)
Rat	Protein	↔ PXR protein stability	Sprague-Dawley rat hepatocytes	(383)
		↔ PXR protein induced by rifampicin stability	Sprague-Dawley rat hepatocytes	(383)
	Activity	↓ PXR-dependent CYP3A23-luciferase activity induced by DEX	Fischer 344 rat hepatocytes	(394-396)
		↓ Ectopic human PXR-dependent CYP3A23-luciferase activity induced by rifampicin	Fischer 344 rat hepatocytes	(366)
	---	↓ PXR nuclear accumulation	Sprague-Dawley rat hepatocytes	(383)
		↓ PXR nuclear accumulation induced by rifampicin	Sprague-Dawley rat hepatocytes	(383)

iAs^{III} exposure significantly increased the constitutive liver, lung, kidney, heart, and brain CYP1B1 mRNA in C57BL/6 mice (Table 1.5). Such increase can be attributed to iAs^{III}-induced inflammation that was evidenced by an increase in serum tumor necrosis factor alpha (TNF-α) which is a potent inducer of CYP1B1 gene expression (385; 397; 398). Though, a study by Liu *et*

al., investigating the effect of iAs^{III}-related stress on the expression of different CYP enzymes, showed a significant decrease in basal hepatic CYP1B1 mRNA along with other CYP enzymes in 129/Sv mice (387; 399). At the inducible level, co-treatment of C57BL/6 mice with iAs^{III} and TCDD resulted in a significant increase in hepatic CYP1B1 protein compared with TCDD treatment alone (380).

1.4.2.1.2. CYP2 family

As shown in (Table 1.5), iAs^{III} increases basal mRNA expression of hepatic CYP2A4 in the C3H mice. Such effect of iAs^{III} on CYP2A4 can alter steroid metabolism because it encodes hepatic microsomal androstenedione 15α-hydroxylase (384; 400). Similarly, iAs^{III} enhances mRNA and activity of constitutive renal CYP2A5 of C57BL/6 mice with no change observed in hepatic and pulmonary levels (304).

In mice, iAs^{III} decreased CYP2B1/2 activity in C57BL/6 mouse liver (Table 1.5), with no change in lung and kidney tissues (304). Exposure to iAs^{III} did not also affect CYP2B1/2 mRNA expression in Sprague-Dawley rat liver, lung, and kidney. Interestingly, it has been found that iAs^{III} inhibits phenobarbital (PB)-mediated induction of CYP2B1/2 mRNA, protein and activity in Fischer 344 rat hepatocytes (299; 382). Moreover, it has been reported that iAs^{III} decreases CYP2B1/2 activity in different rat strains (299; 303; 372). A study by Falkner *et al.* demonstrated that iAs^{III} exposure suppresses CYP2B4 activity in liver and lung tissues of Hartley guinea pigs (298).

Other CYP2B subfamily members, such as CYP2B9, CYP2B10, and CYP2B19, were significantly induced at mRNA level in response to iAs^{III} treatment in different tissues of C57BL/6 and C3H mice. This induction is believed to be mediated by the activation of constitutive androstane receptor (CAR) by iAs^{III} (385; 397; 398). On the contrary, there was a decrease in hepatic CYP2B9 mRNA expression in 129/Sv mice (387).

Table 1.5. The effect of arsenite on the expression of CYP1B, 2A, and 2B subfamilies in different species.

SPECIES	LEVEL	EFFECT	EXPERIMENTAL MODEL	REFERENCE
ARSENITE				
CYP1B1				
Mouse	mRNA	↑ CYP1B1 mRNA	C57BL/6 mice (liver)	(397)
			C57BL/6 mice (lung)	(397)
			C57BL/6 mice (kidney)	(397)
			C57BL/6 mice (heart)	(398)
			C57BL/6 mice (brain)	(385)
		↓ CYP1B1 mRNA	129/Sv mice (liver)	(387)
		↔ CYP1B1 mRNA	C57BL/6 mice (liver)	(380)
		↔ CYP1B1 mRNA induced by TCDD	C57BL/6 mice (liver)	(380)
	Protein	↔ CYP1B1 protein	C57BL/6 mice (liver)	(380)
		↑ CYP1B1 protein induced by TCDD	C57BL/6 mice (liver)	(380)
CYP2A4				
Mouse	mRNA	↑ CYP2A4 mRNA	C3H mice (liver)	(384; 400)
CYP2A5				
Mouse	mRNA	↑ CYP2A5 mRNA	C57BL/6 mice (kidney)	(304)
		↔ CYP2A5 mRNA	C57BL/6 mice (liver)	(304)
			C57BL/6 mice (lung)	(304)
	Activity	↑ CYP2A5 (COH) activity	C57BL/6 mice (kidney)	(304)
		↔ CYP2A5 (COH) activity	C57BL/6 mice (liver)	(304)
			C57BL/6 mice (lung)	(304)
CYP2B1/2				
Mouse	Activity	↓ CYP2B1/2 (PROD) activity	C57BL/6 mice (liver)	(304)
		↔ CYP2B1/2 (PROD) activity	C57BL/6 mice (lung)	(304)
			C57BL/6 mice (kidney)	(304)
Rat	mRNA	↔ CYP2B1/2 mRNA	Sprague-Dawley rats (liver)	(299)
			Sprague-Dawley rats (lung)	(299)
			Sprague-Dawley rats (kidney)	(299)
		↓ CYP2B1 mRNA induced by PB	Fischer 344 rat hepatocytes	(382)

	Protein	↓ CYP2B1/2 protein induced by PB	Fischer 344 rat hepatocytes	(382)
	Activity	↓ CYP2B2 (BROD) activity	Wistar albino rats (liver)	(372)
		↓ CYP2B1/2 (PROD) activity	Sprague-Dawley rats (liver)	(299; 303)
		↔ CYP2B1 (PROD) activity	Wistar albino rats (liver)	(372)
		↔ CYP2B1/2 (PROD) activity	Sprague-Dawley rats (lung)	(299; 303)
		↓ CYP2B1/2 (BROD) activity induced by PB	Fischer 344 rat hepatocytes	(382)
CYP2B4				
Guinea pig	Activity	↓ CYP2B4 (PROD) activity	Hartley guinea pigs (liver)	(298)
			Hartley guinea pigs (lung)	(298)
		↓ CYP2B4 (PROD) activity induced by βNF	Hartley guinea pigs (lung)	(298)
		↔ CYP2B4 (PROD) activity induced by βNF	Hartley guinea pigs (liver)	(298)
CYP2B9				
Mouse	mRNA	↑ CYP2B9 mRNA	C3H mice (liver)	(400)
			C57BL/6 mice (liver)	(397)
			C57BL/6 mice (kidney)	(397)
			C57BL/6 mice (heart)	(398)
			C57BL/6 mice (brain)	(385)
		↓ CYP2B9 mRNA	129/Sv mice (liver)	(387)
		↔ CYP2B9 mRNA	C57BL/6 mice (lung)	(397)
CYP2B10				
Mouse	mRNA	↑ CYP2B10 mRNA	C57BL/6 mice (liver)	(397)
			C57BL/6 mice (lung)	(397)
			C57BL/6 mice (kidney)	(397)
			C57BL/6 mice (heart)	(398)
		↔ CYP2B10 mRNA	C57BL/6 mice (brain)	(385)
CYP2B19				
Mouse	mRNA	↑ CYP2B19 mRNA	C57BL/6 mice (lung)	(397)
			C57BL/6 mice (kidney)	(397)
			C57BL/6 mice (heart)	(398)
			C57BL/6 mice (brain)	(385)
		↔ CYP2B19 mRNA	C57BL/6 mice (liver)	(397)

Considering CYP2C subfamily members (Table 1.6), iAs^{III} treatment has exhibited tissue-specific differential effect on their expression. In the liver and brain of C57BL/6 mice, iAs^{III} treatment increased mRNA level of CYP2C29, CYP2C38, and CYP2C40 but decreased that of hepatic CYP2C44, with no change on liver CYP2C39 and brain CYP2C44. Additionally, iAs^{III} increased mRNA level of renal CYP2C29 and CYP2C40, without affecting CYP2C38 and CYP2C44 mRNA. On the other hand, iAs^{III} decreased pulmonary mRNA of CYP2C29, CYP2C38, and CYP2C40 without altering CYP2C44. Finally, iAs^{III} increased mRNA of CYP2C38, and CYP2C40 in the heart with no change in CYP2C29, and CYP2C44 (385; 397; 398; 400).

Interestingly, it has been found that iAs^{III} increases the protein expression of CYP2C subfamily in the liver, lung, and kidney of C57BL/6 mice (397). Additionally, iAs^{III} can transcriptionally regulate CYP2B and CYP2C subfamilies expression through activating the CAR (385).

A significant induction of CYP2D9 and CYP2D10 mRNA expression was reported in the liver of C3H female mice and brain of C57BL/6 mice, respectively, after iAs^{III} treatment (Table 1.6). On the other hand, iAs^{III} did not significantly affect CYP2D22 in the brain of C57BL/6 mice (385; 400).

In mice, iAs^{III} treatment enhanced the mRNA expression of basal CYP2E1 in the brain of C57BL/6 mice (Table 1.6) (385). In contrast, basal CYP2E1 mRNA expression is inhibited in the liver, lung, kidney, and heart by iAs^{III} (384; 397; 398). Similarly, iAs^{III} has also inhibited CYP2E1 activity, measured by aniline *p*-hydroxylation (APH), in the liver of Wistar albino rats (375). Exposure to iAs^{III} caused marked inhibition of CYP2F2 mRNA expression in the liver of C3H mice (384; 400).

It has been reported that iAs^{III} significantly induces liver CYP2J5 mRNA levels, inhibits that of the lung and heart, and does not affect kidney CYP2J5 and brain CYP2J5/6/9/11/13 mRNA levels in C57BL/6 mice (Table 1.6) (385; 397). Interestingly, while iAs^{III} significantly induced lung, liver, kidney, and heart CYP2J9 mRNA levels, it significantly inhibited heart CYP2J5, CYP2J11, CYP2J13 mRNA levels in C57BL/6 mice (397; 398). At protein level, iAs^{III} significantly induced CYP2J protein expression in the liver and lung while inhibited its expression in the kidney of C57BL/6 mice (397). In contrast to other CYP2 subfamilies, regulation of CYP2J subfamily has been demonstrated to be mediated by activator protein-1 (AP-1), therefore, iAs^{III} might have induced CYP2J through activating AP-1 (397).

Table 1.6. The effect of arsenite on the expression of CYP2C, 2D, 2E, 2F, 2H, and 2J subfamilies in different species.

SPECIES	LEVEL	EFFECT	EXPERIMENTAL MODEL	REFERENCE
ARSENITE				
CYP2C29				
Mouse	mRNA	↑ CYP2C29 mRNA	C57BL/6 mice (liver)	(397)
			C57BL/6 mice (kidney)	(397)
			C57BL/6 mice (brain)	(385)
		↓ CYP2C29 mRNA	C57BL/6 mice (lung)	(397)
		↔ CYP2C29 mRNA	C57BL/6 mice (heart)	(398)
CYP2C38				
Mouse	mRNA	↑ CYP2C38 mRNA	C57BL/6 mice (liver)	(397)
			C57BL/6 mice (heart)	(398)
			C57BL/6 mice (brain)	(385)
		↓ CYP2C38 mRNA	C57BL/6 mice (lung)	(397)
		↔ CYP2C38 mRNA	C57BL/6 mice (kidney)	(397)
CYP2C39				
Mouse	mRNA	↔ CYP2C39 mRNA	C3H mice (liver)	(400)
CYP2C40				
Mouse	mRNA	↑ CYP2C40 mRNA	C57BL/6 mice (liver)	(397)
			C57BL/6 mice (kidney)	(397)
			C57BL/6 mice (heart)	(398)
			C57BL/6 mice (brain)	(385)
		↓ CYP2C40 mRNA	C57BL/6 mice (lung)	(397)
CYP2C44				
Mouse	mRNA	↓ CYP2C44 mRNA	C57BL/6 mice (liver)	(397)
		↔ CYP2C44 mRNA	C57BL/6 mice (lung)	(397)
			C57BL/6 mice (kidney)	(397)
			C57BL/6 mice (heart)	(398)
			C57BL/6 mice (brain)	(385)
CYP2C				
Mouse	Protein	↑ CYP2C protein	C57BL/6 mice (liver)	(397)
			C57BL/6 mice (lung)	(397)
			C57BL/6 mice (kidney)	(397)
CYP2D9				
Mouse	mRNA	↑ CYP2D9 mRNA	C3H mice (liver)	(400)
CYP2D10				
Mouse	mRNA	↑ CYP2D10 mRNA	C57BL/6 mice (brain)	(385)
CYP2D22				

Mouse	mRNA	↔ CYP2D22 mRNA	C57BL/6 mice (brain)	(385)
CYP2E1				
Mouse	mRNA	↑ CYP2E1 mRNA	C57BL/6 mice (brain)	(385)
		↓ CYP2E1 mRNA	C3H mice (liver)	(384)
			C57BL/6 mice (liver)	(397)
			C57BL/6 mice (lung)	(397)
			C57BL/6 mice (kidney)	(397)
			C57BL/6 mice (heart)	(398)
		↔ CYP2E1 mRNA	129/Sv mice (liver)	(387)
			C3H mice (liver)	(400)
Rat	Activity	↓ CYP2E1 (APH) activity	Wistar albino rats (liver)	(375)
CYP2F2				
Mouse	mRNA	↓ CYP2F2 mRNA	C3H mice (liver)	(384; 400)
		↔ CYP2F2 mRNA	129/Sv mice (liver)	(387)
CYP2H1/2				
Chicken	mRNA	↔ CYP2H1 mRNA induced by PB	Chick Embryo hepatocytes	(391; 392)
	Protein	↓ CYP2H1/2 protein induced by PB	Chick Embryo hepatocytes	(391; 392)
	Activity	↓ CYP2H1/2 (BZND) activity induced by PB	Chick Embryo hepatocytes	(391; 392)
CYP2J5				
Mouse	mRNA	↑ CYP2J5 mRNA	C57BL/6 mice (liver)	(397)
		↓ CYP2J5 mRNA	C3H mice (liver)	(384)
			C57BL/6 mice (lung)	(397)
			C57BL/6 mice (heart)	(398)
		↔ CYP2J5 mRNA	C3H mice (liver)	(400)
			C57BL/6 mice (kidney)	(397)
			C57BL/6 mice (brain)	(385)
CYP2J6				
Mouse	mRNA	↔ CYP2J6 mRNA	C57BL/6 mice (brain)	(385)
CYP2J9				
Mouse	mRNA	↑ CYP2J9 mRNA	C57BL/6 mice (liver)	(397)
			C57BL/6 mice (lung)	(397)
			C57BL/6 mice (kidney)	(397)
			C57BL/6 mice (heart)	(398)
		↔ CYP2J9 mRNA	C57BL/6 mice (brain)	(385)
CYP2J11				
Mouse	mRNA	↓ CYP2J11 mRNA	C57BL/6 mice (heart)	(398)
		↔ CYP2J11 mRNA	C57BL/6 mice (brain)	(385)
CYP2J13				

Mouse	mRNA	↓ CYP2J13 mRNA	C57BL/6 mice (heart)	(398)
		↔ CYP2J13 mRNA	C57BL/6 mice (brain)	(385)
CYP2J				
Mouse	Protein	↑ CYP2J protein	C57BL/6 mice (liver)	(397)
			C57BL/6 mice (lung)	(397)
		↓ CYP2J protein	C57BL/6 mice (kidney)	(397)

1.4.2.1.3. CYP3 family

Exposure to iAs^{III} increased CYP3A4 expression (Table 1.7) at the level of mRNA, protein, and activity in the small intestine of transgenic-CYP3A4 mice with a consistent induction of PXR and Retinoid X Receptor alpha (RXRα) mRNA levels (Table 1.4) which may be attributed to iAs^{III}-mediated oxidative stress. However, the magnitude of induction between mRNA and protein is not consistent. This may be attributed to iAs^{III}-mediated protein degradation through ubiquitin-proteasome system that results in low apparent CYP3A4 protein expression (393). Similarly, iAs^{III} exposure induced CYP3A11 mRNA in the brain of C57BL/6 mice (385). On the contrary, it has been found that iAs^{III} decreases mRNA level of CYP3A13 in the liver of 129/Sv mice (387). Moreover, in Fischer 344 primary rat hepatocytes, exposure to a low concentration of iAs^{III} inhibited dexamethasone (DEX)-mediated induction of CYP3A23 transcriptionally, translationally, and at activity level. This has been evidenced by a decrease in PXR-dependent CYP3A23-luciferase activity induced by DEX. In addition, the ectopic human PXR-dependent CYP3A23-luciferase activity induced by rifampicin decreased after iAs^{III} exposure. Interestingly, iAs^{III} produced no effect on CYP3A23 protein stability induced by DEX. Therefore, this effect of translational inhibition is probably not caused by protein degradation but may be attributed to iAs^{III}-mediated decrease in the association of CYP3A23 mRNA with polyribosomes (366; 382; 394-396).

Regarding CYP3A25, although there was an increase in its hepatic mRNA level in 129/Sv mice by iAs^{III}, there was a decrease in its hepatic mRNA level in C3H mice (384; 387). Additionally, there was also a decrease in hepatic CYP3A41 mRNA expression in C3H mice (400). Generally, exposure to iAs^{III} inhibited CYP3A mRNA, protein, and activity induced by rifampicin, DEX, and PB in hepatocytes from different rat strains (382; 383), but it had no effect on its activity in the liver of Hartley guinea pigs (298).

1.4.2.1.4. CYP4 family

From the data shown in (Table 1.7), it seems that there is a differential iAs^{III} exposure outcome regarding CYP4A10 mRNA expression in different species and tissues. For instance, iAs^{III} enhanced the mRNA level in the liver and brain of C57BL/6 mice, while it decreased its level in the liver of C3H mice. Also, iAs^{III} had no effect on pulmonary, renal, and cardiac CYP4A10 in C57BL/6 mice (384; 385; 397; 398). Regarding CYP4A12 and CYP4A14, it has been found that iAs^{III} increases mRNA level of both CYP enzymes in the brain and that of CYP4A14 in the liver of C57BL/6 mice. On the other hand, exposure to iAs^{III} decreased the mRNA level of CYP4A14 in the lung and heart of C57BL/6 mice as well as the liver of C3H mice, with no effect on mRNA level of cardiac CYP4A12 and renal CYP4A14 (384; 385; 397; 398).

Additionaly, iAs^{III} exposure increased the protein expression of CYP4A in the liver while it decreased its expression in the kidney, with no change in the lung and heart of C57BL/6 mice (397; 398). Regarding protein expression of CYP4A in Wistar albino rats, iAs^{III} enhanced the protein expression in both liver and kidney (401).

Although iAs^{III} increased CYP4F13 mRNA level in the liver, lung, and brain of C57BL/6 mice, it had no effect on its level in the kidney and heart (Table 1.7). However, the effect of iAs^{III} on CYP4F15 was different as it induced its mRNA in the liver, kidney, heart, and brain with no effect on the lung. Moreover, iAs^{III} exposure caused induction of CYP4F16 mRNA in the liver and brain but did not affect its levels in the lung, kidney, and heart of C57BL/6 mice. Interestingly, there was an increase in the mRNA of CYP4F18 in all tested tissues (lung, kidney, heart, and brain) with the exception of the liver (385; 397; 398).

Table 1.7. The effect of arsenite on the expression of CYP3A, 4A, 4B, 4F, 7B, and 21A subfamilies in different species.

SPECIES	LEVEL	EFFECT	EXPERIMENTAL MODEL	REFERENCE
ARSENITE				
CYP3A4				
Mouse	mRNA	↑ CYP3A4 mRNA	Transgenic-CYP3A4 mice (small intestine)	(393)
	Protein	↑ CYP3A4 protein	Transgenic-CYP3A4 mice (small intestine)	(393)

	Activity	↑ CYP3A4 (proluciferin metabolism) activity	Transgenic-CYP3A4 mice (small intestine)	(393)
CYP3A11				
Mouse	mRNA	↑ CYP3A11 mRNA	C57BL/6 mice (brain)	(385)
CYP3A13				
Mouse	mRNA	↓ CYP3A13 mRNA	129/Sv mice (liver)	(387)
CYP3A23				
Rat	mRNA	↓ CYP3A23 mRNA induced by DEX	Fischer 344 rat hepatocytes	(382; 394-396)
		↔ CYP3A23 mRNA induced by PB	Fischer 344 rat hepatocytes	(382)
	Protein	↓ CYP3A23 protein induced by DEX	Fischer 344 rat hepatocytes	(394-396)
		↔ CYP3A23 protein induced by DEX stability	Fischer 344 rat hepatocytes	(394-396)
	Activity	↓ CYP3A23 (p-nitrophenol hydroxylation) activity induced by DEX	Fischer 344 rat hepatocytes	(394-396)
CYP3A25				
Mouse	mRNA	↑ CYP3A25 mRNA	129/Sv mice (liver)	(387)
		↓ CYP3A25 mRNA	C3H mice (liver)	(384)
		↔ CYP3A25 mRNA	C3H mice (liver)	(400)
CYP3A41				
Mouse	mRNA	↓ CYP3A41 mRNA	C3H mice (liver)	(400)
CYP3A				
Rat	mRNA	↓ CYP3A mRNA induced by rifampicin	Sprague-Dawley rat hepatocytes	(383)
	Protein	↓ CYP3A protein induced by DEX	Fischer 344 rat hepatocytes	(382)
		↓ CYP3A protein induced by PB	Fischer 344 rat hepatocytes	(382)
		↓ CYP3A protein induced by rifampicin	Sprague-Dawley rat hepatocytes	(383)
	Activity	↓ CYP3A (DFB debenzylation) activity induced by rifampicin	Sprague-Dawley rat hepatocytes	(383)
Guinea pig	Activity	↔ CYP3A (ERND) activity	Hartley guinea pigs (liver)	(298)
CYP4A10				
Mouse	mRNA	↑ CYP4A10 mRNA	C57BL/6 mice (liver)	(397)
			C57BL/6 mice (brain)	(385)
		↓ CYP4A10 mRNA	C3H mice (liver)	(384)
		↔ CYP4A10 mRNA	C57BL/6 mice (lung)	(397)

			C57BL/6 mice (kidney)	(397)
			C57BL/6 mice (heart)	(398)
CYP4A12				
Mouse	mRNA	↑ CYP4A12 mRNA	C57BL/6 mice (brain)	(385)
		↔ CYP4A12 mRNA	C57BL/6 mice (heart)	(398)
CYP4A14				
Mouse	mRNA	↑ CYP4A14 mRNA	C57BL/6 mice (liver)	(397)
			C57BL/6 mice (brain)	(385)
		↓ CYP4A14 mRNA	C3H mice (liver)	(384)
			C57BL/6 mice (lung)	(397)
			C57BL/6 mice (heart)	(398)
		↔ CYP4A14 mRNA	C3H mice (liver)	(400)
			C57BL/6 mice (kidney)	(397)
CYP4A				
Mouse	Protein	↑ CYP4A protein	C57BL/6 mice (liver)	(397)
		↓ CYP4A protein	C57BL/6 mice (kidney)	(397)
		↔ CYP4A protein	C57BL/6 mice (lung)	(397)
			C57BL/6 mice (heart)	(398)
Rat	Protein	↑ CYP4A protein	Wistar albino rats (liver)	(401)
			Wistar albino rats (kidney)	(401)
CYP4B1				
Guinea pig	Activity	↔ CYP4B1 (ABH) activity	Hartley guinea pigs (liver)	(298)
			Hartley guinea pigs (lung)	(298)
CYP4F13				
Mouse	mRNA	↑ CYP4F13 mRNA	C57BL/6 mice (liver)	(397)
			C57BL/6 mice (lung)	(397)
			C57BL/6 mice (brain)	(385)
		↔ CYP4F13 mRNA	C57BL/6 mice (kidney)	(397)
			C57BL/6 mice (heart)	(398)
CYP4F15				
Mouse	mRNA	↑ CYP4F15 mRNA	C57BL/6 mice (liver)	(397)
			C57BL/6 mice (kidney)	(397)
			C57BL/6 mice (heart)	(398)
			C57BL/6 mice (brain)	(385)
		↔ CYP4F15 mRNA	C57BL/6 mice (lung)	(397)
CYP4F16				

Mouse	mRNA	↑ CYP4F16 mRNA	C57BL/6 mice (liver)	(397)
			C57BL/6 mice (brain)	(385)
		↔ CYP4F16 mRNA	C57BL/6 mice (lung)	(397)
			C57BL/6 mice (kidney)	(397)
			C57BL/6 mice (heart)	(398)
CYP4F18				
Mouse	mRNA	↑ CYP4F18 mRNA	C57BL/6 mice (lung)	(397)
			C57BL/6 mice (kidney)	(397)
			C57BL/6 mice (heart)	(398)
			C57BL/6 mice (brain)	(385)
		↔ CYP4F18 mRNA	C57BL/6 mice (liver)	(397)
CYP4F				
Mouse	Protein	↔ CYP4F protein	C57BL/6 mice (heart)	(398)
CYP7B1				
Mouse	mRNA	↓ CYP7B1 mRNA	C3H mice (liver)	(384; 400)
		↔ CYP7B1 mRNA	129/Sv mice (liver)	(387)
CYP21A1				
Mouse	mRNA	↓ CYP21A1 mRNA	129/Sv mice (liver)	(387)

1.4.2.2. The effect of arsenate on the expression of CYP enzymes in different species

As shown in (Table 1.8), iAs^V exposure produces no change in hepatic mRNA expression for several CYP enzymes in 129/Sv mice such as CYP1A1, CYP1B1, CYP2B9, CYP2E1, CYP2F2, CYP3A13, and CYP21A1. However, there was an increase in CYP3A25 mRNA in the liver and a decrease in CYP7B1 mRNA (387). In Wistar albino rats, treatment with iAs^V increased renal CYP4A protein expression while there was no alteration in the liver (401).

Table 1.8. The effect of arsenate on the expression of CYP enzymes in different species.

SPECIES	LEVEL	EFFECT	EXPERIMENTAL MODEL	REFERENCE
ARSENATE				
TOTAL CYP				
Rat	---	↓ CYP content	Wistar albino rats (liver)	(369)
CYP1A1				
Mouse	mRNA	↔ CYP1A1 mRNA	129/Sv mice (liver)	(387)

CYP1B1				
Mouse	mRNA	↔ CYP1B1 mRNA	129/Sv mice (liver)	(387)
CYP2B9				
Mouse	mRNA	↔ CYP2B9 mRNA	129/Sv mice (liver)	(387)
CYP2E1				
Mouse	mRNA	↔ CYP2E1 mRNA	129/Sv mice (liver)	(387)
CYP2F2				
Mouse	mRNA	↔ CYP2F2 mRNA	129/Sv mice (liver)	(387)
CYP3A13				
Mouse	mRNA	↔ CYP3A13 mRNA	129/Sv mice (liver)	(387)
CYP3A25				
Mouse	mRNA	↑ CYP3A25 mRNA	129/Sv mice (liver)	(387)
CYP4A				
Rat	Protein	↑ CYP4A protein	Wistar albino rats (kidney)	(401)
		↔ CYP4A protein	Wistar albino rats (liver)	(401)
CYP7B1				
Mouse	mRNA	↓ CYP7B1 mRNA	129/Sv mice (liver)	(387)
CYP21A1				
Mouse	mRNA	↔ CYP21A1 mRNA	129/Sv mice (liver)	(387)

1.4.2.3. The effect of monomethylarsonous acid and dimethylarsinous acid on the expression of CYP enzymes in mice

It has been previously demonstrated that MMA^{III} increases CYP3A4 expression at the levels of mRNA and catalytic activity, in agreement with the increase in PXR expression in the small intestine of CYP3A4 transgenic mice (393). However, there was no change in the protein level, which may be attributed to MMA^{III}-mediated oxidative stress that resulted in CYP3A4 protein destabilization. In addition, it was hypothesized that MMA^{III} causes inhibition of NF-κB induction which by turn may suppress CYP3A4 protein levels (Table 1.9) (393; 402).

As described in (Table 1.9), DMA^{III} causes up-regulation of CYP3A4 at the level of mRNA, protein, and activity in the small intestine of the CYP3A4 transgenic mice which is accompanied by induction of both PXR and RXRα (393).

Table 1.9. The effect of monomethylarsonous acid and dimethylarsinous acid on the expression of CYP enzymes in mice.

SPECIES	LEVEL	EFFECT	EXPERIMENTAL MODEL	REFERENCE
MONOMETHYLARSONOUS ACID				
CYP3A4				
Mouse	mRNA	↑ CYP3A4 mRNA	Transgenic-CYP3A4 mice (small intestine)	(393)
	Protein	↔ CYP3A4 protein	Transgenic-CYP3A4 mice (small intestine)	(393)
	Activity	↑ CYP3A4 (proluciferin metabolism) activity	Transgenic-CYP3A4 mice (small intestine)	(393)
CYP REGULATION: PXR				
Mouse	mRNA	↑ PXR mRNA	Transgenic-CYP3A4 mice (small intestine)	(393)
		↔ RXRα mRNA	Transgenic-CYP3A4 mice (small intestine)	(393)
DIMETHYLARSINOUS ACID				
CYP3A4				
Mouse	mRNA	↑ CYP3A4 mRNA	Transgenic-CYP3A4 mice (small intestine)	(393)
	Protein	↑ CYP3A4 protein	Transgenic-CYP3A4 mice (small intestine)	(393)
	Activity	↑ CYP3A4 (proluciferin metabolism) activity	Transgenic-CYP3A4 mice (small intestine)	(393)
CYP REGULATION: PXR				
Mouse	mRNA	↑ PXR mRNA	Transgenic-CYP3A4 mice (small intestine)	(393)
		↑ RXRα mRNA	Transgenic-CYP3A4 mice (small intestine)	(393)

1.4.2.4. The effect of monomethylarsonic acid and dimethylarsinic acid on the expression of CYP enzymes in different species

It seems that MMA^V has no effect on the total hepatic CYP content of Fischer 344 rats as shown in (Table 1.10), specifically CYP2B1/2 which was only increased at the level of protein expression with no significant effect being observed in the transcripts. In CYP2E1, there was no alteration in hepatic protein expression (403).

As shown in (Table 1.10), DMA^V causes no change in the basal CYP1A1 and CYP1A2 mRNA, protein, and catalytic activity in the liver, lung, and kidney of C57BL/6 mice. Regarding the TCDD-inducible expression of these enzymes, the influence of DMA^V was tissue-specific. For instance, CYP1A1 and CYP1A2 mRNA expression and activity were increased in the lung as opposed to the kidney where they were decreased, while in the liver they were not affected (302). In addition, exposure to DMA^V in Fischer 344 rats did not alter either CYP2B1/2 or CYP2E1 mRNA and protein expression in the liver (403).

Table 1.10. The effect of monomethylarsonic acid and dimethylarsinic acid on the expression of CYP enzymes in different species.

SPECIES	LEVEL	EFFECT	EXPERIMENTAL MODEL	REFERENCE
MONOMETHYLARSONIC ACID				
TOTAL CYP				
Rat	---	↔ CYP content	Fischer 344 rats (liver)	(403)
CYP2B1/2				
Rat	mRNA	↔ CYP2B1/2 mRNA	Fischer 344 rats (liver)	(403)
	Protein	↑ CYP2B1 protein	Fischer 344 rats (liver)	(403)
CYP2E1				
Rat	Protein	↔ CYP2E1 protein	Fischer 344 rats (liver)	(403)
DIMETHYLARSINIC ACID				
TOTAL CYP				
Rat	---	↔ CYP content	Fischer 344 rats (liver)	(403)
CYP1A1				
Mouse	mRNA	↔ CYP1A1 mRNA	C57BL/6 mice (liver)	(302)
			C57BL/6 mice (lung)	(302)
			C57BL/6 mice (kidney)	(302)
		↑ CYP1A1 mRNA induced by TCDD	C57BL/6 mice (lung)	(302)
		↓ CYP1A1 mRNA induced by TCDD	C57BL/6 mice (kidney)	(302)
		↔ CYP1A1 mRNA induced by TCDD	C57BL/6 mice (liver)	(302)
	Activity	↔ CYP1A1 (EROD) activity	C57BL/6 mice (liver)	(302)
			C57BL/6 mice (lung)	(302)
			C57BL/6 mice (kidney)	(302)

		↑ CYP1A1 (EROD) activity induced by TCDD	C57BL/6 mice (lung)	(302)
		↓ CYP1A1 (EROD) activity induced by TCDD	C57BL/6 mice (kidney)	(302)
		↔ CYP1A1 (EROD) activity induced by TCDD	C57BL/6 mice (liver)	(302)
Guinea pig	Activity	↔ CYP1A1 (EROD) activity (direct effect)	Hartley guinea pig liver microsomes	(298)
CYP1A2				
Mouse	mRNA	↔ CYP1A2 mRNA	C57BL/6 mice (liver)	(302)
			C57BL/6 mice (lung)	(302)
			C57BL/6 mice (kidney)	(302)
		↑ CYP1A2 mRNA induced by TCDD	C57BL/6 mice (lung)	(302)
		↓ CYP1A2 mRNA induced by TCDD	C57BL/6 mice (kidney)	(302)
		↔ CYP1A2 mRNA induced by TCDD	C57BL/6 mice (liver)	(302)
	Activity	↔ CYP1A2 (MROD) activity	C57BL/6 mice (liver)	(302)
			C57BL/6 mice (lung)	(302)
			C57BL/6 mice (kidney)	(302)
		↑ CYP1A2 (MROD) activity induced by TCDD	C57BL/6 mice (lung)	(302)
		↓ CYP1A2 (MROD) activity induced by TCDD	C57BL/6 mice (kidney)	(302)
		↔ CYP1A2 (MROD) activity induced by TCDD	C57BL/6 mice (liver)	(302)
CYP1A				
Mouse	Protein	↔ CYP1A protein	C57BL/6 mice (liver)	(302)
			C57BL/6 mice (lung)	(302)
			C57BL/6 mice (kidney)	(302)
		↑ CYP1A protein induced by TCDD	C57BL/6 mice (lung)	(302)
		↓ CYP1A protein induced by TCDD	C57BL/6 mice (kidney)	(302)
		↔ CYP1A protein induced by TCDD	C57BL/6 mice (liver)	(302)

CYP2B1/2				
Rat	mRNA	↔ CYP2B1/2 mRNA	Fischer 344 rats (liver)	(403)
	Protein	↔ CYP2B1 protein	Fischer 344 rats (liver)	(403)
CYP2E1				
Rat	Protein	↔ CYP2E1 protein	Fischer 344 rats (liver)	(403)

1.4.2.5. The effect of trimethylarsine oxide on the expression of CYP enzymes in different species

In (Table 1.11), $TMAO^V$ differentially affects both constitutive and inducible expressions of different CYP enzymes in tissue- and enzyme-specific manner. It increased the basal level of hepatic and pulmonary CYP1A1 mRNA in C57BL/6 mice as well as their primary hepatocytes, while it caused no change in its renal and cardiac levels. Additionally, $TMAO^V$ potentiated the TCDD-mediated induction of CYP1A1 mRNA in all investigated tissues and primary hepatocytes as well (404). Regarding the protein and catalytic activity levels, $TMAO^V$ increased both of them in all tested tissues such as the liver and lung, in addition to primary hepatocytes, with the exception of the kidney levels which were not affected. Moreover, it potentiated the TCDD-induced protein expression and activity in the liver, lung, kidney, and primary hepatocytes (218; 404).

The basal expression of CYP1A2 mRNA, protein, and activity was increased only in the liver of C57BL/6 mice after $TMAO^V$ exposure, with no change in the lung or the kidney. Moreover, the TCDD-inducible CYP1A2 was potentiated in response to $TMAO^V$ at the mRNA, protein, and activity levels in the lung, but not in the liver or the kidney (218; 404).

Treating C57BL/6 mice with $TMAO^V$ resulted in a significant increase in the hepatic, pulmonary, and renal mRNA basal expression of CYP1B1 in contrast to the heart which exhibited no change. In addition, $TMAO^V$ resulted in potentiating the TCDD-induced CYP1B1 mRNA in the liver, kidney, and heart with no change being observed in the lung. Considering the protein expression of CYP1B1, $TMAO^V$ increased its basal level in the lung and kidney with no change in the liver, while the TCDD-inducible protein was potentiated in the liver and kidney with no change in the lung (218; 404).

Mechanistic studies using the luciferase reporter gene assay and immunocytochemical analysis of AHR localization have revealed that these AHR-regulated enzymes were transcriptionally modulated by $TMAO^V$ at both basal and inducible levels (404).

Table 1.11. The effect of trimethylarsine oxide on the expression of CYP enzymes in different species.

SPECIES	LEVEL	EFFECT	EXPERIMENTAL MODEL	REFERENCE
TRIMETHYLARSINE OXIDE				
TOTAL CYP				
Rat	---	↔ CYP content	Fischer 344 rats (liver)	(403)
CYP1A1				
Mouse	mRNA	↑ CYP1A1 mRNA	C57BL/6 mice (liver)	(404)
			C57BL/6 mice (lung)	(218)
			C57BL/6 mouse hepatocytes	(404)
		↔ CYP1A1 mRNA	C57BL/6 mice (kidney)	(218)
			C57BL/6 mice (heart)	(218)
		↑ CYP1A1 mRNA induced by TCDD	C57BL/6 mice (liver)	(404)
			C57BL/6 mice (lung)	(218)
			C57BL/6 mice (kidney)	(218)
			C57BL/6 mice (heart)	(218)
			C57BL/6 mouse hepatocytes	(404)
	Protein	↑ CYP1A1 protein	C57BL/6 mice (liver)	(404)
			C57BL/6 mice (lung)	(218)
			C57BL/6 mouse hepatocytes	(404)
		↔ CYP1A1 protein	C57BL/6 mice (kidney)	(218)
		↑ CYP1A1 protein induced by TCDD	C57BL/6 mice (liver)	(404)
			C57BL/6 mice (lung)	(218)
			C57BL/6 mice (kidney)	(218)
			C57BL/6 mouse hepatocytes	(404)
	Activity	↑ CYP1A1 (EROD) activity	C57BL/6 mice (liver)	(404)
			C57BL/6 mice (lung)	(218)

			C57BL/6 mouse hepatocytes	(404)
		↔ CYP1A1 (EROD) activity	C57BL/6 mice (kidney)	(218)
		↑ CYP1A1 (EROD) activity induced by TCDD	C57BL/6 mice (liver)	(404)
			C57BL/6 mice (lung)	(218)
			C57BL/6 mice (kidney)	(218)
			C57BL/6 mouse hepatocytes	(404)
CYP1A2				
Mouse	mRNA	↑ CYP1A2 mRNA	C57BL/6 mice (liver)	(404)
		↔ CYP1A2 mRNA	C57BL/6 mice (lung)	(218)
			C57BL/6 mice (kidney)	(218)
			C57BL/6 mice (heart)	(218)
		↑ CYP1A2 mRNA induced by TCDD	C57BL/6 mice (lung)	(218)
		↔ CYP1A2 mRNA induced by TCDD	C57BL/6 mice (liver)	(404)
			C57BL/6 mice (kidney)	(218)
			C57BL/6 mice (heart)	(218)
	Protein	↑ CYP1A2 protein	C57BL/6 mice (liver)	(404)
		↔ CYP1A2 protein	C57BL/6 mice (lung)	(218)
			C57BL/6 mice (kidney)	(218)
		↑ CYP1A2 protein induced by TCDD	C57BL/6 mice (lung)	(218)
		↔ CYP1A2 protein induced by TCDD	C57BL/6 mice (liver)	(404)
			C57BL/6 mice (kidney)	(218)
	Activity	↑ CYP1A2 (MROD) activity	C57BL/6 mice (liver)	(404)
		↔ CYP1A2 (MROD) activity	C57BL/6 mice (lung)	(218)
			C57BL/6 mice (kidney)	(218)
		↑ CYP1A2 (MROD) activity induced by TCDD	C57BL/6 mice (lung)	(218)
		↔ CYP1A2 (MROD) activity induced by TCDD	C57BL/6 mice (liver)	(404)
			C57BL/6 mice (kidney)	(218)
CYP1B1				
Mouse	mRNA	↑ CYP1B1 mRNA	C57BL/6 mice (liver)	(404)
			C57BL/6 mice (lung)	(218)

			C57BL/6 mice (kidney)	(218)
		↔ CYP1B1 mRNA	C57BL/6 mice (heart)	(218)
		↑ CYP1B1 mRNA induced by TCDD	C57BL/6 mice (liver)	(404)
			C57BL/6 mice (kidney)	(218)
			C57BL/6 mice (heart)	(218)
		↔ CYP1B1 mRNA induced by TCDD	C57BL/6 mice (lung)	(218)
	Protein	↑ CYP1B1 protein	C57BL/6 mice (lung)	(218)
			C57BL/6 mice (kidney)	(218)
		↔ CYP1B1 protein	C57BL/6 mice (liver)	(404)
		↑ CYP1B1 protein induced by TCDD	C57BL/6 mice (liver)	(404)
			C57BL/6 mice (kidney)	(218)
		↔ CYP1B1 protein induced by TCDD	C57BL/6 mice (lung)	(218)
CYP2B1/2				
Rat	mRNA	↔ CYP2B1/2 mRNA	Fischer 344 rats (liver)	(403)
	Protein	↔ CYP2B1 protein	Fischer 344 rats (liver)	(403)
CYP2E1				
Rat	Protein	↔ CYP2E1 protein	Fischer 344 rats (liver)	(403)
CYP REGULATION: AHR				
Mouse	Activity	↑ AHR-dependent XRE-luciferase activity	C57BL/6 mouse hepatocytes	(404)
		↑ AHR-dependent XRE-luciferase activity induced by TCDD	C57BL/6 mouse hepatocytes	(404)
	---	↑ AHR nuclear accumulation	C57BL/6 mouse hepatocytes	(404)

1.5. Rationale, hypotheses, and objectives

1.5.1. Rationale

ATO^{III} has evolved from an environmental toxicant to become an indispensable component of the standard of care, along with all-trans-retinoic acid, for the treatment of APL. The clinical success of ATO^{III} in APL patients has opened the door for a plethora of studies investigating its potential efficacy in other hematologic malignancies in addition to solid tumors (203; 216). However, being one of arsenic compounds, ATO^{III} retains at its core the hypertoxic characteristics of that notorious heavy metalloid. The innate toxicity of ATO^{III} results in a constellation of side effects and complications in APL patients (212) including hepatotoxicity (213) which can be severe enough to

result in treatment discontinuation (214). Moreover, these toxicities may stand as a major hurdle against employing ATO^{III} in the treatment of other types of cancer especially solid tumors, where a worse toxicity profile is expected, because much higher ATO^{III} doses, than those used in APL, are required to compensate for the rapid ATO^{III} renal clearance and allow sufficient uptake of it by the tumor mass (215; 216).

As an inorganic arsenical, ATO^{III} undergoes progressive metabolism into a network of methylated intermediates/products, which can, at least partly (19), be held responsible for the overall toxic outcome of exposure to the parent inorganic molecule. Beside methylated metabolites, the sulfur-containing thio-methylated arsenicals, including $MMMTA^{V}$, have been also reported in humans orally exposed to iAs-contaminated drinking water (46; 47) as well as APL patients receiving ATO^{III} (26; 48). Interestingly, some studies have reported significant toxicity for some thioarsenicals that may even exceed that of iAs (43; 45).

While oxidative stress is strongly agreed upon as a common theme of the body-wide ATO^{III}-mediated organ toxicity, such as hepatic (405; 406), renal (407), and cardiac (408) toxicities, the definitive mechanism underlying these toxic events is still lacking. Regarding hepatotoxicity, since the liver is the metabolic powerhouse of the body, it is reasonable to think of hepatic metabolic enzyme systems as a vulnerable target for ATO^{III}. In fact, arsenic-based compounds are known to interfere with the function of a multitude of enzymes, resulting in serious biochemical derangements (50). The hepatic abundance of CYP enzymes reflects their major contribution to metabolic biotransformation. This contribution is not limited to xenobiotics, notably drugs, metabolism (268), but it also extends to catalyzing homeostatic transformation of endobiotics such as arachidonic acid (AA) (409). Also, the abundance of hepatic CYP monooxygenases makes them more likely to be targeted by ATO^{III}.

CYP1A enzymes (CYP1A1 and CYP1A2) are members of the CYP superfamily which play a pivotal role in the endobiotic metabolism (410) and the biotransformation of various commercially available drugs (275; 411-414), therefore, modifying their activity can eventually lead to a disease state (410) or clinically significant drug interactions (415), respectively.

Moreover, CYP1A enzymes are prominently involved in the metabolic transformation of environmental toxicants. The outcome of exposure to these toxicants is determined by CYP1A enzymes which play a crucial role in either mediating or mitigating the biological effects of these

hazardous chemicals. In fact, CYP1A enzymes have drawn significant attention because of their infamous implication in the bioactivation of procarcinogens such as the PAHs; e.g. 3-MC and B[a]P (275; 416-419). These compounds represent the prototypical activators of the AHR which regulates CYP1A expression through its XRE at the promoter region flanking CYP1A1 and CYP1A2 genes. For instance, exposure to the PAHs associated with cigarette smoking results in higher levels of CYP1A1 and CYP1A2 in smokers, especially in the lung cells, compared with non-smokers (420-423).

Several studies over the last few decades have reported that various arsenic compounds are able to differentially modulate the expression of CYP1A1 and CYP1A2 at different levels of their signaling pathway. Because of the environmental omnipresence of the PAHs and other AHR-activating pollutants that renders co-exposure to them almost inescapable, these studies have also investigated the effect of different arsenicals on the inducible expression of CYP1A1 and CYP1A2 mediated by AHR-ligands such as the halogenated aromatic hydrocarbon; TCDD (14).

Considering that polypharmacy is common among cancer patients, especially the elderly; the possible alteration of the drug-metabolizing CYP enzymes, such as CYP1A1 and CYP1A2, by ATO^{III} can result in inevitable drug-drug interactions that may affect the ultimate health outcomes of the co-administered medications. Moreover, such alteration may render ATO^{III}-treated patients vulnerable to detrimental health effects upon exposure to the widely spread AHR-activating pollutants. Characterizing the possible modulatory effect of ATO^{III} on both constitutive and inducible levels of CYP1A1 and CYP1A2 and understanding the underlying mechanisms may help to decipher how ATO^{III} can negatively impact APL patients in an attempt to develop mitigation strategies.

1.5.2. Hypotheses

1- Exposure to ATO^{III} differentially modulates basal and inducible expression of hepatic AHR-regulated phase I enzymes, both *in vivo* and *in vitro*.

2- Exposure to $MMMTA^{V}$ differentially modulates basal and inducible expression of hepatic AHR-regulated phase I enzymes, both *in vivo* and *in vitro*.

3- Differential modulation of hepatic CYP enzymes expression by ATO^{III} exposure *in vivo* is not limited to those regulated by AHR.

1.5.3. Objectives

1- To examine the effects of ATO^{III} in the absence and presence of TCDD on hepatic CYP1A1 and CYP1A2 *in vivo* using C57BL/6 mice.

2- To determine the effects of ATO^{III} in the absence and presence of TCDD on CYP1A1 and CYP1A2 *in vitro* using mouse hepatoma Hepa1c1c7 cells and human hepatocellular carcinoma HepG2 cells, and to investigate the underlying molecular mechanisms of these effects.

3- To examine the effects of $MMMTA^{V}$ in the absence and presence of TCDD on hepatic CYP1A1 and CYP1A2 *in vivo* using C57BL/6 mice.

4- To determine the effects of $MMMTA^{V}$ in the absence and presence of TCDD on CYP1A1 and CYP1A2 *in vitro* using mouse hepatoma Hepa1c1c7 cells and human hepatocellular carcinoma HepG2 cells, and to investigate the underlying molecular mechanisms of these effects.

5- To explore the effects of ATO^{III} on other hepatic non-AHR-regulated CYP enzymes as well as cellular transporters *in vivo* using C57BL/6 mice.

CHAPTER 2.

MATERIALS AND METHODS

Portions of this chapter have been published in:

1. **El-Ghiaty MA**, Alqahtani MA, El-Kadi AOS. Down-regulation of hepatic cytochromes P450 1A1 and 1A2 by arsenic trioxide (ATO) in vivo and in vitro: A role of heme oxygenase 1. *Chem Biol Interact*. 2022 Sep 1;364:110049. doi: 10.1016/j.cbi.2022.110049.

2. **El-Ghiaty MA**, Alqahtani MA, El-Kadi AOS. Arsenic trioxide (ATO) up-regulates cytochrome P450 1A (CYP1A) enzymes in murine hepatoma Hepa-1c1c7 cell line. *Environ Toxicol Pharmacol*. 2023 Aug;101:104214. doi: 10.1016/j.etap.2023.104214.

3. **El-Ghiaty MA**, Alqahtani MA, El-Kadi AOS. Modulation of cytochrome P450 1A (CYP1A) enzymes by monomethylmonothioarsonic acid (MMMTAV) in vivo and in vitro. *Chem Biol Interact*. 2023 May 1;376:110447. doi: 10.1016/j.cbi.2023.110447.

4. **El-Ghiaty MA**, Alqahtani MA, El-Mahrouk SR, Isse FA, Alammari AH, El-Kadi AOS. Alteration of hepatic cytochrome P450 expression and arachidonic acid metabolism by arsenic trioxide (ATO) in C57BL/6 mice. *Biol Trace Elem Res*. 2024. doi: 10.1007/s12011-024-04225-1. (in press)

2.1. Chemicals and materials

Arsenic trioxide (As_2O_3; 99.5%) was purchased from Acros Organics (Geel, Belgium). Monomethyl arsonothioic acid (CH_5AsO_2S; 80%) and 2,3,7,8-tetrachlorodibenzo-*p*-dioxin ($C_{12}H_4Cl_4O_2$) were purchased from Toronto Research Chemicals (Toronto, ON, Canada). Tin (IV) mesoporphyrin (IX) (SnMP) was purchased from Frontier Scientific (Logan, UT, USA). Sodium (meta)arsenite ($NaAsO_2$; ≥90%), 3-(4,5-dimethylthiazol-2-yl)-2,5-diphenyltetrazolium bromide (MTT), 7-ethoxyresorufin, 7-methoxyresorufin, resorufin, fluorescamine, actinomycin-D (Act-D), cycloheximide (CHX), acetonitrile, ethyl acetate, glacial acetic acid, isopropyl alcohol, methanol, magnesium chloride hexahydrate, potassium phosphate dibasic, potassium phosphate monobasic, reduced nicotinamide adenine dinucleotide (NADPH), protease inhibitor cocktail, bovine serum albumin (BSA), and sterile-filtered dimethyl sulfoxide (DMSO) were purchased from MilliporeSigma (Burlington, MA, USA). The endogenous standards (±)5-, (±)8-, (±)11-, (±)12-, (±)15-, (±)16-, (±)17-, (±)18-, (±)19-, and 20-HETE and the deuterated internal standard 20-HETE-d_6 were purchased from Cayman Chemical (Ann Arbor, MI, USA). Dulbecco's Modified Eagle Medium (DMEM), Minimum Essential Medium Alpha (MEM α), phosphate-buffered saline (PBS), and Trypsin-EDTA were purchased from Gibco (Waltham, MA, USA). TRIzol™ Reagent and UltraPure™ DNase/RNase-Free Distilled Water were purchased from Invitrogen (Waltham, MA, USA). Real-time PCR primers were synthesized by Integrated DNA Technologies (Coralville, IA, USA). High-Capacity cDNA Reverse Transcription Kit, SYBR™ Green PCR Master Mix, MicroAmp™ Optical 96-Well Reaction Plates, MicroAmp™ EnduraPlate™ Optical 384-Well Reaction Plates, and MicroAmp™ Optical Adhesive Films were purchased from Applied Biosystems (Waltham, MA, USA). Polyvinylidene difluoride (PVDF) membrane and 2X Laemmli Sample Buffer were purchased from Bio-Rad Laboratories (Hercules, CA, USA). 6X Laemmli Sample Buffer was purchased from Alfa Aesar (Haverhill, MA, USA). NE-PER™ Nuclear and Cytoplasmic Extraction Reagents were purchased from Thermo Scientific (Waltham, MA, USA). Anti-CYP1A1 (sc-393979), anti-CYP1A2 (sc-53241), anti-Ah Receptor (sc-133088), and anti-lamin B1 (sc-374015) mouse monoclonal primary antibodies were purchased from Santa Cruz Biotechnology (Dallas, TX, USA). CYP1A1 rabbit polyclonal primary antibody (ab79819), heme oxygenase 1 (HMOX1) rabbit monoclonal primary antibody (ab52947), and beta-actin (ACTB) mouse monoclonal primary antibody (ab6276), and glyceraldehyde 3-phosphate dehydrogenase (GAPDH) mouse monoclonal primary antibody (ab8245) were purchased from Abcam

(Cambridge, UK). Anti-mouse IgG HRP-linked secondary antibody (7076) and anti-rabbit IgG HRP-linked secondary antibody (7074) were purchased from Cell Signaling Technology (Danvers, MA, USA). Amersham™ ECL™ Western Blotting Detection Reagents were purchased from Cytiva (Marlborough, MA, USA). ViewPlate™ -96 Sterile and Tissue Culture Treated White 96-well Microplate with Clear Bottom and BackSeal-96/384 White Adhesive Bottom Seal for 96-well and 384-well Microplate were purchased from PerkinElmer (Waltham, MA, USA). Dual-Glo® Luciferase Assay System was purchased from Promega (Madison, WI, USA). HPLC grade water and other chemicals and materials were purchased from Fisher Scientific (Waltham, MA, USA).

2.2. Chemical hazards and safety

Arsenicals, such as ATO^{III}, iAs^{III}, and $MMMTA^{V}$, as well as TCDD are highly toxic and have strong potential of carcinogenicity to humans. Therefore, all personnel involved in this work were instructed for safe handling procedures and received comprehensive laboratory and chemical safety training provided by the Health, Safety and Environment Office of the University of Alberta. Moreover, adequate personal protective equipment (PPE); including lab coats, gloves, masks, and safety goggles; was provided to the participants and was used all the time. Contaminated materials and hazardous waste were cautiously collected separately for disposal in accordance with the University of Alberta Health, Safety and Environment Office guidelines.

2.3. Preparation of treatment agents

ATO^{III} solution was prepared by dissolving its powder in a solution of sodium hydroxide (NaOH, 5 N). A clear homogenous solution was obtained with the aid of mechanical stirring at room temperature in a glass bottle protected from light. The solution was then diluted with autoclaved Milli-Q® water (Milli-Q® Water Purification System by MilliporeSigma; Burlington, MA, USA), and was adjusted to pH 8 using hydrochloric acid (HCl, 1 N). Finally, arsenic trioxide solution was sterilized by filtration (through a 0.2 μm filter) and then stored for future use at −20 °C in sterile, airtight, and lightproof tubes.

Clear homogenous solutions of iAs^{III} and $MMMTA^{V}$ were prepared using autoclaved Milli-Q® water (Milli-Q® Water Purification System by MilliporeSigma; Burlington, MA, USA), then sterilized by filtration (through a 0.2 μm filter), and finally stored in sterile, airtight, and lightproof tubes at –20 °C for future use.

TCDD stock solution was prepared in sterile-filtered dimethyl sulfoxide (DMSO) and stored for future use at –20 °C in sterile, airtight, and lightproof tubes.

2.4. Experimental models

2.4.1. Cellular models

Both human hepatocellular carcinoma HepG2 cell line and mouse hepatoma Hepa1c1c7 cell line were employed to test our hypothesis. These liver-derived cells are *in vitro* mirrors to the actual *in vivo* behavior of the hepatocytes which, by turn, have been shown to be one of major targets for metal accumulation and toxicity upon exposure (424).

Because of their unlimited life span, relative phenotype stability, ease of handling, and wide commercial availability, hepatoma cell lines are considered indispensable *in vitro* alternative to primary human hepatocytes. Since their introduction in the 1970s, HepG2 cell line has become the most commonly used in drug metabolism and hepatotoxicity studies (425). While HepG2 cell line does not possess phenotypic characteristics identical to the liver tissue, they exhibit many differentiated hepatic functions (426) such as expressing both phase I and phase II metabolizing enzymes (427). The capability of HepG2 cell line to perform metabolic biotransformation reactions necessary for the detoxification of xenobiotics renders it a useful *in vitro* model for several toxicological studies (425). It has sensitivity to TCDD-mediated AHR induction comparable to that of primary human hepatocytes (428), therefore, it can be utilized for investigating the up-regulation of its associated CYP enzymes (429). In fact, HepG2 cell line is considered an ideal model for studying human CYP1A1 regulation (363; 430-433).

The emergence of Hepa1c1c7 cell line dates back to the 1970s when it was isolated from the BW 7756 hepatoma carried in C57 leaden mice (C57L/J) (434). Hepa1c1c7 cell line has been widely employed in investigating AHR-dependent signaling mechanisms (362; 376; 381). In this cell line, both constitutive and inducible expressions of AHR-regulated genes are much higher than those found in human or rat cell lines (435). This results in tangible and easily measurable changes in the expression of these genes in response to activators/inhibitors exposure. That's why Hepa1c1c7 cell line is considered a powerful model for elucidating the mechanistic influence of metals on the expression of the AHR-regulated genes.

2.4.1.1. Cell culture

Human hepatocellular carcinoma HepG2 cell line (ATCC HB-8065™) and mouse hepatoma Hepa1c1c7 cell line (ATCC CRL-2026™) were purchased from the American Type Culture Collection (Manassas, VA, USA). HepG2 and Hepa1c1c7 cells were maintained in Dulbecco's Modified Eagle Medium (Gibco 11995-065) and Minimum Essential Medium Alpha (Gibco 12561-056), respectively, which were supplemented with 10% thermally inactivated fetal bovine serum (MilliporeSigma F1051) and 1% Antibiotic-Antimycotic (Gibco 15240-062). Cells were grown in T-75 cell culture flasks (75 cm^2 rectangular flasks with canted neck and vent cap) in a 5% CO_2 humidified incubator at 37 °C.

2.4.1.2. Chemical treatment

Right before applying the treatment to each cell line, the working solutions of ATO^{III}, $MMMTA^{V}$, and TCDD were prepared by diluting the stock solution in the respective serum-free culture medium.

Cells were plated in 12-well cell culture plates (Corning 3513) for RNA assay, 6-well cell culture plates (Corning 3516) for protein assay, and 48-well cell culture plates (Corning 3548) for enzyme activity assays. The specific conditions of each assay, such as the duration of treatment, are detailed in its respective section.

Upon reaching ≈80% confluence, each cell line was treated in its respective serum-free culture medium with various concentrations of ATO^{III} or $MMMTA^{V}$ with or without TCDD. In the absence or presence of 1 nM TCDD, HepG2 cells were treated with (0, 1, 5, and 10 μM) ATO^{III} or $MMMTA^{V}$, while Hepa1c1c7 cells were treated with (0, 0.63, 1.25, and 2.5 μM) ATO^{III} or (0, 1, 5, and 10 μM) $MMMTA^{V}$. In all treatments, cells were not exposed to a DMSO concentration beyond 0.1% (v/v).

2.4.2. Animal model

2.4.2.1. Animal handling and ethical considerations

Male C57BL/6 mice (at age of 10–12 weeks and with average weight of 23 g) were purchased from Charles River Laboratories (Montreal, QC, Canada). To adjust to their new environment and overcome stress during transit, all mice underwent acclimatization for seven days in the animal facility of the Health Sciences Laboratory Animal Services (HSLAS) at the University of Alberta before initiating the experiment. Mice were housed in groups of four mice in each cage under

standard conditions, where food and water were available *ad libitum*, and were maintained on a 12 h light/12 h dark diurnal cycle. All experimental procedures involving animals were approved by the University of Alberta Health Sciences Animal Policy and Welfare Committee.

2.4.2.2. Experimental design and treatment protocol

Right before injecting the animals, the working solutions of ATO^{III}, iAs^{III}, and $MMMTA^{V}$ were prepared by diluting the stock solution in normal saline, while TCDD working solution was prepared in corn oil.

Mice were randomized into eight groups (12 mice/group), then intraperitoneally (IP) injected with a single dose of normal saline, ATO^{III} (8 mg/kg body weight), iAs^{III} (12.5 mg/kg body weight), $MMMTA^{V}$ (12.5 mg/kg body weight), TCDD (15 µg/kg body weight), ATO^{III} plus TCDD, iAs^{III} plus TCDD, or $MMMTA^{V}$ plus TCDD. The first group (control; n = 12) received normal saline (0.2 mL) and corn oil (0.2 mL). The second group (ATO^{III}; n = 12) received ATO^{III} (0.2 mL) and corn oil (0.2 mL). The third group (iAs^{III}; n = 12) received iAs^{III} (0.2 mL) and corn oil (0.2 mL). The fourth group ($MMMTA^{V}$; n = 12) received $MMMTA^{V}$ (0.2 mL) and corn oil (0.2 mL). The fifth group (TCDD; n = 12) received normal saline (0.2 mL) and TCDD (0.2 mL). The sixth group (ATO^{III} and TCDD; n = 12) received ATO^{III} (0.2 mL) and TCDD (0.2 mL). The seventh group (iAs^{III} and TCDD; n = 12) received iAs^{III} (0.2 mL) and TCDD (0.2 mL). The eighth group ($MMMTA^{V}$ and TCDD; n = 12) received $MMMTA^{V}$ (0.2 mL) and TCDD (0.2 mL).

The animals were euthanized, through IP injection of pentobarbital sodium (Euthansol®), at 6 (n = 6) or 24 h (n = 6) after the injection, and death was confirmed by cervical dislocation. Liver tissues were rapidly excised and washed in ice-cold phosphate-buffered saline, then flash frozen in liquid nitrogen and ultimately stored at –80 °C until further analysis.

2.5. Experimental methods and protocols

2.5.1. Assessment of cell viability

The effect of ATO^{III} and $MMMTA^{V}$ on cell viability was assessed using the MTT reduction assay as previously described (363). The assay is based on measuring the optical density of formazan dye; a product formed through the reduction of tetrazolium salt (MTT) in living cells via mitochondrial enzymes, thus reflecting the number of viable cells.

In brief, cells were seeded onto 48-well cell culture plates and incubated for 24 h at 37 °C in a 5% CO_2 humidified incubator to reach ≈80% confluence. The treatments were applied, and after 24 h-incubation, the medium was discarded and replaced with serum-free culture medium containing 1.2 mM MTT. After 2 h-incubation, the medium was discarded, and the formed formazan crystals were dissolved in DMSO. The optical density of the wells was measured at a wavelength of 570 nm using the Synergy™ H1 Hybrid Multi-Mode Reader (BioTek Instruments; Winooski, VT, USA).

To determine the non-toxic concentrations of ATO^{III} to be used in HepG2 cell line, the cells were challenged with increasing concentrations of ATO^{III} (0, 5, 10, 15, 20, 25, and 30 μM). Based on this experiment, three relatively non-toxic concentrations of ATO^{III} (1, 5, and 10 μM) were selected and cytotoxicity was reassessed in the absence or presence of 1 nM TCDD. Moreover, the effect of tin (IV) mesoporphyrin (IX) (SnMP) (5 μM) on cell viability was also evaluated in HepG2 cells treated with 1 and 5 μM ATO^{III} in the absence or presence of 1 nM TCDD.

A screening for the non-cytotoxic ATO^{III} concentrations in Hepa1c1c7 cell line was conducted by challenging the cells with ascending ATO^{III} concentrations (0, 0.5, 1, 1.5, 2, 2.5, 3, 3.5, 4, 4.5, and 5 μM). Consequently, three relatively safe ATO^{III} concentrations (0.63, 1.25, and 2.5 μM) were chosen and re-evaluated for cytotoxicity with or without 1 nM TCDD.

For $MMMTA^{V}$, HepG2 cells were initially challenged with increasing concentrations of $MMMTA^{V}$ (0, 1, 5, 10, 25, 50, 75, 100, 500, and 1000 μM). Accordingly, three relatively safe concentrations of $MMMTA^{V}$ (1, 5, and 10 μM) were selected, and the assay was repeated in the absence or presence of 1 nM TCDD. The same concentrations of $MMMTA^{V}$ (1, 5, and 10 μM) were used in Hepa1c1c7 cell line experiments as well.

2.5.2. RNA extraction and cDNA synthesis

The cells were seeded onto 12-well cell culture plates and incubated for 24 h at 37 °C in a 5% CO_2 humidified incubator to reach ≈80% confluence. The cells were then incubated for 6 h with the treatments specified in section (2.4.1.2). For the time-dependent experiment, Hepa1c1c7 cells underwent incubation with 0 and 10 μM $MMMTA^{V}$ for 3, 6, 12, and 24 h.

Total RNA was isolated from the cells, treated as described above, or frozen liver tissues, excised from the aforementioned mice groups, using TRIzol™ Reagent according to the manufacturer's

instructions. RNA quantity and quality were determined by measuring the absorbance at 260 nm and the 260/280 ratio, respectively, using the Synergy™ H1 Hybrid Multi-Mode Reader (BioTek Instruments; Winooski, VT, USA). Thereafter, the first-strand cDNA was synthesized using the High-Capacity cDNA Reverse Transcription Kit according to the manufacturer's instructions. Briefly, 1.25 µg of total RNA, in 10 µL UltraPure™ DNase/RNase-Free Distilled Water, from each sample was added to a mixture of 2 µL 10X RT Buffer, 2 µL 10X RT Random Primers, 0.8 µL 25X dNTP Mix (100mM), 1 µL MultiScribe™ Reverse Transcriptase (50U/µL), and 4.2 µL UltraPure™ DNase/RNase-Free Distilled Water in a MicroAmp™ Optical 96-Well Reaction Plate. Inside the Mastercycler® nexus GSX1 (Eppendorf AG; Hamburg, Germany), the final reaction mixture was kept at 25 °C for 10 min, heated to 37 °C for 120 min, heated for 85 °C for 5 min, and finally cooled to 4 °C.

2.5.3. Quantitative real-time PCR (qPCR)

For quantitative analysis of specific mRNA expression, real-time polymerase chain reaction amplification of target genes in the prepared cDNA was performed using the QuantStudio™ 5 Real-Time PCR System (Applied Biosystems; Waltham, MA, USA). 1 µL from each cDNA sample was added in a MicroAmp™ EnduraPlate™ Optical 384-Well Reaction Plate to a reaction mixture contained 0.04 µL of 12 µM forward primer and 0.04 µL of 12 µM reverse primer (Table 2.1), 10 µL of SYBR™ Green PCR Master Mix, and 8.92 µL of UltraPure™ DNase/RNase-Free Distilled Water. The thermocycling conditions were initiated at 95 °C for 10 min, followed by 40 PCR cycles of denaturation at 95 °C for 15 sec and annealing/extension at 60 °C for 1 min. After completion of the amplification cycles, a melting curve analysis was performed to ascertain the specificity of the primers and the purity of PCR amplicons.

The real time-PCR data were analyzed using the relative gene expression ($\Delta\Delta C_t$) method as described in the Applied Biosystems User Bulletin No. 2 and further explained by Kenneth Livak and Thomas Schmittgen (436). Briefly, the ΔC_t value was calculated in each sample for each gene of interest as follows: $(C_t)_{\text{target gene}} - (C_t)_{\text{reference gene}}$, with beta-actin being the reference gene. Calculation of the relative changes in the expression level of one specific gene ($\Delta\Delta C_t$) was performed by subtracting $(\Delta C_t)_{\text{untreated control}}$ from the (ΔC_t) of the corresponding treatment groups. The values and ranges given in different figures were presented as follows: $2^{-\Delta\Delta Ct} \pm$ SEM, where SEM is the standard error of the mean of the $2^{-\Delta\Delta Ct}$ value.

Table 2.1. Human and mouse primer sequences used in real-time PCR experiments.

Gene	Forward primer	Reverse primer
Human		
ACTB	CTGGCACCCAGCACAATG	GCCGATCCACACGGAGTACT
CYP1A1	CTATCTGGGCTGTGGGCAA	CTGGCTCAAGCACAACTTGG
CYP1A2	CTGGGCACTTCGACCCTTAC	TCTCATCGCTACTCTCAGGGA
HMOX1	ATGGCCTCCCTGTACCACATC	TGTTGCGCTCAATCTCCTCCT
Mouse		
Actb	TATTGGCAACGAGCGGTTCC	GGCATAGAGGTCTTTACGGATGTC
Pla2g4a	GGTGTCCTTTGCCTCTCTTCA	TTCTGTGAGCCAGAAACTCCC
Cyp1a1	GGTTAACCATGACCGGGAACT	TGCCCAAACCAAAGAGAGTGA
Cyp1a2	TGGAGCTGGCTTTGACACAG	CGTTAGGCCATGTCACAAGTAGC
Cyp1b1	AATGAGGAGTTCGGGCGCACA	GGCGTGTGGAATGGTGACAGG
Cyp2a4	TCACCATCTATCTGGGATCTCG	CCCCGAAGACGATTGAGCTAA
Cyp2a5	TGGTCCTGTATTCACCATCTACC	ACTACGCCATAGCCTTTGAAAA
Cyp2b9	GCTGCAGCTCAGCTAGTTATGC	GCCCACTGGCAAAAAATATACC
Cyp2b10	GGGAACCTCTTGCAGATG	CCCAGGTGCACTGTGAA
Cyp2b19	CACAAAGCCTTCCTCACCGAT	ACAAGCAAGCAACCCACACTC
Cyp2c29	TGGTCCACCCAAAAGAAATTGA	GCAGAGAGGCAAATCCATTCA
Cyp2c37	CACGAGGCGTTTCTCACTCA	AGGGCTGCTCAGAATCTTTGT
Cyp2c38	GCATTACTTTTAGCAATGGAAACAGT	CCACAAGACACTGTGCTTCTTCTC
Cyp2c39	GAGGAAGCATTCCAATGGTAGAA	TGTGAAGCGCCTAATCTCTTTC
Cyp2c40	TCCGGTTTTTGACAAGGTTTCTAC	TGCCCAAGTTCCTCAAGGTATTC
Cyp2c44	CTTTTCAACGAGCGATTCCC	TGTTTCTCCTCCTCGATCTTGC
Cyp2c65	ACAACCCAAAGACGGAGTTTAC	CTGTCCCAGCAGCAAACAGAT
Cyp2c66	GGAGTTTGCTGGAAGAGGAACC	GCGTCTCATCTCTTTCCAGGTC
Cyp2d10	TCCACTGAATTTGCCACGC	TCAGCACGGAGGACATGTTG
Cyp2d22	CCACGCTTCATCAGGCTACTG	CACATTCAGGAACATGGGTAGGA
Cyp2e1	CCCAAGTCTTTAACCAAGTTGGC	CTTCCATGTGGGTCCATTATTGA
Cyp2j5	TGTGAATCGCTTTATGACACCG	TGATGGGTCTCCTCCTGAATG
Cyp2j6	TTAGCCACGATCTGGGCAG	CTGGGGGATAGTTCTTGGGG
Cyp2j9	GGGAATGTTCTAAGCCTGGATTT	GAGTGACTGGGCGATTCATAAA
Cyp2j11	GTATGATGGACAGTCACCGGGA	GGTCCAGAGCAGTGCAGATGA
Cyp2j13	GGGAAGAGGAAGGACAGCCTT	GCAGCAGCTCCTGAAACTGACT
Cyp3a11	AGCAGGGATGGACCTGG	CGGTAGAGGAGCACCAA
Cyp3a13	GACGATTCTTGCTTACCAGAAGG	CCGGTTTGTGAAGGTAGAGTAAC
Cyp4a10	GTGCTGAGGTGGACACATTCAT	TGTGGCCAGAGCATAGAAGATC
Cyp4a12	TGACCCCAGCTTTCCACTATG	TTGTTCAGGTCCTCAACTGCC
Cyp4a14	GTCTCTCGGGGAGCAATATACG	ACCAATCCAGGGAGCAAAGAA
Cyp4f13	CCCTAAACCGAGCTGGTTCTG	GAGTCGCAGGATTGGGTACAC
Cyp4f15	CCTGTGCTGTGTTCCTTAGGG	GACGGGAAATGACCGTGACT
Cyp4f16	CCGCCTCAGTTGTTTCCCTC	TGCCCAAGTGACCTGAAAACC
Cyp4f18	CTGCATCCTCCCGTCACTG	GGATTGTGATGTGTCCCGAAA
Ptgs1	GACTATGGGGTTGAGGCACTG	CTCCAGGGTAATCTGGCACAC
Ptgs2	CTGGTGCCTGGTCTGATGATG	GGCAATGCGGTTCTGATACTG
Alox5	GCCATCTAAGGCCTTGCCTC	CAGACCACCTAGGCCCAAGA
Alox12	TGGCAGGAGACAATGCCTTAG	GGTCCATCCTCAGCATGACAA
Alox15	CTACAGCTCATTGTGTCCCCC	ACTATGGAAAGCGGGCTCTTG

Hmox1	GTGATGGAGCGTCCACAGC	TGGTGGCCTCCTTCAAGG
Aqp3	GCTTTTGGCTTCGCTGTCAC	TAGATGGGCAGCTTGATCCAG
Aqp7	AATATGGTGCGAGAGTTTCTGG	AACCCAAGTTGACACCGAGAT
Aqp9	TGGTGTCTACCATGTTCCTCC	AACCAGAGTTGAGTCCGAGAG
Abcb1	CAGCAGTCAGTGTGCTTACAA	ATGGCTCTTTTATCGGCCTCA
Abcc1	CATGTGGACGTGTTTCGAGATT	CACGAGCTGAACAAGCACAAG
Abcc2	GTGTGGATTCCCTTGGGCTTT	CACAACGAACACCTGCTTGG
Abcc3	AGTCTTCGGGAGTGCTCATCA	AGGATTTGTGTCAAGATTCTCCG
Abcc4	ACGCTTCCCAGACTTTGCA	AACAACACGGGAGCCTTCAG
Abcc5	CCCTTCCGGACCACTACCA	TGTAGGAGAAAAGTCCAGCATTGT
Abcc6	CAGCTCAAACAACTGGAATCTGA	GCTCGAAGTGTCCAGAGTCCTT

2.5.4. Preparation of cell lysate and protein extraction

2.5.4.1. Total protein extraction

Cells were seeded onto 6-well cell culture plates and incubated for 24 h at 37 °C in a 5% CO_2 humidified incubator to reach ≈80% confluence. The cells were then incubated for 24 h with the treatments specified in section (2.4.1.2).

Cells were collected in ice-cold mixture of protease inhibitor cocktail (5 µL/mL) and a lysis buffer containing 50 mM HEPES, 0.5 M sodium chloride, 1.5 mM magnesium chloride, 1 mM EDTA, 10% (v/v) glycerol, and 1% Triton X-100. Total cell lysates were then incubated on ice for 1 h, with intermittent vortex mixing every 10 min, followed by centrifugation at 12000 × g for 10 min at 4 °C. The resulting supernatant was collected and stored at –80 °C for further analysis. Thereafter, total protein concentration in each sample was determined by the Lowry protein assay using bovine serum albumin as a standard (437).

2.5.4.2. Nuclear protein extraction

Hepa1c1c7 cells were incubated in 6-well cell culture plates for 24 h in a humidified 5% CO_2 incubator at 37 °C until ≈80% confluence. Thereafter, cells underwent 3 h-incubation with 0 and 2.5 µM ATO^{III}.

On ice, nuclear protein extraction was done using ice-cold NE-PER™ Nuclear and Cytoplasmic Extraction Reagents (Thermo Scientific 78833) according to the manufacturer's instructions. The resulting nuclear protein fractions were collected and stored for further analysis at –80 °C. Afterwards, the Lowry protein assay was used for protein quantification in each sample, with bovine serum albumin being the standard (437).

2.5.5. Preparation of tissue homogenate and microsomal protein extraction

Liver microsomes (from the 24 h-treated animals) were prepared by differential centrifugation of the homogenized tissues as previously described (438). In brief, individual frozen liver tissues were cut into pieces (0.5 g) and homogenized separately in 2 mL ice-cold homogenization mixture of 0.25 M sucrose solution containing protease inhibitor cocktail (5 µL/mL). The homogenate was centrifuged at 10000 × g for 20 min at 4 °C, then the resulting supernatant (S9 fraction) was separated and re-centrifuged at 100000 × g for 60 min at 4 °C, yielding the microsomal pellet and the cytosolic fraction. The microsomal pellet was reconstituted in ice-cold sucrose-protease inhibitor cocktail mixture and stored at –80 °C until further analysis. Thereafter, total protein concentration in each sample was determined by the Lowry protein assay using bovine serum albumin as a standard (437).

2.5.6. Western blotting analysis

Western blotting analysis of target proteins was performed using denaturing gel electrophoresis as previously described (439). Total cell lysate (150 µg for Hepa1c1c7 cells and 50 µg for HepG2 cells) or microsomal (15 µg) proteins were mixed with an equal volume of 2X, or a suitable volume of 6X, Laemmli Sample Buffer, boiled for 5 min, separated by 10% sodium dodecyl sulfate-polyacrylamide gel electrophoresis (SDS-PAGE), and electrophoretically transferred to polyvinylidene difluoride (PVDF) membrane. Protein blots were then blocked overnight at 4 °C in a blocking buffer (pH 7.4) containing 0.15 M sodium chloride, 3 mM potassium chloride, 25 mM UltraPure™ Tris Buffer, 0.1% (v/v) Tween® 20, 5% (w/v) skimmed dry milk, and 2% (w/v) bovine serum albumin.

After blocking, the blots were probed with antibodies through 2 h-incubation with primary antibodies at 4 °C, followed by 45 min-incubation with horseradish peroxidase (HRP)-conjugated IgG secondary antibodies at room temperature. Finally, protein bands were visualized by the ChemiDoc™ Imaging System (Bio-Rad Laboratories; Hercules, CA, USA) using the enhanced chemiluminescence (ECL) method.

Using the GeneTools Analysis Software, version 4.3.9.0 (Syngene; Cambridge, UK), the intensity of target protein bands was quantified relative to the signals obtained for either beta-actin (ACTB) or glyceraldehyde 3-phosphate dehydrogenase (GAPDH) (as loading controls) and was expressed

as percentage of the untreated control (set at 100%). Of note, AHR protein bands intensity was measured relative to the lamin B1 (LMNB1) signals (as a nuclear loading control).

2.5.7. Determination of CYP1A1 and CYP1A2 catalytic activities in intact cells

In a monolayer of intact living cells, 7-ethoxyresorufin was used as a substrate for evaluating CYP1A1-dependent 7-ethoxyresorufin O-deethylase (EROD) activity, while CYP1A2-dependent 7-methoxyresorufin O-demethylase (MROD) activity was assessed using 7-methoxyresorufin, as previously reported (335).

Cells were seeded onto 48-well cell culture plates and incubated for 24 h at 37 °C in a 5% CO_2 humidified incubator to reach ≈80% confluence. The cells were then incubated for 24 h with the treatments specified in section (2.4.1.2). Thereafter, the medium was discarded and replaced with 200 µL of serum-free medium containing 2 µM 7-ethoxyresorufin or 7-methoxyresorufin. The fluorescence of resorufin formed in the wells was recorded every 1 min at excitation and emission wavelengths of 550 nm and 585 nm, respectively, using the Synergy™ H1 Hybrid Multi-Mode Reader (BioTek Instruments; Winooski, VT, USA). The amount of resorufin formed was determined by a standard curve of known resorufin concentrations.

Enzymatic activity was normalized for cellular protein content after determination of protein concentration in each well by a fluorescence-based protein assay using fluorescamine, as previously described (440). The linear rate of resorufin formation was expressed as pmol/min/mg protein.

For the heme oxygenase 1 (HMOX1) inhibition experiment, HepG2 cells underwent a 24 h-incubation with 0 and 1 µM ATO^{III} in the absence or presence of 1 nM TCDD and/or 5 µM of the heme oxygenase 1 (HMOX1) inhibitor, tin (IV) mesoporphyrin (IX) (SnMP). Of note, SnMP was dissolved in sterile-filtered dimethyl sulfoxide (DMSO), then a working solution was freshly prepared in serum-free medium (the final DMSO concentration did not exceed 0.1% (v/v)).

2.5.8. Determination of hepatic microsomal CYP1A1 and CYP1A2 catalytic activities

CYP1A1-dependent EROD and CYP1A2-dependent MROD activities were assessed using 7-ethoxyresorufin and 7-methoxyresorufin as substrates, respectively.

Liver microsomes from each sample of the 24 h-treated animals (0.2 mg protein/mL) were incubated in an incubation buffer (5 mM magnesium chloride hexahydrate-supplemented 100 mM

potassium phosphate buffer, pH 7.4) mixed with 2 μM of the substrate (7-ethoxyresorufin for the EROD or 7-methoxyresorufin for the MROD assays) at 37 °C in a shaking water bath (50 rpm). The mixture was pre-equilibrated for 5 min, then the reaction was initiated by adding 0.6 mM NADPH. After incubation at 37 °C (1 min for the EROD and 3 min for the MROD assays), the reaction was terminated by adding 0.5 mL ice-cold methanol. The fluorescence of the formed resorufin in the resulting supernatant, after precipitating protein pellet, was measured using the Synergy™ H1 Hybrid Multi-Mode Reader (BioTek Instruments; Winooski, VT, USA) at excitation and emission wavelengths of 550 nm and 585 nm, respectively. The amount of resorufin formed was determined by a standard curve of known resorufin concentrations. Resorufin formation was linear with the incubation time and protein amount.

Enzymatic activities were expressed as picomoles of resorufin formed per minute and per milligram of microsomal proteins.

2.5.9. XRE-dependent luciferase reporter gene assay

HepG2 and Hepa1c1c7 cells, that were employed in the reporter gene assay, underwent stable transfection with the pGudLuc7.5, a firefly luciferase reporter gene plasmid which carries 20 copies of the xenobiotic response element (XRE) (441). These cells, with highly AHR-responsive reporter gene constructs, were generously donateded by the late Dr. Michael S. Denison (University of California, Davis, CA, USA).

Transfected cells were seeded onto the ViewPlate™ -96 Sterile and Tissue Culture Treated White 96-well Microplate with Clear Bottom and incubated for 24 h at 37 °C in a 5% CO_2 humidified incubator to reach ≈80% confluence. In the absence or presence of 1 nM TCDD, transfected HepG2 cells were incubated for 24 h with ATO^{III} (0 and 5 μM) or $MMMTA^{V}$ (0 and 10 μM), while transfected Hepa1c1c7 cells were incubated for 24 h with ATO^{III} (0 and 2.5 μM) or $MMMTA^{V}$ (0 and 10 μM). Luciferase assay was performed using the Dual-Glo® Luciferase Assay System (Promega E2920) according to the manufacturer's instructions.

Briefly, the Dual-Glo® Luciferase Reagent was prepared by mixing the buffer with the lyophilized substrate, then added to the cells in a volume equal to the culture medium present in the wells, with continuous shaking for 20 min. The bottom of the plate was covered by the BackSeal-96/384 White Adhesive Bottom Seal for 96-well and 384-well Microplate, then the luminescence signal from

luciferase/luciferin interaction was measured in each well using the Synergy™ H1 Hybrid Multi-Mode Reader (BioTek Instruments; Winooski, VT, USA).

2.5.10. Assessment of CYP1A1 transcriptional regulation

Hepa1c1c7 cells were incubated in 12-well cell culture plates for 24 h in a humidified 5% CO_2 incubator at 37 °C until ≈80% confluence. Thereafter, cells underwent preincubation with 5 µg/mL actinomycin-D (Act-D) for 30 min, to block mRNA synthesis, then 6 h-treatment with either 2.5 µM ATO^{III} or 1 nM TCDD. Total RNA isolation from the cells was carried out using the method described above, and *Cyp1a1* mRNA expression was quantitatively analyzed via qPCR.

2.5.11. Assessment of *Cyp1a1* mRNA stability

Act-D chase assay was used to evaluate the effect of ATO^{III} and $MMMTA^{V}$ on *Cyp1a1* mRNA stability by measuring and comparing its half-life in the absence or presence of ATO^{III} or $MMMTA^{V}$. The assay is based on inducing *Cyp1a1* mRNA synthesis, then monitoring its gradual decay over time after inhibiting *de novo* mRNA synthesis using Act-D.

In 12-well cell culture plates, Hepa1c1c7 cells were incubated in a 5% CO_2 humidified incubator at 37 °C for 24 h till ≈80% confluence was reached. The cells were then pretreated with 1 nM TCDD for 12 h. Thereafter, cells were incubated with 5 µg/mL Act-D for 30 min, to inhibit further mRNA synthesis, prior to a treatment with 2.5 µM ATO^{III} or 10 µM $MMMTA^{V}$. Total RNA was isolated from the cells, as described above, at 0, 1, 3, 6, and 12 h after incubation with ATO^{III} or $MMMTA^{V}$. Quantitative analysis of *Cyp1a1* mRNA expression was done through qPCR as previously detailed.

Data was fitted into straight lines on semi-log plots using linear regression analysis where mRNA half-life values were estimated from the slope of these lines.

2.5.12. Assessment of CYP1A1 protein stability

Cycloheximide (CHX) chase assay was used for assessing the effect of ATO^{III} and $MMMTA^{V}$ on CYP1A1 protein stability by measuring and comparing its half-life in the absence or presence of ATO^{III} or $MMMTA^{V}$. The principle of this assay is to induce CYP1A1 protein synthesis, then monitoring the decrease in its abundance (i.e., degradation) following the inhibition of translating new protein using CHX.

In 6-well cell culture plates, Hepa1c1c7 cells were incubated in a 5% CO_2 humidified incubator at 37 °C for 24 h till ≈80% confluence was reached. The cells were then pretreated with 1 nM TCDD for 24 h. Thereafter, cells were incubated with 10 µg/mL CHX for 30 min, to inhibit further protein synthesis, before the treatment with 2.5 µM ATO^{III} or 10 µM $MMMTA^{V}$. Total cell lysate proteins were extracted, as described above, at 0, 3, 6, 12, 24, and 36 h after incubation with $MMMTA^{V}$. Quantitative analysis of CYP1A1 protein expression was carried out via western blotting as previously detailed.

Data was fitted into straight lines on semi-log plots using linear regression analysis where protein half-life values were estimated from the slope of these lines.

2.5.13. Microsomal incubation of arachidonic acid and extraction of its metabolites

The isolated hepatic microsomes from each sample of the 24 h-treated animals (1 mg protein/mL) were incubated in an incubation buffer (5 mM magnesium chloride hexahydrate-supplemented 100 mM potassium phosphate buffer, pH 7.4) mixed with 100 µM of AA (total reaction volume is 200 µL) inside a shaking water bath (90 rpm) at 37 °C for a pre-equilibration period of 5 min, then the reaction was initiated by adding 1 mM NADPH. After 30 min-incubation, the reaction was terminated by adding 600 µL ice-cold acetonitrile, then the internal standard (20-HETE-d_6) was added. Thereafter, arachidonic acid metabolites underwent a single liquid-liquid extraction from the incubation mixture**,** where 1 mL ethyl acetate was added to each sample. After vortex mixing and centrifugation, 1 mL of the supernatant was removed then dried using the Savant™ SpeedVac™ SPD130 Deluxe Vacuum Concentrator (Thermo Scientific; Waltham, MA, USA), and finally the resulting residue was reconstituted in 100 µL acetonitrile (311).

2.5.14. Separation and quantification of arachidonic acid metabolites

Enantioselective separation and quantification of the extracted arachidonic acid metabolites were carried out by chiral liquid chromatography-tandem mass spectrometry (LC-MS/MS) using the Reflect™ Coated Amylose A Chiral Column (Regis Technologies Inc.; Morton Grove, IL, USA) and the LCMS-8030 Triple Quadrupole Mass Spectrometer (Shimadzu Corporation; Kyoto, Japan), respectively, according to our in-house developed method (311). Data analysis was performed using the LabSolutions™ LCMS software, version 5.91 (Shimadzu Corporation; Kyoto, Japan).

2.5.15. Data and statistical analyses

The comparative statistical analysis of the data was performed using the Prism for Windows software, version 8.3.0 (GraphPad Software; San Diego, CA, USA).

Comparisons of the results from the experimental groups with each other or with their corresponding controls were carried out by the one-way analysis of variance (ANOVA) followed by Tukey's post-hoc pairwise multiple comparisons test, or by the unpaired Student's t-test, when applicable. The mean differences between groups were deemed statistically significant when $p < 0.05$. Data are presented as the mean ± standard error of the mean.

CHAPTER 3.

RESULTS

Portions of this chapter have been published in:

1. **El-Ghiaty MA**, Alqahtani MA, El-Kadi AOS. Down-regulation of hepatic cytochromes P450 1A1 and 1A2 by arsenic trioxide (ATO) in vivo and in vitro: A role of heme oxygenase 1. *Chem Biol Interact*. 2022 Sep 1;364:110049. doi: 10.1016/j.cbi.2022.110049.

2. **El-Ghiaty MA**, Alqahtani MA, El-Kadi AOS. Arsenic trioxide (ATO) up-regulates cytochrome P450 1A (CYP1A) enzymes in murine hepatoma Hepa-1c1c7 cell line. *Environ Toxicol Pharmacol*. 2023 Aug;101:104214. doi: 10.1016/j.etap.2023.104214.

3. **El-Ghiaty MA**, Alqahtani MA, El-Kadi AOS. Modulation of cytochrome P450 1A (CYP1A) enzymes by monomethylmonothioarsonic acid (MMMTAV) in vivo and in vitro. *Chem Biol Interact*. 2023 May 1;376:110447. doi: 10.1016/j.cbi.2023.110447.

4. **El-Ghiaty MA**, Alqahtani MA, El-Mahrouk SR, Isse FA, Alammari AH, El-Kadi AOS. Alteration of hepatic cytochrome P450 expression and arachidonic acid metabolism by arsenic trioxide (ATO) in C57BL/6 mice. *Biol Trace Elem Res*. 2024. doi: 10.1007/s12011-024-04225-1. (in press)

3.1. Down-regulation of hepatic CYP1A enzymes by ATO^{III} in C57BL/6 mice

3.1.1. Effect of ATO^{III} and TCDD on hepatic *Cyp1a1* and *Cyp1a2* mRNA in C57BL/6 mice

At 6 h, ATO^{III} alone significantly increased hepatic *Cyp1a1* mRNA level by 100%, while a significant 30% decrease was observed at 24 h compared to the control (Figure 3.1A). On the other hand, the constitutive level of hepatic *Cyp1a2* mRNA was not significantly affected by ATO^{III} alone at both durations of treatment (Figure 3.1B).

TCDD alone significantly induced hepatic *Cyp1a1* and *Cyp1a2* mRNA levels at 6 h by 529,600% and 590%, respectively, compared to the control (Figure 3.1A and B). Also, a significant induction of 1720000% and 4590% in hepatic *Cyp1a1* and *Cyp1a2* mRNA levels, respectively, was obtained in response to the 24 h treatment of TCDD alone compared to the control (Figure 3.1A and B).

In animals co-exposed to ATO^{III} and TCDD, ATO^{III} significantly inhibited the TCDD-mediated induction of hepatic *Cyp1a1* and *Cyp1a2* mRNA levels by 99.7% and 68.1% at 6 h, and by 59.3% and 48.8% at 24 h, respectively, compared to the treatment of TCDD alone (Figure 3.1A and B).

3.1.2. Effect of ATO^{III} and TCDD on hepatic CYP1A1 and CYP1A2 proteins in C57BL/6 mice

Our results showed that ATO^{III} alone caused a significant 47.7% and –29.8% changes in the constitutive levels of hepatic CYP1A1 and CYP1A2 proteins, respectively (Figure 3.2A and B). The treatment of TCDD alone resulted in a significant induction of hepatic CYP1A1 and CYP1A2 protein expression by 1033% and 314.2%, respectively, compared to the control (Figure 3.2A and B). Compared to the animals treated with TCDD alone, animals co-exposed to ATO^{III} and TCDD showed significant decrease in the TCDD-mediated induction of hepatic CYP1A1 and CYP1A2 proteins by 49.2% and 38.2%, respectively (Figure 3.2A and B).

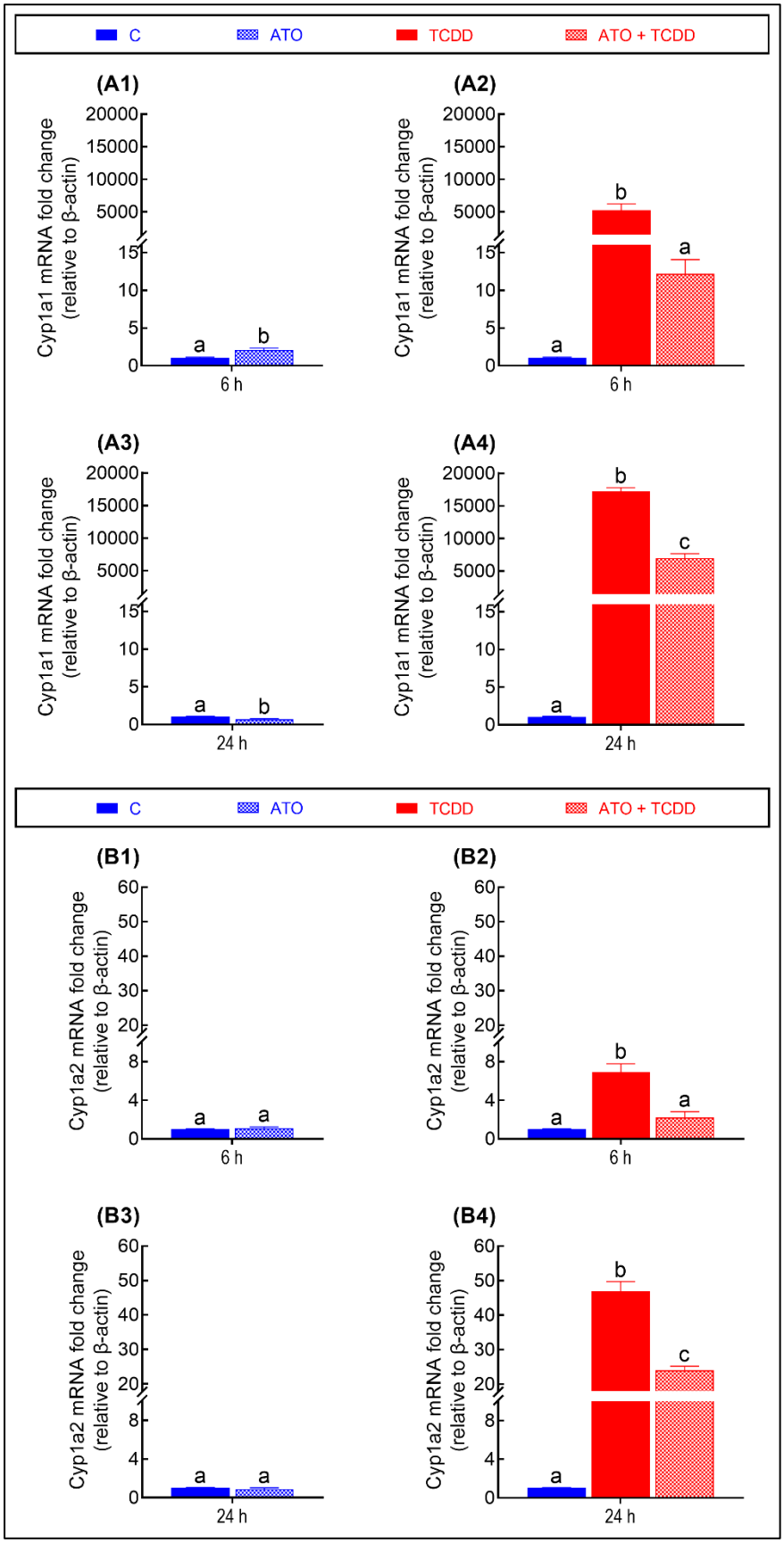

Figure 3.1. Effect of ATO^{III} and TCDD on hepatic *Cyp1a1* (A) and *Cyp1a2* (B) mRNA in C57BL/6 mice. Results are presented as mean ± SEM (n = 6). Different lowercase letters indicate statistically significant difference ($p < 0.05$). Bars not sharing any letter are significantly different.

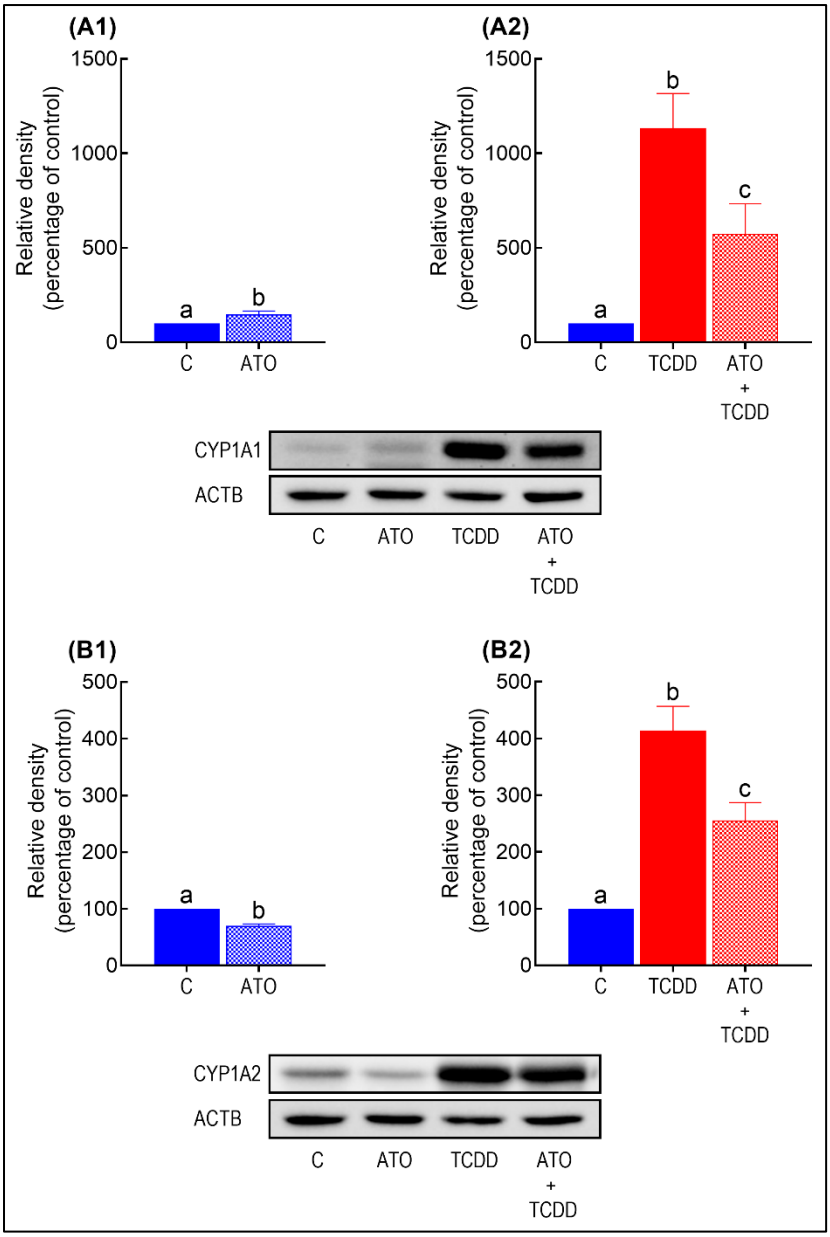

Figure 3.2. Effect of ATO^{III} and TCDD on hepatic CYP1A1 (A) and CYP1A2 (B) proteins in C57BL/6 mice. Results are presented as mean ± SEM (n = 6) representing the relative amounts of protein (expressed as percentage of the control (C) which is set at 100%) normalized to ACTB signals. Different lowercase letters indicate statistically significant difference ($p < 0.05$). Bars not sharing any letter are significantly different.

3.1.3. Effect of ATO^{III} and TCDD on hepatic CYP1A1 and CYP1A2 activities in C57BL/6 mice

At the catalytic activity level, ATO^{III} alone did not significantly alter hepatic EROD activity (Figure 3.3A), whereas MROD activity was significantly decreased by 40.4% in response to this treatment compared to the control (Figure 3.3B). TCDD alone significantly induced both hepatic EROD and MROD activities by 1015.8% and 790.4%, respectively, compared to the control (Figure 3.3A and B). When animals were co-exposed to ATO^{III} and TCDD, ATO^{III} significantly inhibited the TCDD-mediated induction of hepatic EROD and MROD activities by 25.8% and 34.7%, respectively, compared to the treatment of TCDD alone (Figure 3.3A and B).

3.1.4. Effect of ATO^{III} and TCDD on hepatic HMOX1 mRNA and protein in C57BL/6 mice

At 6 h, ATO^{III} alone significantly increased hepatic *Hmox1* mRNA level by 14,470%, while a significant 45.4% decrease was observed at 24 h, compared to the control (Figure 3.4A). At both durations of treatment, TCDD alone failed to significantly affect the constitutive level of hepatic *Hmox1* mRNA (Figure 3.4A). Compared to the animals treated with TCDD alone, co-exposure to ATO^{III} and TCDD resulted in a significant increase in hepatic *Hmox1* mRNA expression by 31,125% at 6 h, whereas a significant 58.3% decrease was obtained at 24 h (Figure 3.4A).

At protein level, the expression of hepatic HMOX1 significantly increased by 9897% in response to ATO^{III} alone compared to the control (Figure 3.4B). TCDD alone did not significantly change the constitutive level of hepatic HMOX1 protein (Figure 3.4B). Co-exposure to ATO^{III} and TCDD significantly increased hepatic HMOX1 protein by 10,574% compared to the exposure to TCDD alone (Figure 3.4B).

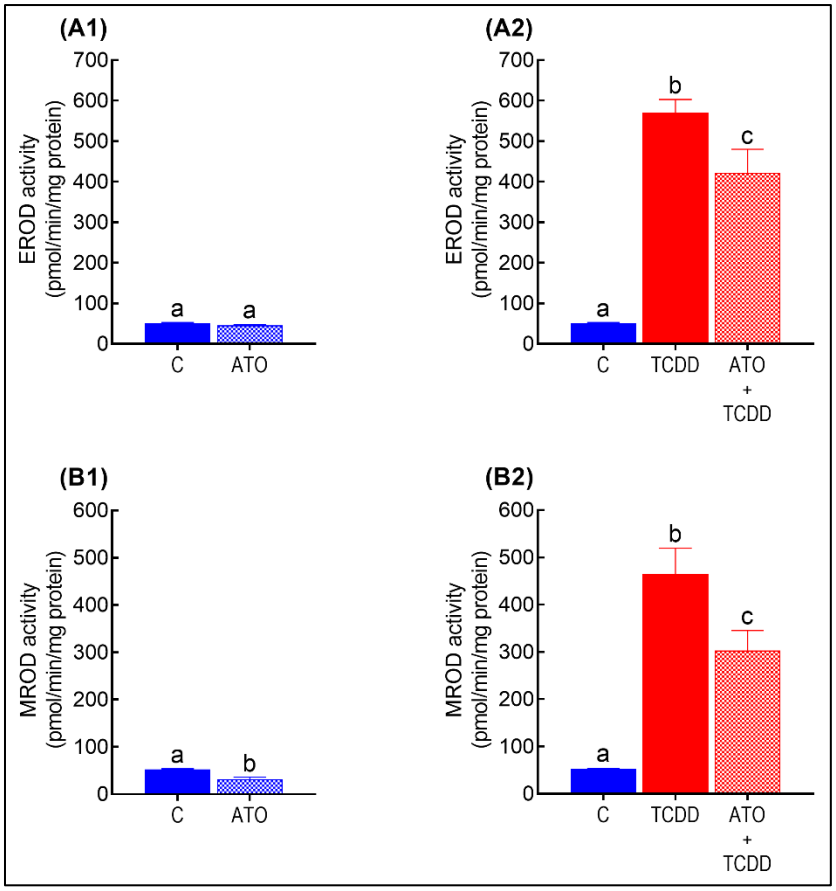

Figure 3.3. Effect of ATO^{III} and TCDD on hepatic CYP1A1 (A) and CYP1A2 (B) activities in C57BL/6 mice. Results are presented as mean ± SEM (n = 6). Different lowercase letters indicate statistically significant difference ($p < 0.05$). Bars not sharing any letter are significantly different.

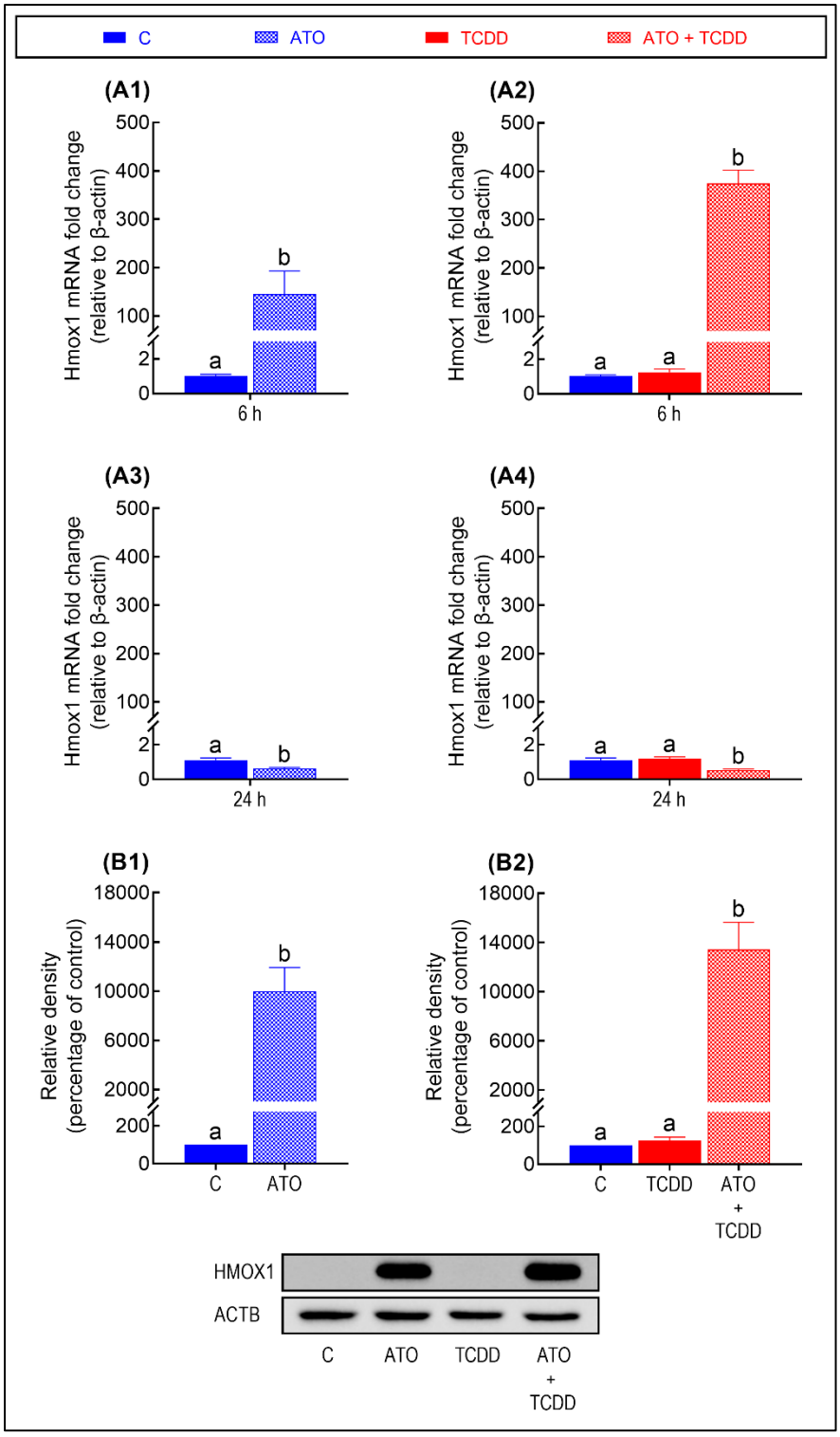

Figure 3.4. Effect of ATO^{III} and TCDD on hepatic HMOX1 mRNA (A) and protein (B) in C57BL/6 mice. Results are presented as mean ± SEM (n = 6). Protein results represent the relative amounts of protein (expressed as percentage of the control (C) which is set at 100%) normalized to ACTB signals. Different lowercase letters indicate statistically significant difference ($p < 0.05$). Bars not sharing any letter are significantly different.

3.2. Differential modulation of CYP1A enzymes by ATO^{III} in mouse Hepa1c1c7 and human HepG2 cells

3.2.1. Up-regulation of CYP1A enzymes by ATO^{III} in mouse Hepa1c1c7 cells

3.2.1.1. Effect of ATO^{III} and TCDD on viability of Hepa1c1c7 cells

Screening of different ATO^{III} concentrations via a 24 h-exposure MTT assay demonstrated that ATO^{III} is relatively non-toxic to Hepa1c1c7 cells at up to 3 μM, while significant 10.1%, 25%, 43.3%, and 52% reductions in cell viability were observed in response to 3.5, 4, 4.5, and 5 μM ATO^{III} exposure, respectively (Figure 3.5A). Subsequently, three ATO^{III} concentrations (0.63, 1.25, and 2.5 μM) were selected and underwent cell viability reassessment with or without 1 nM TCDD. The three concentrations, alone or in combination with TCDD, did not significantly alter cell viability (Figure 3.5B).

3.2.1.2. Effect of ATO^{III} and TCDD on *Cyp1a1* and *Cyp1a2* mRNA in Hepa1c1c7 cells

Exposure to ATO^{III} increased mRNA transcripts of both *Cyp1a1* and *Cyp1a2* at constitutive and inducible levels. Upon exposure to 1.25 and 2.5 μM ATO^{III} alone, *Cyp1a1* mRNA significantly increased by 140.2% and 400.9%, respectively, while *Cyp1a2* mRNA increased by 166.7%, 189.3%, and 385.3% in response to 0.63, 1.25, and 2.5 μM ATO^{III} treatment, respectively (Figure 3.6A and B). Both Cyp1a1 and *Cyp1a2* mRNA transcripts were significantly induced by 6714.9% and 2628.5%, respectively, by TCDD treatment in comparison with the control (Figure 3.6A and B).

Compared with the TCDD group, 1.25 or 2.5 μM ATO^{III} co-exposure with TCDD caused significant increase in the TCDD-induced *Cyp1a1* mRNA by 78.3% and 132.6%, respectively, while TCDD-induced *Cyp1a2* mRNA was significantly elevated by 83.1% and 114.7%, respectively (Figure 3.6A and B).

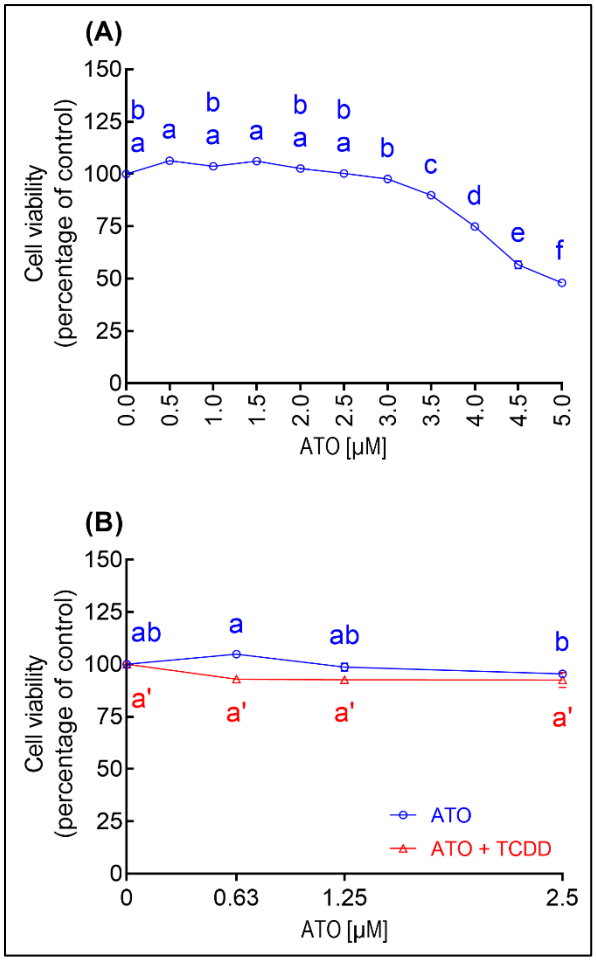

Figure 3.5. Effect of ATO^{III} and TCDD on viability of Hepa1c1c7 cells. Results are expressed as percentage of control (set at 100%) ± SEM (n = 6). Different lowercase letters indicate statistically significant difference ($p < 0.05$). Points not sharing any letter are significantly different.

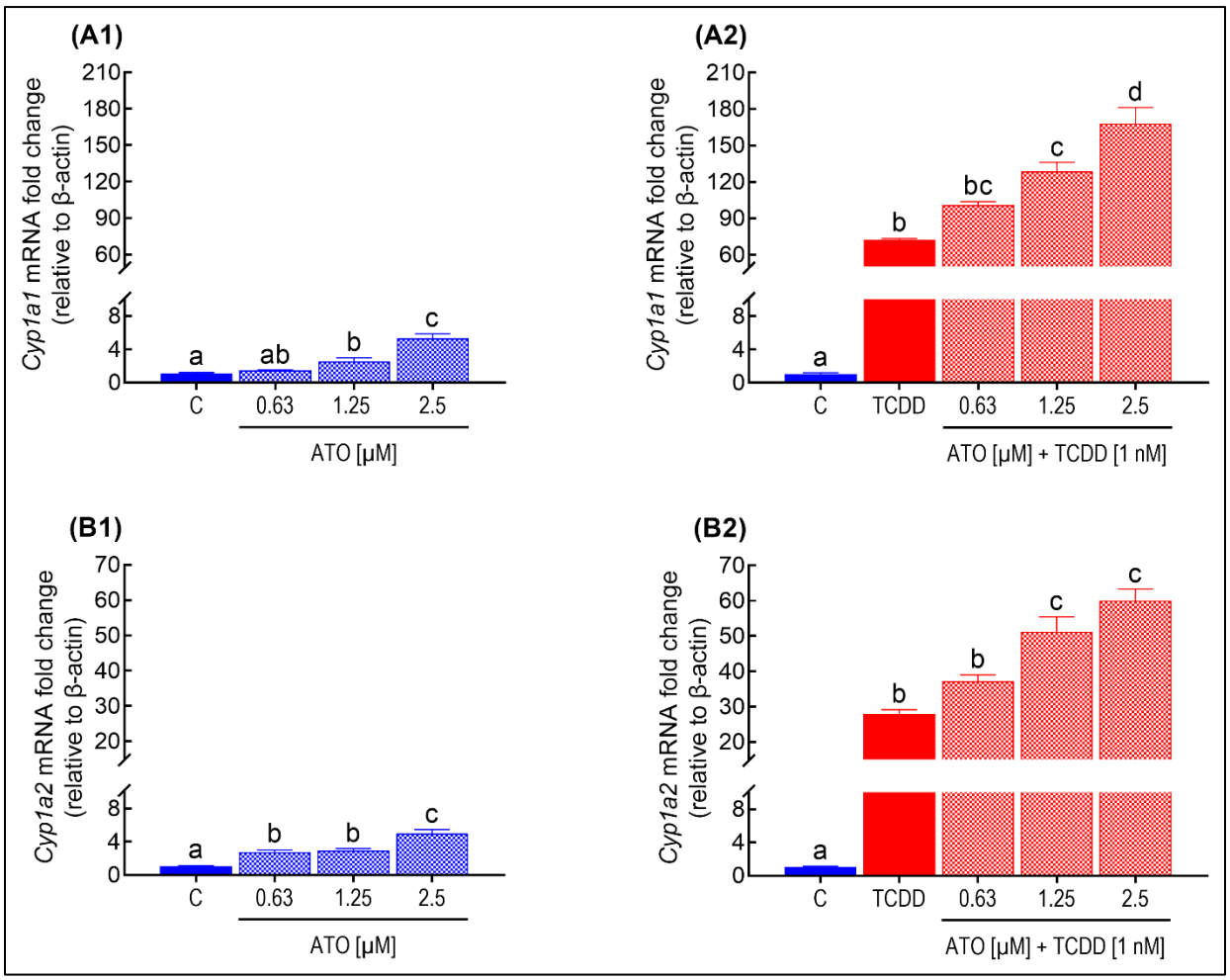

Figure 3.6. Effect of ATO^{III} and TCDD on *Cyp1a1* (A) and *Cyp1a2* (B) mRNA in Hepa1c1c7 cells. Results are presented as mean ± SEM (representing duplicate reactions performed for each experiment of three independent experiments). Different lowercase letters indicate statistically significant difference ($p < 0.05$). Bars not sharing any letter are significantly different.

3.2.1.3. Effect of ATO^{III} and TCDD on CYP1A1 and CYP1A2 proteins in Hepa1c1c7 cells

At basal level, CYP1A2, but not CYP1A1, protein was significantly increased by ATO^{III}. Significant 136.8%, 184.4%, and 257.8% increases in CYP1A2 protein were observed in response to 0.63, 1.25, and 2.5 μM ATO^{III}, respectively (Figure 3.7B). Both CYP1A1 and CYP1A2 proteins were significantly induced in response to TCDD treatment by 2066% and 19835%, respectively, in comparison with the control (Figure 3.7A and B). The co-exposure to 0.63, 1.25, and 2.5 μM ATO^{III} resulted in significant increase in the TCDD-induced CYP1A1 protein by 27.7%, 27.6%, and 48.1%, respectively, while TCDD-induced CYP1A2 protein was increased by 11.0%, 13.7%, and 15.9%, respectively (Figure 3.7A and B).

3.2.1.4. Effect of ATO^{III} and TCDD on CYP1A1 and CYP1A2 activities in Hepa1c1c7 cells

The basal levels of both EROD and MROD catalytic activities were not significantly affected by the treatment of ATO^{III} alone (Figure 3.8A and B). However, TCDD treatment significantly induced both EROD and MROD activities by 1268.1% and 372.4%, respectively, compared to the control (Figure 3.8A and B). Compared to TCDD treatment, significant increase in the TCDD-mediated induction of EROD and MROD activities resulted from the co-exposure to both ATO^{III} and TCDD, where EROD activity increased by 20.6%, 42.4%, and 53% in response to 0.63, 1.25, and 2.5 μM ATO^{III} co-treatment, respectively, while 17.4% and 34.1% increases in MROD activity were obtained in the 1.25 and 2.5 μM ATO^{III} co-treated groups, respectively (Figure 3.8A and B).

3.2.1.5. Effect of ATO^{III} on nuclear AHR protein in Hepa1c1c7 cells

The effect of ATO^{III} on AHR activation, and its consequent translocation from the cytosol to the nucleus, was examined through measuring AHR protein level in the nuclear protein extracts after treatment with ATO^{III}. Compared to control group, a significant 48.3% increase in AHR protein level was observed in response to 3 h-treatment with 2.5 μM ATO^{III} (Figure 3.9).

3.2.1.6. Effect of ATO^{III} and TCDD on XRE-driven luciferase activity in transfected Hepa1c1c7 cells

At a concentration of 2.5 μM, ATO^{III} significantly enhanced the basal luciferase activity by 154.9% (Figure 3.10A), while 1 nM TCDD resulted in a 3113.5% increase in the activity in comparison with the control (Figure 3.10B). Co-exposure to ATO^{III} and TCDD significantly increased the TCDD-induced luminescence signal by 51.3% (Figure 3.10B).

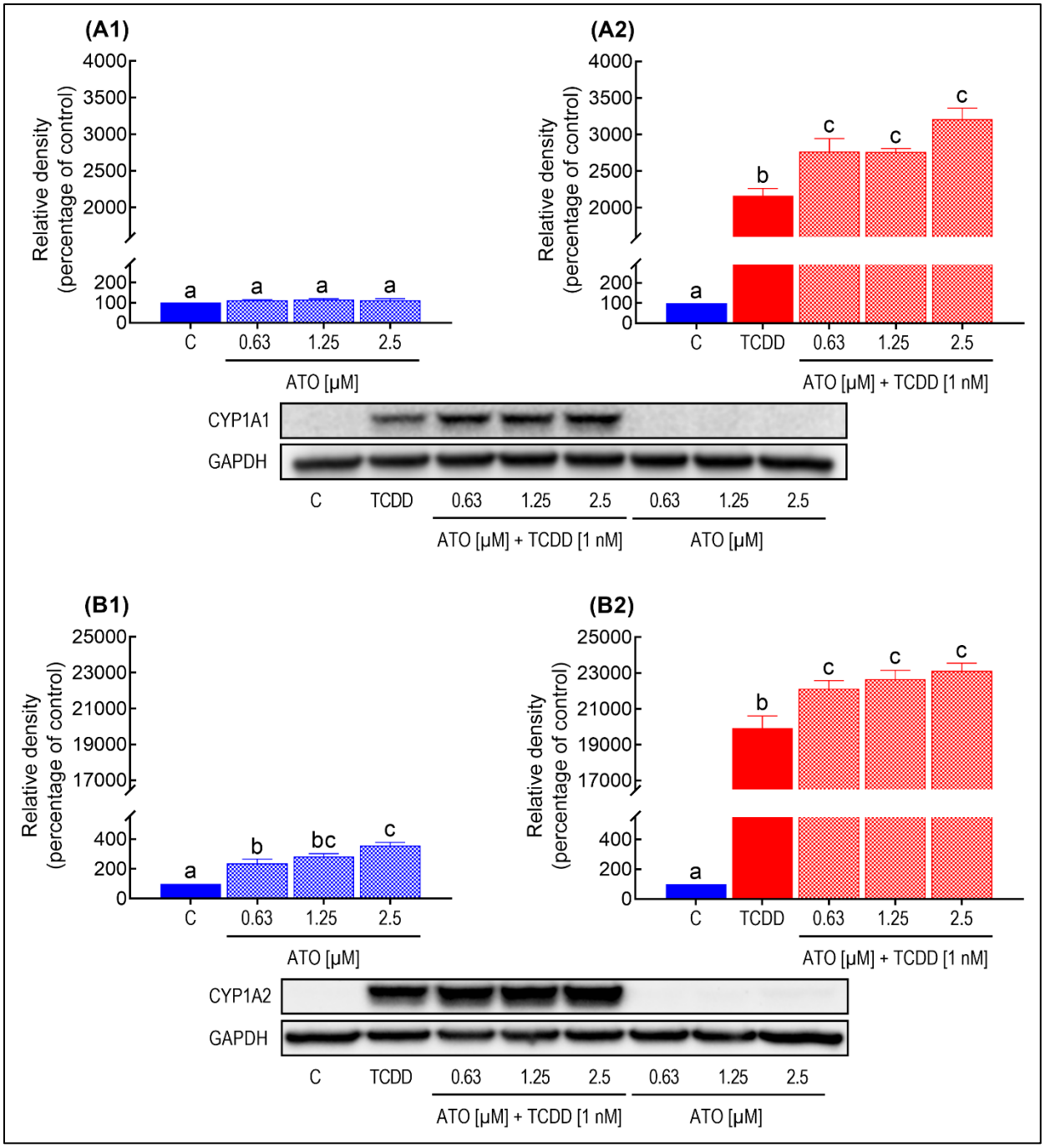

Figure 3.7. Effect of ATO^{III} and TCDD on CYP1A1 (A) and CYP1A2 (B) proteins in Hepa1c1c7 cells. Results are presented as mean ± SEM (one of three representative experiments is shown) representing the relative amounts of protein (expressed as percentage of the control (C) which is set at 100%) normalized to GAPDH signals. Different lowercase letters indicate statistically significant difference ($p < 0.05$). Bars not sharing any letter are significantly different.

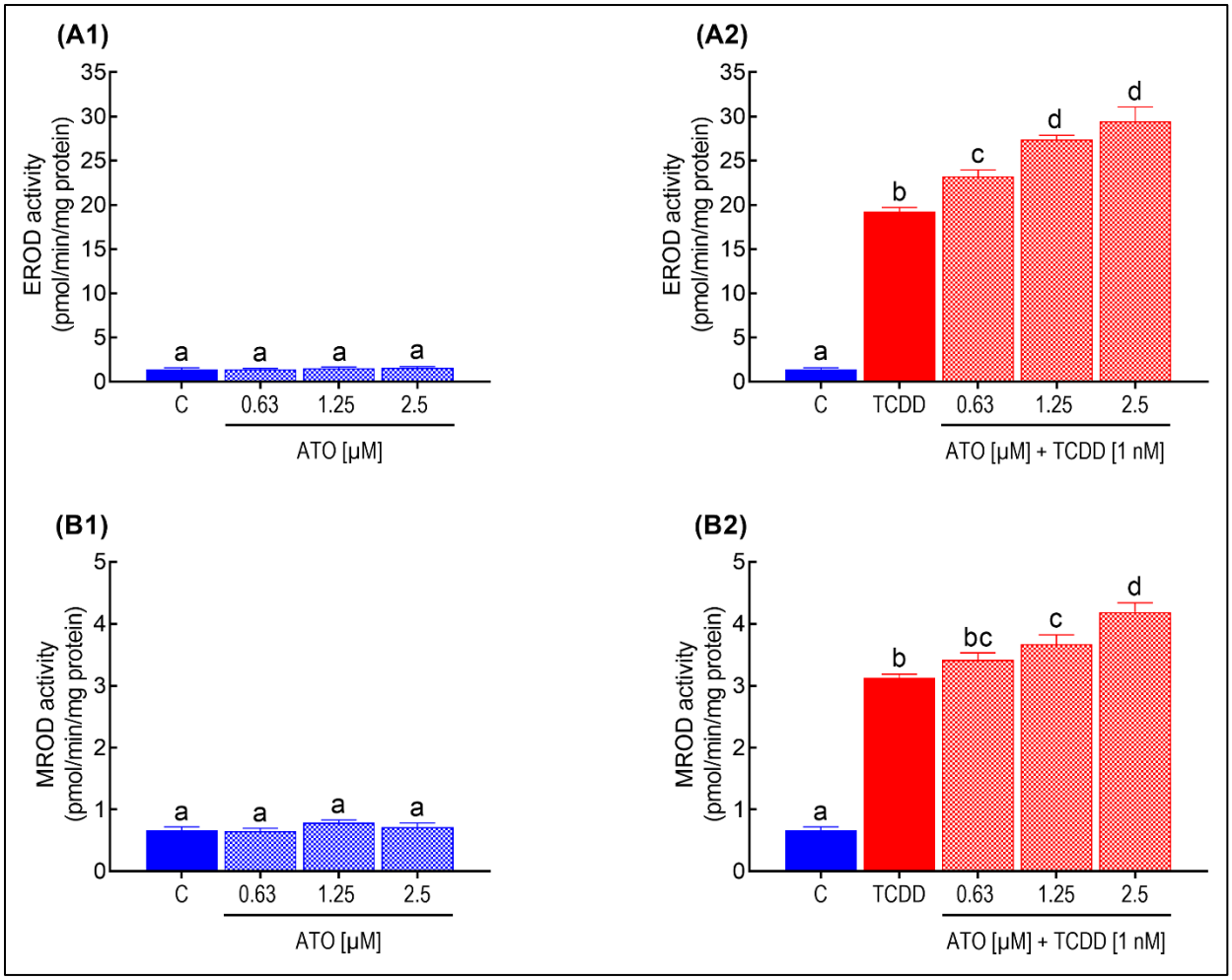

Figure 3.8. Effect of ATO^{III} and TCDD on CYP1A1 (A) and CYP1A2 (B) activities in Hepa1c1c7 cells. Results are presented as mean ± SEM (n = 6). Different lowercase letters indicate statistically significant difference ($p < 0.05$). Bars not sharing any letter are significantly different.

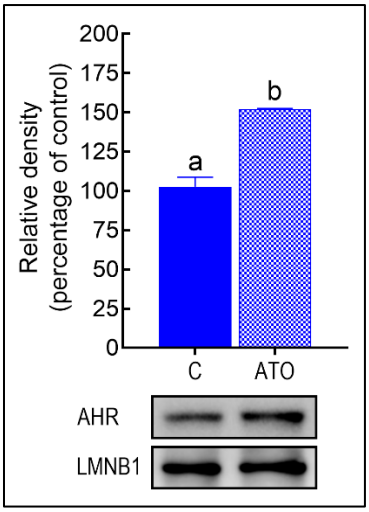

Figure 3.9. Effect of ATO^{III} on nuclear AHR protein in Hepa1c1c7 cells. Results are presented as mean ± SEM (one of three representative experiments is shown) representing the relative amounts of protein (expressed as percentage of the control (C) which is set at 100%) normalized to LMNB1 signals. Different lowercase letters indicate statistically significant difference ($p < 0.05$). Bars not sharing any letter are significantly different.

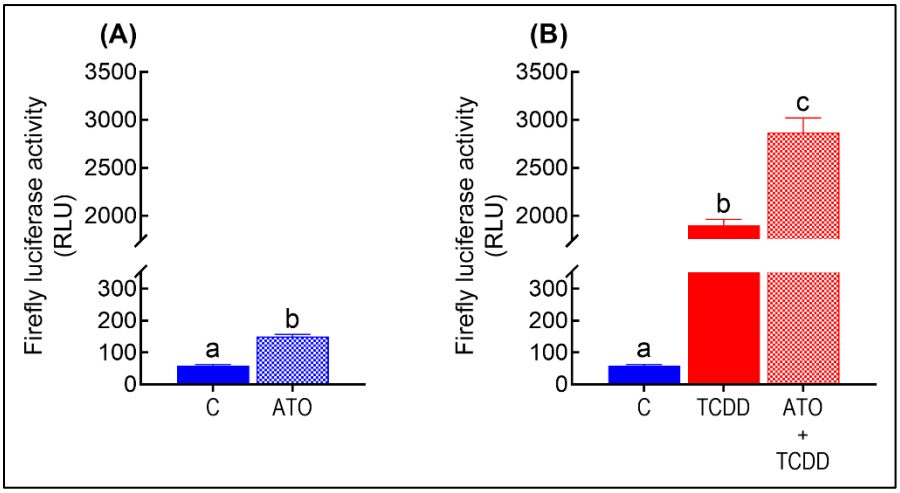

Figure 3.10. Effect of ATO^{III} and TCDD on XRE-driven luciferase activity in transfected Hepa1c1c7 cells. Luciferase activity is reported as relative light units. Results are presented as mean ± SEM (n = 6). Different lowercase letters indicate statistically significant difference ($p < 0.05$). Bars not sharing any letter are significantly different.

3.2.1.7. Effect of Act-D on ATO^{III}-mediated induction of *Cyp1a1* mRNA in Hepa1c1c7 cells

To examine whether transcriptional mechanisms are involved in the *Cyp1a1* mRNA induction by ATO^{III}, the transcription inhibitor Act-D was used to block de novo mRNA synthesis. The incubation with Act-D resulted in a significant 64.4% decrease in the constitutively expressed *Cyp1a1* mRNA compared to the control group (Figure 3.11A). While ATO^{III} alone significantly elevated the basal level of *Cyp1a1* mRNA by 103.7%, Act-D preincubation abolished such effect and significantly diminished *Cyp1a1* mRNA by 73% (Figure 3.11B). The induction of *Cyp1a1* mRNA by ATO^{III} and its inhibition by Act-D co-treatment followed a pattern like the one that was observed in TCDD and Act-D/TCDD groups. TCDD alone increased *Cyp1a1* mRNA significantly by 4700.9%, while Act-D/TCDD group showed a significant 99.3% less *Cyp1a1* mRNA (Figure 3.11C).

3.2.1.8. Effect of ATO^{III} on *Cyp1a1* mRNA half-life in Hepa1c1c7 cells

Since the level of mRNA transcripts is dependent on both transcription as well as turnover rates, the collective effect of ATO^{III} on *Cyp1a1* mRNA can be ascribed to altered production and/or degradation. The possibility of *Cyp1a1* mRNA undergoing ATO^{III}-mediated post-transcriptional alteration was assessed by the Act-D chase assay. Our data demonstrated that TCDD-induced *Cyp1a1* mRNA degraded with a 4.2 h half-life ($t_{1/2}$), and that ATO^{III} co-treatment significantly increased *Cyp1a1* mRNA half-life to 5.5 h (Figure 3.12).

3.2.1.9. Effect of ATO^{III} on CYP1A1 protein half-life in Hepa1c1c7 cells

The amount of protein is an outcome of translation/elimination rates. Therefore, the net impact of ATO^{III} on CYP1A1 protein can be attributed to modulated synthesis and/or decay. The possibility of CYP1A1 protein undergoing ATO^{III}-mediated post-translational modulation was evaluated by the CHX chase assay. Our findings showed that TCDD-induced CYP1A1 protein decayed with a half-life of 7.3 h, and that ATO^{III} co-exposure significantly increased CYP1A1 protein half-life ($t1/2 = 11.8$ h) (Figure 3.13).

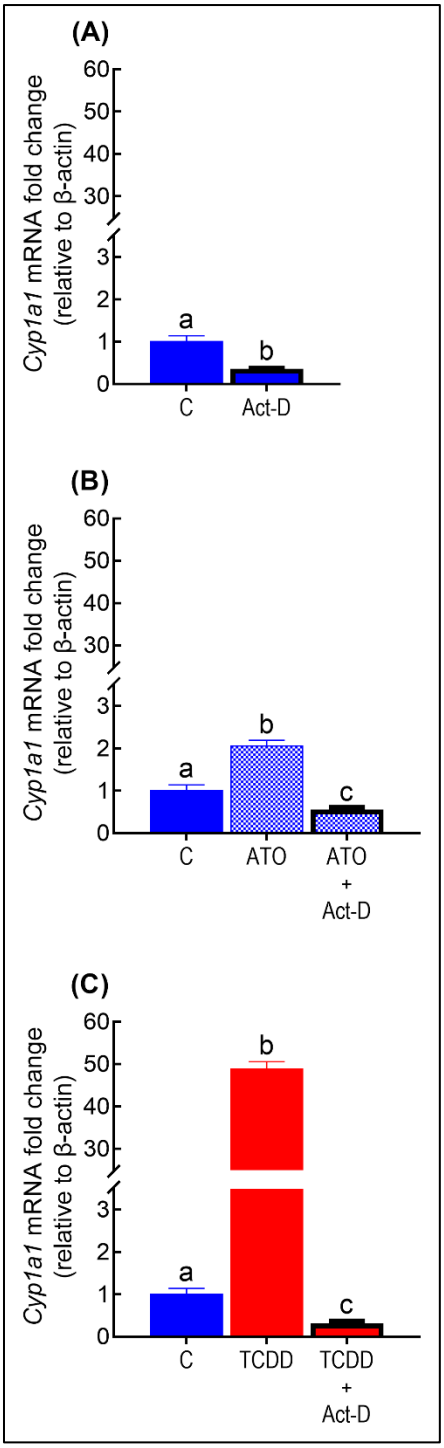

Figure 3.11. Effect of Act-D on ATO^{III}-mediated induction of *Cyp1a1* mRNA in Hepa1c1c7 cells. Results are presented as mean ± SEM (representing duplicate reactions performed for each experiment of three independent experiments). Different lowercase letters indicate statistically significant difference ($p < 0.05$). Bars not sharing any letter are significantly different.

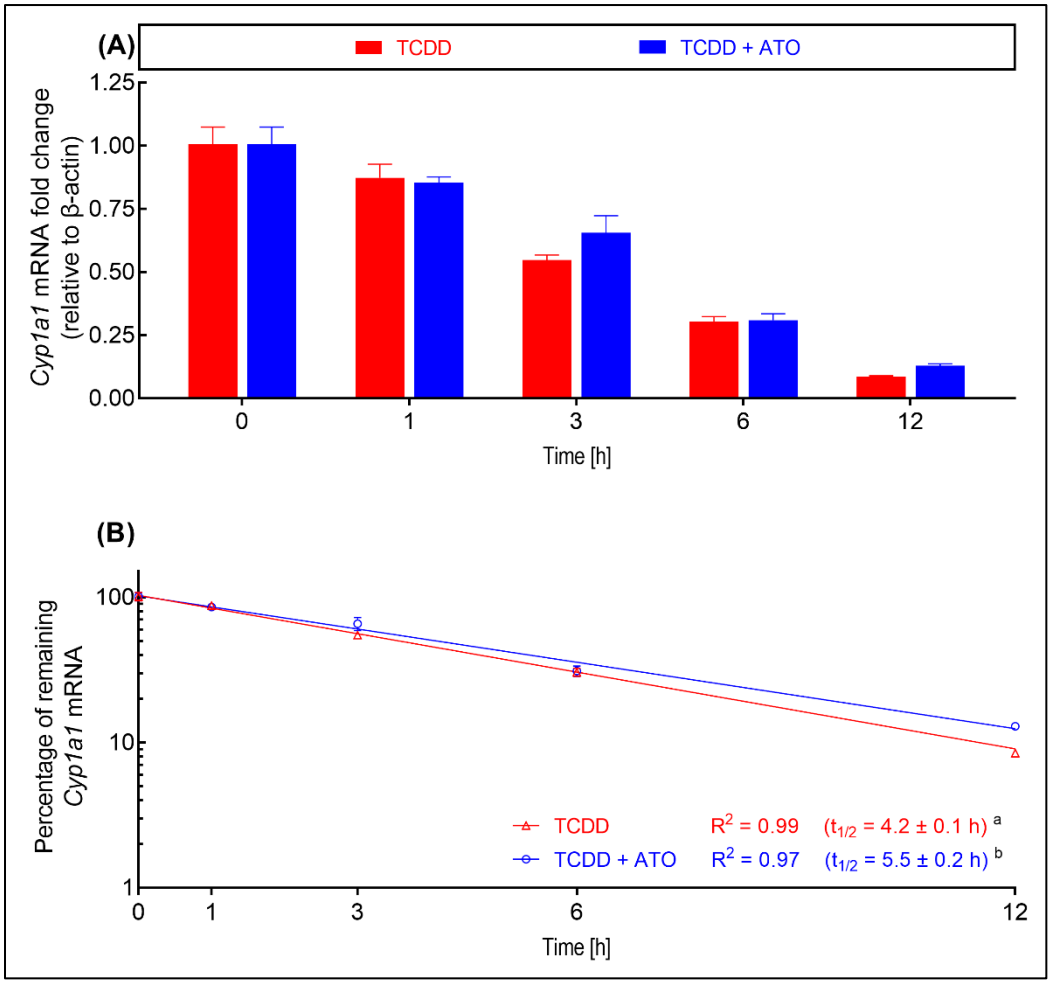

Figure 3.12. Effect of ATO^{III} on *Cyp1a1* mRNA half-life in Hepa1c1c7 cells. Results are presented as mean ± SEM (representing duplicate reactions performed for each experiment of two independent experiments). The mRNA decay curve from each experiment was analyzed individually, and the obtained half-life values were then used to calculate the mean half-life. Different lowercase letters indicate statistically significant difference ($p < 0.05$).

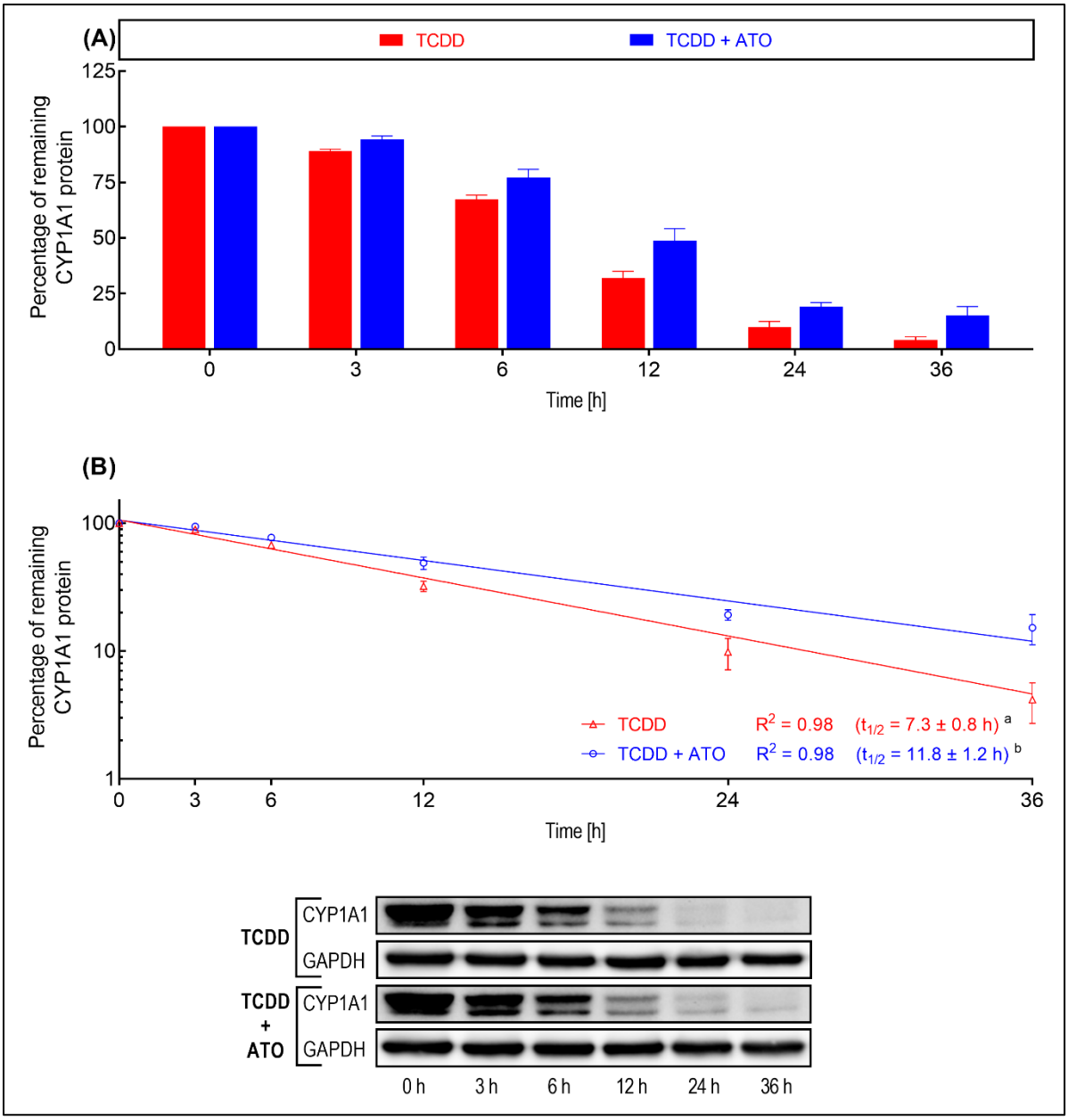

Figure 3.13. Effect of ATO^{III} on CYP1A1 protein half-life in Hepa1c1c7 cells. Results are presented as mean ± SEM (one of three representative experiments is shown) representing the relative amounts of protein (expressed as percentage of the control (C) which is set at 100%) normalized to GAPDH signals. The protein decay curve from each experiment was analyzed individually, and the obtained half-life values were then used to calculate the mean half-life. Different lowercase letters indicate statistically significant difference ($p < 0.05$).

3.2.2. Down-regulation of CYP1A enzymes by ATO^{III} in human HepG2 cells

3.2.2.1. Effect of ATO^{III} and TCDD in the absence and presence of SnMP on viability of HepG2 cells

The MTT reduction assay showed that 24 h-exposure to ATO^{III} alone at the concentrations of 5 and 10 μM did not significantly affect cell viability, while at the concentrations of 15, 20, 25, and 30 μM, cell viability significantly decreased to approximately 92%, 91%, 89%, and 85%, respectively (Figure 3.14A).

Our results also showed that co-exposure to ATO^{III} (1, 5, and 10 μM) and 1 nM TCDD did not significantly affect cell viability (Figure 3.14B). Finally, SnMP (5 μM) had no significant effect on the viability of the cells treated with 1 and 5 μM ATO^{III} in the absence and presence of 1 nM TCDD (Figure 3.14C).

3.2.2.2. Effect of ATO^{III} and TCDD on *CYP1A1* mRNA in HepG2 cells

Exposure to ATO^{III} alone at the concentrations of 1, 5 and 10 μM resulted in a significant decrease in the constitutive *CYP1A1* mRNA level by 40%, 50%, and 30%; respectively (Figure 3.15). TCDD alone caused a significant 4840% increase in *CYP1A1* mRNA that was inhibited in a concentration-dependent manner by ATO^{III} (Figure 3.15). ATO^{III} at the concentration of 1 μM resulted in a significant decrease in the TCDD-mediated induction of *CYP1A1* mRNA by 60.5%. A much more inhibition, by 93.5%, was observed when cells were co-exposed to 5 μM ATO^{III} with TCDD, while the maximum inhibition took place at the highest concentration tested, 10 μM, which caused a 97.7% decrease in the TCDD-induced *CYP1A1* mRNA (Figure 3.15).

3.2.2.3. Effect of ATO^{III} and TCDD on CYP1A1 and CYP1A2 proteins in HepG2 cells

At the constitutive level, neither CYP1A1 nor CYP1A2 protein expression was affected by ATO^{III} alone (Figure 3.16A and B). However, TCDD alone significantly induced both CYP1A1 and CYP1A2 proteins by 2423% and 7970%, respectively compared to the control (Figure 3.16A and B). The TCDD-mediated induction of CYP1A1 and CYP1A2 proteins was significantly inhibited in a concentration-dependent manner by co-exposure to ATO^{III}. At the concentrations of 1, 5, and 10 μM; ATO^{III} significantly decreased the TCDD-mediated induction of CYP1A1 protein by 70.1%, 85.8, and 89.6%; respectively, while CYP1A2 protein had 33.8%, 67.2%, and 91% decrease; respectively (Figure 3.16A and B).

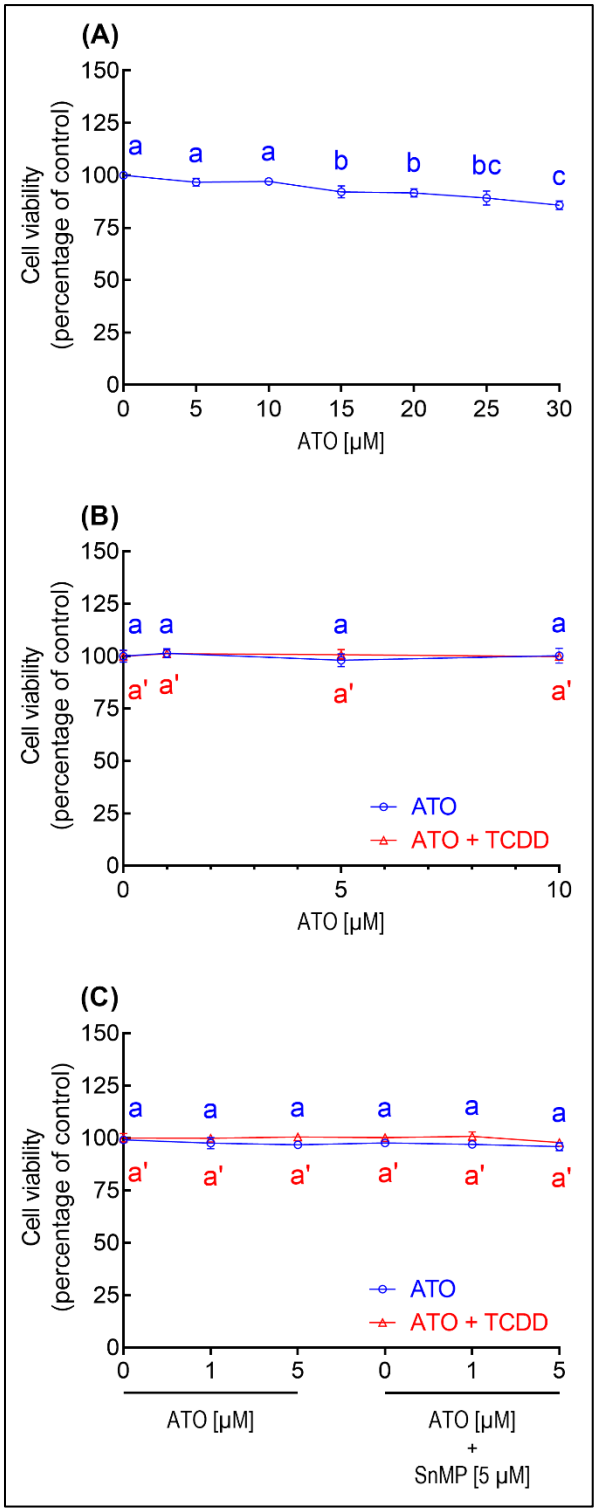

Figure 3.14. Effect of ATO^{III} and TCDD, in the absence and presence of SnMP, on viability of HepG2 cells. Results are expressed as percentage of control (set at 100%) ± SEM (n = 6). Different lowercase letters indicate statistically significant difference ($p < 0.05$). Points not sharing any letter are significantly different.

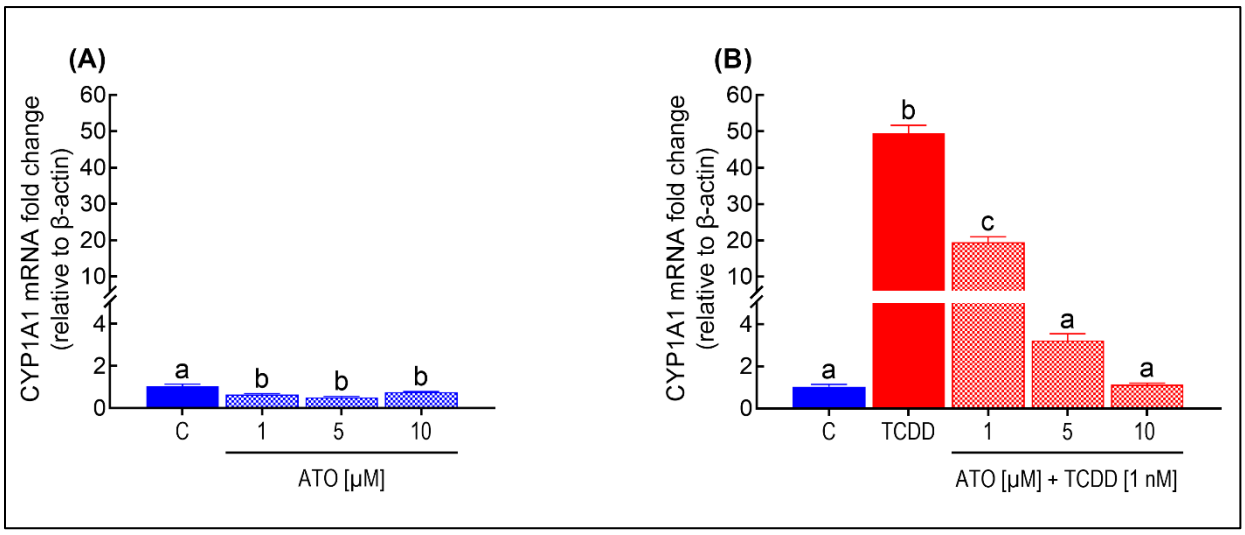

Figure 3.15. Effect of ATO^{III} and TCDD on *CYP1A1* mRNA in HepG2 cells. Results are presented as mean ± SEM (representing duplicate reactions performed for each experiment of three independent experiments). Different lowercase letters indicate statistically significant difference ($p < 0.05$). Bars not sharing any letter are significantly different.

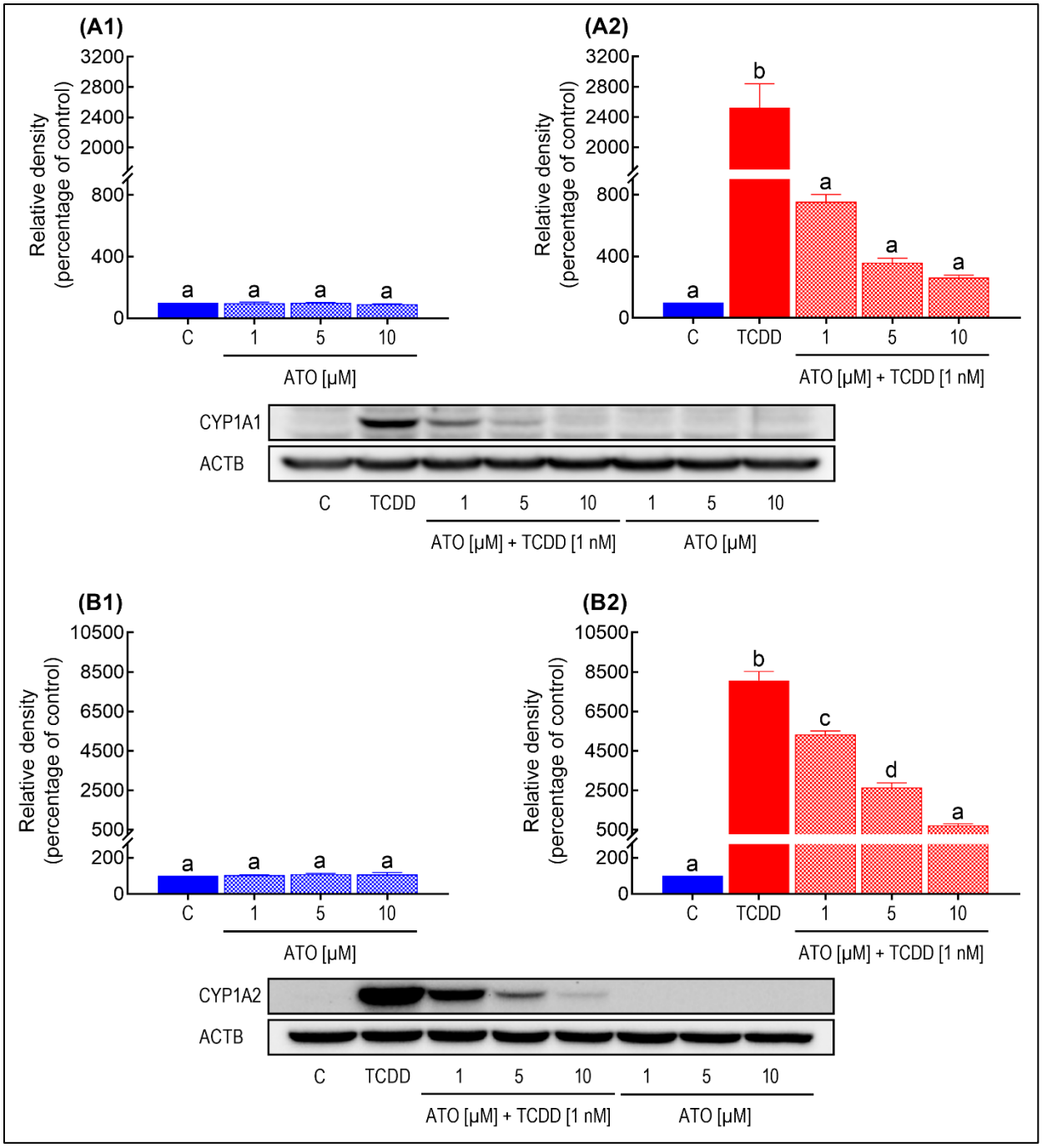

Figure 3.16. Effect of ATO^{III} and TCDD on CYP1A1 (A) and CYP1A2 (B) proteins in HepG2 cells. Results are presented as mean ± SEM (one of three representative experiments is shown) representing the relative amounts of protein (expressed as percentage of the control (C) which is set at 100%) normalized to ACTB signals. Different lowercase letters indicate statistically significant difference ($p < 0.05$). Bars not sharing any letter are significantly different.

3.2.2.4. Effect of ATO^{III} and TCDD on CYP1A1 and CYP1A2 activities in HepG2 cells

At the catalytic activity level, ATO^{III} alone did not significantly affect EROD or MROD activities (Figure 3.17A and B). However, TCDD alone significantly induced both EROD and MROD activities by 3800% and 4290%, respectively compared to the control (Figure 3.17A and B). A concentration-dependent inhibition of the TCDD-mediated induction of EROD and MROD activities resulted from the co-exposure to both ATO^{III} and TCDD. A significant reduction in activity was observed at 1, 5, and 10 μM ATO^{III} by 22.6%, 49.6%, and 68.5%; respectively, for the EROD; and by 55.4%, 77.2%, and 89%; respectively, for the MROD (Figure 3.17A and B).

3.2.2.5. Effect of ATO^{III} and TCDD on HMOX1 mRNA and protein in HepG2 cells

ATO^{III} alone, at all concentrations tested, significantly increased the constitutive *HMOX1* mRNA level in a concentration-dependent fashion by 1770%, 5900%, and 7380%; at 1, 5, and 10 μM; respectively (Figure 3.18A). On the other hand, TCDD alone failed to significantly alter *HMOX1* mRNA in comparison with the control (Figure 3.18A). Compared to the treatment with TCDD alone, co-exposure to ATO^{III} and TCDD resulted in a significant increase in hepatic *HMOX1* mRNA expression in a concentration-dependent pattern by 1670%, 6060%, and 7070%; for the 1, 5, and 10 μM ATO^{III}; respectively (Figure 3.18A).

Similarly, the constitutive expression of HMOX1 protein significantly increased by 2281%, 12,073%, and 14,529% in response to 1, 5, and 10 μM ATO^{III}; respectively (Figure 3.18B). TCDD alone did not significantly change HMOX1 protein level compared to the control (Figure 3.18B). Co-exposure to TCDD and 1, 5, or 10 μM ATO^{III} resulted in a significant increase in HMOX1 protein by 1647%, 8001%, and 9394%; respectively, compared to the exposure to TCDD alone (Figure 3.18B).

3.2.2.6. Effect of ATO^{III} and TCDD on XRE-driven luciferase activity in transfected HepG2 cells

Our results showed that 5 μM ATO^{III} alone caused a significant 63.5% inhibition in the constitutive expression of the luciferase activity (Figure 3.19). On the other hand, 1 nM TCDD alone significantly increased luciferase activity by 351% compared to the control (Figure 3.19). Co-treatment with ATO^{III} and TCDD significantly decreased the TCDD-mediated induction of luciferase activity by 74.2% (Figure 3.19).

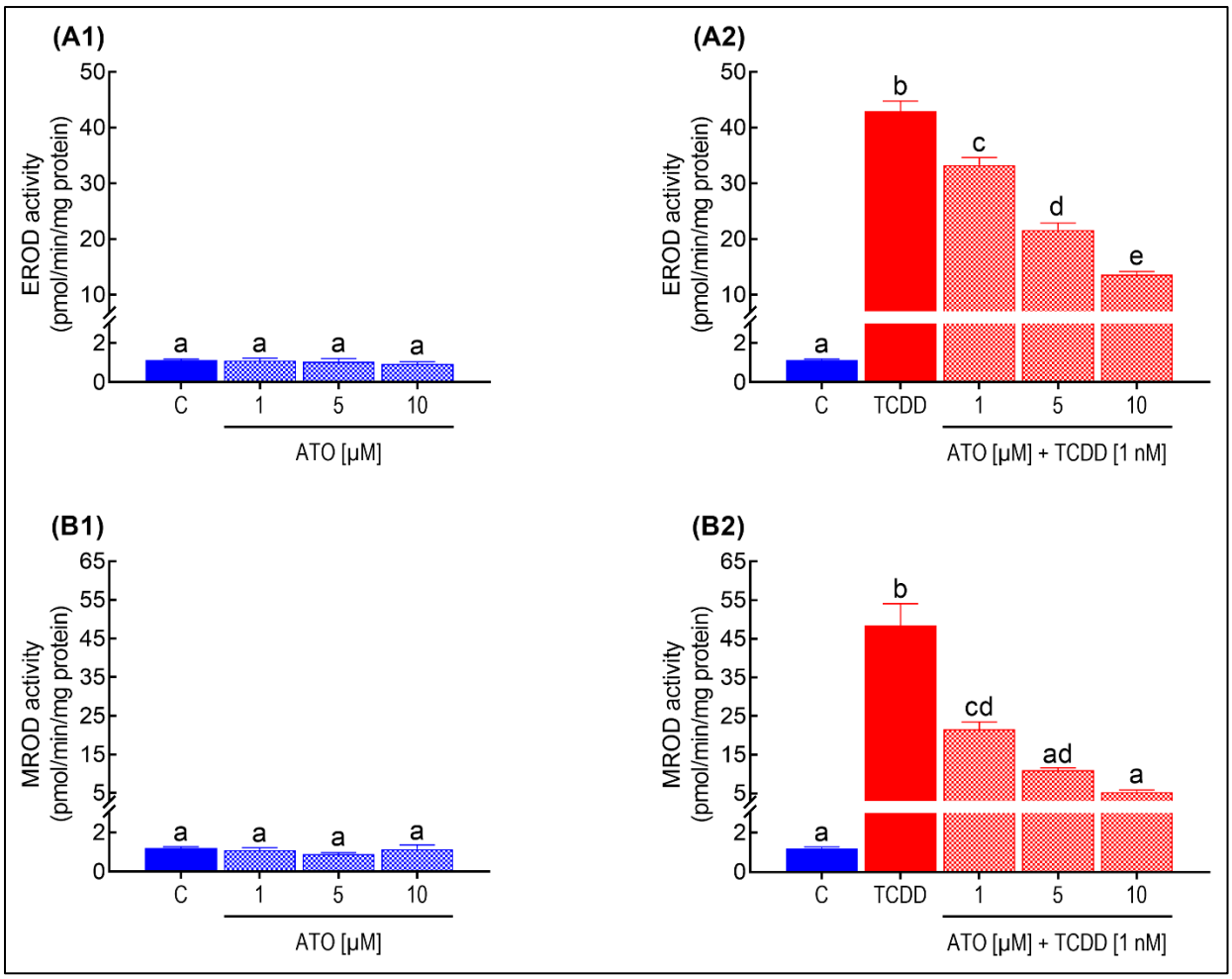

Figure 3.17. Effect of ATO^{III} and TCDD on CYP1A1 (A) and CYP1A2 (B) activities in HepG2 cells. Results are presented as mean ± SEM (n = 6). Different lowercase letters indicate statistically significant difference ($p < 0.05$). Bars not sharing any letter are significantly different.

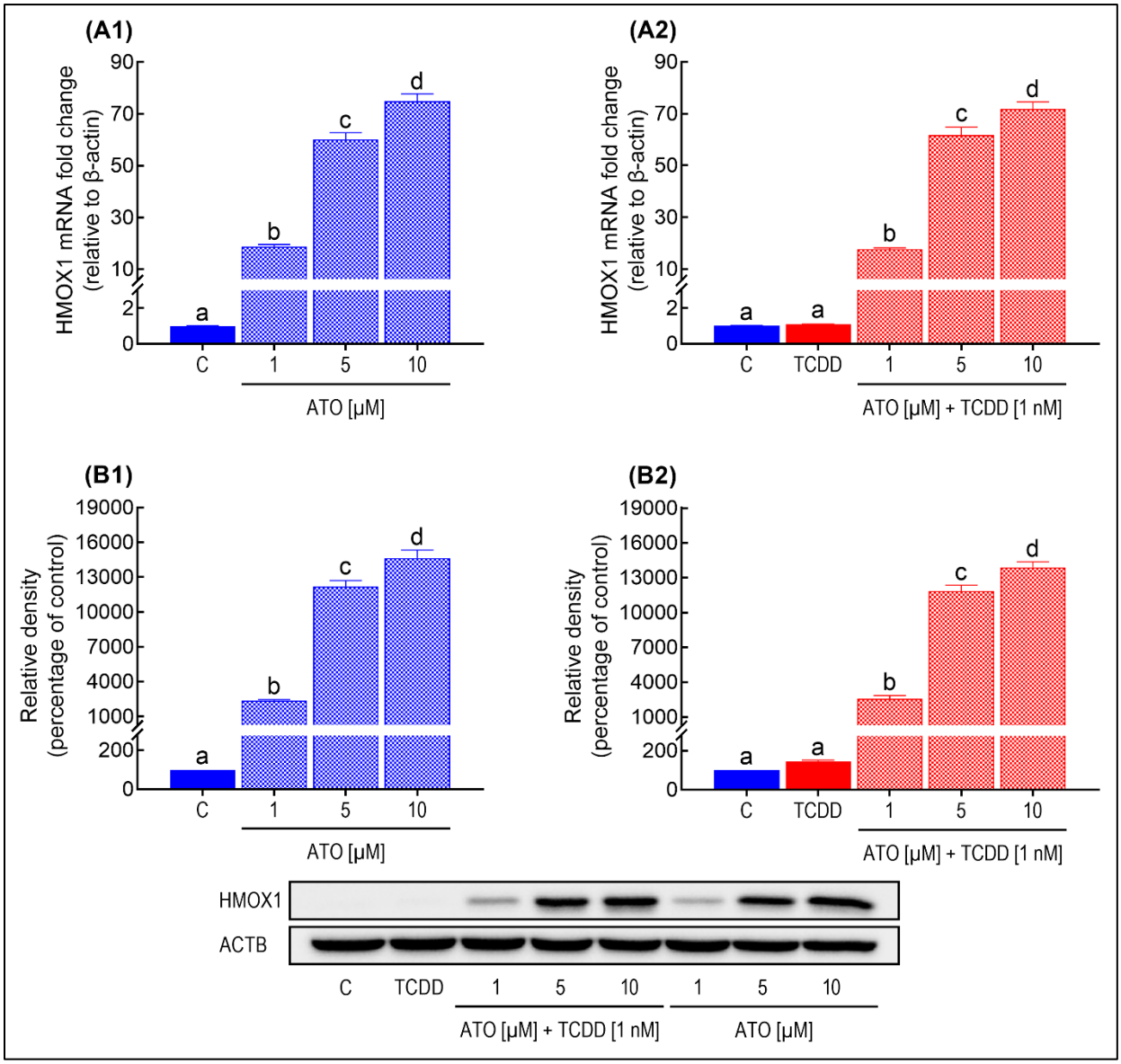

Figure 3.18. Effect of ATO^{III} and TCDD on HMOX1 mRNA (A) and protein (B) in HepG2 cells. Results are presented as mean ± SEM (representing duplicate reactions performed for each experiment of three independent experiments). Protein results (one of three representative experiments is shown) represent the relative amounts of protein (expressed as percentage of the control (C) which is set at 100%) normalized to ACTB signals. Different lowercase letters indicate statistically significant difference ($p < 0.05$). Bars not sharing any letter are significantly different.

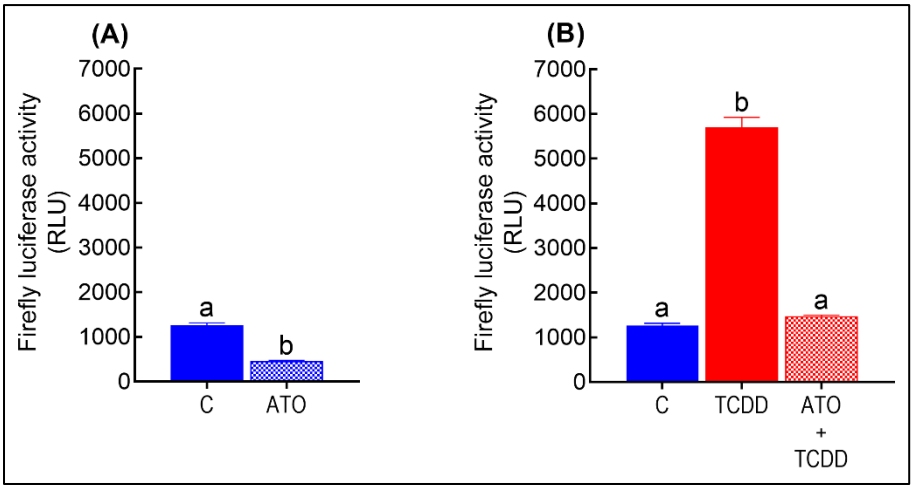

Figure 3.19. Effect of ATO^{III} and TCDD on XRE-driven luciferase activity in transfected HepG2 cells. Luciferase activity is reported as relative light units. Results are presented as mean ± SEM (n = 6). Different lowercase letters indicate statistically significant difference ($p < 0.05$). Bars not sharing any letter are significantly different.

3.2.2.7. Effect of ATO^{III} and TCDD on CYP1A1 activity in HepG2 cells in the presence of SnMP

The treatment of SnMP alone or in the presence of ATO^{III} caused no effect on EROD activity compared to the control or ATO^{III} alone, respectively (Figure 3.20). Similarly, the significant TCDD-mediated induction of EROD activity was not affected by SnMP co-treatment (Figure 3.20). On the other hand, ATO^{III} at the concentration of 1 μM significantly decreased the TCDD-mediated induction of EROD activity. However, co-treatment with SnMP partially reversed the ATO^{III}-mediated inhibition of EROD activity induced by TCDD (Figure 3.20).

The formerly mentioned findings about the failure of SnMP alone or in the presence of ATO^{III} or TCDD to alter EROD activity eliminate the possibility that such partial restoration of the inhibition resulted from inducing EROD activity by SnMP itself. Also, despite being successful in partially reversing the ATO^{III}-mediated decrease in EROD activity by inhibiting HMOX1, SnMP was unable to completely restore EROD activity, implying the presence of an additional transcriptional mechanism underlying such decrease.

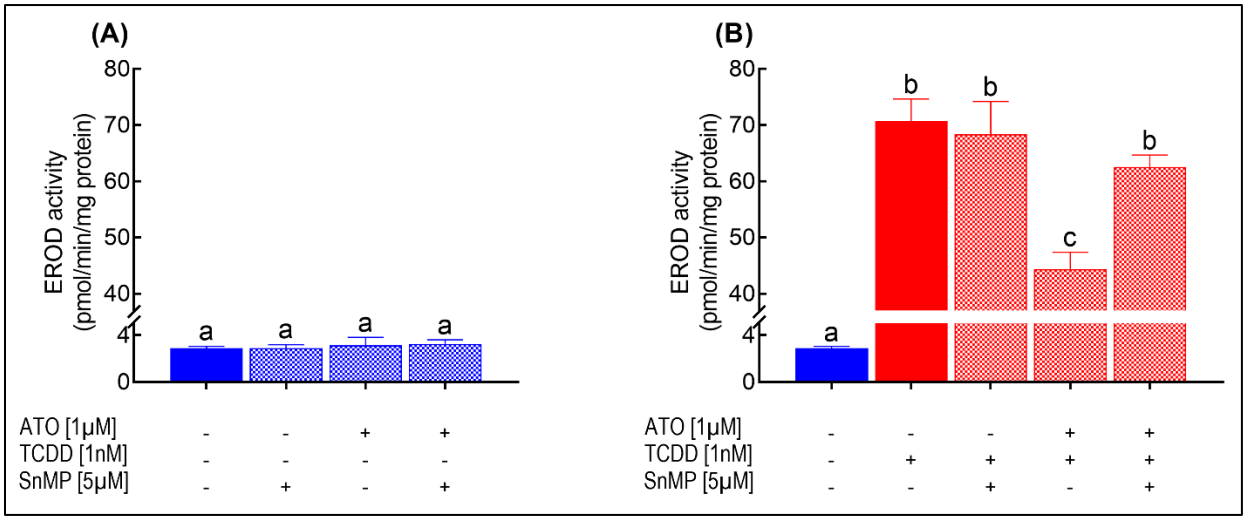

Figure 3.20. Effect of ATO^{III} and TCDD on CYP1A1 activity in HepG2 cells in the presence of SnMP as a competitive inhibitor of HMOX1. Results are presented as mean ± SEM (n = 6). Different lowercase letters indicate statistically significant difference ($p < 0.05$). Bars not sharing any letter are significantly different.

3.3. Up-regulation of hepatic CYP1A enzymes by $MMMTA^{V}$ in C57BL/6 mice

3.3.1. Effect of $MMMTA^{V}$ and TCDD on hepatic *Cyp1a1* and *Cyp1a2* mRNA in C57BL/6 mice

The constitutive levels of hepatic *Cyp1a1* and *Cyp1a2* mRNA were not significantly affected by $MMMTA^{V}$ at both durations of treatment (6 h and 24 h), similar to its inorganic precursor, iAs^{III} (Figure 3.21A and B). Compared to the control, TCDD alone significantly induced hepatic *Cyp1a1* and *Cyp1a2* mRNA levels at 6 h by 529600% and 593.6%, respectively (Figure 3.21A and B). Also, a significant increase of 1720000% and 4597% in hepatic *Cyp1a1* and *Cyp1a2* mRNA levels, respectively, was obtained in response to the 24 h-treatment of TCDD alone compared to the control (Figure 3.21A and B).

Upon co-exposure to $MMMTA^{V}$ and TCDD, $MMMTA^{V}$ significantly inhibited the TCDD-mediated induction of hepatic *Cyp1a1* mRNA level by 67.3% and 28.5% at 6 h and 24 h, respectively, compared to the treatment of TCDD alone (Figure 3.21A). The effect of $MMMTA^{V}$ on TCDD-inducible *Cyp1a1* mRNA followed a pattern similar to iAs^{III}, which caused 95.6% and 56.9% reduction in TCDD-mediated induction at 6 h and 24 h, respectively (Figure 3.21A).

For *Cyp1a2* mRNA, the combined iAs^{III} and TCDD treatment showed also significant 57% and 56.4% lower induction compared to that observed in TCDD treatment group at 6 h and 24 h, respectively (Figure 3.21B). Interestingly, combining $MMMTA^{V}$ treatment with TCDD resulted in an opposite effect by increasing the TCDD-mediated induction of *Cyp1a2* mRNA at both treatment durations (6 h and 24 h) by 41.1% and 64.1%, respectively (Figure 3.21B).

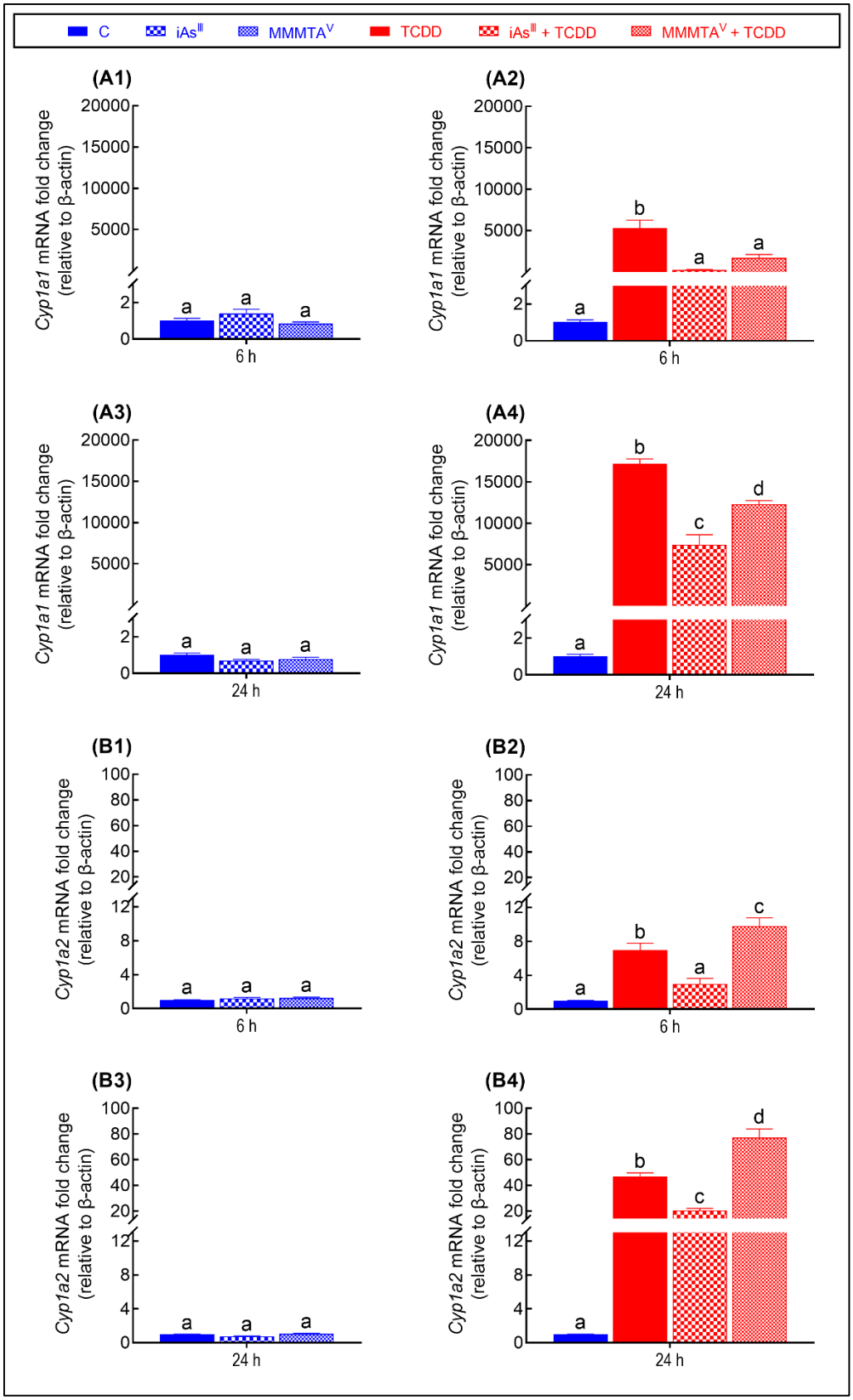

Figure 3.21. Effect of MMMTA^{V} and TCDD on hepatic *Cyp1a1* (A) and *Cyp1a2* (B) mRNA in C57BL/6 mice. Results are presented as mean ± SEM (n = 6). Different lowercase letters indicate statistically significant difference ($p < 0.05$). Bars not sharing any letter are significantly different.

3.3.2. Effect of $MMMTA^{V}$ and TCDD on hepatic CYP1A1 and CYP1A2 proteins in C57BL/6 mice

Neither iAs^{III} nor $MMMTA^{V}$ alone caused a change in the constitutive levels of hepatic CYP1A1 and CYP1A2 proteins (Figure 3.22A and B). The treatment of TCDD alone caused a significant induction of hepatic CYP1A1 and CYP1A2 proteins expression by 256.5% and 86%, respectively, compared to the control (Figure 3.22A and B).

Animals co-exposed to $MMMTA^{V}$ and TCDD showed significant increase in the TCDD-mediated induction of hepatic CYP1A1 and CYP1A2 proteins by 76.2% and 46.1%, respectively, compared to the animals treated with TCDD alone (Figure 3.22A and B). Interestingly, iAs^{III} did not alter TCDD-mediated induction of both proteins when combined with TCDD treatment.

3.3.3. Effect of $MMMTA^{V}$ and TCDD on hepatic CYP1A1 and CYP1A2 activities in C57BL/6 mice

At catalytic activity level, the treatment with either iAs^{III} or $MMMTA^{V}$ alone did not significantly alter hepatic EROD or MROD significantly induced both hepatic EROD and MROD activities by 724.1% and 789.3%, respectively, compared to the control (Figure 3.23A and B). Co-exposure of animals to TCDD with iAs^{III} or $MMMTA^{V}$ significantly increased the TCDD-mediated induction of hepatic EROD activity by 67.7% and 117.8%, respectively, compared to the treatment of TCDD alone (Figure 3.23A).

While the combination of iAs^{III} and TCDD did not exhibit significant difference in MROD activity compared to the treatment with TCDD alone, the combined $MMMTA^{V}$ and TCDD treatment showed significantly higher, 66.3%, MROD activity compared to the TCDD group (Figure 3.23B).

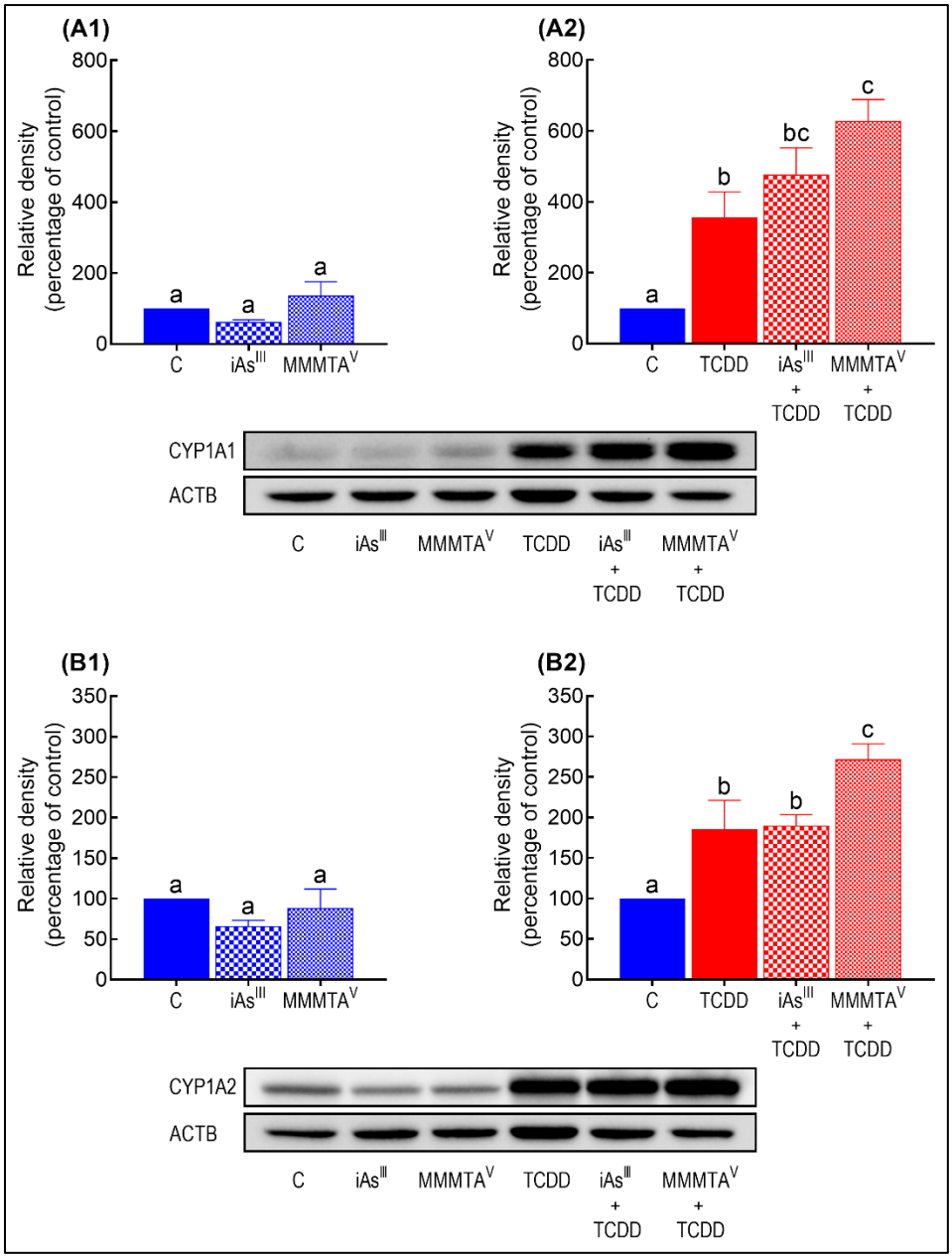

Figure 3.22. Effect of MMMTA^{V} and TCDD on hepatic CYP1A1 (A) and CYP1A2 (B) proteins in C57BL/6 mice. Results are presented as mean ± SEM (n = 6) representing the relative amounts of protein (expressed as percentage of the control (C) which is set at 100%) normalized to ACTB signals. Different lowercase letters indicate statistically significant difference ($p < 0.05$). Bars not sharing any letter are significantly different.

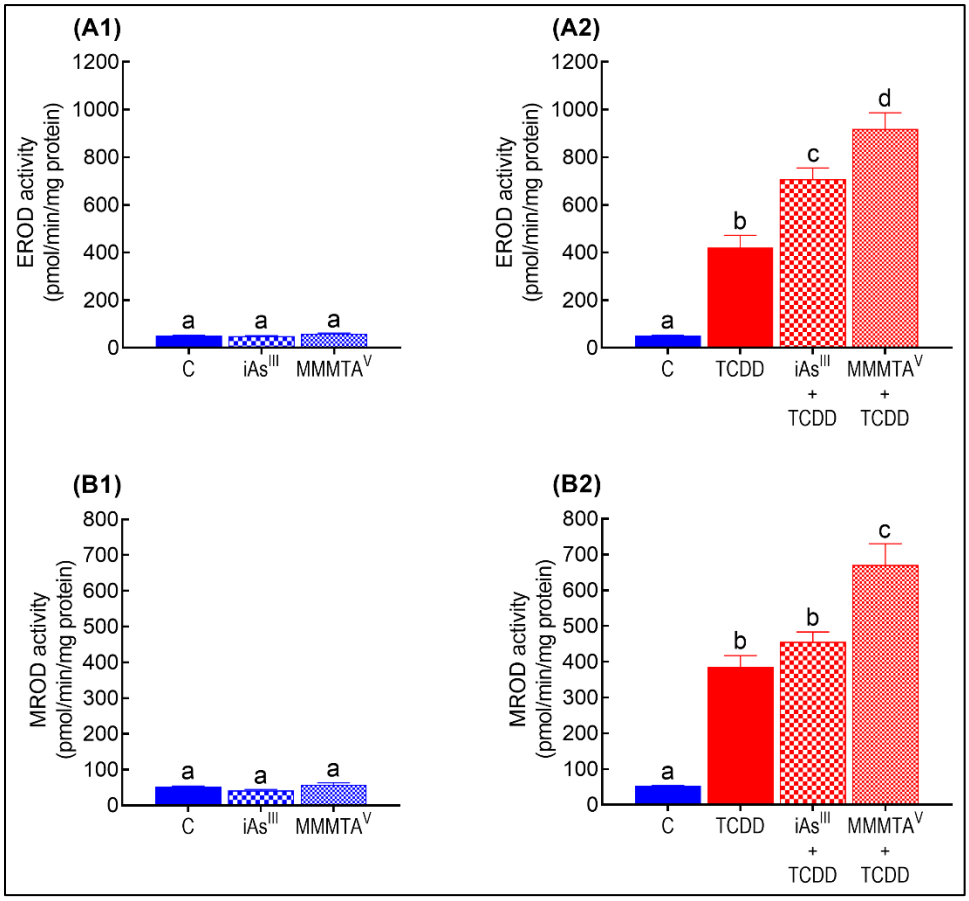

Figure 3.23. Effect of MMMTA^{V} and TCDD on hepatic CYP1A1 (A) and CYP1A2 (B) activities in C57BL/6 mice. Results are presented as mean ± SEM (n = 6). Different lowercase letters indicate statistically significant difference ($p < 0.05$). Bars not sharing any letter are significantly different.

3.4. Differential modulation of CYP1A enzymes by MMMTA^{V} in mouse Hepa1c1c7 and human HepG2 cells

3.4.1. Up-regulation of CYP1A enzymes by MMMTA^{V} in mouse Hepa1c1c7 cells

3.4.1.1. Effect of MMMTA^{V} and TCDD on viability of Hepa1c1c7 cells

The MTT reduction assay showed that 24 h-exposure to MMMTA^{V} alone at the concentrations of 1, 5, and 10 μM did not significantly affect cell viability in Hepa1c1c7 cells (Figure 3.24). Our results also demonstrated that co-exposure to MMMTA^{V} (1, 5, and 10 μM) and 1 nM TCDD did not cause significant cytotoxicity (Figure 3.24).

3.4.1.2. Effect of MMMTA^{V} and TCDD on *Cyp1a1* and *Cyp1a2* mRNA in Hepa1c1c7 cells

Exposure to MMMTA^{V} alone at the concentrations of 1, 5, and 10 μM resulted in a significant decrease in the constitutive *Cyp1a1* mRNA level by 30.4%, 31.4%, and 34.9%, respectively, but did not affect the basal *Cyp1a2* mRNA (Figure 3.25A and B). TCDD alone caused significant 4848% and 1190% increase in the levels of *Cyp1a1* and *Cyp1a2* mRNA, respectively (Figure 3.25A and B).

Compared to the TCDD treatment group, co-exposure to TCDD and 10 μM MMMTA^{V} resulted in a significant decrease in the TCDD-mediated induction of *Cyp1a1* mRNA by 31.1%, whereas TCDD-inducible *Cyp1a2* mRNA was significantly increased by 33.2% at the same MMMTA^{V} concentration (Figure 3.25A and B). The TCDD-induced *Cyp1a1* and *Cyp1a2* mRNA levels were not significantly altered by co-exposure to either 1 or 5 μM MMMTA^{V} (Figure 3.25A and B).

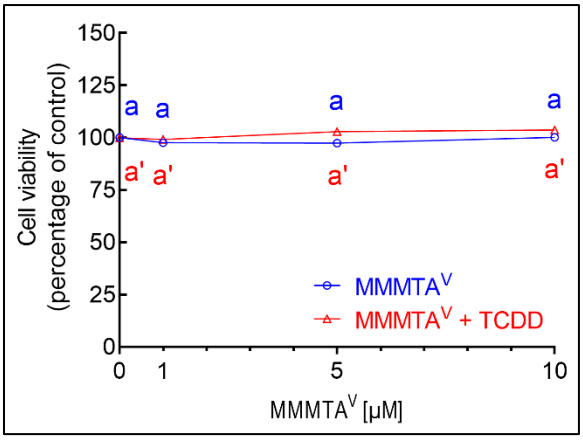

Figure 3.24. Effect of MMMTA^V and TCDD on viability of Hepa1c1c7 cells. Results are expressed as percentage of control (set at 100%) ± SEM (n = 6). Different lowercase letters indicate statistically significant difference ($p < 0.05$). Points not sharing any letter are significantly different.

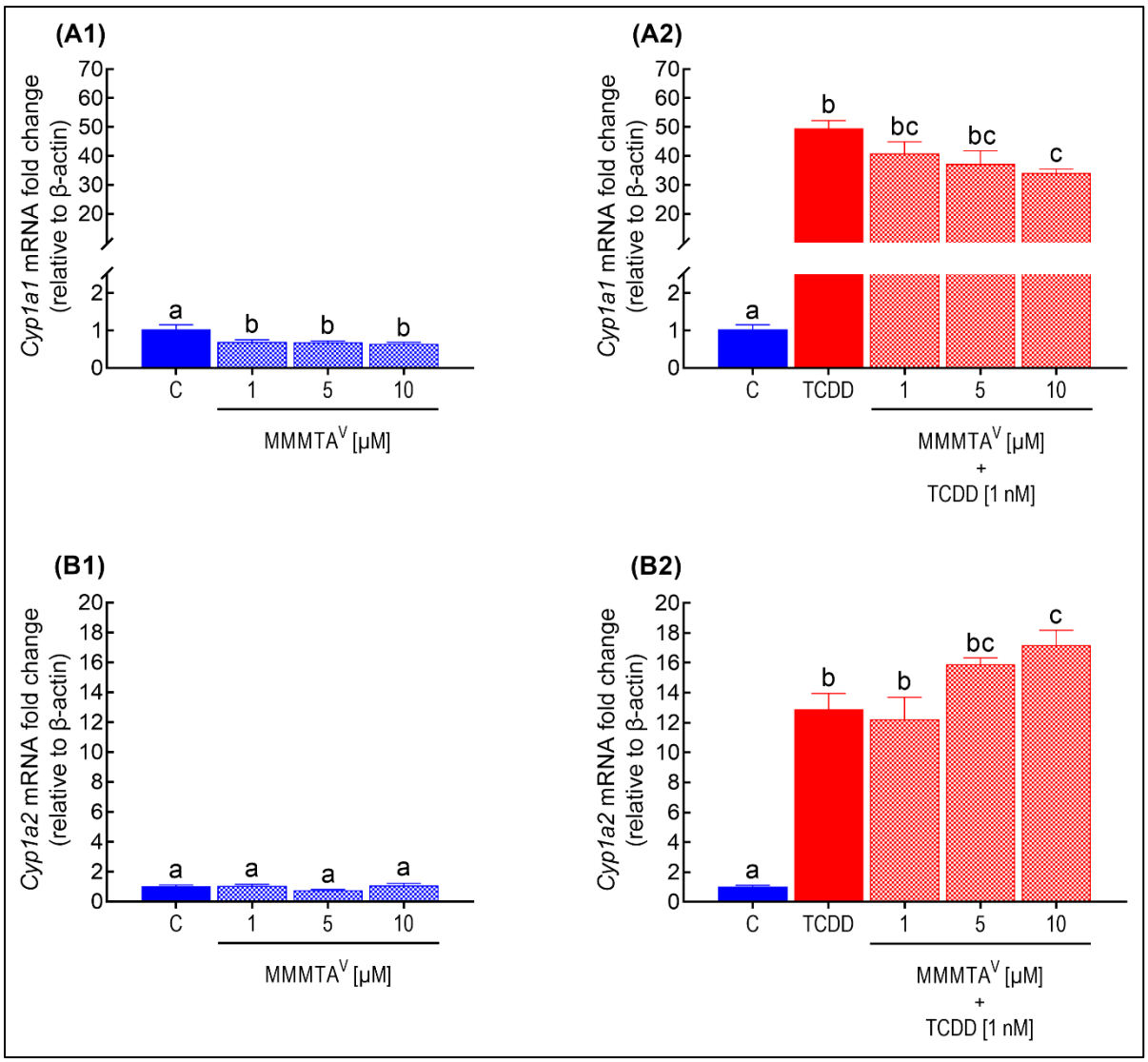

Figure 3.25. Effect of MMMTA^{V} and TCDD on *Cyp1a1* (A) and *Cyp1a2* (B) mRNA in Hepa1c1c7 cells. Results are presented as mean ± SEM (representing duplicate reactions performed for each experiment of three independent experiments). Different lowercase letters indicate statistically significant difference ($p < 0.05$). Bars not sharing any letter are significantly different.

3.4.1.3. Time-dependent effect of $MMMTA^V$ and TCDD on *Cyp1a1* and *Cyp1a2* mRNA in Hepa1c1c7 cells

The effect of 10 μM $MMMTA^V$ on the expression levels of *Cyp1a1* and *Cyp1a2* mRNA was evaluated at 3, 6, 12, and 24 h. The basal level of *Cyp1a1* mRNA significantly decreased at 6, 12, and 24 h by 53.5%, 52.5%, and 47%, respectively, in response to $MMMTA^V$ treatment, while *Cyp1a2* mRNA level showed no change at all tested time points (Figure 3.26A and B).

Compared to the control, treatment with TCDD alone caused significant induction in *Cyp1a1* mRNA at all time points, with the maximum induction being observed at 6 h by a value of 20730% (Figure 3.26A). The significant induction of *Cyp1a2* mRNA in response to TCDD was obtained at 6, 12, and 24 h, with a maximum value of 3742% at the 24 h-treatment (Figure 3.26B).

Compared to the TCDD treatment group at the respective time point, co-exposure to TCDD and $MMMTA^V$ resulted in a significant decrease in the TCDD-mediated induction of *Cyp1a1* mRNA by 20.3% only at the 6 h-treatment (Figure 3.26A). On the other hand, TCDD-inducible *Cyp1a2* mRNA was significantly increased by 47.2%, 21.6%, and 43.4% at 6, 12, and 24 h of $MMMTA^V$ co-treatment, respectively (Figure 3.26B).

3.4.1.4. Effect of $MMMTA^V$ and TCDD on CYP1A1 and CYP1A2 proteins in Hepa1c1c7 cells

Neither CYP1A1 nor CYP1A2 basal protein expression was affected by $MMMTA^V$ treatment alone (Figure 3.27A and B). However, TCDD alone significantly induced both CYP1A1 and CYP1A2 proteins by 3301% and 23576%, respectively, compared to the control (Figure 3.27A and B). The TCDD-mediated induction of CYP1A1 protein significantly increased by 12.9% upon co-exposure to 10 μM $MMMTA^V$, while TCDD-inducible CYP1A2 protein was not significantly affected by $MMMTA^V$ co-treatment at all tested concentrations (Figure 3.27A and B).

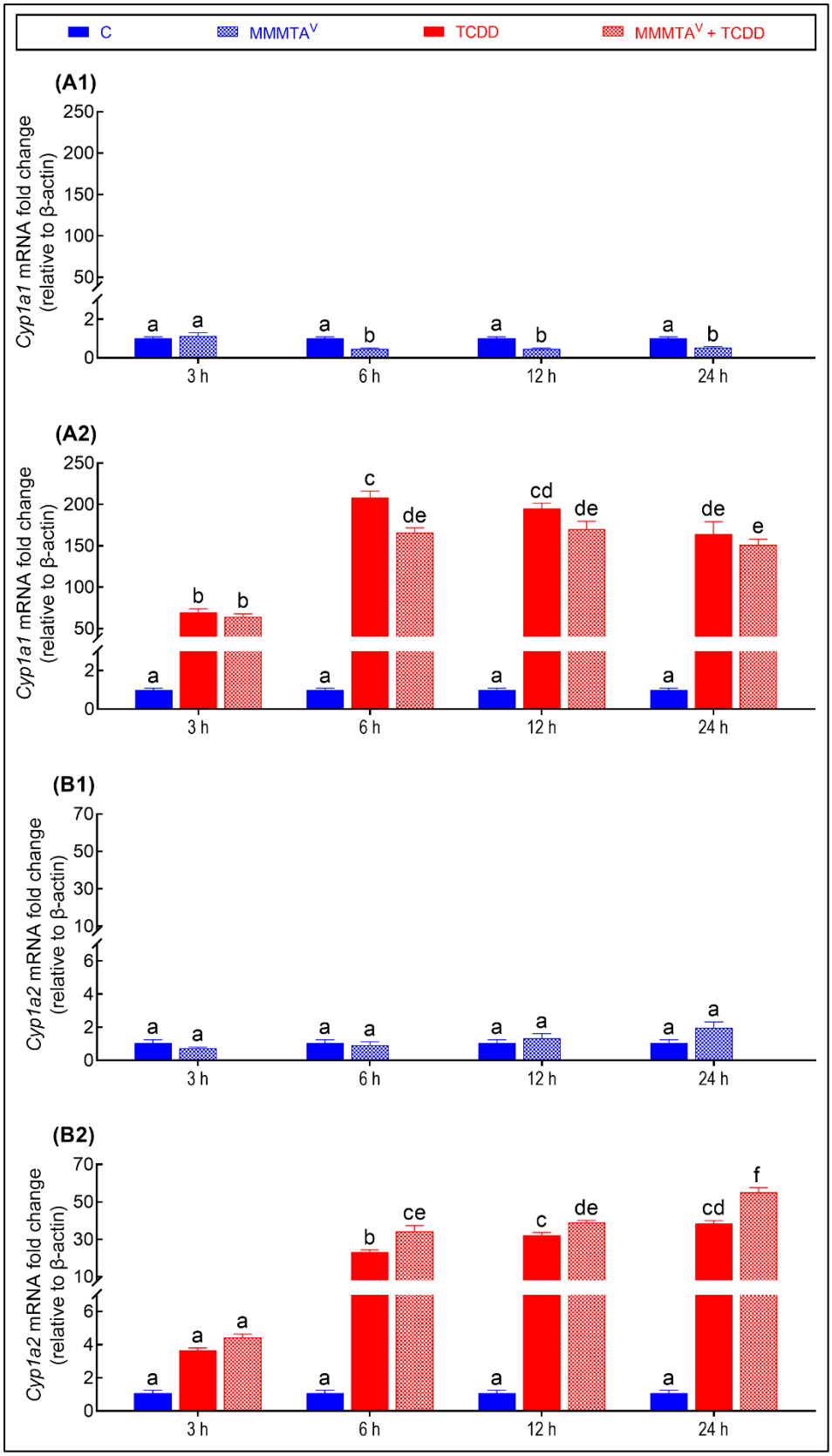

Figure 3.26. Time-dependent effect of MMMTA^V and TCDD on *Cyp1a1* (A) and *Cyp1a2* (B) mRNA in Hepa1c1c7 cells. Results are presented as mean ± SEM (representing duplicate reactions performed for each experiment of three independent experiments). Different lowercase letters indicate statistically significant difference ($p < 0.05$). Bars not sharing any letter are significantly different.

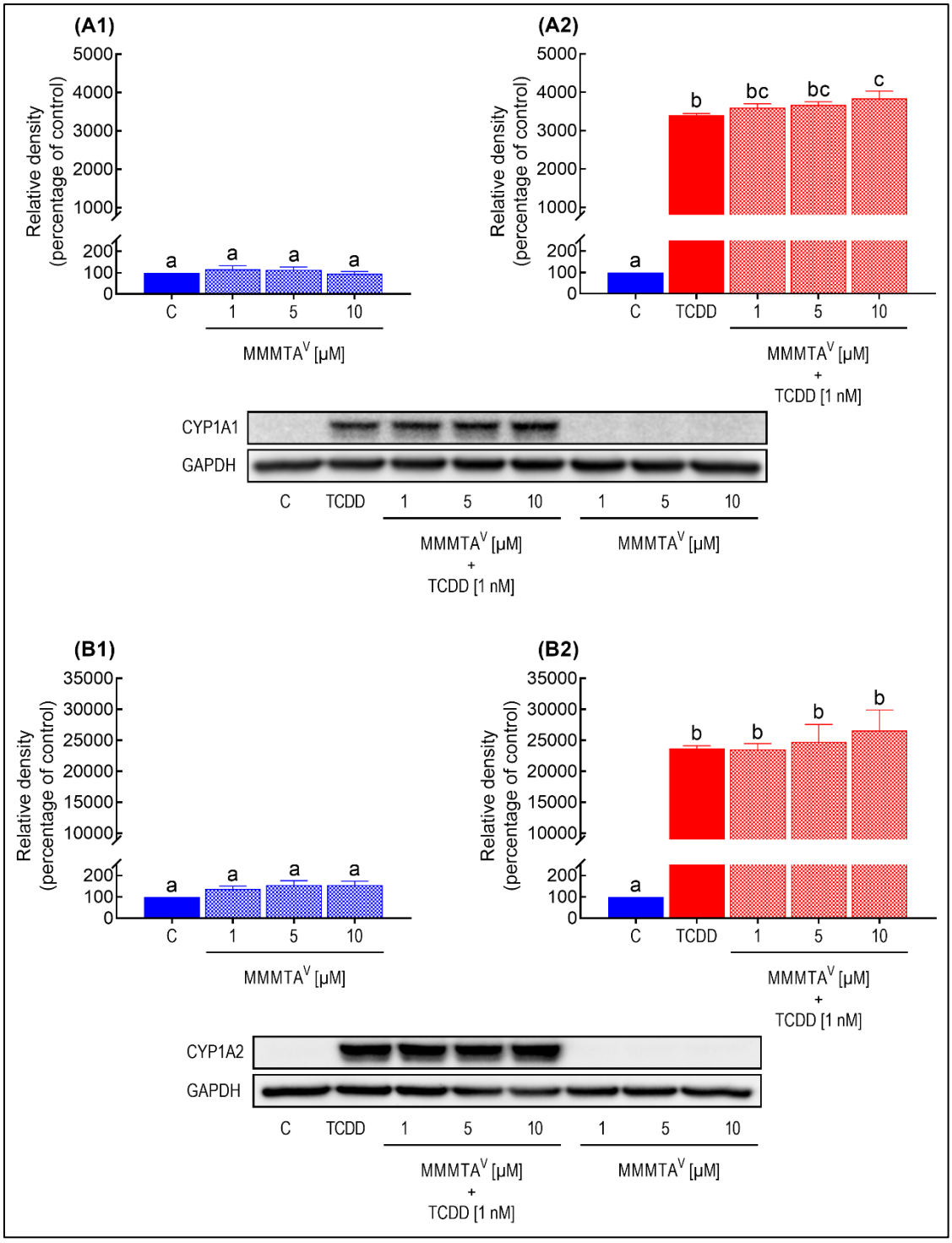

Figure 3.27. Effect of MMMTA^{V} and TCDD on CYP1A1 (A) and CYP1A2 (B) proteins in Hepa1c1c7 cells. Results are presented as mean ± SEM (one of three representative experiments is shown) representing the relative amounts of protein (expressed as percentage of the control (C) which is set at 100%) normalized to GAPDH signals. Different lowercase letters indicate statistically significant difference ($p < 0.05$). Bars not sharing any letter are significantly different.

3.4.1.5. Effect of MMMTA^V and TCDD on CYP1A1 and CYP1A2 activities in Hepa1c1c7 cells

The basal levels of both EROD or MROD catalytic activities were not significantly affected by the treatment of MMMTA^V alone (Figure 3.28A and B). However, TCDD treatment significantly induced both EROD and MROD activities by 1297.4% and 494.8%, respectively, compared to the control (Figure 3.28A and B). Compared to TCDD treatment, significant increase in the TCDD-mediated induction of EROD and MROD activities resulted from the co-exposure to both MMMTA^V and TCDD, where EROD activity increased by 23.4% in response to 10 μM MMMTA^V co-treatment, while 12.8% and 16% increases in MROD activity were observed in the 5 and 10 μM MMMTA^V co-treatment groups, respectively (Figure 3.28A and B).

3.4.1.6. Effect of MMMTA^V and TCDD on XRE-driven luciferase activity in transfected Hepa1c1c7 cells

Our findings demonstrated that 10 μM MMMTA^V alone did not alter the constitutive expression of the luciferase activity (Figure 3.29A). On the other hand, 1 nM TCDD alone significantly increased luciferase activity by 3022.2% compared to the control (Figure 3.29B). Co-exposure to both MMMTA^V and TCDD significantly decreased the TCDD-mediated induction of luciferase activity by 9.1% (Figure 3.29B).

3.4.1.7. Effect of MMMTA^V on *Cyp1a1* mRNA half-life in Hepa1c1c7 cells

Because mRNA expression level is a function of both transcription and elimination rates, the overall effect of MMMTA^V on *Cyp1a1* mRNA can be attributed not only to modulating its synthesis, but also to modifying its degradation. The Act-D chase assay was performed to assess whether *Cyp1a1* mRNA undergoes MMMTA^V-mediated post-transcriptional modification. Our results showed that TCDD-induced *Cyp1a1* mRNA decayed with a half-life ($t_{1/2}$) of 4.2 h, and that the co-exposure to MMMTA^V and TCDD did not significantly alter *Cyp1a1* mRNA half-life, which was 4.1 h in this case (Figure 3.30).

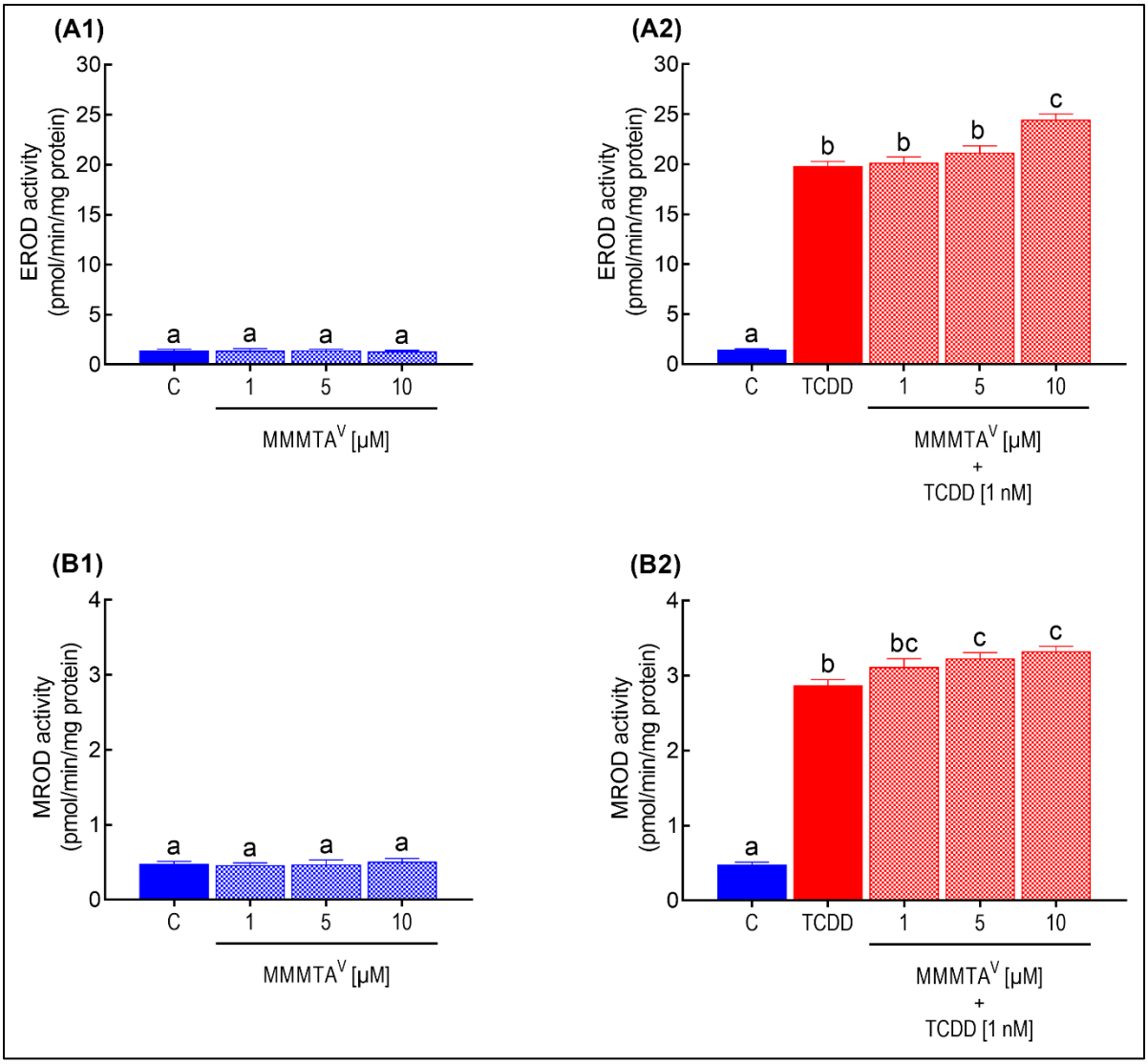

Figure 3.28. Effect of MMMTA^{V} and TCDD on CYP1A1 (A) and CYP1A2 (B) activities in Hepa1c1c7 cells. Results are presented as mean ± SEM (n = 6). Different lowercase letters indicate statistically significant difference ($p < 0.05$). Bars not sharing any letter are significantly different.

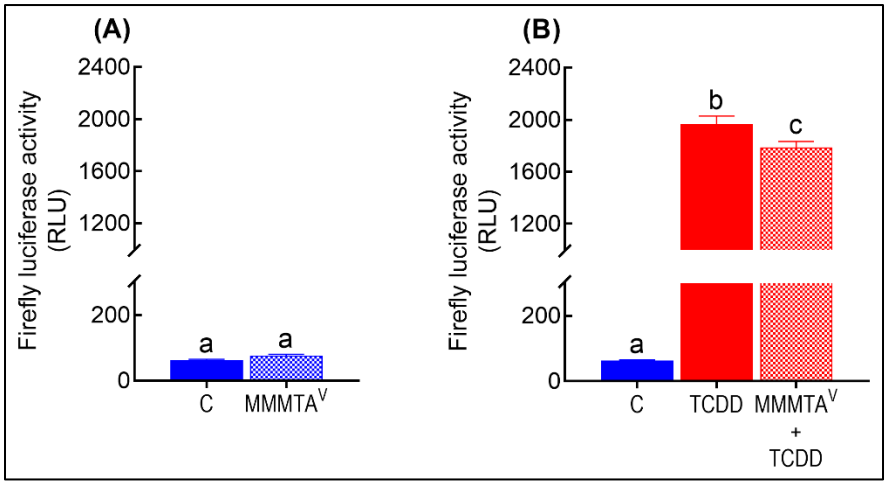

Figure 3.29. Effect of MMMTA^V and TCDD on XRE-driven luciferase activity in transfected Hepa1c1c7 cells. Luciferase activity is reported as relative light units. Results are presented as mean ± SEM (n = 6). Different lowercase letters indicate statistically significant difference ($p < 0.05$). Bars not sharing any letter are significantly different.

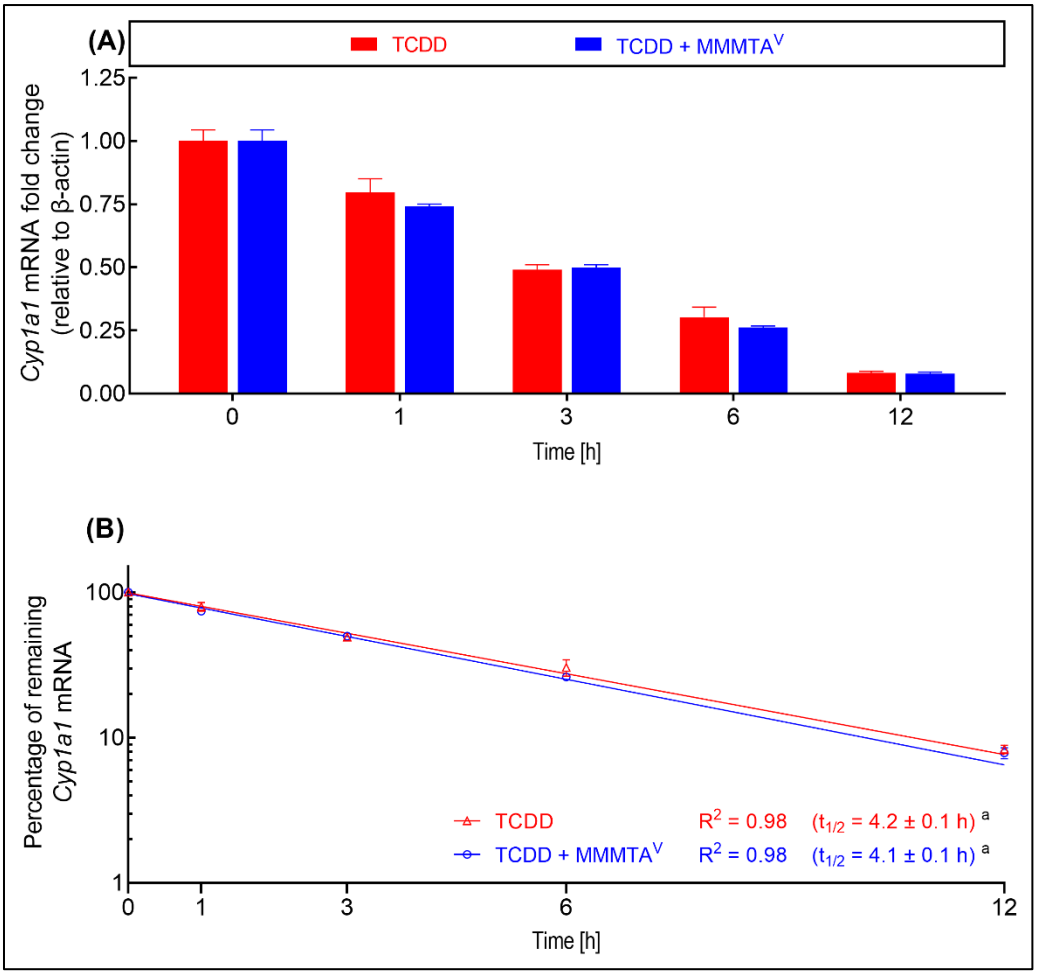

Figure 3.30. Effect of MMMTA^{V} on *Cyp1a1* mRNA half-life in Hepa1c1c7 cells. Results are presented as mean ± SEM (representing duplicate reactions performed for each experiment of two independent experiments). The mRNA decay curve from each experiment was analyzed individually, and the obtained half-life values were then used to calculate the mean half-life. Different lowercase letters indicate statistically significant difference ($p < 0.05$).

3.4.1.8. Effect of MMMTA^{V} on CYP1A1 protein half-life in Hepa1c1c7 cells

Similar to mRNA, the expression level of certain protein is dependent on its rate of translation from mRNA transcripts as well as its turnover rate. Therefore, the collective impact of MMMTA^{V} on CYP1A1 protein can be ascribed to alteration in its production and/or decay. The CHX chase assay was performed to evaluate the possibility of MMMTA^{V} involvement in post-translational modification of CYP1A1 protein. Our findings demonstrated that TCDD-induced CYP1A1 protein degraded with a half-life of 7.3 h, and that the co-treatment with MMMTA^{V} did not significantly change CYP1A1 protein half-life ($t_{1/2}$ = 7 h) (Figure 3.31).

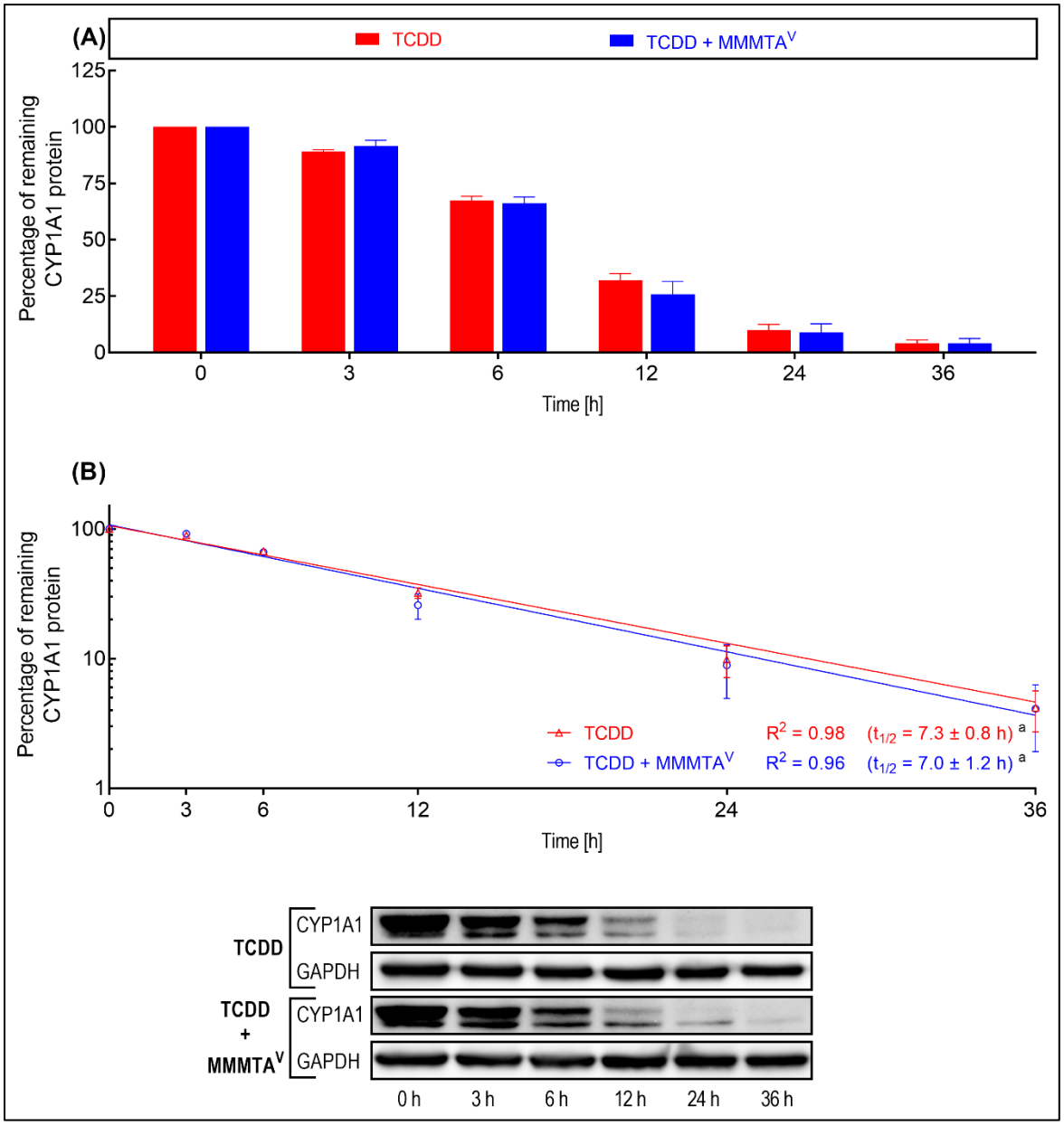

Figure 3.31. Effect of MMMTA^V on CYP1A1 protein half-life in Hepa1c1c7 cells. Results are presented as mean ± SEM (one of three representative experiments is shown) representing the relative amounts of protein (expressed as percentage of the control (C) which is set at 100%) normalized to GAPDH signals. The protein decay curve from each experiment was analyzed individually, and the obtained half-life values were then used to calculate the mean half-life. Different lowercase letters indicate statistically significant difference ($p < 0.05$).

3.4.2. Down-regulation of CYP1A1 enzyme by MMMTA^V in human HepG2 cells

3.4.2.1. Effect of MMMTA^V and TCDD on viability of HepG2 cells

In an attempt to correlate rodent data to humans, we used human HepG2 cells. Screening of different MMMTA^V concentrations through the MTT reduction assay revealed a significant 30.3% reduction in HepG2 cells viability after 24 h-exposure to 1000 μM MMMTA^V, while other tested concentrations did not significantly affect cell viability (Figure 3.32A). Additionally, our results also showed that co-exposure to MMMTA^V (1, 5, and 10 μM) and 1 nM TCDD had no significant effect on cell viability (Figure 3.32B).

3.4.2.2. Effect of MMMTA^V and TCDD on CYP1A1 mRNA, protein, and activity in HepG2 cells

MMMTA^V alone, at all tested concentrations, did not affect the constitutive level of *CYP1A1* mRNA, while TCDD alone caused a significant induction of 14830% compared to the control (Figure 3.33). Co-exposure to 10 μM MMMTA^V and TCDD resulted in a significant 43.4% decrease in *CYP1A1* mRNA compared to the treatment with TCDD alone (Figure 3.33).

Similarly, CYP1A1 protein was not altered by MMMTA^V alone, but was significantly induced by 333.5% in response to TCDD (Figure 3.34). The TCDD-inducible CYP1A1 protein was significantly reduced by 28.8% upon the co-exposure to 10 μM MMMTA^V (Figure 3.34).

EROD activity was affected in a way similar to that of the CYP1A1 transcripts and protein. None of the tested MMMTA^V concentrations was able to alter the basal EROD activity, whereas TCDD alone significantly increased it by 2025.1% (Figure 3.35). When combined with TCDD, MMMTA^V at 10 μM was able to significantly decrease EROD activity by 18.3% compared to TCDD treatment (Figure 3.35).

3.4.2.3. Effect of MMMTA^V and TCDD on XRE-driven luciferase activity in transfected HepG2 cells

The treatment with 10 μM MMMTA^V alone did not change the basal luciferase activity (Figure 3.36A). However, 1 nM TCDD alone significantly increased the luminescence signal of luciferase activity by 351.5% compared to the control (Figure 3.36B). Co-exposure to both MMMTA^V and TCDD significantly decreased the TCDD-mediated induction of luciferase activity by 12.8% (Figure 3.36B).

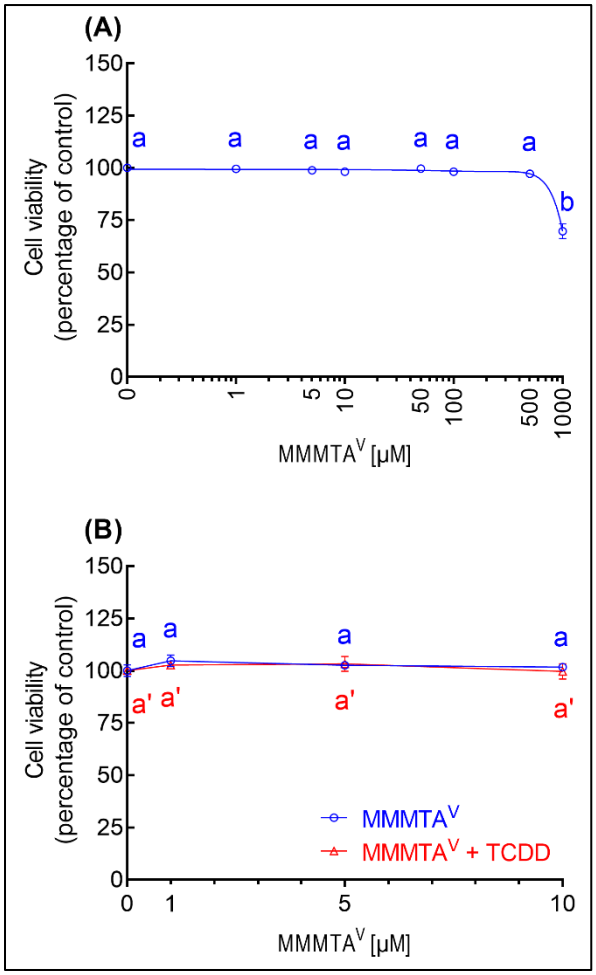

Figure 3.32. Effect of MMMTA^V and TCDD on viability of HepG2 cells. Results are expressed as percentage of control (set at 100%) ± SEM (n = 6). Different lowercase letters indicate statistically significant difference ($p < 0.05$). Points not sharing any letter are significantly different.

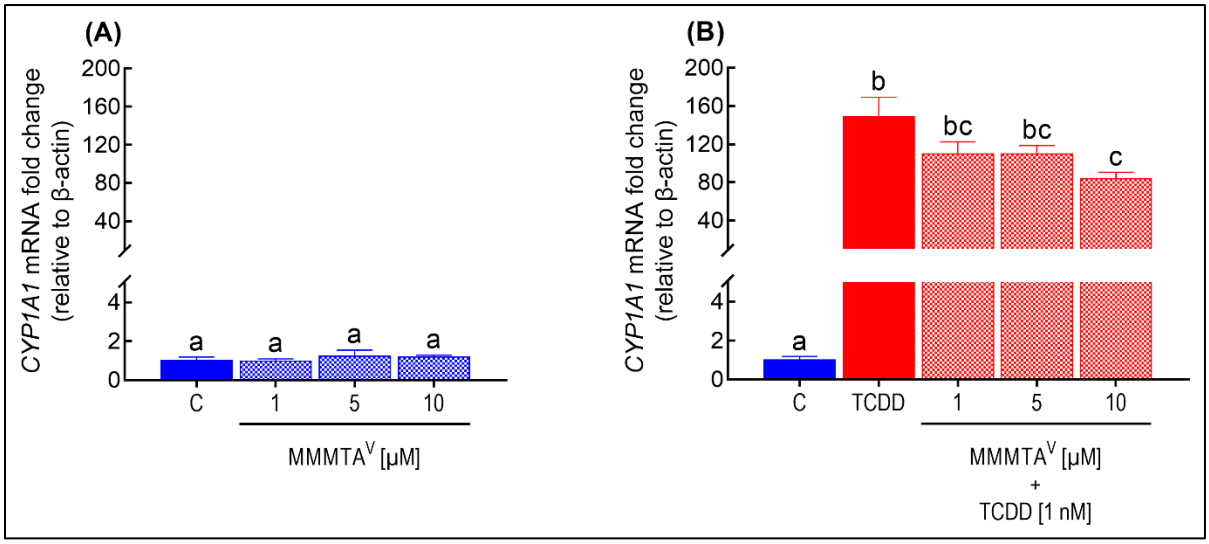

Figure 3.33. Effect of MMMTA^V and TCDD on *CYP1A1* mRNA in HepG2 cells. Results are presented as mean ± SEM (representing duplicate reactions performed for each experiment of three independent experiments). Different lowercase letters indicate statistically significant difference ($p < 0.05$). Bars not sharing any letter are significantly different.

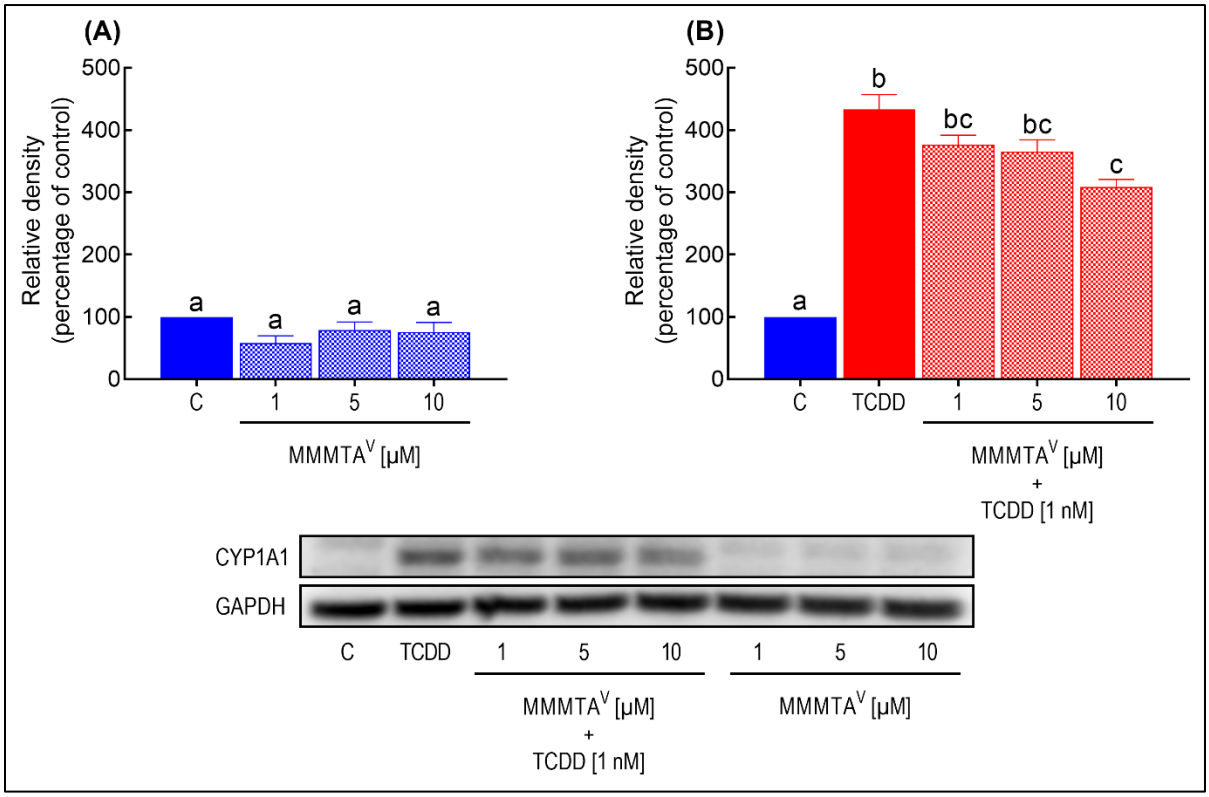

Figure 3.34. Effect of MMMTA^{V} and TCDD on CYP1A1 protein in HepG2 cells. Results are presented as mean ± SEM (one of three representative experiments is shown) representing the relative amounts of protein (expressed as percentage of the control (C) which is set at 100%) normalized to GAPDH signals. Different lowercase letters indicate statistically significant difference ($p < 0.05$). Bars not sharing any letter are significantly different.

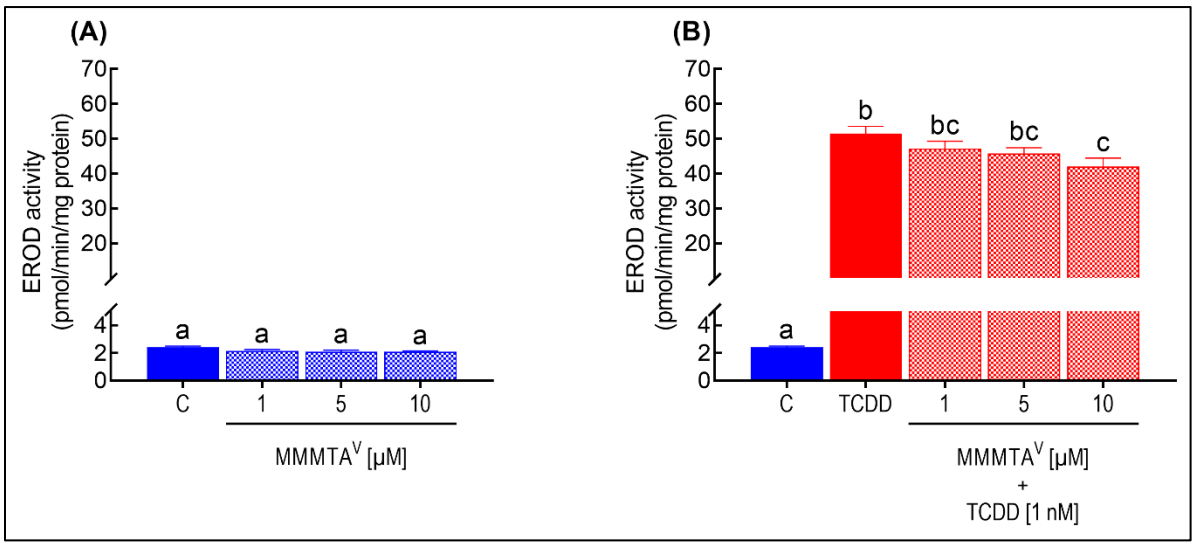

Figure 3.35. Effect of MMMTA^{V} and TCDD on CYP1A1 activity in HepG2 cells. Results are presented as mean ± SEM (n = 6). Different lowercase letters indicate statistically significant difference ($p < 0.05$). Bars not sharing any letter are significantly different.

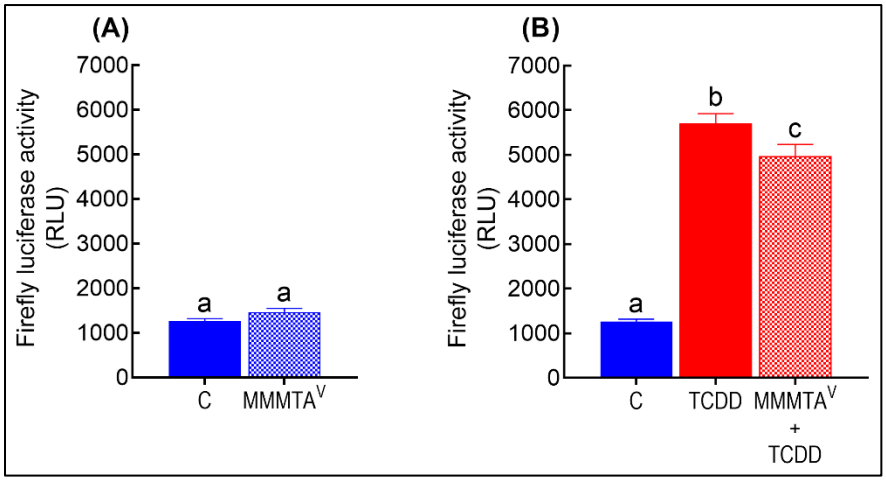

Figure 3.36. Effect of MMMTA^V and TCDD on XRE-driven luciferase activity in transfected HepG2 cells. Luciferase activity is reported as relative light units. Results are presented as mean ± SEM (n = 6). Different lowercase letters indicate statistically significant difference ($p < 0.05$). Bars not sharing any letter are significantly different.

3.5. Modulation of hepatic CYP enzymes and cellular transporters by ATO^{III} in C57BL/6 mice

3.5.1. Differential modulation of hepatic CYP enzymes by ATO^{III} in C57BL/6 mice

ATO^{III} significantly altered mRNA expression of the *Cyp1* family members (Figure 3.37) after both durations of treatment, with the exception of *Cyp1a2* which exhibited no significant change at both time points. At 6 h, ATO^{III} significantly potentiated *Cyp1a1* mRNA level by 99.5% compared to the control (Figure 3.37). However, this effect was inverted into a significant 31% decrease at the 24 h time point. For *Cyp1b1* mRNA, there was a significant increase at both 6 h and 24 h, with increments of 161% and 61%, respectively, compared to their respective control levels (Figure 3.37).

Differential modulation of mRNA expression by ATO^{III} was observed across the different *Cyp2* subfamilies (Figure 3.38). Compared to the control, there was a significant induction of *Cyp2a4* and *Cyp2a5* in response to 6 h and 24 h ATO^{III} treatments. Specifically, *Cyp2a4* was increased by 413% at 6 h and 246% at 24 h, while *Cyp2a5* was increased by 316% and 202% at 6 h and 24 h, respectively (Figure 3.38A).

For the *Cyp2b* subfamily, ATO^{III} significantly induced the mRNA expression of *Cyp2b9*, *Cyp2b10*, and *Cyp2b19* at 6 h by 872%, 88%, and 111%, respectively (Figure 3.38B). At 24 h, *Cyp2b9* and *Cyp2b10* also exhibited a significant increase in mRNA by 191% and 53%, respectively, while *Cyp2b19* showed a significant decrease by 54% compared to the control (Figure 3.38B).

In the *Cyp2c* subfamily, ATO^{III} had gene- and time-dependent effects on their expression. At 24 h, ATO^{III} significantly increased the mRNA levels of *Cyp2c38*, *Cyp2c39*, and *Cyp2c40* by 109%, 200%, and 114%, respectively, compared to their respective controls, while *Cyp2c29* exhibited a significant 21% decrease (Figure 3.38C). *Cyp2c39* showed a significant 108% increase in response to ATO^{III} at 6 h as well, while neither *Cyp2c29* nor *Cyp2c40* had a significant change (Figure 3.38C). Additionally, the 6 h mRNA levels of both *Cyp2c38* and *Cyp2c44* significantly decreased by 41% and 31%, respectively, compared to the control (Figure 3.38C).

As shown in (Figure 3.38D) *Cyp2d10* exhibited a significant 28% decrease in mRNA expression at the 24 h time point, with no change at 6 h, compared to the control. In contrast, *Cyp2e1* showed significant down-regulation of its mRNA level only at 6 h, with a decrease of 32%, while there was no significant alteration at the 24 h time point, compared to the control (Figure 3.38E).

The influence of ATO^{III} on the *Cyp2j* subfamily was observed only at the 6 h time point, with no significant changes in mRNA expression at 24 h (Figure 3.38F). Specifically, *Cyp2j6*, *Cyp2j9*, and *Cyp2j13* exhibited significant up-regulation, with increases of 42%, 44%, and 38%, respectively. Conversely, *Cyp2j5* displayed a significant decrease of 19%, compared to the control (Figure 3.38F).

Exposure to ATO^{III} resulted in significant up-regulation of the mRNA expression of *Cyp3a11* and *Cyp3a13*, only at 6 h, by 28% and 68%, respectively, without changing their expression at 24 h, as compared to the control (Figure 3.39).

Regarding the *Cyp4a* subfamily (Figure 3.40A), several changes in gene expression were observed as a result of ATO^{III} treatment. There was a significant increase in the gene expression of *Cyp4a10* at 6 h and 24 h by 42% and 81%, respectively (Figure 3.40A). Additionally, *Cyp4a14* exhibited a significant increase in its mRNA level at 6 h by 64% (Figure 3.40A). Inversely, *Cyp4a12* showed a considerable 48% decrease at the 24 h time point compared to the control (Figure 3.40A).

Also, ATO^{III} had a significant impact on certain members of the *Cyp4f* subfamily. Specifically, *Cyp4f13* exhibited a significant mRNA increase at 6 h by 31%, in contrast to a notable decrease of 25% at 24 h (Figure 3.40B). Interestingly, *Cyp4f16* displayed a significant increase at both 6 h and 24 h, with a rise of 124% and 69%, respectively (Figure 3.40B). In contrast, *Cyp4f18* mRNA levels increased by 107% at 6 h, with no corresponding change at the 24 h time point when compared to the control (Figure 3.40B).

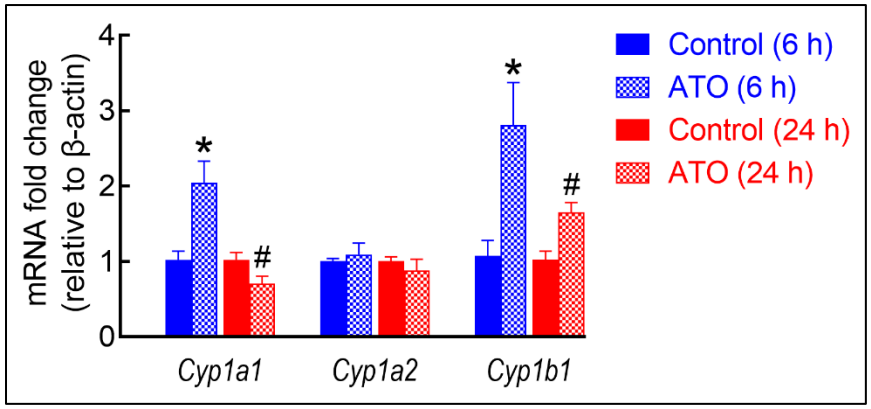

Figure 3.37. Effect of ATO^{III} on hepatic *Cyp1* family mRNA in C57BL/6 mice. Results are presented as mean ± SEM (n = 4–6). * and # designate statistically significant difference in comparison with the 6 h control and 24 h control, respectively ($p < 0.05$).

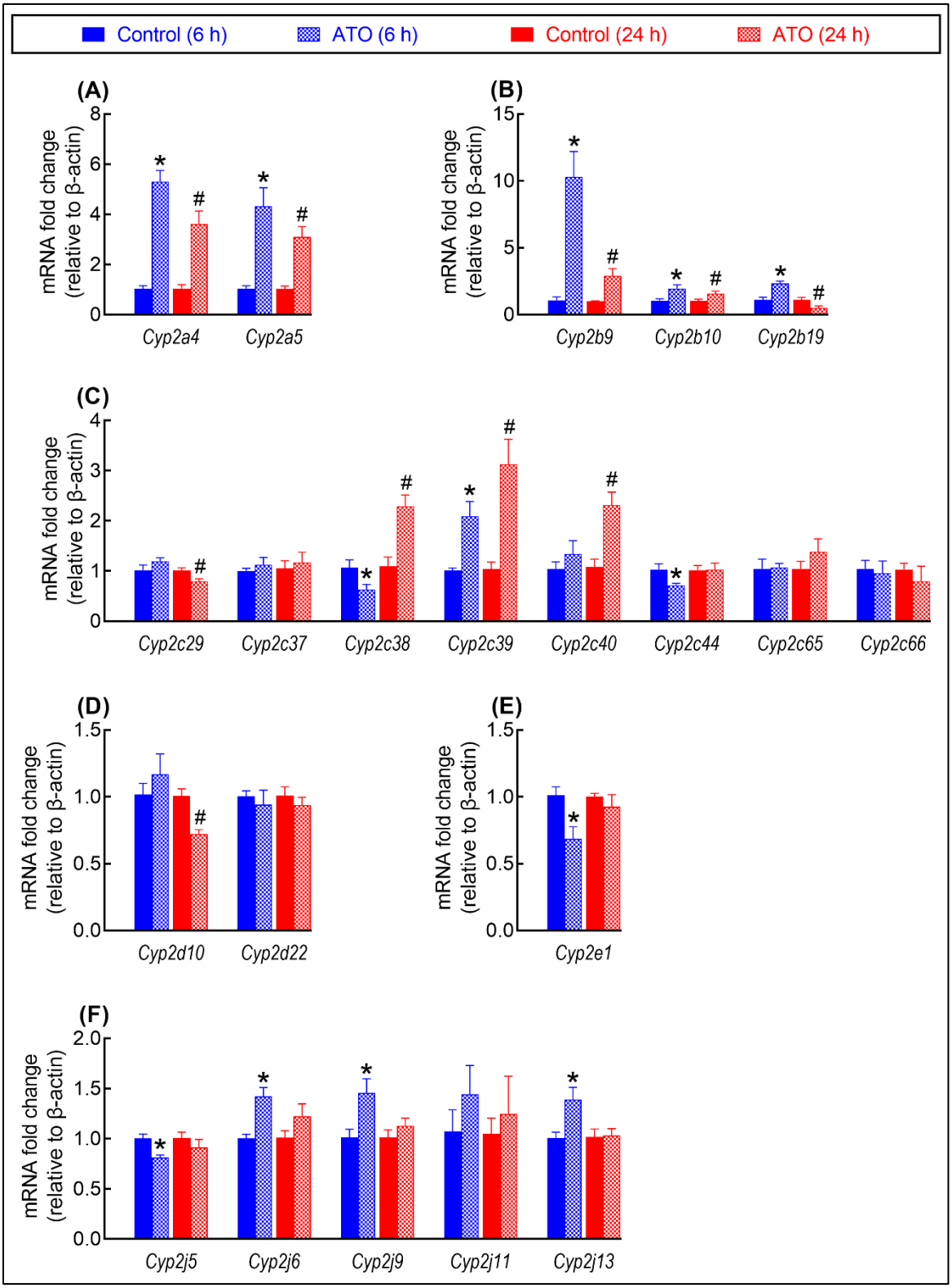

Figure 3.38. Effect of ATO^{III} on hepatic *Cyp2* family mRNA in C57BL/6 mice. Results are presented as mean ± SEM (n = 4–6). * and # designate statistically significant difference in comparison with the 6 h control and 24 h control, respectively ($p < 0.05$).

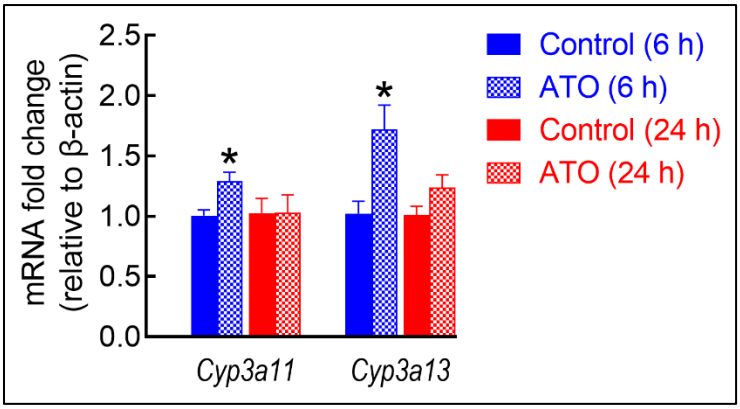

Figure 3.39. Effect of ATO^{III} on hepatic *Cyp3* family mRNA in C57BL/6 mice. Results are presented as mean ± SEM (n = 4–6). * and # designate statistically significant difference in comparison with the 6 h control and 24 h control, respectively ($p < 0.05$).

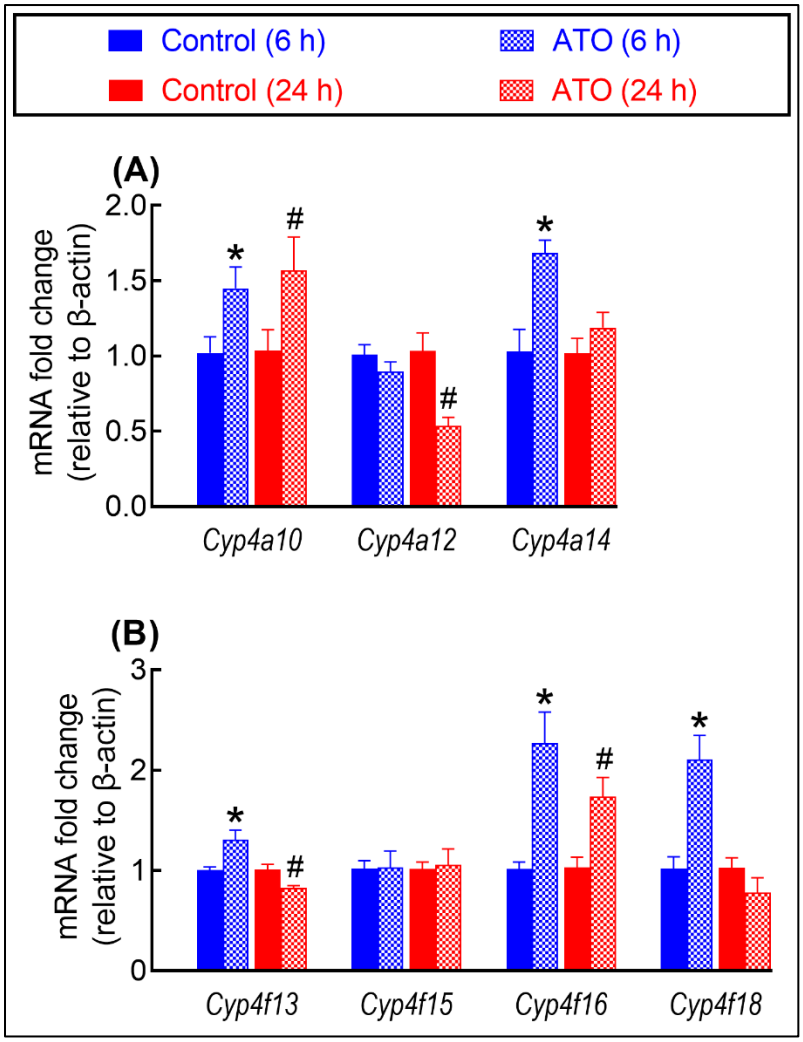

Figure 3.40. Effect of ATO^{III} on hepatic *Cyp4* family mRNA in C57BL/6 mice. Results are presented as mean ± SEM (n = 4–6). * and # designate statistically significant difference in comparison with the 6 h control and 24 h control, respectively ($p < 0.05$).

3.5.2. Modulation of hepatic *Pla2g4a*, *Ptgs*, and *Alox* mRNA by ATO^{III} in C57BL/6 mice

At 6 h and 24 h, exposure to ATO^{III} significantly increased the mRNA levels of phospholipase A_2 group IV A (*Pla2g4a*), commonly referred to as cytosolic phospholipase A_2-alpha, in the liver by 67% and 49%, respectively, compared to the control (Figure 3.41).

In line with the findings presented in (Figure 3.42A), the exposure to ATO^{III} led to a notable 52% reduction in prostaglandin-endoperoxide synthase 1 (*Ptgs1*), commonly referred to as cyclooxygenase 1 (COX-1), mRNA expression at 6 h, with no significant change observed at 24 h (Figure 3.42A). Conversely, prostaglandin-endoperoxide synthase 2 (*Ptgs2*), commonly referred to as cyclooxygenase 2 (COX-2), exhibited a significant increase of 519%, only at the 6 h time point (Figure 3.42A).

Both arachidonate 5-lipoxygenase (*Alox5*) and arachidonate 15-lipoxygenase (*Alox15*) demonstrated significant decrease in mRNA levels, only at 6 h, with reductions of 40% and 37%, respectively, in comparison to the control (Figure 3.42B).

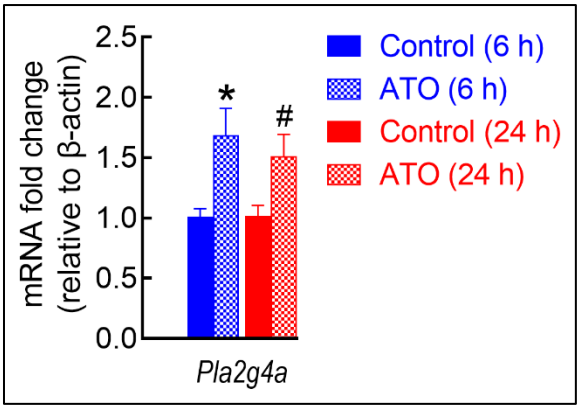

Figure 3.41. Effect of ATO[III] on hepatic *Pla2g4a* (cytosolic phospholipase A2-alpha) mRNA in C57BL/6 mice. Results are presented as mean ± SEM (n = 4–6). * and # designate statistically significant difference in comparison with the 6 h control and 24 h control, respectively ($p < 0.05$).

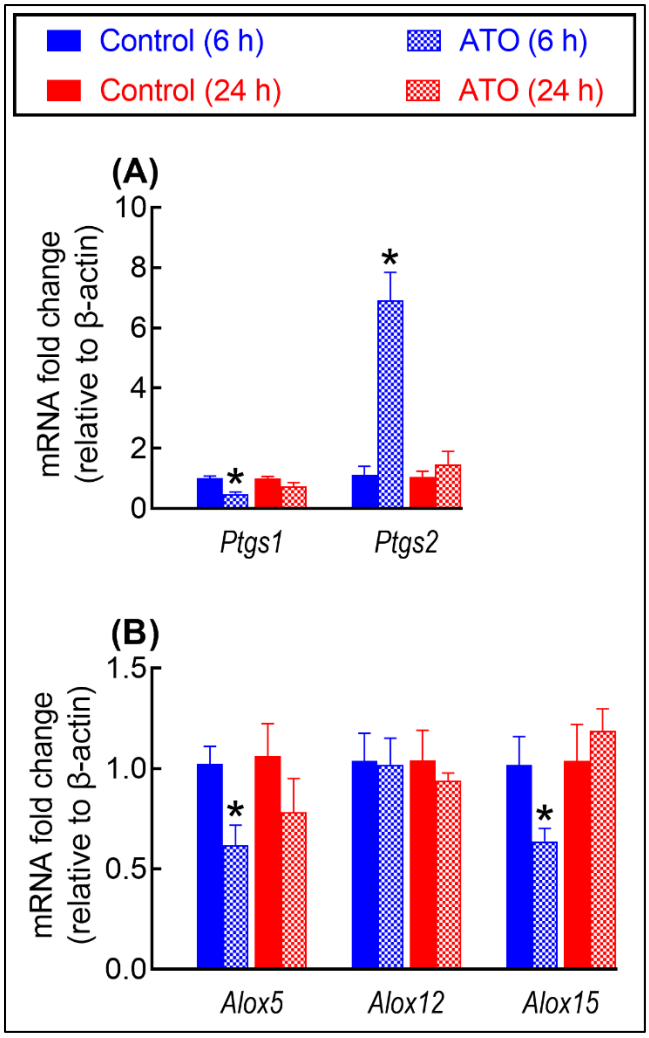

Figure 3.42. Effect of ATO^{III} on hepatic *Ptgs* (cyclooxygenases) (A) and *Alox* (lipoxygenases) (B) mRNA in C57BL/6 mice. Results are presented as mean ± SEM (n = 4–6). * and # designate statistically significant difference in comparison with the 6 h control and 24 h control, respectively ($p < 0.05$).

3.5.3. Alteration of hepatic HETEs formation by ATO^{III} in C57BL/6 mice

Both enantiomers of all HETEs were detected in the liver, except for the 9-HETE (Figure 3.43). Among these, 20-HETE was the most abundantly formed HETE in hepatic microsomes (Figure 3.43J). Of all mid-chain HETEs, only 5-HETE and 15-HETE showed significant enantiospecific changes in response to 24 h ATO^{III} exposure. Compared to their respective controls, the R enantiomer of 5-HETE decreased significantly by 16%, while the S enantiomer of 15-HETE exhibited a significant reduction of 25% (Figure 3.43A and E).

For mid-chain HETEs in ATO^{III}-treated mice, the S enantiomer was found to be significantly higher than the R enantiomer in 5-, 8-, and 11-HETEs, whereas the R enantiomer predominated in 12- and 15-HETEs (Figure 3.43). In case of subterminal HETEs, the R enantiomer generally surpassed the S enantiomer, except for 19-HETE, where the S enantiomer was significantly higher (Figure 3.43). Additionally, exposure to ATO^{III} resulted in a significant 25% increase in the S enantiomer of 17-HETE compared to the respective control (Figure 3.43G). For 18-HETE, a significant 33% increase was noticed in the R enantiomer, in contrast to the S enantiomer, which decreased by 30%, compared to the control (Figure 3.43H). Interestingly, ATO^{III} exposure led to a significant 30% increase in 20-HETE levels compared to the control (Figure 3.43J).

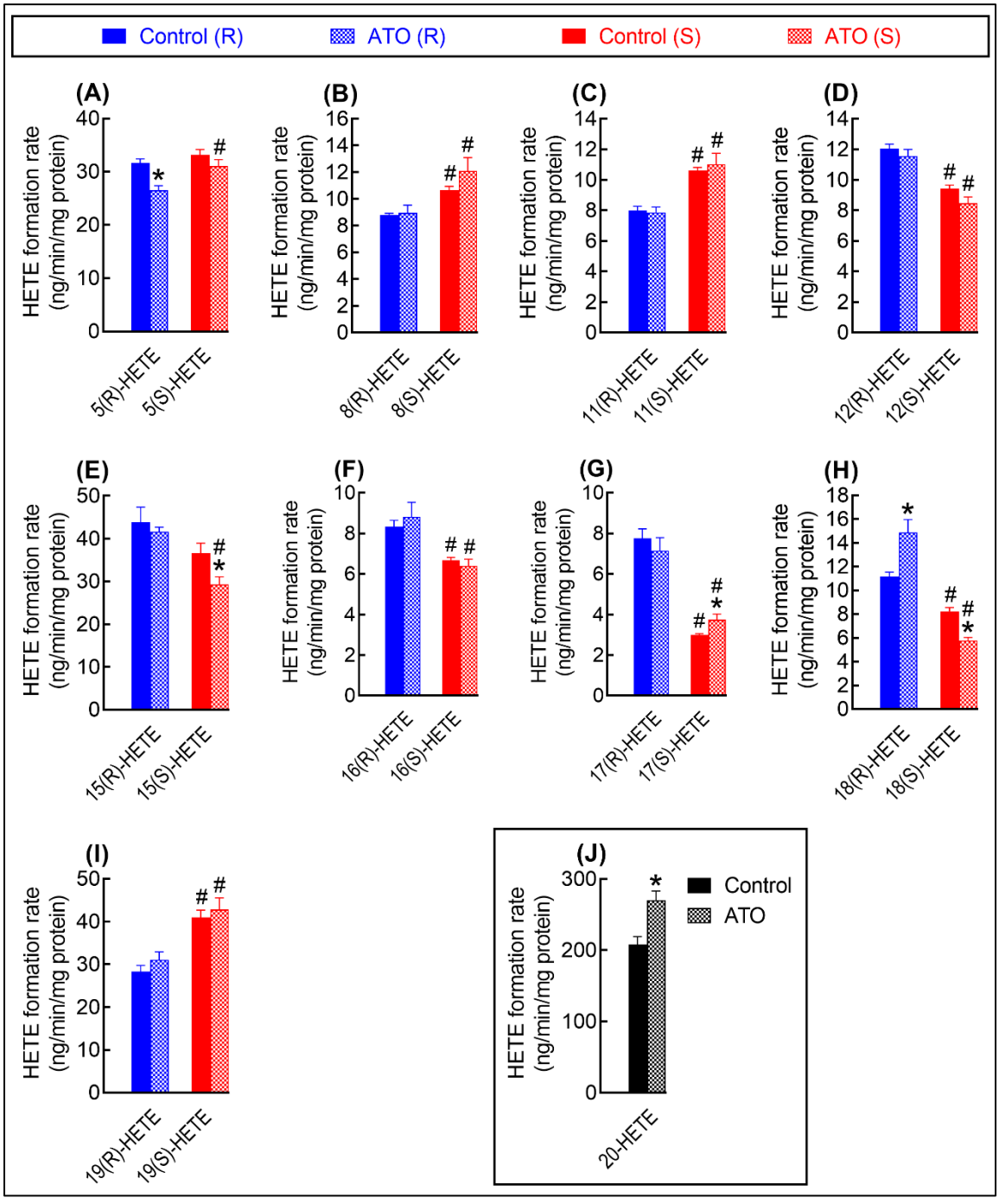

Figure 3.43. Effect of ATO^{III} on enantiospecific formation rates of hepatic HETEs (hydroxyeicosatetraenoic acids) in C57BL/6 mice. Results are presented as mean ± SEM (n = 4–6). * designates statistically significant difference in comparison with the respective control for each enantiomer, while # denotes significant difference in comparison with the respective optical antipode within each experimental group ($p < 0.05$).

3.5.4. Differential modulation of hepatic cellular transporters by ATO^{III} in C57BL/6 mice

Both arsenic influx and efflux transporters were affected by ATO^{III} treatment. Exposure to ATO^{III} resulted in altered mRNA expression of the aquaporin (*Aqp*) uptake channels. As early as 6 h, ATO^{III} significantly increased the mRNA levels of *Aqp3* and *Aqp9* by 71% and 92%, respectively, but this effect faded into insignificant change at 24 h (Figure 3.44A). Conversely, there was a significant up-regulation of *Aqp7* mRNA transcripts by 197% at 24 h, while no significant change was noticed at 6 h when compared to the control (Figure 3.44A).

ATO^{III} treatment also modulated the mRNA expression of some members of the ATP-binding cassette (*Abc*) superfamily of efflux transporters (Figure 3.44B). Subfamily B member 1 (*Abcb1*), commonly referred to as P-glycoprotein (P-gp) or multidrug resistance protein 1 (MDR1), mRNA was significantly increased after 6 h- and 24 h-exposure to ATO^{III} by 64% and 82%, respectively, compared to the control (Figure 3.44B). At 6 h only, ATO^{III} significantly elevated the mRNA expression of the members 1, 2, 4, 5, and 6 of the subfamily C, commonly referred to as multidrug resistance-associated proteins (MRPs), by 177%, 49%, 298%, 102%, and 109%, respectively, compared to their respective controls (Figure 3.44B).

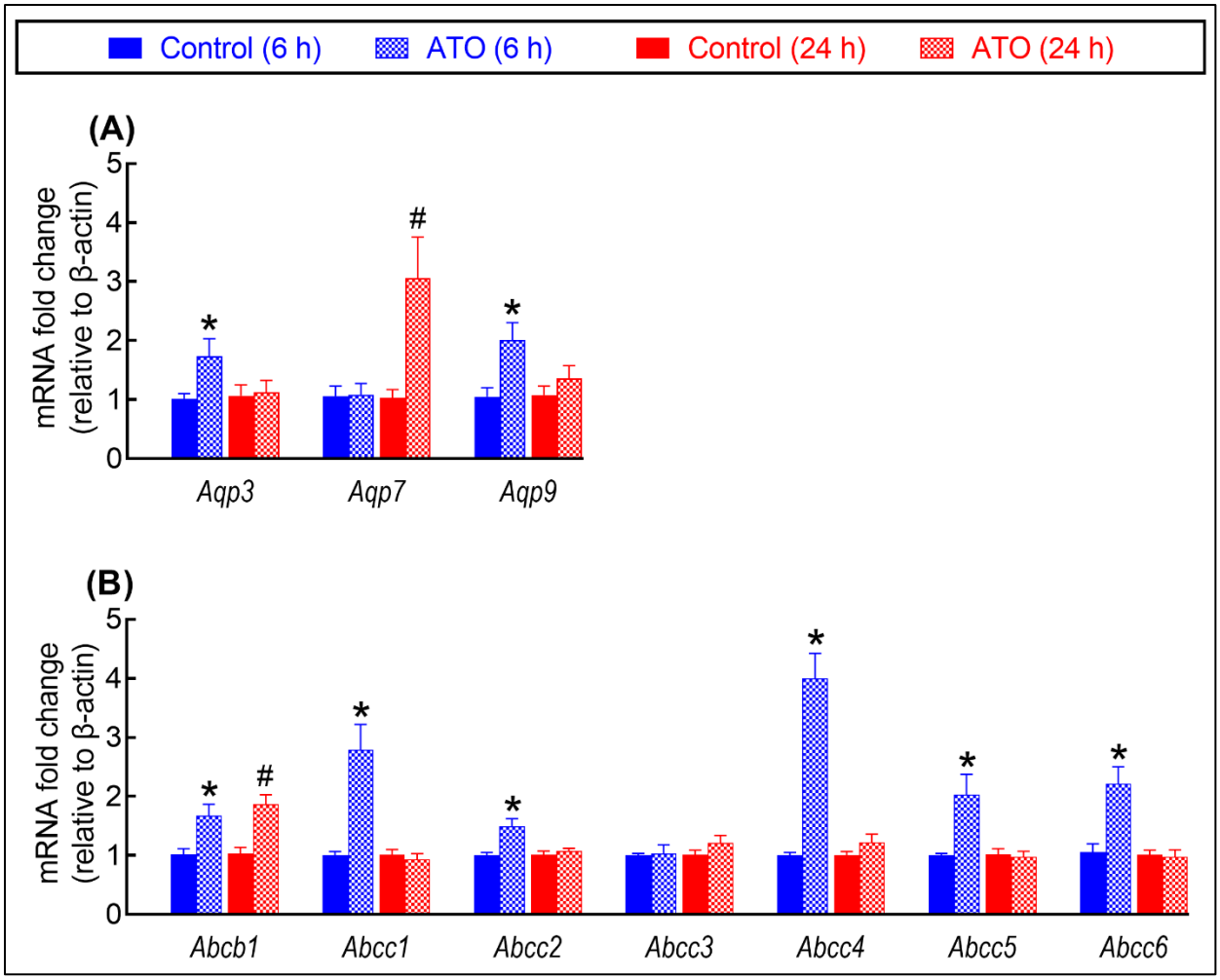

Figure 3.44. Effect of ATO^{III} on hepatic arsenic uptake channels (A) and efflux pumps (B) mRNA in C57BL/6 mice. Results are presented as mean ± SEM (n = 4–6). * and # designate statistically significant difference in comparison with the 6 h control and 24 h control, respectively ($p < 0.05$).

CHAPTER 4.

DISCUSSION

Portions of this chapter have been published in:

1. **El-Ghiaty MA**, Alqahtani MA, El-Kadi AOS. Down-regulation of hepatic cytochromes P450 1A1 and 1A2 by arsenic trioxide (ATO) in vivo and in vitro: A role of heme oxygenase 1. *Chem Biol Interact*. 2022 Sep 1;364:110049. doi: 10.1016/j.cbi.2022.110049.

2. **El-Ghiaty MA**, Alqahtani MA, El-Kadi AOS. Arsenic trioxide (ATO) up-regulates cytochrome P450 1A (CYP1A) enzymes in murine hepatoma Hepa-1c1c7 cell line. *Environ Toxicol Pharmacol*. 2023 Aug;101:104214. doi: 10.1016/j.etap.2023.104214.

3. **El-Ghiaty MA**, Alqahtani MA, El-Kadi AOS. Modulation of cytochrome P450 1A (CYP1A) enzymes by monomethylmonothioarsonic acid (MMMTAV) in vivo and in vitro. *Chem Biol Interact*. 2023 May 1;376:110447. doi: 10.1016/j.cbi.2023.110447.

4. **El-Ghiaty MA**, Alqahtani MA, El-Mahrouk SR, Isse FA, Alammari AH, El-Kadi AOS. Alteration of hepatic cytochrome P450 expression and arachidonic acid metabolism by arsenic trioxide (ATO) in C57BL/6 mice. *Biol Trace Elem Res*. 2024. doi: 10.1007/s12011-024-04225-1. (in press)

4.1. Differential modulation of basal and TCDD-inducible CYP1A enzymes by ATO^{III} *in vivo* and *in vitro*

We demonstrate for the first time that ATO^{III}, at clinically relevant dose or concentrations, modulates both constitutive and TCDD-inducible expressions of cytochromes P450 1A1 and 1A2 in C57BL/6 mice and HepG2 cells. Moreover, we show that ATO^{III} can alter these enzymes through both transcriptional and post-translational mechanisms.

In clinical practice, ATO^{III} is administered to APL patients at a regimen of 0.15 mg/kg body weight repeated daily for multiple weeks depending on the phase of treatment (i.e., induction of remission or consolidation). This dose can be allometrically scaled to about 1.85 mg/kg body weight for mice (442). However, selection of the dose (8 mg/kg body weight) in our *in vivo* experiment was based on published studies that investigated the effect of a higher single dose exposure of ATO^{III} on other malignancies in mice (443-448). Additionally, monitoring and evaluation of animals' health status during the study, according to the University of Alberta Health Sciences Animal Policy and Welfare Committee guidelines, have shown that ATO^{III} at a dose of 8 mg/kg body weight, either alone or in combination with TCDD, was well tolerated by the animals.

In human HepG2 cells experiments, to mimic the circulating therapeutic levels of ATO^{III}, we selected a range of concentrations (1, 5, and 10 μM) covering its clinical peak plasma concentration (Cp_{max}) (449) observed in APL patients after administration of the conventional dose (0.15 mg/kg body weight) (450-453). Assessment of cytotoxicity, via MTT reduction assay, has shown that ATO^{III} concentrations used in HepG2 cells experiments did not significantly affect cell viability, either alone or in combination with TCDD and/or SnMP.

Selection of the *in vivo* dose of TCDD (15 μg/kg body weight) and the *in vitro* concentrations of TCDD (1 nM) and SnMP (5 μM) used in our experiments was based on the previous studies that used the same dose and concentrations in the same experimental models (C57BL/6 mice (380) and HepG2 cells (354)). The experimental times were determined in accordance with preliminary time-dependent experiments (not reported) that were conducted to spot the timepoint of peak induction of the target (mRNA, protein, or activity) to be assessed.

Arsenic trioxide (As_2O_3) and sodium arsenite ($NaAsO_2$) are the two main chemical forms of trivalent inorganic arsenic to which humans are commonly exposed. As_2O_3 sparingly dissolves in water in the form of arsenious acid (H_3AsO_3), but by increasing the pH using an alkali such as

NaOH, the readily soluble sodium salt ($NaAsO_2$) is produced. The finished commercial arsenic trioxide product is then adjusted to pH 8 by adding HCl (454; 455).

Accordingly, arsenic trioxide and sodium arsenite are somewhat related because, under the slightly alkaline conditions of the finished arsenic trioxide product, the dominant species is possibly the sodium salt. However, depending on several factors; such as pH, temperature, and ionic strength; a number of arsenic species could also be present in equilibrium in the solution. Conventionally, arsenic trioxide is regarded as the active ingredient, despite the presence of other species in solution which may ultimately contribute to the pharmacological activity (456). That is probably why arsenic trioxide, but not sodium arsenite, is currently used as a therapeutic agent.

A lot of studies have investigated the effects of different arsenic species on the CYP enzymes, but most of them have focused on sodium arsenite as the prototypical trivalent inorganic form because of its relatively higher environmental prevalence with subsequent higher risk of human exposure. In this regard, only a very limited number of studies are available on ATO^{III} (14).

To the best of our knowledge, we are the first to test the effect of ATO^{III} on CYP1A1 and CYP1A2 *in vivo*. In C57BL/6 mice, ATO^{III} significantly inhibited the TCDD-mediated induction of hepatic CYP1A1 and CYP1A2 at the mRNA, protein, and catalytic activity (EROD and MROD activities, respectively) levels (Figure 3.1, 3.2, and 3.3). Similarly, a significant inhibitory effect on the constitutive expression of hepatic CYP1A2 was produced by ATO^{III} alone at the protein and catalytic (MROD) activity levels (Figure 3.2 and 3.3). Interestingly, the basal level of hepatic *Cyp1a1* mRNA expression was inhibited by the treatment of ATO^{III} alone 24 h post-IP injection, following an initial induction, as observed in the 6 h-treatment groups, that was reflected as significant induction in the basal CYP1A1 protein too (Figure 3.1 and 3.2).

Additionally, ATO^{III} both alone and in the presence of TCDD significantly induced hepatic *Hmox1* mRNA levels after 6 h-treatment as well as its protein expression (Figure 3.4). However, hepatic *Hmox1* mRNA induction at 6 h was inverted into significant decrease in the 24 h-treatment groups (Figure 3.4).

Enhanced HMOX1 production by ATO^{III} is one part of its impact on the cellular redox system (457). The transcriptional activation of HMOX1 has been attributed to the role of ATO^{III} in promoting the nuclear translocation of its key regulator; the nuclear factor erythroid 2-related factor

2 (NFE2L2) (458). Some studies have reported that the effect of inorganic arsenic on hepatic *Hmox1* mRNA completely disappears after 24 h of treatment, and this can be ascribed to its total elimination at this time point (380; 459). However, *Hmox1* mRNA may become down-regulated as a sign of ATO^{III} organ toxicity (406; 460).

In HepG2 cells, increasing ATO^{III} concentration resulted in concentration-dependent inhibition of TCDD-inducible CYP1A1 expression at the mRNA, protein, and catalytic (EROD) activity levels (Figure 3.15, 3.16, and 3.17). ATO^{III} also concentration-dependently decreased the TCDD-mediated induction of CYP1A2 protein expression and catalytic (MROD) activity (Figure 3.16 and 3.17). At basal level, only *CYP1A1* mRNA was significantly decreased by the treatment of ATO^{III} alone (Figure 3.15). Minimal *CYP1A2* mRNA expression was observed in all groups at our chosen duration (6 h) of treatment (data not shown). That's probably why studies assessing *CYP1A2* mRNA level in HepG2 cells are usually performed at longer treatment durations (429; 461).

There is no previous study that examined the effect of ATO^{III} on both constitutive and TCDD-induced CYP1A1 and CYP1A2 in HepG2 cells. Using Hep3B cells, Vernhet *et al.* have reported that ATO^{III}, at varying concentrations (0.25–5 μM), significantly decreased the 3-MC-mediated induction of CYP1A1 mRNA, protein, and catalytic (EROD) activity in a concentration-dependent manner. In this study, the same effect on the EROD activity was also obtained when B[a]P or 50 nM TCDD were used as CYP1A1 inducers in Hep3B cells. Similarly, ATO^{III} inhibited 3-MC-induced EROD activity in HepG2 cells and human primary hepatocytes (352).

We investigated the effect of ATO^{III} on the AHR-mediated transcriptional regulation of CYP1A expression using HepG2 cells stably transfected with a genetic construct containing their upstream regulatory element (XRE) linked to the firefly luciferase reporter gene. Our findings revealed that 5 μM ATO^{III} alone or in the presence of TCDD significantly decreased the AHR-dependent XRE-driven luciferase reporter activity (Figure 3.19).

In a previous study, Vernhet *et al.* assessed such transcriptional regulation using Hep3B cells transiently transfected with the p1A1-FL construct, which contains the human CYP1A1 gene 5'-flanking region upstream of the firefly luciferase reporter gene. They showed that 5 μM ATO^{III} inhibited the 3-MC-induced luciferase activity in p1A1-FL-loaded cells (352).

In HepG2 cells, exposure to ATO^{III} alone or co-exposure to both ATO^{III} and TCDD significantly induced HMOX1 mRNA and protein expression in a concentration-dependent fashion (Figure 3.18). Several *in vitro* studies have reported the prominent effect of ATO^{III} on HMOX1 (462; 463).

Exposure to heavy metals, including arsenic, has been associated with HMOX1 induction along with CYP enzymes inhibition (285). HMOX1 is the key enzyme in heme catabolism into biliverdin (subsequently reduced to bilirubin), free iron, and carbon monoxide. Induction of HMOX1 can provide cytoprotection by promoting the conversion of a powerful pro-oxidant (heme) into effective antioxidants (biliverdin and bilirubin). Conversely, HMOX1 overexpression may be counter-protective due to excessive production of reactive iron which by turn can exacerbate cellular oxidative damage (464; 465).

Another important aspect of HMOX1 up-regulation, other than lowering excessive heme, is the accompanying decrease in the content and activity of cellular hemoproteins. The prosthetic heme is an indispensable element for CYP enzymes catalytic activity. In fact, CYP enzymes are the major heme-consuming hepatic hemoproteins, with over 50% of liver-produced heme being directed to fuel their synthesis. The induction of HMOX1, e.g. by heavy metals, can adversely affect the CYP enzymes by depleting the cellular heme pool, with ensuing failure to form a fully functioning enzyme (466). Additionally, HMOX1 inducers as metals may affect heme affinity to its apoprotein with subsequent partial dissociation from the holoenzyme rendering it liable to degradation by HMOX1, thus yielding eventually a functionless protein (467).

If ATO^{III} decreases the TCDD-mediated induction of CYP1A1 catalytic activity by degrading its heme through excessive HMOX1 production, then inhibiting HMOX1 should restore the TCDD-mediated induction of CYP1A1 catalytic activity levels. Therefore, we treated HepG2 cells with SnMP, an inhibitor of HMOX1, in an attempt to restore the TCDD-induced EROD activity decreased by 1 µM ATO^{III}. Our findings showed that inhibiting HMOX1 partially restored the ATO^{III}-mediated decrease in the EROD activity, thus confirming the role of HMOX1 in the ATO^{III}-mediated post-translational modification of CYP1A1 (Figure 3.20).

The post-translational direct interaction between ATO^{III} and CYP1A1 enzyme was previously evaluated by Vernhet *et al.* In their study, incubating 5 µM ATO^{III} with the microsomes from 3-MC-treated Hep3B cells did not alter EROD activity. This team has also tested the impact of N-acetylcysteine (NAC), a potent reducing agent, on 5 µM ATO^{III}-mediated inhibition of 3-MC-

induced EROD activity in Hep3B cells. Through its activity against the reactive oxygen species (ROS), significantly produced by ATO^{III} treatment, NAC resulted in complete restoration of EROD activity. However, other antioxidant agents such as catalase and superoxide dismutase could not restore EROD activity, implying that ROS partially contribute to ATO^{III}-mediated effect on CYP1A1 (352).

We also tested, for the first time, the effects of ATO^{III} on CYP1A1 and CYP1A2 using an *in vitro* model of mouse-derived cells (Hepa1c1c7 cells) in an attempt to expand our understanding and gain mechanistic insights into ATO^{III}-mediated modulation of these enzymes.

In this model, while ATO^{III} concentrations selection was based on an initial MTT assay screening conducted to identify tolerable concentrations in Hepa1c1c7 cells, TCDD concentration (1 nM) was selected on the basis of previous studies that were conducted in the same experimental model (468; 469). This concentration is optimal for inducing the AHR in Hepa1c1c7 cells without imparting significant toxicity when used alone or in combination with toxic heavy metals including arsenic (377; 470).

Our findings show that ATO^{III}, at well-tolerable concentrations in Hepa1c1c7 cells, significantly increased the basal *Cyp1a1* mRNA transcripts, while in the presence of the inducer TCDD, ATO^{III} significantly enhanced the induced CYP1A1 mRNA, protein, and activity (Figure 3.6, 3.7, and 3.8). Similarly, TCDD-induced CYP1A2 was significantly increased by ATO^{III} co-treatment at the same three levels of expression, while the increase in the constitutive CYP1A2 was only significant at mRNA and protein levels (Figure 3.6, 3.7, and 3.8).

Because CYP1A1 and CYP1A2 are both controlled by the AHR, we tried to dissect its signaling pathway to decipher the mechanism behind their ATO^{III}-mediated up-regulation. Up-stream in the AHR signaling pathway, ATO^{III} alone caused a significant increase in the nuclear recruitment of AHR, and this translocation was most likely triggered by cytosolic AHR complex activation (Figure 3.9). Generally, AHR activation is mostly mediated by ligand binding, however, ATO^{III}, like other arsenicals (351; 353), probably does not fit structurally as a typical AHR ligand to initiate the signaling pathway (377). In this case, a plausible explanation might be a non-classical ligand-independent mechanism in which the cytosolic AHR complex is disrupted, and subsequently translocated, by the ROS generated by exposure to arsenicals (353) including ATO^{III} (471). Interestingly, arsenic-induced oxidative stress can be also indirectly implicated in ligand-dependent

AHR activation through mediating metabolic alterations that result ultimately in the production of endogenous AHR ligands (468).

Another possible mechanism for the ligand-independent AHR activation is the direct arsenic interaction with its chaperone protein, heat shock protein 90 (HSP90), thus disrupting its molecular interaction with AHR. In this case, contrary to what happens in ligand-mediated activation, AHR is believed to subsequently migrate to the nucleus without HSP90. Additionally, arsenic might activate AHR, in the absence of a true ligand, similar to the proteasome inhibitor, MG-132, which triggers events of phosphorylation/dephosphorylation in the AHR nuclear export signal and other domains (376).

The increase in the nuclear recruitment of AHR was subsequently reflected as enhanced transcriptional activation of its response element, XRE, as revealed by the reporter gene assay at both basal and inducible levels (Figure 3.10). The ability of ATO^{III} to transcriptionally increase *Cyp1a1* mRNA expression was further evidenced by the abolishment of ATO^{III}-induced *Cyp1a1* mRNA in the presence of the transcription inhibitor, Act-D (Figure 3.11). The induction of *Cyp1a1* mRNA was similarly affected in the case of TCDD, a well-known transcriptional inducer (Figure 3.11). Of note, Act-D pretreatment significantly decreased *Cyp1a1* mRNA below its basal level (Figure 3.11). This is because of the duration of this experiment, 6 h, which was beyond the estimated *Cyp1a1* mRNA half-life, 4.2 h, resulting inevitably in, at least, 50% decrease in its abundance. We also examined ATO^{III} effects on CYP1A1 beyond the transcriptional level of regulation through Act-D and CHX chase assays, which demonstrated that ATO^{III} positively affects mRNA and protein stabilities of CYP1A1, respectively (Figure 3.12 and 3.13). The definitive mechanisms of arsenic-mediated stabilization of CYP1A1 mRNA and protein are yet to be elucidated (377).

Interestingly, our findings of the down-regulatory effect of ATO^{III} on both CYP1A enzymes in human HepG2 cells and C57BL/6 mice are opposing the up-regulatory effect in Hepa1c1c7 cells. Generally, the differential modulation of the CYP enzymes is a common feature among different arsenicals, which can be not only dependent on the arsenical of interest, but also species-, tissue-, and enzyme-specific (14). Indeed, such a phenomenon can be partly attributed to the extensive and differential metabolic handling of the arsenical being tested in different experimental models, which can result in arsenic metabolites, each of which having a different biological behavior (50).

This may explain the opposite effects observed previously in human HepG2 cells and currently in murine Hepa1c1c7 where species-based difference in genetic make-up can result in different arsenic metabolizing activity (351). On the other hand, the differential modulation reported in Hepa1c1c7 cells and C57BL/6 mice can be attributed to difference between *in vitro* an *in vivo* metabolic environments, something that has been previously reported for sodium arsenite in C57BL/6 mice and their derived primary hepatocytes (380). An additional factor in our case is that Hepa1c1c7 are murine cells but derived from a different strain of mice.

4.2. Differential modulation of basal and TCDD-inducible CYP1A enzymes by $MMMTA^{V}$ *in vivo* and *in vitro*

While methylated oxo-arsenic forms are the most commonly identified metabolites of iAs, several sulfur-containing derivatives have been also detected in both humans and animals. $MMMTA^{V}$ is one of iAs-derived thioarsenicals that have been reported in mammals. Because of their relatively recent discovery, little is known about the metabolism and toxicity of these thiolated arsenic metabolites (472).

Modulation of the CYP enzymes by different arsenicals has been reported in several studies, with the main focus being on sodium arsenite because of its relatively higher environmental prevalence with subsequent higher risk for human exposure. Methylated arsenic metabolites have also drawn a lot of attention because of the evident toxicity of some of them. In this regard, only very limited data are currently available on thio-methylated arsenicals, especially $MMMTA^{V}$ (14).

In the current study, we report for the first time that $MMMTA^{V}$ alters the expression of CYP1A1 and 1A2 *in vivo* and *in vitro*. Moreover, we show that $MMMTA^{V}$ modulates these enzymes through interfering with the AHR signaling pathway.

In this study, all *in vivo* doses and *in vitro* concentrations of the chemical agents were selected on the basis of their ability to induce changes in enzyme expression without significantly affecting animals or cells viability, respectively. Both dose (15 µg/kg body weight) and concentration (1 nM) of TCDD used in this study were previously employed in the same experimental models (C57BL/6 mice (380), Hepa1c1c7 cells (377), and HepG2 cells (354)). $MMMTA^{V}$ dose and concentrations were chosen to match those of iAs^{III} that were tested previously in different

experimental models (354; 380), and also in agreement with what has been observed in human populations chronically exposed to arsenic-contaminated drinking water (365; 473; 474).

Arsenicals undergo excessive metabolism and that is why their behavior might vary among different models based on their metabolic capacity. Our study utilized C57BL/6 mice as an *in vivo* model to gain insight into how $MMMTA^{V}$ behaves inside mammalian body upon exposure. For elucidating the possible mechanisms driving $MMMTA^{V}$ effects in C57BL/6 mice, we used murine Hepa1c1c7 cell line which is a well-suited model for studying the AHR and CYP1A regulation. Because of the difference in genetic make-up, human HepG2 cell line was used to get a closer look on human response to $MMMTA^{V}$.

In our *in vivo* experiment, we used iAs^{III}, which is the parent inorganic molecule for $MMMTA^{V}$, to compare its effect on CYP1A1/2 expression with that of $MMMTA^{V}$. While this is the first study examining the effect of $MMMTA^{V}$ on both basal and TCDD-inducible expressions of CYP1A1 and CYP1A2, previously published studies have reported iAs^{III}-related findings similar to these reported here (380).

In this study, the effect of $MMMTA^{V}$ alone on CYP1A1 expression was only observed at mRNA level in Hepa1c1c7 cells (Figure 3.25 and 3.26). *In vivo*, $MMMTA^{V}$ inhibited the TCDD-mediated induction of hepatic *Cyp1a1* mRNA levels at 6 and 24 h (Figure 3.21). This effect was also observed in both *in vitro* models (Figure 3.25, 3.26, and 3.33) and was mechanistically explained by the decreased XRE activation as demonstrated by the luciferase reporter gene assay (Figure 3.29 and 3.36). Of note, the magnitude of reduction in the TCDD-mediated *Cyp1a1* mRNA induction caused by $MMMTA^{V}$ co-exposure decreased over time (67.3% and 28.5% at 6 h and 24 h, respectively) (Figure 3.26). Also, the time-dependent experiment of *Cyp1a1* mRNA expression in Hepa1c1c7 cells has revealed that the peak of significant effect of $MMMTA^{V}$ co-exposure was reached around 6 h, then the effect started to fade afterwards (Figure 3.26). Interestingly, the down-regulatory effect of $MMMTA^{V}$ on TCDD-inducible *Cyp1a1* mRNA was inverted into significant potentiation downstream in its expression pathway (i.e., at protein and activity levels) in C57BL/6 mice liver (Figure 3.22 and 3.23) and Hepa1c1c7 cells (Figure 3.27 and 3.28), but not HepG2 cells (Figure 3.34 and 3.35).

We investigated the possibility of the involvement of post-transcriptional and post-translational mechanisms in the $MMMTA^{V}$-mediated up-regulation of CYP1A1 protein expression and catalytic

activity through examining its effect on CYP1A1 mRNA and protein half-lives as a measure of their stability. However, $MMMTA^{V}$ did not alter the decay rate of either mRNA or protein (Figure 3.30 and 3.31).

Therefore, to explain this inverted effect, we hypothesize that there is an initial (at early exposure time) decrease in *Cyp1a1* mRNA expression attributed to a direct effect of the non-metabolized $MMMTA^{V}$. As the exposure time (24 h in protein and activity experiments) increases, a late increase in CYP1A1 expression results as an indirect effect of the metabolic transformation of $MMMTA^{V}$ into other arsenic species, which by turn may have opposing effect on CYP1A1 expression. Such biotransformation has been previously reported for other thioarsenicals (475). Another factor that may contribute to this late potentiation effect *in vivo* is the possible impact of $MMMTA^{V}$ on other biochemical pathways with subsequent release of certain modulators such as the endogenous AHR ligand, bilirubin (476).

Interestingly, $MMMTA^{V}$ caused a significant reduction in TCDD-inducible CYP1A1 at all expression levels (mRNA, protein, and activity) in HepG2 cells (Figure 3.33, 3.34, and 3.35). The different genetic make-up of these human cells, as opposed to the murine *in vivo* and *in vitro* models, may result in different arsenic metabolizing capacity (351). The delayed $MMMTA^{V}$ metabolism in HepG2 cells, beyond the durations of treatment in our study, can result in its persistent down-regulatory effect on CYP1A1 protein and activity.

Comparative *in vitro* toxicity studies have shown that $MMMTA^{V}$ is one of the least arsenic compounds to affect cell viability (43; 45). In agreement with this finding, challenging HepG2 cells with high concentrations (up to 1000 μM) in our study showed a wide range of relatively safe $MMMTA^{V}$ concentrations (Figure 3.32). Such *in vitro* assessment of toxicity does not essentially reflect real-life toxic consequences *in vivo*. In the current *in vivo* study, $MMMTA^{V}$ was able, at the same dose as iAs^{III}, to significantly potentiate TCDD-inducible CYP1A1 and CYP1A2 activities to levels significantly higher than those of its parent inorganic molecule, which by turn did not significantly alter inducible CYP1A2 activity (Figure 3.23). While iAs^{III} is notoriously toxic, its metabolite, $MMMTA^{V}$, may contribute to such toxicity by enhancing the expression of the procarcinogen-activating CYP1A enzymes.

Other arsenic species formed downstream in the iAs^{III} metabolic pathway can produce effects either similar or different from those of $MMMTA^{V}$. For instance, trimethylarsine oxide ($TMAO^{V}$) has

been reported to increase TCDD-induced CYP1A1, but not CYP1A2, activity in C57BL/6 mice (404). On the other hand, dimethylarsinic acid (DMA^V) has shown organ-specific pattern of inducible CYP1A potentiation, with no significant effect being observed in the liver (302).

4.3. Modulation of hepatic CYP enzymes and cellular transporters by ATO^{III} *in vivo*

In the current study, we show for the first time how a clinically relevant dose of ATO^{III} (475) can alter the hepatic AA metabolism along with the underlying network of enzymes, the most notable of which are the CYP enzymes, *in vivo* using C57BL/6 mice. Moreover, we report that ATO^{III} can also change the expression of transporters that control its intracellular burden beside other co-administered medications.

We have demonstrated that ATO^{III} treatment increases the hepatic expression of *Pla2g4a* which may inevitably result in elevation of the free AA available for eicosanoids production (385) (Figure 3.41). In addition to the cyclooxygenases and lipoxygenases pathways, the CYP enzymes constitute the third major route for metabolizing AA (398; 477) which catalyzes AA conversion into bioactive EETs through epoxygenation, and HETEs through hydroxylation (306; 477). Our findings show that ATO^{III} can significantly modulate the enzymes involved in the three pathways of eicosanoids production.

ATO^{III} induced hepatic *Cyp1a1* (at 6 h) and *Cyp1b1* with no significant effect on *Cyp1a2* (Figure 3.37). Despite the overarching role of the aryl hydrocarbon receptor (AHR) in regulating all the three enzymes, *Cyp1b1* up-regulated expression appears to be caused by other additional factors. This may explain the different behavior of *Cyp1a1/2*, where *Cyp1a1* (at 24 h) was suppressed, rather than being stimulated, and *Cyp1a2* showed no significant alteration (Figure 3.37). The sustained induction of *Cyp1b1* by ATO^{III} at 6 h and 24 h is likely a result of ATO^{III}-induced inflammation. It has been previously reported that ATO^{III} leads to an increase in serum tumor necrosis factor-alpha (TNF-α) (478; 479) which is a known potent stimulator of *Cyp1b1* gene expression in certain liver cells (480; 481), therefore, ATO^{III} may induce *Cyp1b1* gene expression through this particular mechanism (482).

In the *Cyp2* family, ATO^{III} exhibited diverse effects on hepatic mRNA levels. Broadly, ATO^{III} treatment triggered the mRNA induction of some CYP epoxygenases within the *Cyp2a*, *Cyp2b*, *Cyp2c*, and *Cyp2j* (at 6 h) subfamilies while leaving others unaffected (Figure 3.38). Specifically, ATO^{III} exposure induced *Cyp2a4*, *Cyp2a5*, *Cyp2b9*, *Cyp2b10*, *Cyp2b19* (at 6 h), *Cyp2c38* (at 24

h), *Cyp2c39*, *Cyp2c40* (at 24 h), *Cyp2j6* (at 6 h), *Cyp2j9* (at 6 h), and *Cyp2j13* (at 6 h) (Figure 3.38). It is well-established that the transcriptional regulation of the *Cyp2a*, *Cyp2b*, and *Cyp2c* subfamilies is mediated by the constitutive androstane receptor (CAR) (483; 484). Notably, previous research has substantiated the capacity of ATO^{III} to activate CAR in different cell lines (485). Thus, it is reasonable to postulate that the induction of the *Cyp2a*, *Cyp2b*, and *Cyp2c* subfamilies in this study is attributed to CAR activation by ATO. The *Cyp2j* subfamily regulation, distinct from the other *Cyp2* subfamilies, is known to be governed by the activation of the activator protein-1 (AP-1). Given the potent ability of ATO^{III} to stimulate AP-1 (486), it is conceivable that ATO^{III} induced some of the *Cyp2j* subfamily members by activating AP-1.

Investigating the influence of ATO^{III} on the CYP hydroxylases mRNA levels, we observed a suppression of *Cyp2e1* (at 6 h), *Cyp4a12* (at 24 h), and *Cyp4f13* (at 24 h) (Figure 3.38 and 3.40). Conversely, there was an increase in *Cyp4a10*, *Cyp4a14* (at 6 h), *Cyp4f13* (at 6 h), *Cyp4f16*, and *Cyp4f18* (at 6 h), while no significant changes were observed in the mRNA levels of *Cyp4f15* (Figure 3.40). Previous studies have shown that CYP4A and CYP4F enzymes are induced in the heart, kidney, and liver in various inflammation animal models (487-489). Our experiment has demonstrated that ATO^{III} increases the expression of *Ptgs2*, which is an indicator of inflammation (Figure 3.42). Hence, we can attribute the induction of *Cyp4a* and *Cyp4f*, at least partially, to ATO^{III}-induced inflammation. Additionally, in agreement with a previous study by Habib *et al.*, ATO^{III} inhibited the mRNA expression of *Ptgs1* (490) (Figure 3.42).

Prior research has demonstrated that the key enzymes involved in ω-hydroxylation of AA, known as ω-hydroxylases, were found within the CYP family 4, specifically in subfamilies A (CYP4A) and F (CYP4F), in addition to CYP2E1 and CYP2J9. These enzymes are responsible for the conversion of AA into various HETEs (477; 491). In our study, ATO^{III} suppressed hepatic *Cyp2e1* mRNA levels, while induced *Cyp2j9* as well as the majority of *Cyp4a* and *Cyp4f* mRNA levels (Figure 3.38 and 3.40). These variations may account for the differences in the formation rates of subterminal HETEs, with an increase in 17(S)-HETE and 18(R)-HETE, but a decrease in 18(S)-HETE (Figure 3.43). In mice, the synthesis of 20-HETE from AA primarily involves the CYP4A10, CYP4A12, and CYP4A14 isoforms. Among these, CYP4A12 exhibits higher catalytic activity for 20-HETE production compared to CYP4A10. Aside from the CYP4A enzymes, CYP4F isoforms also play a significant role in the production of 20-HETE (492; 493). In our

current investigation, we observed notable increases in the expression of *Cyp4a10*, *Cyp4a14*, *Cyp4f13*, *Cyp4f16*, and *Cyp4f18* following ATO^{III} treatment (Figure 3.40). Consequently, the observed higher hepatic production of 20-HETE in response to ATO^{III} (Figure 3.43) can be linked to the heightened mRNA levels of the majority of *Cyp4a* and *Cyp4f* subfamily members (397) as well as *Cyp1b1* (494).

20-HETE represents the primary pro-inflammatory metabolite produced by hydroxylase enzymes. It plays a crucial role in regulating vascular remodeling and neovascularization, especially in conditions characterized by ischemia or hypoxia. It is responsible for triggering the activation of nuclear factor kappa-light-chain-enhancer of activated B cells (NF-κB) which mediates pro-inflammatory effects. Additionally, it significantly influences the activation of epidermal growth factor (EGF), hypoxia-inducible factor (HIF), and vascular endothelial growth factor (VEGF), thus promoting angiogenesis. This metabolite also plays a pivotal role in stimulating endothelial cell proliferation, migration, and overall cell survival (495-498).

Interestingly, we investigated the impact of ATO^{III} treatment on the hepatic lipoxygenases pathway which produces midchain HETEs corresponding to the specific ALOX enzymes generating them. Our findings revealed a significant reduction in the mRNA levels of *Alox5* and *Alox15* after 6 h-exposure to ATO^{III} (Figure 3.42), resulting in decreased hepatic levels of 5-HETE (R enantiomer) and 15-HETE (S enantiomer), respectively (Figure 3.43). However, hepatic levels of *Alox12* mRNA remained unaffected by ATO^{III} leading to no significant changes in its corresponding metabolite.

The lipoxygenases pathway generates various compounds, including leukotrienes (LTs), lipoxins (LXs), hepoxilins (HXs), and HETEs. These substances play roles in inflammation, allergic reactions, bronchoconstriction, and vasoconstriction (499; 500). The ALOX5 pathway is responsible for generating critical pro-inflammatory LT mediators, such as leukotriene A4 (LTA4) and leukotriene B4 (LTB4) (501). Notably, ALOX12 plays a vital role in tumor angiogenesis, motility, invasion, and metastasis. It is the primary enzyme responsible for generating 12-HETE in humans (500; 502). The ALOX15 enzyme has two isoforms, ALOX15-1 and ALOX15-2, found in various tissues but primarily expressed in reticulocytes, eosinophils, pulmonary epithelial cells, and macrophages. The activity of ALOX15 has been reported to be implicated in enhancing tumorigenesis (500).

Regarding arsenic cellular transport, the aquaporin channels AQP3, AQP7, and AQP9 play a pivotal role in facilitating the cellular uptake of arsenicals. Among the AQP family members, AQP9 is the most efficient transporter for ATO^{III} and most arsenic species (11; 503; 504). In our study, ATO^{III} exposure resulted in a significant increase in the mRNA expression of *Aqp3*, *Aqp7*, and *Aqp9* (Figure 3.44). The up-regulation of AQP3 in response to arsenic has been previously reported (505).

Although AQPs function bidirectionally, they primarily facilitate the entry of arsenicals into cells, potentially increasing their toxicity. Understanding both the chemical properties of metalloids and their mechanisms of transport is crucial for developing new drugs and combating drug-resistant cells. For instance, the level of AQP9 is critical for tumor sensitivity to chemotherapy in colorectal cancer (CRC) patients (506). Similarly, AQP9 abundance may dictate the degree of APL patients' responsiveness to ATO^{III} by facilitating its diffusion into the leukemic cells, thus increasing its intracellular concentration and enhancing its cytotoxic effect (507; 508). Interestingly, the pharmacological enhancement of AQP9 expression represents a promising strategy to augment ATO^{III} sensitivity in neoplastic cells (509; 510). Being primarily expressed in hepatocytes, AQP9 may also serve as a key player in the ATO^{III}-induced hepatotoxicity in APL patients (507).

The ATP-binding cassette (ABC) proteins play a major role in actively transporting heavy metals. The ABC subfamily C members, the multidrug resistance-associated proteins, ABCC1-6 are known for their function as efflux pumps for arsenic and its metabolites (11). Our study has demonstrated that ATO^{III} increases the mRNA expression of some members including *Abcc1*, *Abcc2*, *Abcc4*, *Abcc5*, and *Abcc6* (Figure 3.44). While the apical ABCC2 handles the biliary excretion of arsenic metabolites through the canalicular surface of hepatocytes (511), the basolateral ABCC3, ABCC4, and ABCC6 are expressed at the sinusoidal surface of hepatocytes and are responsible for the substrate extrusion into the blood (512). ABCC1 and ABCC5 are also basolateral transporters involved in arsenic efflux (11; 513). Interestingly, ABCC1 and ABCC5 have minimal expression in normal liver (514), but they become up-regulated in hepatocytes under stress conditions (515; 516).

The ABC subfamily B member, the P-glycoprotein or multidrug resistance protein 1, ABCB1 is recognized for its role in providing cellular defense against a wide range of xenobiotics (517; 518). In our study, ATO^{III} has also significantly up-regulated the mRNA expression of *Abcb1* in the liver

(Figure 3.44). The increase in the expression of *Abcb1* as well as *Cyp3a* (Figure 3.39) might be attributed to an ATO^{III}-mediated activation of their regulator, the PXR (519). ABCB1 is regarded as a protective shield against arsenic. That is why mice lacking the *Abcb1* gene displayed increased susceptibility to arsenite and with higher levels of tissue accumulation compared to their wild-type counterparts (520; 521). However, the magnitude of ABCB1 contribution to arsenic cellular expulsion and resistance is still debatable (11).

4.4. Summary and general conclusions

ATO^{III} is a prominent example of arsenic duality being a notorious environmental toxicant that has been medicinally exploited. However, the clinical efficacy of ATO^{III} in APL patients comes at a cost of multi-organ toxicity whose mechanisms remain unresolved. Deciphering such mechanisms is critical for developing mitigation strategies that will not only improve the treatment outcome in APL patients but also allow expanding the use of ATO^{III} to other clinical applications.

Hepatotoxicity is one of ATO^{III} complications which can be severe enough to result in treatment discontinuation. Being the metabolic powerhouse of the body, targeting enzyme machinery in the liver can be a plausible cause of such toxicity. CYP1A monooxygenases are members of one of the major hepatic enzyme systems that are involved in the metabolism of endogenous substrates, such as AA, commercial drugs, and environmental carcinogens. Altering CYP1A activity can inevitably entail metabolic perturbations with subsequent negative outcomes. It is widely reported that various arsenic-based compounds can modulate the expression of different CYP enzymes, most notably the AHR-regulated CYP1A1/1A2. Being an arsenical, the potential modulation of these enzymes by ATO^{III} might be the key for understanding its related toxicities.

In humans, the inorganic ATO^{III} undergoes progressive metabolism into a network of methylated intermediates/products, which can, at least partly, be held responsible for the overall toxic outcome of ATO^{III} exposure. Among these metabolites, thio-methylated arsenicals, including $MMMTA^{V}$, have been reported in APL patients receiving ATO^{III}.

Therefore, this work aimed to determine the possible modulatory effects of ATO^{III} and its metabolite, $MMMTA^{V}$, on both constitutive and TCDD-mediated inducible levels of hepatic CYP1A1 and CYP1A2 using both *in vivo* (C57BL/6 mice) and *in vitro* (HepG2 and Hepa1c1c7 cell lines) models. We also aimed to investigate the *in vivo* effects of ATO^{III} on other hepatic non-AHR-regulated CYP enzymes with the associated perturbations in AA metabolism. Finally, we

explored the potential *in vivo* alterations in cellular transporters expression as a result of ATO^{III} exposure.

At clinically relevant levels, ATO^{III} differentially modified the expressions of CYP1A1 and CYP1A2 in C57BL/6 mice as well as HepG2 and Hepa1c1c7 cell lines. In C57BL/6 mice, ATO^{III} inhibited the TCDD-mediated induction of hepatic CYP1A1 and CYP1A2 at the mRNA, protein, and catalytic activity levels. Significant reductions in CYP1A2, but not CYP1A1, protein and activity were observed at basal expression levels. In HepG2 cells, a similar inhibitory effect was only observed in the inducible CYP1A1 and CYP1A2 at all levels of expression. Such inhibition was mechanistically explained to be transcriptionally regulated by interfering with the AHR-mediated activation of the XRE. Also, a potential post-translational modification through the up-regulated HMOX1 might be, at least partially, implicated in reducing enzyme activity. Such inhibitory effects on CYP1A enzymes implies the possible involvement of ATO^{III} in clearance-related consequences for the substrates of these enzymes such as interactions with co-administered drugs, like the anti-emetic granisetron which is widely used for chemotherapy-induced nausea and vomiting, or suboptimal environmental toxicant elimination.

Interestingly, a differential modulation of CYP1A1/1A2 was obtained in Hepa1c1c7 cells in response to tolerable ATO^{III} concentrations. At all expression levels, TCDD-inducible CYP1A1/1A2 expressions were increased while only basal levels of mRNA transcripts, in addition to protein in case of CYP1A2, were up-regulated. Such contradicting behavior, compared to the *in vivo* murine model, was attributed to a transcriptional level of regulation related to the AHR nuclear accumulation as well as XRE activation. Moreover, post-transcriptional and post-translational mechanisms were also involved in the regulation, with the ultimate result being increased production and decreased degradation of the CYP gene products.

The thiolated metabolite of ATO^{III}, $MMMTA^{V}$, ultimately increased both CYP1A1 and CYP1A2 inducible activities in C57BL/6 mice. The same pattern of effect was also observed in Hepa1c1c7 cells. At the early stage of CYP1A1 gene expression, i.e., mRNA transcripts formation, a significant decrease was obtained in both models. Such effect was only explained by transcriptional regulation mediated by interference with the XRE activation by AHR. As opposed to these murine models, the effect on inducible CYP1A1 in HepG2 cells was consistently inhibitory across all levels of expression. Similarly, this inhibition was attributed to transcriptional regulation at the

level of XRE activation. Investigating post-transcriptional and post-translational modifications of CYP1A1 in murine *in vitro* model could not clarify the reason behind the inversion of $MMMTA^{V}$ effect on CYP1A1 expression. However, a possible cause of such inversion might be the transformation of $MMMTA^{V}$ into a different arsenic species, by certain murine enzymes that are absent in human HepG2 cells, at the later time points of protein and activity measurement experiments.

While arsenic studies, involving experimental models, are usually based on exposure to a single arsenic species, the inevitable generation of different metabolites makes it difficult to attribute the final outcome to that single species. However, these studies, when using a specific metabolite, give us an indication about the type of effect bestowed by each of these metabolites to ultimately yield the apparent collective outcome of the original parent species. It is also important to know that the relative formation of each metabolite varies depending on multiple factors such as interspecies genetic variability, which may explain the disparity in effect among different model species.

Our last study has revealed that the *in vivo* alteration of CYP enzymes by ATO^{III} goes beyond the AHR regulated CYP1A subfamily to include other CYP families (CYP2, CYP3, and CYP4). A clinically relevant dose of ATO^{III} altered the hepatic AA metabolism in C57BL/6 mice through modulating gene expression of the underlying network of enzymes. Such modulation impacts the AA biotransformation pathway from its beginning at the step of AA liberation by PLA2G4A and extends through the eicosanoids-generating cyclooxygenases, lipoxygenases, and CYP enzymes routes. ATO^{III} suppressed *Cyp2e1*, while induced *Cyp2j9* and most of *Cyp4a* and *Cyp4f*, causing 17(S)-HETE and 18(R)-HETE increase, and 18(S)-HETE decrease. ATO^{III} also induced *Cyp4a10*, *Cyp4a14*, *Cyp4f13*, *Cyp4f16*, and *Cyp4f18*, causing 20-HETE elevation. Modifying the homeostatic production of bioactive AA metabolites, such as HETEs, can entail toxic events that compromise the overall body tolerability to ATO^{III} treatment. Additionally, this situation may be aggravated by unfavorable changes in the expression of ATO^{III} transport systems, such as increased expression of the influx AQP transporters, with ensuing enhancement of its toxicity.

4.5. Future research directions

The results obtained from the present work have highlighted the interaction of the anti-leukemic ATO^{III} and one of its metabolites, $MMMTA^{V}$, with the hepatic CYP enzymes especially the AHR-regulated CYP1A which are widely involved in physiologic homeostasis as well as xenobiotic

clearance. However, further studies are needed to provide comprehensive characterization of ATO^{III} behavior, along with its other recently identified thiolated metabolites, in biological systems, with subsequent understanding of its toxic interactions. Such understanding should advance our findings into clinical practice through, for instance, implementing drug-drug interactions management protocols or prescribing adjuvant supportive agents that maximize the benefit from ATO^{III}.

Further research is required to address the following objectives:

1- To examine the effects of ATO^{III} (and $MMMTA^{V}$) in the absence and presence of AHR ligands (e.g., TCDD) on hepatic phase II AHR-regulated enzymes, typified by the NAD(P)H:quinone oxidoreductase 1 (NQO1), *in vivo* and *in vitro*.

Rationale: NQO1 catalyzes the reduction and detoxification of highly reactive quinones that can cause redox cycling and oxidative stress. It is also co-regulated by the NFE2L2 and is regarded as its prototypical target protein. Interestingly, some studies have reported a cross-talk between AHR and NFE2L2 (522). Moreover, our research group has previously reported that some arsenicals act as bifunctional modulators of both transcription factors (353). This can be helpful for understanding how ATO^{III} (and $MMMTA^{V}$) might trigger a dual effect in which it additionally impacts the cytoprotective proteins via modulating the NFE2L2.

2- To investigate the effects of ATO^{III} (and $MMMTA^{V}$) in the absence and presence of AHR ligands (e.g., TCDD) on extra-hepatic AHR-regulated enzymes, *in vivo*.

Rationale: While the liver is the powerhouse of enzymatic biotransformation in the body, AHR-regulated enzymes are also expressed, to a varying degree, in other organs such as lung and kidney. Our research group has previous reports regarding modulation of these extra-hepatic enzymes by different arsenicals (301; 302). Characterizing how ATO^{III} (and $MMMTA^{V}$) affects AHR-regulated enzymes in extra-hepatic tissues can provide a clue for organ-specific toxicity.

3- To explore the chronic effects of ATO^{III} on hepatic and extra-hepatic AHR-regulated enzymes, *in vivo*.

Rationale: A chronic study can provide valuable information about the sustained effects of ATO^{III} exposure on the AHR and its associated enzymes. This should give a closer look at

the real-life scenario of ATO^{III} exposure where ATO^{III} is administered to APL patients at a regimen of 0.15 mg/kg body weight repeated daily for multiple weeks depending on the phase of treatment (i.e., induction of remission or consolidation) (523).

4- To explore the sex-specific differences in the effects of ATO^{III} on hepatic and extra-hepatic AHR-regulated enzymes, *in vivo*.

Rationale: Our research group and others have previously reported the sexual dimorphism in the expression of CYP enzymes across different organs (524; 525), which was also associated with sex-related differential modulation of endobiotic metabolism (526) as well as xenobiotic biotransformation (527; 528). Interestingly, both phase I (529) and phase II (525; 530) AHR-regulated enzymes have also shown sex-specific expression differences, therefore, these enzymes are more likely to be affected differently in response to ATO^{III} exposure.

5- To examine the effects of other ATO^{III}-related thio-metabolites in the absence and presence of AHR ligands (e.g., TCDD) on hepatic and extra-hepatic AHR-regulated enzymes, *in vivo* and *in vitro*.

Rationale: Besides $MMMTA^{V}$, other thiolated arsenic metabolites, such as $DMMTA^{V}$, have been also reported in humans intravenously receiving ATO^{III}-based treatment for APL (26; 48). This will help us to identify the potential contribution of ATO^{III} metabolites to its collective effect on AHR-regulated enzymes.

6- To explore the hepatic effects of ATO^{III} in mice with humanized liver through proteomic analysis.

Rationale: ATO^{III} causes body-wide toxicities, including hepatotoxicity, mediated mainly through cellular protein alterations (50). A comprehensive proteomic analysis of ATO^{III}-dependent hepatic effects is important for identifying target proteins involved in the toxicopathic pathways and responses to ATO^{III} exposure. The humanized liver chimeric mice are mice with livers that are largely repopulated by human hepatocytes, therefore, this model will provide a closer look at the *in vivo* toxic response of human hepatocytes to ATO^{III}.

REFERENCES

1. Meharg AA. 2005. *Venomous earth: How arsenic caused the world's worst mass poisoning*. Hampshire: Macmillan
2. Parascandola J. 2012. *King of poisons: A history of arsenic*. Dulles: Potomac Books
3. Marsh J. 1836. Account of a method of separating small quantities of arsenic from substances with which it may be mixed. *Edinburgh New Philosophical Journal* 21:229-36
4. Bishop C, Kipling MD. 1978. Dr J Ayrton Paris and cancer of the scrotum: 'Honour the physician with the honour due unto him'. *J Soc Occup Med* 28:3-5
5. ATSDR. 2007. *Toxicological profile for arsenic*. Atlanta: Agency for Toxic Substances and Disease Registry
6. CEPA. 1993. *Arsenic and its compounds Priority substances list 1 assessment report*. Ottawa: Government of Canada
7. IARC. 2004. *Monographs on the evaluation of carcinogenic risks to humans*. Lyon: International Agency for Cancer Research
8. Chen QY, Costa M. 2021. Arsenic: A Global Environmental Challenge. *Annu Rev Pharmacol Toxicol* 61:47-63
9. Uthus EO. 2003. Arsenic essentiality: A role affecting methionine metabolism. *J Trace Elem Exp Med* 16:345-55
10. Mukhopadhyay R, Bhattacharjee H, Rosen BP. 2014. Aquaglyceroporins: generalized metalloid channels. *Biochimica et biophysica acta* 1840:1583-91
11. Roggenbeck BA, Banerjee M, Leslie EM. 2016. Cellular arsenic transport pathways in mammals. *J Environ Sci (China)* 49:38-58
12. Xue J, Zartarian V, Wang SW, Liu SV, Georgopoulos P. 2010. Probabilistic Modeling of Dietary Arsenic Exposure and Dose and Evaluation with 2003-2004 NHANES Data. *Environ Health Perspect* 118:345-50
13. Lomax C, Liu WJ, Wu L, Xue K, Xiong J, et al. 2012. Methylated arsenic species in plants originate from soil microorganisms. *New Phytol* 193:665-72
14. El-Ghiaty MA, El-Kadi AOS. 2021. Arsenic: Various species with different effects on cytochrome P450 regulation in humans. *EXCLI journal* 20:1184-242
15. Challenger F. 1945. Biological Methylation. *Chemical Reviews* 36:315-61

16. Hayakawa T, Kobayashi Y, Cui X, Hirano S. 2005. A new metabolic pathway of arsenite: arsenic–glutathione complexes are substrates for human arsenic methyltransferase Cyt19. *Archives of Toxicology* 79:183-91
17. Naranmandura H, Suzuki N, Suzuki KT. 2006. Trivalent Arsenicals Are Bound to Proteins during Reductive Methylation. *Chemical Research in Toxicology* 19:1010-8
18. Watanabe T, Hirano S. 2013. Metabolism of arsenic and its toxicological relevance. *Archives of toxicology* 87:969-79
19. Cohen SM, Arnold LL, Eldan M, Lewis AS, Beck BD. 2006. Methylated arsenicals: the implications of metabolism and carcinogenicity studies in rodents to human risk assessment. *Critical reviews in toxicology* 36:99-133
20. Hirano S. 2020. Biotransformation of arsenic and toxicological implication of arsenic metabolites. *Archives of toxicology* 94:2587-601
21. Council NR. 2013. *Critical Aspects of EPA's IRIS Assessment of Inorganic Arsenic: Interim Report*. Washington, DC: The National Academies Press. 127 pp.
22. Cohen SM, Arnold LL, Beck BD, Lewis AS, Eldan M. 2013. Evaluation of the carcinogenicity of inorganic arsenic. *Critical reviews in toxicology* 43:711-52
23. Vahter M. 1999. Variation in Human Metabolism of Arsenic. In *Arsenic Exposure and Health Effects III*, ed. WR Chappell, CO Abernathy, RL Calderon:267-79. Oxford: Elsevier Science Ltd. Number of 267-79 pp.
24. Aposhian HV, Aposhian MM. 2006. Arsenic toxicology: five questions. *Chem Res Toxicol* 19:1-15
25. North DW. 1992. Risk assessment for ingested inorganic arsenic: A review and status report. *Environ Geochem Health* 14:59-62
26. Chen B, Cao F, Yuan C, Lu X, Shen S, et al. 2013. Arsenic speciation in saliva of acute promyelocytic leukemia patients undergoing arsenic trioxide treatment. *Anal Bioanal Chem* 405:1903-11
27. Vahter M. 1999. Methylation of inorganic arsenic in different mammalian species and population groups. *Science progress* 82 (Pt 1):69-88
28. Eichstaedt CA, Antao T, Cardona A, Pagani L, Kivisild T, Mormina M. 2015. Positive selection of AS3MT to arsenic water in Andean populations. *Mutation research* 780:97-102

29. Li J, Packianathan C, Rossman TG, Rosen BP. 2017. Nonsynonymous Polymorphisms in the Human AS3MT Arsenic Methylation Gene: Implications for Arsenic Toxicity. *Chem Res Toxicol* 30:1481-91
30. Lu J, Hu S, Wang W, Li J, Dong Z, et al. 2018. AS3MT Polymorphisms, Arsenic Metabolism, and the Hematological and Biochemical Values in APL Patients Treated with Arsenic Trioxide. *Toxicological sciences : an official journal of the Society of Toxicology* 166:219-27
31. Pu YS, Yang SM, Huang YK, Chung CJ, Huang SK, et al. 2007. Urinary arsenic profile affects the risk of urothelial carcinoma even at low arsenic exposure. *Toxicology and applied pharmacology* 218:99-106
32. Lin YC, Chen WJ, Huang CY, Shiue HS, Su CT, et al. 2018. Polymorphisms of Arsenic (+3 Oxidation State) Methyltransferase and Arsenic Methylation Capacity Affect the Risk of Bladder Cancer. *Toxicological sciences : an official journal of the Society of Toxicology* 164:328-38
33. Hernández A, Xamena N, Surrallés J, Sekaran C, Tokunaga H, et al. 2008. Role of the Met(287)Thr polymorphism in the AS3MT gene on the metabolic arsenic profile. *Mutation research* 637:80-92
34. Lindberg AL, Kumar R, Goessler W, Thirumaran R, Gurzau E, et al. 2007. Metabolism of low-dose inorganic arsenic in a central European population: influence of sex and genetic polymorphisms. *Environ Health Perspect* 115:1081-6
35. Agusa T, Iwata H, Fujihara J, Kunito T, Takeshita H, et al. 2009. Genetic polymorphisms in AS3MT and arsenic metabolism in residents of the Red River Delta, Vietnam. *Toxicology and applied pharmacology* 236:131-41
36. Hernández A, Paiva L, Creus A, Quinteros D, Marcos R. 2014. Micronucleus frequency in copper-mine workers exposed to arsenic is modulated by the AS3MT Met287Thr polymorphism. *Mutation research. Genetic toxicology and environmental mutagenesis* 759:51-5
37. Sampayo-Reyes A, Hernández A, El-Yamani N, López-Campos C, Mayet-Machado E, et al. 2010. Arsenic induces DNA damage in environmentally exposed Mexican children and adults. Influence of GSTO1 and AS3MT polymorphisms. *Toxicological sciences : an official journal of the Society of Toxicology* 117:63-71

38. Valenzuela OL, Drobná Z, Hernández-Castellanos E, Sánchez-Peña LC, García-Vargas GG, et al. 2009. Association of AS3MT polymorphisms and the risk of premalignant arsenic skin lesions. *Toxicology and applied pharmacology* 239:200-7
39. Drobná Z, Del Razo LM, García-Vargas GG, Sánchez-Peña LC, Barrera-Hernández A, et al. 2013. Environmental exposure to arsenic, AS3MT polymorphism and prevalence of diabetes in Mexico. *Journal of exposure science & environmental epidemiology* 23:151-5
40. Beebe-Dimmer JL, Iyer PT, Nriagu JO, Keele GR, Mehta S, et al. 2012. Genetic variation in glutathione S-transferase omega-1, arsenic methyltransferase and methylene-tetrahydrofolate reductase, arsenic exposure and bladder cancer: a case-control study. *Environmental health : a global access science source* 11:43
41. Cullen WR. 2014. Chemical mechanism of arsenic biomethylation. *Chem Res Toxicol* 27:457-61
42. Rehman K, Naranmandura H. 2012. Arsenic metabolism and thioarsenicals. *Metallomics : integrated biometal science* 4:881-92
43. Moe B, Peng H, Lu X, Chen B, Chen LWL, et al. 2016. Comparative cytotoxicity of fourteen trivalent and pentavalent arsenic species determined using real-time cell sensing. *J Environ Sci (China)* 49:113-24
44. Borak J, Hosgood HD. 2007. Seafood arsenic: implications for human risk assessment. *Regulatory toxicology and pharmacology : RTP* 47:204-12
45. Naranmandura H, Carew MW, Xu S, Lee J, Leslie EM, et al. 2011. Comparative toxicity of arsenic metabolites in human bladder cancer EJ-1 cells. *Chem Res Toxicol* 24:1586-96
46. Raml R, Rumpler A, Goessler W, Vahter M, Li L, et al. 2007. Thio-dimethylarsinate is a common metabolite in urine samples from arsenic-exposed women in Bangladesh. *Toxicology and applied pharmacology* 222:374-80
47. Mandal BK, Suzuki KT, Anzai K, Yamaguchi K, Sei Y. 2008. A SEC-HPLC-ICP MS hyphenated technique for identification of sulfur-containing arsenic metabolites in biological samples. *Journal of chromatography. B, Analytical technologies in the biomedical and life sciences* 874:64-76
48. Chen B, Cao F, Lu X, Shen S, Zhou J, Le XC. 2018. Arsenic speciation in hair and nails of acute promyelocytic leukemia (APL) patients undergoing arsenic trioxide treatment. *Talanta* 184:446-51

49. SS DCR, Alava P, Zekker I, Du Laing G, Van de Wiele T. 2014. Arsenic thiolation and the role of sulfate-reducing bacteria from the human intestinal tract. *Environ Health Perspect* 122:817-22
50. El-Ghiaty MA, El-Kadi AOS. 2023. The Duality of Arsenic Metabolism: Impact on Human Health. *Annu Rev Pharmacol Toxicol* 63:341-58
51. Suzuki KT, Mandal BK, Katagiri A, Sakuma Y, Kawakami A, et al. 2004. Dimethylthioarsenicals as arsenic metabolites and their chemical preparations. *Chem Res Toxicol* 17:914-21
52. Bu N, Wang HY, Hao WH, Liu X, Xu S, et al. 2011. Generation of thioarsenicals is dependent on the enterohepatic circulation in rats. *Metallomics : integrated biometal science* 3:1064-73
53. Yoshimura Y, Endo Y, Shimoda Y, Yamanaka K, Endo G. 2011. Acute arsine poisoning confirmed by speciation analysis of arsenic compounds in the plasma and urine by HPLC-ICP-MS. *Journal of occupational health* 53:45-9
54. Tsuji JS, Lennox KP, Watson HN, Chang ET. 2021. Essential concepts for interpreting the dose-response of low-level arsenic exposure in epidemiological studies. *Toxicology* 457:152801
55. Datta BK, Mishra A, Singh A, Sar TK, Sarkar S, et al. 2010. Chronic arsenicosis in cattle with special reference to its metabolism in arsenic endemic village of Nadia district West Bengal India. *The Science of the total environment* 409:284-8
56. Lynch HN, Greenberg GI, Pollock MC, Lewis AS. 2014. A comprehensive evaluation of inorganic arsenic in food and considerations for dietary intake analyses. *The Science of the total environment* 496:299-313
57. Luvonga C, Rimmer CA, Yu LL, Lee SB. 2020. Organoarsenicals in Seafood: Occurrence, Dietary Exposure, Toxicity, and Risk Assessment Considerations - A Review. *J Agric Food Chem* 68:943-60
58. Harrington CF, Brima EI, Jenkins RO. 2008. Biotransformation of arsenobetaine by microorganisms from the human gastrointestinal tract. *Chemical Speciation & Bioavailability* 20:173-80
59. Taylor V, Goodale B, Raab A, Schwerdtle T, Reimer K, et al. 2017. Human exposure to organic arsenic species from seafood. *The Science of the total environment* 580:266-82

60. Buchet JP, Lauwerys R, Roels H. 1981. Comparison of the urinary excretion of arsenic metabolites after a single oral dose of sodium arsenite, monomethylarsonate, or dimethylarsinate in man. *Int Arch Occup Environ Health* 48:71-9
61. Marafante E, Vahter M, Norin H, Envall J, Sandström M, et al. 1987. Biotransformation of dimethylarsinic acid in mouse, hamster and man. *J Appl Toxicol* 7:111-7
62. Shen S, Li XF, Cullen WR, Weinfeld M, Le XC. 2013. Arsenic binding to proteins. *Chem Rev* 113:7769-92
63. Dopp E, Hartmann LM, von Recklinghausen U, Florea AM, Rabieh S, et al. 2005. Forced uptake of trivalent and pentavalent methylated and inorganic arsenic and its cyto-/genotoxicity in fibroblasts and hepatoma cells. *Toxicological sciences : an official journal of the Society of Toxicology* 87:46-56
64. Bertolero F, Pozzi G, Sabbioni E, Saffiotti U. 1987. Cellular uptake and metabolic reduction of pentavalent to trivalent arsenic as determinants of cytotoxicity and morphological transformation. *Carcinogenesis* 8:803-8
65. Kurosawa H, Shimoda Y, Miura M, Kato K, Yamanaka K, et al. 2016. A novel metabolic activation associated with glutathione in dimethylmonothioarsinic acid (DMMTA(V))-induced toxicity obtained from in vitro reaction of DMMTA(V) with glutathione. *Journal of trace elements in medicine and biology : organ of the Society for Minerals and Trace Elements (GMS)* 33:87-94
66. Delnomdedieu M, Basti MM, Otvos JD, Thomas DJ. 1994. Reduction and binding of arsenate and dimethylarsinate by glutathione: a magnetic resonance study. *Chemico-biological interactions* 90:139-55
67. Sakurai T, Qu W, Sakurai MH, Waalkes MP. 2002. A major human arsenic metabolite, dimethylarsinic acid, requires reduced glutathione to induce apoptosis. *Chem Res Toxicol* 15:629-37
68. Hughes MF. 2002. Arsenic toxicity and potential mechanisms of action. *Toxicology letters* 133:1-16
69. Naranmandura H, Ogra Y, Iwata K, Lee J, Suzuki KT, et al. 2009. Evidence for toxicity differences between inorganic arsenite and thioarsenicals in human bladder cancer cells. *Toxicology and applied pharmacology* 238:133-40

70. Ochi T, Kita K, Suzuki T, Rumpler A, Goessler W, Francesconi KA. 2008. Cytotoxic, genotoxic and cell-cycle disruptive effects of thio-dimethylarsinate in cultured human cells and the role of glutathione. *Toxicology and applied pharmacology* 228:59-67
71. Miller CG, Schmidt EE. 2019. Disulfide reductase systems in liver. *British journal of pharmacology* 176:532-43
72. Wang Z, Zhang H, Li XF, Le XC. 2007. Study of interactions between arsenicals and thioredoxins (human and E. coli) using mass spectrometry. *Rapid communications in mass spectrometry : RCM* 21:3658-66
73. Lin S, Del Razo LM, Styblo M, Wang C, Cullen WR, Thomas DJ. 2001. Arsenicals inhibit thioredoxin reductase in cultured rat hepatocytes. *Chem Res Toxicol* 14:305-11
74. Lu J, Chew EH, Holmgren A. 2007. Targeting thioredoxin reductase is a basis for cancer therapy by arsenic trioxide. *Proc Natl Acad Sci U S A* 104:12288-93
75. Styblo M, Serves SV, Cullen WR, Thomas DJ. 1997. Comparative inhibition of yeast glutathione reductase by arsenicals and arsenothiols. *Chem Res Toxicol* 10:27-33
76. Bergquist ER, Fischer RJ, Sugden KD, Martin BD. 2009. Inhibition by methylated organo-arsenicals of the respiratory 2-oxo-acid dehydrogenases. *Journal of organometallic chemistry* 694:973-80
77. Paul DS, Harmon AW, Devesa V, Thomas DJ, Stýblo M. 2007. Molecular mechanisms of the diabetogenic effects of arsenic: inhibition of insulin signaling by arsenite and methylarsonous acid. *Environ Health Perspect* 115:734-42
78. Huang M, Douillet C, Stýblo M. 2019. Arsenite and its trivalent methylated metabolites inhibit glucose-stimulated calcium influx and insulin secretion in murine pancreatic islets. *Archives of toxicology* 93:2525-33
79. Witkiewicz-Kucharczyk A, Bal W. 2006. Damage of zinc fingers in DNA repair proteins, a novel molecular mechanism in carcinogenesis. *Toxicology letters* 162:29-42
80. Zhou X, Sun X, Mobarak C, Gandolfi AJ, Burchiel SW, et al. 2014. Differential binding of monomethylarsonous acid compared to arsenite and arsenic trioxide with zinc finger peptides and proteins. *Chem Res Toxicol* 27:690-8
81. Walter I, Schwerdtle T, Thuy C, Parsons JL, Dianov GL, Hartwig A. 2007. Impact of arsenite and its methylated metabolites on PARP-1 activity, PARP-1 gene expression and poly(ADP-ribosyl)ation in cultured human cells. *DNA repair* 6:61-70

82. Schwerdtle T, Walter I, Hartwig A. 2003. Arsenite and its biomethylated metabolites interfere with the formation and repair of stable BPDE-induced DNA adducts in human cells and impair XPAzf and Fpg. *DNA repair* 2:1449-63
83. Piatek K, Schwerdtle T, Hartwig A, Bal W. 2008. Monomethylarsonous acid destroys a tetrathiolate zinc finger much more efficiently than inorganic arsenite: mechanistic considerations and consequences for DNA repair inhibition. *Chem Res Toxicol* 21:600-6
84. Spuches AM, Wilcox DE. 2008. Monomethylarsenite competes with Zn2+ for binding sites in the glucocorticoid receptor. *Journal of the American Chemical Society* 130:8148-9
85. Kligerman AD, Doerr CL, Tennant AH. 2005. Oxidation and methylation status determine the effects of arsenic on the mitotic apparatus. *Molecular and cellular biochemistry* 279:113-21
86. Bustaffa E, Stoccoro A, Bianchi F, Migliore L. 2014. Genotoxic and epigenetic mechanisms in arsenic carcinogenicity. *Archives of toxicology* 88:1043-67
87. WHO. 2001. *Air Quality Guidelines for Europe*. Copenhagen: World Health Organization
88. Masuda H. 2018. Arsenic cycling in the Earth's crust and hydrosphere: interaction between naturally occurring arsenic and human activities. *Progress in Earth and Planetary Science* 5:68
89. Wang S, Mulligan CN. 2006. Occurrence of arsenic contamination in Canada: Sources, behavior and distribution. *Science of The Total Environment* 366:701-21
90. Bennett B, Dudas M. 2011. Release of arsenic and molybdenum by reductive dissolution of iron oxides in a soil with enriched levels of native arsenic. *Journal of Environmental Engineering and Science* 2:265-72
91. Warren HV, Delavault RE, Barakso J. 1964. The role of arsenic as a pathfinder in biogeochemical prospecting. *Economic Geology* 59:1381-5
92. Ng J. 2005. Environmental Contamination of Arsenic and its Toxicological Impact on Humans. *Environmental Chemistry* 2:146-60
93. Matschullat J. 2000. Arsenic in the geosphere - A review. *Science of The Total Environment* 249:297-312
94. Signorelli S. 1997. Arsenic in volcanic gases. *Environmental Geology* 32:239-44

95. Juncos R, Arcagni M, Rizzo A, Campbell L, Arribére M, Ribeiro Guevara S. 2015. Natural origin arsenic in aquatic organisms from a deep oligotrophic lake under the influence of volcanic eruptions. *Chemosphere* 144:2277-89

96. Morales-Simfors N, Bundschuh J, Herath I, Inguaggiato C, Caselli A, et al. 2019. Arsenic in Latin America: A critical overview on the geochemistry of arsenic originating from geothermal features and volcanic emissions for solving its environmental consequences. *Science of The Total Environment* 716:135564

97. Finlay SE, Moffat A, Gazzard R, Baker D, Murray V. 2012. Health impacts of wildfires. *PLoS Curr* 4:e4f959951cce2c-e4fcce2c

98. Johnston SG, Karimian N, Burton ED. 2019. Fire Promotes Arsenic Mobilization and Rapid Arsenic(III) Formation in Soil via Thermal Alteration of Arsenic-Bearing Iron Oxides. *Frontiers in Earth Science* 7

99. Makkonen U, Hellén H, Anttila P, Ferm M. 2009. Size distribution and chemical composition of airborne particles in south-eastern Finland during different seasons and wildfire episodes in 2006. *Science of The Total Environment* 408:644-51

100. Wolf RE, Morman SA, Hageman PL, Hoefen TM, Plumlee GS. 2011. Simultaneous speciation of arsenic, selenium, and chromium: species stability, sample preservation, and analysis of ash and soil leachates. *Analytical and Bioanalytical Chemistry* 401:2733

101. Wittig V, Williams S, DuTeaux SB. 2008. Public Health Impacts of Residential Wildfires: Analysis of Ash and Debris from the 2007 Southern California Fires. *Epidemiology* 19

102. Stocks B, Mason JA, Todd J, Bosch E, Wotton M, et al. 2003. Large forest fires in Canada, 1959–1997. *Journal of Geophysical Research* 108

103. Beck J, Simpson B. 2007. Wildfire threat analysis and the development of a fuel management strategy for British Columbia. *Proceedings of Wildfire*:1-12

104. Kohl L, Meng M, de Vera J, Bergquist B, Cooke CA, et al. 2019. Limited Retention of Wildfire-Derived PAHs and Trace Elements in Indoor Environments. *Geophysical Research Letters* 46:383-91

105. Leist M, Casey RJ, Caridi D. 2000. The management of arsenic wastes: problems and prospects. *Journal of Hazardous Materials* 76:125-38

106. Basha CA, Selvi SJ, Ramasamy E, Chellammal S. 2008. Removal of arsenic and sulphate from the copper smelting industrial effluent. *Chemical Engineering Journal* 141:89-98

107. Razo I, Carrizales L, Castro J, Díaz-Barriga F, Monroy M. 2004. Arsenic and Heavy Metal Pollution of Soil, Water and Sediments in a Semi-Arid Climate Mining Area in Mexico. *Water, Air, & Soil Pollution* 152:129-52

108. Straskraba V, Moran RE. 1990. Environmental occurrence and impacts of arsenic at gold mining sites in the western United States. *International journal of mine water* 9:181-91

109. Kesici GG, Ünlü İ, Topçu AB, Bal CD, Tutkun E, Yılmaz ÖH. 2016. Arsenic related hearing loss in miners. *American Journal of Otolaryngology* 37:6-11

110. Dartey E, Sarpong K, Darko G, Acheampong-Marfo M. 2013. Urinary arsenic and mercury levels in artisanal miners in some communities in the Obuasi Municipality of Ghana. *Journal of Environmental Chemistry and Ecotoxicology* 5:113-8

111. Murao S, Baatar T, Sera K, S.futatsugawa, T.waza. 2011. FINDING OF HIGH LEVEL ARSENIC FOR MONGOLIAN VILLAGERS' HAIR. *International Journal of PIXE* 14

112. Weisenberg IJ, Bakshi PS, Vervaert AE. 1979. Arsenic Distribution and Control in Copper Smelters. *JOM* 31:38-44

113. Chen B, Stein AF, Castell N, de la Rosa JD, Sanchez de la Campa AM, et al. 2012. Modeling and surface observations of arsenic dispersion from a large Cu-smelter in southwestern Europe. *Atmospheric Environment* 49:114-22

114. Hansen HK, Ottosen LM. 2010. Removal of Arsenic from Wastewaters by Airlift Electrocoagulation: Part 3: Copper Smelter Wastewater Treatment. *Separation Science and Technology* 45:1326-30

115. Vahter M, Friberg L, Rahnster B, Nygren Å, Nolinder P. 1986. Airborne arsenic and urinary excretion of metabolites of inorganic arsenic among smelter workers. *International Archives of Occupational and Environmental Health* 57:79-91

116. Feldman RG, Niles CA, Kelly-Hayes M, Sax DS, Djxon WJ, et al. 1979. Peripheral neuropathy in arsenic smelter workers. *Neurology* 29:939-44

117. Lagerkvist BJ, Zetterlund B. 1994. Assessment of exposure to arsenic among smelter workers: A five-year follow-up. *Am J Ind Med* 25:477-88

118. Lagerkvist B, Linderholm H, Nordberg GF. 1986. Vasospastic tendency and raynaud's phenomenon in smelter workers exposed to arsenic. *Environmental Research* 39:465-74

119. Enterline PE, Day R, Marsh GM. 1995. Cancers related to exposure to arsenic at a copper smelter. *Occupational and Environmental Medicine* 52:28

120. Axelson O, Dahlgren E, Jansson CD, Rehnlund SO. 1978. Arsenic exposure and mortality: a case-referent study from a Swedish copper smelter. *Br J Ind Med* 35:8-15
121. Järup L, Pershagen G, Wall S. 1989. Cumulative arsenic exposure and lung cancer in smelter workers: A dose-response study. *Am J Ind Med* 15:31-41
122. Lubin JH, Moore LE, Fraumeni JF, Jr., Cantor KP. 2008. Respiratory cancer and inhaled inorganic arsenic in copper smelters workers: a linear relationship with cumulative exposure that increases with concentration. *Environmental health perspectives* 116:1661-5
123. Wester PO, Brune D, Nordberg G. 1981. Arsenic and selenium in lung, liver, and kidney tissue from dead smelter workers. *Br J Ind Med* 38:179-84
124. PERSHAGEN G. 1985. LUNG CANCER MORTALITY AMONG MEN LIVING NEAR AN ARSENIC-EMITTING SMELTER. *American Journal of Epidemiology* 122:684-94
125. Jamieson H. 2014. The Legacy of Arsenic Contamination from Mining and Processing Refractory Gold Ore at Giant Mine, Yellowknife, Northwest Territories, Canada. *Reviews in Mineralogy and Geochemistry* 79:533-51
126. Sprague DD, Vermaire JC. 2018. Legacy Arsenic Pollution of Lakes Near Cobalt, Ontario, Canada: Arsenic in Lake Water and Sediment Remains Elevated Nearly a Century After Mining Activity Has Ceased. *Water, Air, & Soil Pollution* 229:87
127. Moldovan B, Jiang D-T, Hendry M. 2003. Mineralogical Characterization of Arsenic in Uranium Mine Tailings Precipitated from Iron-Rich Hydrometallurgical Solutions. *Environmental Science & Technology* 37:873-9
128. Walker S, Parsons M, Jamieson H, Lanzirotti A. 2009. Arsenic Mineralogy of Near-surface Tailings and Soils: Influences on Arsenic Mobility and Bioaccessibility in the Nova Scotia Mining Districts. *The Canadian Mineralogist* 47:533-56
129. Donner MW, Javed MB, Shotyk W, Francesconi KA, Siddique T. 2017. Arsenic speciation in the lower Athabasca River watershed: A geochemical investigation of the dissolved and particulate phases. *Environmental Pollution* 224:265-74
130. Zhang H, Huang G-h, Zeng G-m. 2009. Health risks from arsenic-contaminated soil in Flin Flon–Creighton, Canada: Integrating geostatistical simulation and dose–response model. *Environmental Pollution* 157:2413-20

131. Parsons MB, Cranston RE. 2006. Influence of lead smelter emissions on the distribution of metals in marine sediments from Chaleur Bay, eastern Canada. *Geochemistry: Exploration, Environment, Analysis* 6:259
132. Bonham-Carter GF, Henderson PJ, Kliza D, Kettles IM. 2006. Comparison of metal distributions in snow, peat, lakes and humus around a Cu smelter in western Quebec, Canada. *Geochemistry: Exploration, Environment, Analysis* 6:215-28
133. Caplette J, Schindler M. 2018. Black Rock-Coatings In Trail, British Columbia, Canada: Records of Past Emissions of Lead, Zinc, Antimony, Arsenic, Tellurium, Tin, Selenium, Silver, Bismuth, and Indium-Bearing Atmospheric Contaminants. *The Canadian Mineralogist* 56:canmin.1700069
134. Yudovich YE, Ketris MP. 2005. Arsenic in coal: a review. *International Journal of Coal Geology* 61:141-96
135. Mattigod SV, Rai D, Eary LE, Ainsworth CC. 1990. Geochemical Factors Controlling the Mobilization of Inorganic Constituents from Fossil Fuel Combustion Residues: I. Review of the Major Elements. *Journal of Environmental Quality* 19:188-201
136. Wang C, Liu H, Zhang Y, Zou C, Anthony EJ. 2018. Review of arsenic behavior during coal combustion: Volatilization, transformation, emission and removal technologies. *Progress in Energy and Combustion Science* 68:1-28
137. Yager JW, Hicks JB, Fabianova E. 1997. Airborne arsenic and urinary excretion of arsenic metabolites during boiler cleaning operations in a Slovak coal-fired power plant. *Environmental health perspectives* 105:836-42
138. Pesch B, Ranft U, Jakubis P, Nieuwenhuijsen MJ, Hergemöller A, et al. 2002. Environmental Arsenic Exposure from a Coal-burning Power Plant as a Potential Risk Factor for Nonmelanoma Skin Carcinoma: Results from a Case-Control Study in the District of Prievidza, Slovakia. *American Journal of Epidemiology* 155:798-809
139. Bencko V, Rameš J, Fabiánová E, Pešek J, Jakubis M. 2009. Ecological and human health risk aspects of burning arsenic-rich coal. *Environmental Geochemistry and Health* 31:239-43
140. Pulles T, Denier van der Gon H, Appelman W, Verheul M. 2012. Emission factors for heavy metals from diesel and petrol used in European vehicles. *Atmospheric Environment* 61:641-51

141. Talebi S, Abedi M. 2005. Determination of arsenic in air particulates and diesel exhaust particulates by spectrophotometry. *Journal of environmental sciences (China)* 17:156-8
142. Donahue WF, Allen EW, Schindler DW. 2006. Impacts of Coal-Fired Power Plants on Trace Metals and Polycyclic Aromatic Hydrocarbons (PAHs) in Lake Sediments in Central Alberta, Canada. *Journal of Paleolimnology* 35:111-28
143. Lalonde BA, Ernst W, Comeau F. 2011. Trace Metal Concentrations in Sediments and Fish in the Vicinity of Ash Lagoon Discharges from Coal-Combustion Plants in New Brunswick and Nova Scotia, Canada. *Archives of Environmental Contamination and Toxicology* 61:472-81
144. Neamen DA. 2012. *Semiconductor physics and devices: basic principles*. New York: McGraw-Hill
145. Tanaka A. 2004. Toxicity of indium arsenide, gallium arsenide, and aluminium gallium arsenide. *Toxicology and Applied Pharmacology* 198:405-11
146. Park D, Yang H, Jeong J, Ha K, Choi S, et al. 2010. A Comprehensive Review of Arsenic Levels in the Semiconductor Manufacturing Industry. *The Annals of Occupational Hygiene* 54:869-79
147. Ham S, Yoon C, Kim S, Park J, Kwon O, et al. 2017. Arsenic Exposure during Preventive Maintenance of an Ion Implanter in a Semiconductor Manufacturing Factory. *Aerosol and Air Quality Research* 17:990-9
148. Byun K, Won YL, Hwang YI, Koh D-H, Im H, Kim E-A. 2013. Assessment of arsenic exposure by measurement of urinary speciated inorganic arsenic metabolites in workers in a semiconductor manufacturing plant. *Ann Occup Environ Med* 25:21-
149. Hu C-W, Pan C-H, Huang Y-L, Wu M-T, Chang LW, et al. 2006. Effects of arsenic exposure among semiconductor workers: A cautionary note on urinary 8-oxo-7,8-dihydro-2′-deoxyguanosine. *Free Radic Biol Med* 40:1273-8
150. Torrance KW, Keenan HE, Hursthouse AS, Stirling D. 2010. Measurement of arsenic and gallium content of gallium arsenide semiconductor waste streams by ICP-MS. *Journal of Environmental Science and Health, Part A* 45:471-5
151. Chen HW. 2006. Gallium, Indium, and Arsenic Pollution of Groundwater from a Semiconductor Manufacturing Area of Taiwan. *Bulletin of Environmental Contamination and Toxicology* 77:289-96

152. Chein H, Hsu Y-D, Aggarwal SG, Chen T-M, Huang C-C. 2006. Evaluation of arsenical emission from semiconductor and opto-electronics facilities in Hsinchu, Taiwan. *Atmospheric Environment* 40:1901-7

153. Forti V, Balde CP, Kuehr R, Bel G. 2020. *The Global E-waste Monitor 2020: Quantities, flows and the circular economy potential*. Bonn, Geneva and Rotterdam: United Nations University/United Nations Institute for Training and Research, International Telecommunication Union, and International Solid Waste Association

154. Heacock M, Kelly CB, Asante KA, Birnbaum LS, Bergman ÅL, et al. 2016. E-Waste and Harm to Vulnerable Populations: A Growing Global Problem. *Environ Health Perspect* 124:550-5

155. Yao C-X, Yin X-b, Song J, Li C-x, Qian W, et al. 2008. Arsenic contents in soil, water, and crops in an e-waste disposal area. *Huan Jing Ke Xue* 29:1713-8

156. Ackah M. 2019. Soil elemental concentrations, geoaccumulation index, non-carcinogenic and carcinogenic risks in functional areas of an informal e-waste recycling area in Accra, Ghana. *Chemosphere* 235:908-17

157. Kumar A, Holuszko M. 2016. Electronic waste and existing processing routes: A Canadian perspective. *Resources* 5

158. Kumar A, Kuppusamy VK, Holuszko M, Song S, Loschiavo A. 2019. LED lamps waste in Canada: Generation and characterization. *Resources, Conservation and Recycling* 146:329-36

159. Eckel WP, Rabinowitz MB, Foster GD. 2002. Investigation of unrecognized former secondary lead smelting sites: confirmation by historical sources and elemental ratios in soil. *Environmental Pollution* 117:273-9

160. Ettler V, Mihaljevič M, Šebek O. 2010. Antimony and arsenic leaching from secondary lead smelter air-pollution-control residues. *Waste Manag Res* 28:587-95

161. Chai L-y, Shi M-q, Liang Y-j, Tang J-w, Li Q-z. 2015. Behavior, distribution and environmental influence of arsenic in a typical lead smelter. *Journal of Central South University* 22:1276-86

162. Johnston JE, Franklin M, Roh H, Austin C, Arora M. 2019. Lead and Arsenic in Shed Deciduous Teeth of Children Living Near a Lead-Acid Battery Smelter. *Environmental Science & Technology* 53:6000-6

163. Temple PJ, Linzon SN, Chai BL. 1977. Contamination of vegetation and soil by arsenic emissions from secondary lead smelters. *Environmental Pollution (1970)* 12:311-20
164. Morrell J, Huffman J. 2004. Copper, chromium, and arsenic levels in soils surrounding posts treated with chromated copper arsenate (CCA). *Wood Fiber Sci* 36
165. Khan BI, Solo-Gabriele HM, Townsend TG, Cai Y. 2006. Release of Arsenic to the Environment from CCA-Treated Wood. 1. Leaching and Speciation during Service. *Environmental Science & Technology* 40:988-93
166. Khan BI, Jambeck J, Solo-Gabriele HM, Townsend TG, Cai Y. 2006. Release of arsenic to the environment from CCA-treated wood. 2. Leaching and speciation during disposal. *Environmental Science & Technology* 40:994-9
167. Moghaddam AH, Mulligan CN. 2008. Leaching of heavy metals from chromated copper arsenate (CCA) treated wood after disposal. *Waste Management* 28:628-37
168. Wasson SJ, Linak WP, Gullett BK, King CJ, Touati A, et al. 2005. Emissions of Chromium, Copper, Arsenic, and PCDDs/Fs from Open Burning of CCA-Treated Wood. *Environmental Science & Technology* 39:8865-76
169. Zagury GJ, Samson R, Deschênes L. 2003. Occurrence of Metals in Soil and Ground Water Near Chromated Copper Arsenate–Treated Utility Poles. *Journal of Environmental Quality* 32:507-14
170. Coles CA, Arisi JA, Organ M, Veinott GI. 2014. Leaching of Chromium, Copper, and Arsenic from CCA-Treated Utility Poles. *Applied and Environmental Soil Science* 2014:167971
171. Kwon E, Zhang H, Wang Z, Jhangri GS, Lu X, et al. 2004. Arsenic on the hands of children after playing in playgrounds. *Environmental health perspectives* 112:1375-80
172. Environment F-P-TCoDWotF-P-TCoHat. 2006. *Guidelines for Canadian Drinking Water Quality: Guideline Technical Document: Arsenic*. Ottawa: Health Canada
173. Bencko V, Yan Li Foong F. 2017. The history of arsenical pesticides and health risks related to the use of Agent Blue. *Ann Agric Environ Med* 24:312-6
174. Quazi S, Datta R, Sarkar D. 2011. Effects of soil types and forms of arsenical pesticide on rice growth and development. *International Journal of Environmental Science & Technology* 8:445-60

175. Li Y, Ye F, Wang A, Wang D, Yang B, et al. 2016. Chronic Arsenic Poisoning Probably Caused by Arsenic-Based Pesticides: Findings from an Investigation Study of a Household. *Int J Environ Res Public Health* 13:133

176. Whitmore TJ, Riedinger-Whitmore MA, Smoak JM, Kolasa KV, Goddard EA, Bindler R. 2008. Arsenic contamination of lake sediments in Florida: evidence of herbicide mobility from watershed soils. *Journal of Paleolimnology* 40:869-84

177. Dennis LK, Lynch CF, Sandler DP, Alavanja MCR. 2010. Pesticide use and cutaneous melanoma in pesticide applicators in the agricultural heath study. *Environmental health perspectives* 118:812-7

178. Boulanger M, Tual S, Pons R, Busson A, Delafosse P, et al. 2019. *O6B.1 Use of arsenical pesticides and risk of lung cancer among french farmers*. A53.1-A pp.

179. Cancès B, Juillot F, Morin G, Laperche V, Alvarez L, et al. 2005. XAS Evidence of As(V) Association with Iron Oxyhydroxides in a Contaminated Soil at a Former Arsenical Pesticide Processing Plant. *Environmental Science & Technology* 39:9398-405

180. Keimowitz AR, Zheng Y, Chillrud SN, Mailloux B, Jung HB, et al. 2005. Arsenic Redistribution between Sediments and Water near a Highly Contaminated Source. *Environmental Science & Technology* 39:8606-13

181. Quazi S, Sarkar D, Datta R. 2010. Effect of soil aging on arsenic fractionation and bioaccessibility in inorganic arsenical pesticide contaminated soils. *Applied Geochemistry* 25:1422-30

182. Hughes MF, Beck BD, Chen Y, Lewis AS, Thomas DJ. 2011. Arsenic exposure and toxicology: a historical perspective. *Toxicological sciences* 123:305-32

183. Frank R, Braun HE, Ishida K, Suda P. 1976. PERSISTENT ORGANIC AND INORGANIC PESTICIDE RESIDUES IN ORCHARD SOILS AND VINEYARDS OF SOUTHERN ONTARIO. *Canadian Journal of Soil Science* 56:463-84

184. Bishop RF, Chisholm D. 1962. ARSENIC ACCUMULATION IN ANNAPOLIS VALLEY ORCHARD SOILS. *Canadian Journal of Soil Science* 42:77-80

185. MacLean KS, Langille WM. 1981. Arsenic in orchard and potato soils and plant tissue. *Plant and Soil* 61:413-8

186. Martin RR, Tomlin A, Marsello B. 2000. Arsenic uptake in orchard trees: implications for dendroanalysis. *Chemosphere* 41:635-7

187. Nachman KE, Baron PA, Raber G, Francesconi KA, Navas-Acien A, Love DC. 2013. Roxarsone, inorganic arsenic, and other arsenic species in chicken: a U.S.-based market basket sample. *Environmental health perspectives* 121:818-24

188. Nachman KE, Love DC, Baron PA, Nigra AE, Murko M, et al. 2017. Nitarsone, Inorganic Arsenic, and Other Arsenic Species in Turkey Meat: Exposure and Risk Assessment Based on a 2014 U.S. Market Basket Sample. *Environmental health perspectives* 125:363-9

189. Chen J, Zhang J, Rosen BP. 2019. Role of ArsEFG in Roxarsone and Nitarsone Detoxification and Resistance. *Environmental Science & Technology* 53:6182-91

190. Han J-C, Zhang F, Cheng L, Mu Y, Liu D-F, et al. 2017. Rapid Release of Arsenite from Roxarsone Bioreduction by Exoelectrogenic Bacteria. *Environmental Science & Technology Letters* 4:350-5

191. Garbarino JR, Bednar AJ, Rutherford DW, Beyer RS, Wershaw RL. 2003. Environmental Fate of Roxarsone in Poultry Litter. I. Degradation of Roxarsone during Composting. *Environmental Science & Technology* 37:1509-14

192. Cortinas I, Field JA, Kopplin M, Garbarino JR, Gandolfi AJ, Sierra-Alvarez R. 2006. Anaerobic Biotransformation of Roxarsone and Related N-Substituted Phenylarsonic Acids. *Environmental Science & Technology* 40:2951-7

193. Bednar AJ, Garbarino JR, Ferrer I, Rutherford DW, Wershaw RL, et al. 2003. Photodegradation of roxarsone in poultry litter leachates. *Science of The Total Environment* 302:237-45

194. Rutherford DW, Bednar AJ, Garbarino JR, Needham R, Staver KW, Wershaw RL. 2003. Environmental Fate of Roxarsone in Poultry Litter. Part II. Mobility of Arsenic in Soils Amended with Poultry Litter. *Environmental Science & Technology* 37:1515-20

195. Huang L, Yao L, He Z, Zhou C, Li G, et al. 2014. Roxarsone and its metabolites in chicken manure significantly enhance the uptake of As species by vegetables. *Chemosphere* 100:57-62

196. Yao L, Huang L, He Z, Zhou C, Lu W, Bai C. 2016. Delivery of roxarsone via chicken diet→chicken→chicken manure→soil→rice plant. *Science of The Total Environment* 566-567:1152-8

197. Henke K. 2009. *Arsenic: environmental chemistry, health threats and waste treatment*. New York: John Wiley & Sons

198. Waxman S, Anderson KC. 2001. History of the development of arsenic derivatives in cancer therapy. *Oncologist* 6 Suppl 2:3-10
199. Riethmiller S. 2005. From Atoxyl to Salvarsan: Searching for the Magic Bullet. *Chemotherapy* 51:234-42
200. Bosch F, Rosich L. 2008. The contributions of Paul Ehrlich to pharmacology: a tribute on the occasion of the centenary of his Nobel Prize. *Pharmacology* 82:171-9
201. Steverding D. 2010. The development of drugs for treatment of sleeping sickness: a historical review. *Parasites & Vectors* 3:15
202. Büscher P, Cecchi G, Jamonneau V, Priotto G. 2017. Human African trypanosomiasis. *The Lancet* 390:2397-409
203. Hoonjan M, Jadhav V, Bhatt P. 2018. Arsenic trioxide: insights into its evolution to an anticancer agent. *Journal of biological inorganic chemistry : JBIC : a publication of the Society of Biological Inorganic Chemistry* 23:313-29
204. Khairul I, Wang Q, Jiang Y, Wang C, Naranmandura H. 2015. Metabolism, toxicity and anticancer activities of arsenic compounds. *Oncotarget* 8
205. Kakizuka A, Miller WH, Umesono K, Warrell RP, Frankel SR, et al. 1991. Chromosomal translocation t(15;17) in human acute promyelocytic leukemia fuses RARα with a novel putative transcription factor, PML. *Cell* 66:663-74
206. Liquori A, Ibañez M, Sargas C, Sanz M, Barragán E, Cervera J. 2020. Acute Promyelocytic Leukemia: A Constellation of Molecular Events around a Single PML-RARA Fusion Gene. *Cancers* 12
207. Tomita A, Kiyoi H, Naoe T. 2013. Mechanisms of action and resistance to all-trans retinoic acid (ATRA) and arsenic trioxide (As2O 3) in acute promyelocytic leukemia. *International journal of hematology* 97:717-25
208. Sadaf N, Kumar N, Ali M, Ali V, Bimal S, Haque R. 2018. Arsenic trioxide induces apoptosis and inhibits the growth of human liver cancer cells. *Life Sciences* 205:9-17
209. Huang W, Zeng YC. 2019. A candidate for lung cancer treatment: arsenic trioxide. *Clinical and Translational Oncology* 21:1115-26
210. Ally MS, Ransohoff K, Sarin K, Atwood SX, Rezaee M, et al. 2016. Effects of Combined Treatment With Arsenic Trioxide and Itraconazole in Patients With Refractory Metastatic Basal Cell Carcinoma. *JAMA Dermatol* 152:452-6

211. Wu B, Tan M, Cai W, Wang B, He P, Zhang X. 2018. Arsenic trioxide induces autophagic cell death in osteosarcoma cells via the ROS-TFEB signaling pathway. *Biochemical and Biophysical Research Communications* 496:167-75

212. Wang QQ, Hua HY, Naranmandura H, Zhu HH. 2020. Balance between the toxicity and anticancer activity of arsenic trioxide in treatment of acute promyelocytic leukemia. *Toxicology and applied pharmacology* 409:115299

213. Zhang Z, Zhang S, Zhang F, Zhang Q, Wei H, et al. 2023. Clinical Indicators of Hepatotoxicity in Newly Diagnosed Acute Promyelocytic Leukemia Patients Undergoing Arsenic Trioxide Treatment. *Biological trace element research*

214. Au WY, Kwong YL. 2008. Arsenic trioxide: safety issues and their management. *Acta pharmacologica Sinica* 29:296-304

215. Miodragović Đ, Swindell EP, Waxali ZS, Bogachkov A, O'Halloran TV. 2019. Beyond Cisplatin: Combination Therapy with Arsenic Trioxide. *Inorganica chimica acta* 496

216. Murgo AJ. 2001. Clinical trials of arsenic trioxide in hematologic and solid tumors: overview of the National Cancer Institute Cooperative Research and Development Studies. *Oncologist* 6 Suppl 2:22-8

217. Cubadda F, Jackson BP, Cottingham KL, Van Horne YO, Kurzius-Spencer M. 2017. Human exposure to dietary inorganic arsenic and other arsenic species: State of knowledge, gaps and uncertainties. *Science of The Total Environment* 579:1228-39

218. Elshenawy OH, El-Kadi AO. 2015. Modulation of aryl hydrocarbon receptor regulated genes by acute administration of trimethylarsine oxide in the lung, kidney and heart of C57BL/6 mice. *Xenobiotica* 45:930-43

219. Smedley PL, Kinniburgh DG. 2002. A review of the source, behaviour and distribution of arsenic in natural waters. *Applied Geochemistry* 17:517-68

220. Raessler M. 2018. The Arsenic Contamination of Drinking and Groundwaters in Bangladesh: Featuring Biogeochemical Aspects and Implications on Public Health. *Archives of Environmental Contamination and Toxicology* 75:1-7

221. Greco SL, Belova A, Haskell J, Backer L. 2019. Estimated burden of disease from arsenic in drinking water supplied by domestic wells in the United States. *Journal of Water and Health* 17:801-12

222. Meranger JC, Subramanian KS, McCurdy RF. 1984. Arsenic in Nova Scotian groundwater. *Science of The Total Environment* 39:49-55

223. Thirunavukkarasu OS, Viraraghavan T, Subramanian KS, Tanjore S. 2002. Organic arsenic removal from drinking water. *Urban Water* 4:415-21

224. Hu G, Mian HR, Dyck R, Mohseni M, Jasim S, et al. 2019. Drinking Water Treatments for Arsenic and Manganese Removal and Health Risk Assessment in White Rock, Canada. *Exposure and Health*

225. Saint-Jacques N, Brown P, Nauta L, Boxall J, Parker L, Dummer TJB. 2018. Estimating the risk of bladder and kidney cancer from exposure to low-levels of arsenic in drinking water, Nova Scotia, Canada. *Environment International* 110:95-104

226. Moncur MC, Paktunc D, Jean Birks S, Ptacek CJ, Welsh B, Thibault Y. 2015. Source and distribution of naturally occurring arsenic in groundwater from Alberta's Southern Oil Sands Regions. *Applied Geochemistry* 62:171-85

227. McGuigan CF, Hamula CLA, Huang S, Gabos S, Le XC. 2010. A review on arsenic concentrations in Canadian drinking water. *Environmental Reviews* 18:291-307

228. Kreutzwiser R, de Loë R, Imgrund K, Conboy MJ, Simpson H, Plummer R. 2011. Understanding stewardship behaviour: Factors facilitating and constraining private water well stewardship. *Journal of Environmental Management* 92:1104-14

229. Chappells H, Parker L, Fernandez CV, Conrad C, Drage J, et al. 2014. Arsenic in private drinking water wells: an assessment of jurisdictional regulations and guidelines for risk remediation in North America. *Journal of Water and Health* 12:372-92

230. Gagnon F, Lampron-Goulet E, Normandin L, Langlois M-F. 2016. Measurements of Arsenic in the Urine and Nails of Individuals Exposed to Low Concentrations of Arsenic in Drinking Water From Private Wells in a Rural Region of Quebec, Canada. *Journal of environmental health* 78:76-83

231. Dummer TJB, Yu ZM, Nauta L, Murimboh JD, Parker L. 2015. Geostatistical modelling of arsenic in drinking water wells and related toenail arsenic concentrations across Nova Scotia, Canada. *Science of The Total Environment* 505:1248-58

232. Pratt M, Wadden P, Gulliver W. 2016. Arsenic Keratosis in a Patient from Newfoundland and Labrador, Canada:Case Report and Review. *J Cutan Med Surg* 20:67-71

233. Uneyama C, Toda M, Yamamoto M, Morikawa K. 2007. Arsenic in various foods: Cumulative data. *Food additives and contaminants* 24:447-534

234. Mania M, Rebeniak M, Szynal T, Wojciechowska-Mazurek M, Starska K, et al. 2015. Total and inorganic arsenic in fish, seafood and seaweeds - exposure assessment. *Roczniki Panstwowego Zakladu Higieny* 66:203-10

235. Upadhyay MK, Shukla A, Yadav P, Srivastava S. 2019. A review of arsenic in crops, vegetables, animals and food products. *Food chemistry* 276:608-18

236. Nigra AE, Nachman KE, Love DC, Grau-Perez M, Navas-Acien A. 2017. Poultry Consumption and Arsenic Exposure in the U.S. Population. *Environmental health perspectives* 125:370-7

237. Ruiz-de-Cenzano M, Cava-Montesinos P, Cervera ML, de la Guardia M. 2017. Fast extraction methodologies for the determination of toxic arsenic in meat. *Int J Food Sci Technol* 52:2531-7

238. Datta BK, Bhar MK, Patra PH, Majumdar D, Dey RR, et al. 2012. Effect of environmental exposure of arsenic on cattle and poultry in nadia district, west bengal, India. *Toxicol Int* 19:59-62

239. Ghosh A, Awal MA, Majumder S, Mostofa M, Khair A, et al. 2012. Arsenic in eggs and excreta of laying hens in Bangladesh: a preliminary study. *J Health Popul Nutr* 30:383-93

240. Liu Q, Peng H, Lu X, Zuidhof MJ, Li X-F, Le XC. 2016. Arsenic Species in Chicken Breast: Temporal Variations of Metabolites, Elimination Kinetics, and Residual Concentrations. *Environ Health Perspect* 124:1174-81

241. Huang J-H, Hu K-N, Decker B. 2011. Organic Arsenic in the Soil Environment: Speciation, Occurrence, Transformation, and Adsorption Behavior. *Water, Air, & Soil Pollution* 219:401-15

242. Zhao FJ, Ma JF, Meharg AA, McGrath SP. 2009. Arsenic uptake and metabolism in plants. *New Phytol* 181:777-94

243. Kumarathilaka P, Seneweera S, Ok YS, Meharg AA, Bundschuh J. 2020. Mitigation of arsenic accumulation in rice: An agronomical, physico-chemical, and biological approach – A critical review. *Critical Reviews in Environmental Science and Technology* 50:31-71

244. Tang Z, Lv Y, Chen F, Zhang W, Rosen BP, Zhao F-J. 2016. Arsenic Methylation in Arabidopsis thaliana Expressing an Algal Arsenite Methyltransferase Gene Increases Arsenic Phytotoxicity. *J Agric Food Chem* 64:2674-81

245. Chen Y, Han Y-H, Cao Y, Zhu Y-G, Rathinasabapathi B, Ma LQ. 2017. Arsenic Transport in Rice and Biological Solutions to Reduce Arsenic Risk from Rice. *Front Plant Sci* 8:268-

246. Davis MA, Signes-Pastor AJ, Argos M, Slaughter F, Pendergrast C, et al. 2017. Assessment of human dietary exposure to arsenic through rice. *Science of The Total Environment* 586:1237-44

247. Khush GS. 2005. What it will take to Feed 5.0 Billion Rice consumers in 2030. *Plant Molecular Biology* 59:1-6

248. Jackson BP, Taylor VF, Punshon T, Cottingham KL. 2012. Arsenic concentration and speciation in infant formulas and first foods. *Pure Appl Chem* 84:215-23

249. Signes-Pastor AJ, Carey M, Meharg AA. 2016. Inorganic arsenic in rice-based products for infants and young children. *Food Chemistry* 191:128-34

250. Mierzwa J, B. Adeloju S, S. Dhindsa H. 1997. Slurry Sampling for Hydride Generation Atomic Absorption Spectrometric Determination of Arsenic in Cigarette Tobaccos. *Analyst* 122:539-42

251. Taebunpakul S, Liu C, Wright C, McAdam K, Heroult J, et al. 2011. Determination of total arsenic and arsenic speciation in tobacco products: from tobacco leaf and cigarette smoke. *Journal of Analytical Atomic Spectrometry* 26:1633-40

252. Hertz-Picciotto I, Smith AH, Holtzman D, Lipsett M, Alexeeff G. 1992. Synergism between Occupational Arsenic Exposure and Smoking in the Induction of Lung Cancer. *Epidemiology* 3:23-31

253. Meacher DM, Menzel DB, Dillencourt MD, Bic LF, Schoof RA, et al. 2002. Estimation of Multimedia Inorganic Arsenic Intake in the U.S. Population. *Human and Ecological Risk Assessment: An International Journal* 8:1697-721

254. Lewis AS, Reid KR, Pollock MC, Campleman SL. 2012. Speciated arsenic in air: Measurement methodology and risk assessment considerations. *Journal of the Air & Waste Management Association* 62:2-17

255. IARC. 2012. *Arsenic, metals, fibres, and dusts*. Lyon: International Agency for Cancer Research

256. IARC. 2016. *Outdoor air pollution*. Lyon: International Agency for Cancer Research
257. Setton E, Hystad P, Poplawski K, Cheasley R, Cervantes-Larios A, et al. 2013. Risk-based indicators of Canadians' exposures to environmental carcinogens. *Environmental Health* 12:15
258. Ouypornkochagorn S, Feldmann J. 2010. Dermal Uptake of Arsenic through Human Skin Depends Strongly on Its Speciation. *Environmental Science & Technology* 44:3972-8
259. Smith AE, Lincoln RA, Paulu C, Simones TL, Caldwell KL, et al. 2016. Assessing arsenic exposure in households using bottled water or point-of-use treatment systems to mitigate well water contamination. *Science of The Total Environment* 544:701-10
260. Lowney YW, Wester RC, Schoof RA, Cushing CA, Edwards M, Ruby MV. 2007. Dermal Absorption of Arsenic from Soils as Measured in the Rhesus Monkey. *Toxicological Sciences* 100:381-92
261. Chen AY-Y, Olsen T. 2016. Chromated copper arsenate-treated wood: a potential source of arsenic exposure and toxicity in dermatology. *Int J Womens Dermatol* 2:28-30
262. Hemond HF, Solo-Gabriele HM. 2004. Children's Exposure to Arsenic from CCA-Treated Wooden Decks and Playground Structures. *Risk Anal* 24:51-64
263. Irfan Z. 2012. Arsenic contamination in water: A conceptual framework of policy options with particular reference to Bengal delta basin. *Int. J. of Hydrology Science and Technology* 2:391-401
264. Tseng CH. 2005. Blackfoot disease and arsenic: a never-ending story. *Journal of environmental science and health. Part C, Environmental carcinogenesis & ecotoxicology reviews* 23:55-74
265. Ljung K, Selinus O, Otabbong E, Berglund M. 2006. Metal and arsenic distribution in soil particle sizes relevant to soil ingestion by children. *Applied Geochemistry* 21:1613-24
266. Bacigalupo C, Hale B. 2012. Human health risks of Pb and As exposure via consumption of home garden vegetables and incidental soil and dust ingestion: A probabilistic screening tool. *Science of The Total Environment* 423:27-38
267. De Kanter R, De Jager MH, Draaisma AL, Jurva JU, Olinga P, et al. 2002. Drug-metabolizing activity of human and rat liver, lung, kidney and intestine slices. *Xenobiotica* 32:349-62

268. Guengerich FP. 2008. Cytochrome p450 and chemical toxicology. *Chem Res Toxicol* 21:70-83

269. Lamb DC, Lei L, Warrilow AGS, Lepesheva GI, Mullins JGL, et al. 2009. The First Virally Encoded Cytochrome P450. *Journal of Virology* 83:8266

270. Ding X, Kaminsky L. 2003. Human Extrahepatic Cytochromes P450: Function in Xenobiotic Metabolism and Tissue-Selective Chemical Toxicity in the Respiratory and Gastrointestinal Tracts. *Annu Rev Pharmacol Toxicol* 43:149-73

271. Nebert DW, Russell DW. 2002. Clinical importance of the cytochromes P450. *The Lancet* 360:1155-62

272. Navarro-Mabarak C, Camacho-Carranza R, Espinosa-Aguirre JJ. 2018. Cytochrome P450 in the central nervous system as a therapeutic target in neurodegenerative diseases. *Drug Metabolism Reviews* 50:95-108

273. Xu X, Zhang XA, Wang DW. 2011. The roles of CYP450 epoxygenases and metabolites, epoxyeicosatrienoic acids, in cardiovascular and malignant diseases. *Advanced Drug Delivery Reviews* 63:597-609

274. Wang W, Yang J, Edin ML, Wang Y, Luo Y, et al. 2019. Targeted Metabolomics Identifies the Cytochrome P450 Monooxygenase Eicosanoid Pathway as a Novel Therapeutic Target of Colon Tumorigenesis. *Cancer Research* 79:1822

275. Zanger UM, Schwab M. 2013. Cytochrome P450 enzymes in drug metabolism: regulation of gene expression, enzyme activities, and impact of genetic variation. *Pharmacology & therapeutics* 138:103-41

276. Zanger UM, Turpeinen M, Klein K, Schwab M. 2008. Functional pharmacogenetics/genomics of human cytochromes P450 involved in drug biotransformation. *Analytical and Bioanalytical Chemistry* 392:1093-108

277. McDonnell AM, Dang CH. 2013. Basic review of the cytochrome p450 system. *J Adv Pract Oncol* 4:263-8

278. Storelli F, Samer C, Reny J-L, Desmeules J, Daali Y. 2018. Complex Drug–Drug–Gene–Disease Interactions Involving Cytochromes P450: Systematic Review of Published Case Reports and Clinical Perspectives. *Clinical Pharmacokinetics* 57:1267-93

279. Yoshida N, Yamada A, Mimura Y, Kawakami J, Adachi I. 2006. Trends in new drug interactions for pharmaceutical products in Japan. *Pharmacoepidemiol Drug Saf* 15:421-7

280. Manzetti S. 2013. Polycyclic Aromatic Hydrocarbons in the Environment: Environmental Fate and Transformation. *Polycyclic Aromatic Compounds* 33:311-30
281. Kim K-H, Jahan SA, Kabir E, Brown RJC. 2013. A review of airborne polycyclic aromatic hydrocarbons (PAHs) and their human health effects. *Environment International* 60:71-80
282. Hecht SS. 1999. Tobacco Smoke Carcinogens and Lung Cancer. *JNCI: Journal of the National Cancer Institute* 91:1194-210
283. Badal S, Delgoda R. 2014. Role of the modulation of CYP1A1 expression and activity in chemoprevention. *J Appl Toxicol* 34:743-53
284. Shimada T, Inoue K, Suzuki Y, Kawai T, Azuma E, et al. 2002. Arylhydrocarbon receptor-dependent induction of liver and lung cytochromes P450 1A1, 1A2, and 1B1 by polycyclic aromatic hydrocarbons and polychlorinated biphenyls in genetically engineered C57BL/6J mice. *Carcinogenesis* 23:1199-207
285. Anwar-Mohamed A, Elbekai RH, El-Kadi AO. 2009. Regulation of CYP1A1 by heavy metals and consequences for drug metabolism. *Expert opinion on drug metabolism & toxicology* 5:501-21
286. Pershagen G, Wall S, Taube A, Linnman L. 1981. On the interaction between occupational arsenic exposure and smoking and its relationship to lung cancer. *Scand J Work Environ Health*:302-9
287. Järup L, Pershagen G. 1991. Arsenic Exposure, Smoking, and Lung Cancer in Smelter Workers—A Case-Control Study. *American Journal of Epidemiology* 134:545-51
288. Hertz-Picciotto I, Smith AH. 1993. Observations on the dose-response curve for arsenic exposure and lung cancer. *Scand J Work Environ Health*:217-26
289. Tsuda T, Babazono A, Yamamoto E, Kurumatani N, Mino Y, et al. 1995. Ingested Arsenic and Internal Cancer: A Historical Cohort Study Followed for 33 Years. *American Journal of Epidemiology* 141:198-209
290. Ferreccio C, González C, Milosavjlevic V, Marshall G, Sancha AM, Smith AH. 2000. Lung Cancer and Arsenic Concentrations in Drinking Water in Chile. *Epidemiology* 11:673-9
291. Chen C-L, Hsu L-I, Chiou H-Y, Hsueh Y-M, Chen S-Y, et al. 2004. Ingested Arsenic, Cigarette Smoking, and Lung Cancer RiskA Follow-up Study in Arseniasis-Endemic Areas in Taiwan. *JAMA* 292:2984-90

292. Ishinishi N, Kodama Y, Nobutomo K, Hisanaga A. 1977. Preliminary experimental study on carcinogenicity of arsenic trioxide in rat lung. *Environmental health perspectives* 19:191-6

293. Pershagen G, Nordberg G, Björklund N-E. 1984. Carcinomas of the respiratory tract in hamsters given arsenic trioxide and/or benzo[a]pyrene by the pulmonary route. *Environmental Research* 34:227-41

294. Wei S, Zhang H, Tao S. 2019. A review of arsenic exposure and lung cancer. *Toxicology Research* 8:319-27

295. Lau ATY, Chiu J-F. 2006. Proteomic and biochemical analyses of in vitro carcinogen-induced lung cell transformation: Synergism between arsenic and benzo[a]pyrene. *Proteomics* 6:1619-30

296. Chiang H-c, Tsou T-C. 2009. Arsenite enhances the benzo[a]pyrene diol epoxide (BPDE)-induced mutagenesis with no marked effect on repair of BPDE-DNA adducts in human lung cells. *Toxicology in Vitro* 23:897-905

297. Evans CD, LaDow K, Schumann BL, Savage RE, Jr, Caruso J, et al. 2004. Effect of arsenic on benzo[a]pyrene DNA adduct levels in mouse skin and lung. *Carcinogenesis* 25:493-7

298. Falkner KC, McCallum GP, Cherian MG, Bend JR. 1993. Effects of acute sodium arsenite administration on the pulmonary chemical metabolizing enzymes, cytochrome P-450 monooxygenase, NAD(P)H:quinone acceptor oxidoreductase and glutathione S-transferase in guinea pig: comparison with effects in liver and kidney. *Chemico-biological interactions* 86:51-68

299. Seubert JM, Sinal CJ, Bend JR. 2002. Acute sodium arsenite administration induces pulmonary CYP1A1 mRNA, protein and activity in the rat. *J Biochem Mol Toxicol* 16:84-95

300. Wu JP, Chang LW, Yao HT, Chang H, Tsai HT, et al. 2009. Involvement of oxidative stress and activation of aryl hydrocarbon receptor in elevation of CYP1A1 expression and activity in lung cells and tissues by arsenic: an in vitro and in vivo study. *Toxicological sciences : an official journal of the Society of Toxicology* 107:385-93

301. Anwar-Mohamed A, Abdelhamid G, Amara IE, El-Kadi AO. 2012. Differential modulation of aryl hydrocarbon receptor regulated enzymes by arsenite in the kidney, lung, and heart of C57BL/6 mice. *Archives of toxicology* 86:897-910

302. Elshenawy OH, Abdelhamid G, Althurwi HN, El-Kadi AOS. 2018. Dimethylarsinic acid modulates the aryl hydrocarbon receptor-regulated genes in C57BL/6 mice: in vivo study. *Xenobiotica* 48:124-34

303. Albores A, Sinal CJ, Cherian MG, Bend JR. 1995. Selective increase of rat lung cytochrome P450 1A1 dependent monooxygenase activity after acute sodium arsenite administration. *Can J Physiol Pharmacol* 73:153-8

304. Seubert JM, Webb CD, Bend JR. 2002. Acute sodium arsenite treatment induces Cyp2a5 but not Cyp1a1 in the C57Bl/6 mouse in a tissue (kidney) selective manner. *J Biochem Mol Toxicol* 16:96-106

305. Ho IC, Lee T-C. 2002. ARSENITE PRETREATMENT ATTENUATES BENZO[a]PYRENE CYTOTOXICITY IN A HUMAN LUNG ADENOCARCINOMA CELL LINE BY DECREASING CYCLOOXYGENASE-2 LEVELS. *Journal of Toxicology and Environmental Health, Part A* 65:245-63

306. Shoieb SM, El-Ghiaty MA, Alqahtani MA, El-Kadi AOS. 2020. Cytochrome P450-derived eicosanoids and inflammation in liver diseases. *Prostaglandins & other lipid mediators* 147:106400

307. Evangelista EA, Cho CW, Aliwarga T, Totah RA. 2020. Expression and Function of Eicosanoid-Producing Cytochrome P450 Enzymes in Solid Tumors. *Frontiers in pharmacology* 11:828

308. Powell WS, Rokach J. 2015. Biosynthesis, biological effects, and receptors of hydroxyeicosatetraenoic acids (HETEs) and oxoeicosatetraenoic acids (oxo-ETEs) derived from arachidonic acid. *Biochimica et biophysica acta* 1851:340-55

309. Wang B, Wu L, Chen J, Dong L, Chen C, et al. 2021. Metabolism pathways of arachidonic acids: mechanisms and potential therapeutic targets. *Signal transduction and targeted therapy* 6:94

310. El-Sherbeni AA, El-Kadi AO. 2017. Microsomal cytochrome P450 as a target for drug discovery and repurposing. *Drug Metab Rev* 49:1-17

311. Isse FA, Alammari AH, El-Sherbeni AA, Brocks DR, El-Kadi AOS. 2023. The enantioselective separation and quantitation of the hydroxy-metabolites of arachidonic acid by liquid chromatography - tandem mass spectrometry. *Prostaglandins & other lipid mediators* 165:106701

312. Sonnweber T, Pizzini A, Nairz M, Weiss G, Tancevski I. 2018. Arachidonic Acid Metabolites in Cardiovascular and Metabolic Diseases. *International journal of molecular sciences* 19

313. Dong L, Wang H, Chen K, Li Y. 2022. Roles of hydroxyeicosatetraenoic acids in diabetes (HETEs and diabetes). *Biomedicine & pharmacotherapy = Biomedecine & pharmacotherapie* 156:113981

314. Harizi H, Corcuff JB, Gualde N. 2008. Arachidonic-acid-derived eicosanoids: roles in biology and immunopathology. *Trends in molecular medicine* 14:461-9

315. Sokolowska M, Rovati GE, Diamant Z, Untersmayr E, Schwarze J, et al. 2021. Current perspective on eicosanoids in asthma and allergic diseases: EAACI Task Force consensus report, part I. *Allergy* 76:114-30

316. Ni KD, Liu JY. 2021. The Functions of Cytochrome P450 ω-hydroxylases and the Associated Eicosanoids in Inflammation-Related Diseases. *Frontiers in pharmacology* 12:716801

317. Titz B, Luettich K, Leroy P, Boue S, Vuillaume G, et al. 2016. Alterations in Serum Polyunsaturated Fatty Acids and Eicosanoids in Patients with Mild to Moderate Chronic Obstructive Pulmonary Disease (COPD). *International journal of molecular sciences* 17

318. Charbeneau RP, Peters-Golden M. 2005. Eicosanoids: mediators and therapeutic targets in fibrotic lung disease. *Clinical science (London, England : 1979)* 108:479-91

319. Alvarez ML, Lorenzetti F. 2021. Role of eicosanoids in liver repair, regeneration and cancer. *Biochem Pharmacol* 192:114732

320. Fan F, Muroya Y, Roman RJ. 2015. Cytochrome P450 eicosanoids in hypertension and renal disease. *Current opinion in nephrology and hypertension* 24:37-46

321. Fava C, Bonafini S. 2018. Eicosanoids via CYP450 and cardiovascular disease: Hints from genetic and nutrition studies. *Prostaglandins & other lipid mediators* 139:41-7

322. Alsaad AM, Zordoky BN, Tse MM, El-Kadi AO. 2013. Role of cytochrome P450-mediated arachidonic acid metabolites in the pathogenesis of cardiac hypertrophy. *Drug Metab Rev* 45:173-95

323. Panigrahy D, Kaipainen A, Greene ER, Huang S. 2010. Cytochrome P450-derived eicosanoids: the neglected pathway in cancer. *Cancer metastasis reviews* 29:723-35

324. Omiecinski CJ, Vanden Heuvel JP, Perdew GH, Peters JM. 2011. Xenobiotic metabolism, disposition, and regulation by receptors: from biochemical phenomenon to predictors of major toxicities. *Toxicological sciences : an official journal of the Society of Toxicology* 120 Suppl 1:S49-75

325. Beischlag TV, Luis Morales J, Hollingshead BD, Perdew GH. 2008. The aryl hydrocarbon receptor complex and the control of gene expression. *Crit Rev Eukaryot Gene Expr* 18:207-50

326. Larigot L, Juricek L, Dairou J, Coumoul X. 2018. AhR signaling pathways and regulatory functions. *Biochimie Open* 7:1-9

327. Soshilov A, Denison MS. 2008. Role of the Per/Arnt/Sim domains in ligand-dependent transformation of the aryl hydrocarbon receptor. *J Biol Chem* 283:32995-3005

328. Ciolino HP, Daschner PJ, Yeh GC. 1999. Dietary flavonols quercetin and kaempferol are ligands of the aryl hydrocarbon receptor that affect CYP1A1 transcription differentially. *Biochem J* 340 715-22

329. Casper RF, Quesne M, Rogers IM, Shirota T, Jolivet A, et al. 1999. Resveratrol Has Antagonist Activity on the Aryl Hydrocarbon Receptor: Implications for Prevention of Dioxin Toxicity. *Molecular Pharmacology* 56:784

330. Hammerschmidt-Kamper C, Biljes D, Merches K, Steiner I, Daldrup T, et al. 2017. Indole-3-carbinol, a plant nutrient and AhR-Ligand precursor, supports oral tolerance against OVA and improves peanut allergy symptoms in mice. *PLoS One* 12:e0180321-e

331. Heath-Pagliuso S, Rogers WJ, Tullis K, Seidel SD, Cenijn PH, et al. 1998. Activation of the Ah Receptor by Tryptophan and Tryptophan Metabolites. *Biochemistry* 37:11508-15

332. Hubbard TD, Murray IA, Perdew GH. 2015. Indole and Tryptophan Metabolism: Endogenous and Dietary Routes to Ah Receptor Activation. *Drug Metabolism and Disposition* 43:1522

333. DiNatale BC, Murray IA, Schroeder JC, Flaveny CA, Lahoti TS, et al. 2010. Kynurenic Acid Is a Potent Endogenous Aryl Hydrocarbon Receptor Ligand that Synergistically Induces Interleukin-6 in the Presence of Inflammatory Signaling. *Toxicological Sciences* 115:89-97

334. Adachi J, Mori Y, Matsui S, Takigami H, Fujino J, et al. 2001. Indirubin and Indigo Are Potent Aryl Hydrocarbon Receptor Ligands Present in Human Urine. *J Biol Chem* 276:31475-8

335. Sinal CJ, Bend JR. 1997. Aryl hydrocarbon receptor-dependent induction of cyp1a1 by bilirubin in mouse hepatoma hepa 1c1c7 cells. *Mol Pharmacol* 52:590-9

336. Phelan D, Winter GM, Rogers WJ, Lam JC, Denison MS. 1998. Activation of the Ah Receptor Signal Transduction Pathway by Bilirubin and Biliverdin. *Archives of Biochemistry and Biophysics* 357:155-63

337. Schaldach CM, Riby J, Bjeldanes LF. 1999. Lipoxin A4: A New Class of Ligand for the Ah Receptor. *Biochemistry* 38:7594-600

338. Seidel SD, Winters GM, Rogers WJ, Ziccardi MH, Li V, et al. 2001. Activation of the Ah Receptor Signaling Pathway by Prostaglandins. *J Biochem Mol Toxicol* 15:187-96

339. Ueda R, Iketaki H, Nagata K, Kimura S, Gonzalez FJ, et al. 2006. A common regulatory region functions bidirectionally in transcriptional activation of the human CYP1A1 and CYP1A2 genes. *Molecular Pharmacology* 69:1924

340. Jorge-Nebert LF, Jiang Z, Chakraborty R, Watson J, Jin L, et al. 2010. Analysis of human CYP1A1 and CYP1A2 genes and their shared bidirectional promoter in eight world populations. *Hum Mutat* 31:27-40

341. Kerzee J, Ramos K. 2001. Constitutive and Inducible Expression of Cyp1a1 and Cyp1b1 in Vascular Smooth Muscle Cells: Role of the Ahr bHLH/PAS Transcription Factor. *Circulation research* 89:573-82

342. Saarikoski ST, Rivera SP, Hankinson O, Husgafvel-Pursiainen K. 2005. CYP2S1: A short review. *Toxicology and Applied Pharmacology* 207:62-9

343. Deb S, Bandiera SM. 2009. Characterization and expression of extrahepatic CYP2S1. *Expert Opinion on Drug Metabolism & Toxicology* 5:367-80

344. Shimada T, Guengerich FP. 2006. Inhibition of Human Cytochrome P450 1A1-, 1A2-, and 1B1-Mediated Activation of Procarcinogens to Genotoxic Metabolites by Polycyclic Aromatic Hydrocarbons. *Chemical Research in Toxicology* 19:288-94

345. Shimada T, Fujii-Kuriyama Y. 2004. Metabolic activation of polycyclic aromatic hydrocarbons to carcinogens by cytochromes P450 1A1 and1B1. *Cancer Sci* 95:1-6

346. Wrighton SA, Ring BJ, VandenBranden M. 1995. The use of in vitro metabolism techniques in the planning and interpretation of drug safety studies. *Toxicologic pathology* 23:199-208

347. Astashkina A, Mann B, Grainger DW. 2012. A critical evaluation of in vitro cell culture models for high-throughput drug screening and toxicity. *Pharmacology & therapeutics* 134:82-106

348. Martignoni M, Groothuis GMM, de Kanter R. 2006. Species differences between mouse, rat, dog, monkey and human CYP-mediated drug metabolism, inhibition and induction. *Expert Opinion on Drug Metabolism & Toxicology* 2:875-94

349. Costa A, Sarmento B, Seabra V. 2014. An evaluation of the latest in vitro tools for drug metabolism studies. *Expert opinion on drug metabolism & toxicology* 10:103-19

350. Zhang D, Luo G, Ding X, Lu C. 2012. Preclinical experimental models of drug metabolism and disposition in drug discovery and development. *Acta Pharmaceutica Sinica B* 2:549-61

351. Elshenawy OH, Abdelhamid G, Soshilov AA, Denison MS, El-Kadi AO. 2017. Down-regulation of cytochrome P450 1A1 by monomethylarsonous acid in human HepG2 cells. *Toxicology letters* 270:34-50

352. Vernhet L, Allain N, Le Vée M, Morel F, Guillouzo A, Fardel O. 2003. Blockage of multidrug resistance-associated proteins potentiates the inhibitory effects of arsenic trioxide on CYP1A1 induction by polycyclic aromatic hydrocarbons. *The Journal of pharmacology and experimental therapeutics* 304:145-55

353. Anwar-Mohamed A, Elshenawy OH, Soshilov AA, Denison MS, Chris Le X, et al. 2014. Methylated pentavalent arsenic metabolites are bifunctional inducers, as they induce cytochrome P450 1A1 and NAD(P)H:quinone oxidoreductase through AhR- and Nrf2-dependent mechanisms. *Free Radic Biol Med* 67:171-87

354. Anwar-Mohamed A, El-Kadi AO. 2010. Arsenite down-regulates cytochrome P450 1A1 at the transcriptional and posttranslational levels in human HepG2 cells. *Free Radic Biol Med* 48:1399-409

355. Spink DC, Katz BH, Hussain MM, Spink BC, Wu SJ, et al. 2002. Induction of CYP1A1 and CYP1B1 in T-47D human breast cancer cells by benzo[a]pyrene is diminished by arsenite. *Drug Metabolism and Disposition* 30:262

356. Wu SJ, Spink DC, Spink BC, Kaminsky LS. 2003. Quantitation of CYP1A1 and 1B1 mRNA in polycyclic aromatic hydrocarbon-treated human T-47D and HepG2 cells by a modified bDNA assay using fluorescence detection. *Analytical Biochemistry* 312:162-6

357. Vakharia DD, Liu N, Pause R, Fasco M, Bessette E, et al. 2001. Effect of Metals on Polycyclic Aromatic Hydrocarbon Induction of CYP1A1 and CYP1A2 in Human Hepatocyte Cultures. *Toxicology and Applied Pharmacology* 170:93-103

358. Mondal B, Chen H, Wen W, Cavalieri EL, Rogan EG, Zahid M. 2018. Modulation of Cellular Response to Arsenic Trioxide Toxicity by Resveratrol. *ACS omega* 3:5511-5

359. Bessette EE, Fasco MJ, Pentecost BT, Kaminsky LS. 2005. Mechanisms of arsenite-mediated decreases in benzo[k]fluoranthene-induced human cytochrome P4501A1 levels in HepG2 cells. *Drug Metabolism and Disposition* 33:312-20

360. Tully DB, Collins BJ, Overstreet JD, Smith CS, Dinse GE, et al. 2000. Effects of Arsenic, Cadmium, Chromium, and Lead on Gene Expression Regulated by a Battery of 13 Different Promoters in Recombinant HepG2 Cells. *Toxicology and Applied Pharmacology* 168:79-90

361. Todd MD, Lee MJ, Williams JL, Nalezny JM, Gee P, et al. 1995. The CAT-Tox (L) assay: a sensitive and specific measure of stress-induced transcription in transformed human liver cells. *Fundamental and applied toxicology : official journal of the Society of Toxicology* 28:118-28

362. Bonzo JA, Chen S, Galijatovic A, Tukey RH. 2005. Arsenite inhibition of CYP1A1 induction by 2,3,7,8-tetrachlorodibenzo-p-dioxin is independent of cell cycle arrest. *Mol Pharmacol* 67:1247-56

363. Vakharia DD, Liu N, Pause R, Fasco M, Bessette E, et al. 2001. Polycyclic aromatic hydrocarbon/metal mixtures: effect on PAH induction of CYP1A1 in human HEPG2 cells. *Drug Metab Dispos* 29:999-1006

364. Bessette EE, Fasco MJ, Pentecost BT, Reilly A, Kaminsky LS. 2009. Investigations of the posttranslational mechanism of arsenite-mediated downregulation of human cytochrome P4501A1 levels: the role of heme oxygenase-1. *J Biochem Mol Toxicol* 23:222-32

365. Chao HR, Tsou TC, Li LA, Tsai FY, Wang YF, et al. 2006. Arsenic inhibits induction of cytochrome P450 1A1 by 2,3,7,8-tetrachlorodibenzo-p-dioxin in human hepatoma cells. *J Hazard Mater* 137:716-22

366. Noreault TL, Kostrubsky VE, Wood SG, Nichols RC, Strom SC, et al. 2005. Arsenite decreases CYP3A4 and RXRalpha in primary human hepatocytes. *Drug Metab Dispos* 33:993-1003

367. Noreault-Conti TL, Fellows A, Jacobs JM, Trask HW, Strom SC, et al. 2012. Arsenic decreases RXRα-dependent transcription of CYP3A and suppresses immune regulators in hepatocytes. *International immunopharmacology* 12:651-6

368. Sardana MK, Drummond GS, Sassa S, Kappas A. 1981. The potent heme oxygenase inducing action of arsenic and parasiticidal arsenicals. *Pharmacology* 23:247-53

369. Cebrián ME, Albores A, Connelly JC, Bridges JW. 1988. Assessment of arsenic effects on cytosolic heme status using tryptophan pyrrolase as an index. *J Biochem Toxicol* 3:77-86

370. Albores A, Cebrián ME, Bach PH, Connelly JC, Hinton RH, Bridges JW. 1989. Sodium arsenite induced alterations in bilirubin excretion and heme metabolism. *J Biochem Toxicol* 4:73-8

371. Albores A, Cebrian ME, Connelly JC, Bach PH, Bridges JW. 1992. Effects of arsenite on hepatic mixed-function oxidase activity in rats. *Xenobiotica* 22:591-7

372. Siller FR, Quintanilla-Vega B, Cebrián ME, Albores A. 1997. Effects of arsenite pretreatment on the acute toxicity of parathion. *Toxicology* 116:59-65

373. Ramanathan K, Shila S, Kumaran S, Panneerselvam C. 2003. Protective role of ascorbic acid and alpha-tocopherol on arsenic-induced microsomal dysfunctions. *Hum Exp Toxicol* 22:129-36

374. Naraharisetti SB, Aggarwal M, Sarkar SN, Malik JK. 2008. Concurrent subacute exposure to arsenic through drinking water and malathion via diet in male rats: effects on hepatic drug-metabolizing enzymes. *Archives of toxicology* 82:543-51

375. Rajpoot DS, Prakash A, Mandil R, Rahal A, Garg SK. 2013. Differential modulation of xenobiotic-metabolizing enzymes in rats following single and concurrent exposure to chlorpyrifos, arsenic, and ascorbic acid. *J Toxicol Environ Health A* 76:1354-65

376. Kann S, Huang MY, Estes C, Reichard JF, Sartor MA, et al. 2005. Arsenite-induced aryl hydrocarbon receptor nuclear translocation results in additive induction of phase I genes and synergistic induction of phase II genes. *Mol Pharmacol* 68:336-46

377. Elbekai RH, El-Kadi AO. 2007. Transcriptional activation and posttranscriptional modification of Cyp1a1 by arsenite, cadmium, and chromium. *Toxicology letters* 172:106-19

378. Zhao H, Wang Y, Guo M, Fei D, Mu M, et al. 2019. Hepatoprotective effects of zinc (II) via cytochrome P-450/reactive oxygen species and canonical apoptosis pathways after arsenite waterborne exposure in common carp. *Chemosphere* 236:124869

379. Elbekai RH, El-Kadi AO. 2004. Modulation of aryl hydrocarbon receptor-regulated gene expression by arsenite, cadmium, and chromium. *Toxicology* 202:249-69

380. Anwar-Mohamed A, Abdelhamid G, Amara IE, El-Kadi AO. 2013. Differential modulation of cytochrome P450 1a1 by arsenite in vivo and in vitro in C57BL/6 mice. *Free Radic Biol Med* 58:52-63

381. Maier A, Dalton TP, Puga A. 2000. Disruption of dioxin-inducible phase I and phase II gene expression patterns by cadmium, chromium, and arsenic. *Mol Carcinog* 28:225-35

382. Jacobs JM, Nichols CE, Andrew AS, Marek DE, Wood SG, et al. 1999. Effect of arsenite on induction of CYP1A, CYP2B, and CYP3A in primary cultures of rat hepatocytes. *Toxicology and applied pharmacology* 157:51-9

383. Anwar-Mohamed A, Klotz LO, El-Kadi AO. 2012. Inhibition of heme oxygenase-1 partially reverses the arsenite-mediated decrease of CYP1A1, CYP1A2, CYP3A23, and CYP3A2 catalytic activity in isolated rat hepatocytes. *Drug Metab Dispos* 40:504-14

384. Xie Y, Liu J, Benbrahim-Tallaa L, Ward JM, Logsdon D, et al. 2007. Aberrant DNA methylation and gene expression in livers of newborn mice transplacentally exposed to a hepatocarcinogenic dose of inorganic arsenic. *Toxicology* 236:7-15

385. Anwar-Mohamed A, Elshenawy OH, El-Sherbeni AA, Abdelrady M, El-Kadi AO. 2014. Acute arsenic treatment alters arachidonic acid and its associated metabolite levels in the brain of C57Bl/6 mice. *Can J Physiol Pharmacol* 92:693-702

386. Bashir S, Sharma Y, Irshad M, Gupta SD, Dogra TD. 2006. Arsenic-induced cell death in liver and brain of experimental rats. *Basic & clinical pharmacology & toxicology* 98:38-43

387. Liu J, Kadiiska MB, Liu Y, Lu T, Qu W, Waalkes MP. 2001. Stress-related gene expression in mice treated with inorganic arsenicals. *Toxicological sciences : an official journal of the Society of Toxicology* 61:314-20

388. Maier A, Schumann BL, Chang X, Talaska G, Puga A. 2002. Arsenic co-exposure potentiates benzo[a]pyrene genotoxicity. *Mutation research* 517:101-11

389. Thompson ED, Burwinkel KE, Chava AK, Notch EG, Mayer GD. 2010. Activity of Phase I and Phase II enzymes of the benzo[a]pyrene transformation pathway in zebrafish (Danio rerio) following waterborne exposure to arsenite. *Comp Biochem Physiol C Toxicol Pharmacol* 152:371-8

390. Jacobs JM, Nichols C, Marek D, Gorman N, Walton HS, et al. 2000. Effect of arsenite on the induction of CYP1A4 and CYP1A5 in cultured chick embryo hepatocytes. *Toxicology and applied pharmacology* 168:177-82

391. Jacobs J, Roussel R, Roberts M, Marek D, Wood S, et al. 1998. Effect of arsenite on induction of CYP1A and CYP2H in primary cultures of chick hepatocytes. *Toxicology and applied pharmacology* 150:376-82

392. Jacobs JM, Marek D, Walton HS, Sinclair PR, Sinclair JF. 1999. Effect of sodium arsenite on heme metabolism in cultured chick embryo hepatocytes. *Arch Biochem Biophys* 371:8-14

393. Medina-Díaz IM, Estrada-Muñiz E, Reyes-Hernández OD, Ramírez P, Vega L, Elizondo G. 2009. Arsenite and its metabolites, MMA(III) and DMA(III), modify CYP3A4, PXR and RXR alpha expression in the small intestine of CYP3A4 transgenic mice. *Toxicology and applied pharmacology* 239:162-8

394. Noreault TL, Jacobs JM, Nichols RC, Trask HW, Wrighton SA, et al. 2005. Arsenite decreases CYP3A23 induction in cultured rat hepatocytes by transcriptional and translational mechanisms. *Toxicology and applied pharmacology* 209:174-82

395. Noreault TL, Jacobs JM, Nichols RC, Trask HW, Wrighton SA, et al. 2005. Mechanism of arsenite-mediated decreases in CYP3A23 in rat hepatocytes. *Biochem Biophys Res Commun* 333:1211-7

396. Noreault-Conti TL, Jacobs JM, Trask HW, Wrighton SA, Sinclair JF, Nichols RC. 2006. Effect of proteasome inhibition on toxicity and CYP3A23 induction in cultured rat hepatocytes: comparison with arsenite. *Toxicology and applied pharmacology* 217:245-51

397. Anwar-Mohamed A, El-Sherbeni A, Kim SH, Elshenawy OH, Althurwi HN, et al. 2013. Acute arsenic treatment alters cytochrome P450 expression and arachidonic acid metabolism in lung, liver and kidney of C57Bl/6 mice. *Xenobiotica* 43:719-29

398. Anwar-Mohamed A, El-Sherbeni AA, Kim SH, Althurwi HN, Zordoky BN, El-Kadi AO. 2012. Acute arsenic toxicity alters cytochrome P450 and soluble epoxide hydrolase and their associated arachidonic acid metabolism in C57Bl/6 mouse heart. *Xenobiotica* 42:1235-47

399. Dalton TP, Shertzer HG, Puga A. 1999. Regulation of gene expression by reactive oxygen. *Annu Rev Pharmacol Toxicol* 39:67-101

400. Liu J, Xie Y, Ducharme DM, Shen J, Diwan BA, et al. 2006. Global gene expression associated with hepatocarcinogenesis in adult male mice induced by in utero arsenic exposure. *Environ Health Perspect* 114:404-11

401. Yang HT, Chou HJ, Han BC, Huang SY. 2007. Lifelong inorganic arsenic compounds consumption affected blood pressure in rats. *Food and chemical toxicology : an international journal published for the British Industrial Biological Research Association* 45:2479-87

402. Zangar RC, Bollinger N, Verma S, Karin NJ, Lu Y. 2008. The nuclear factor-kappa B pathway regulates cytochrome P450 3A4 protein stability. *Mol Pharmacol* 73:1652-8

403. Nishikawa T, Wanibuchi H, Ogawa M, Kinoshita A, Morimura K, et al. 2002. Promoting effects of monomethylarsonic acid, dimethylarsinic acid and trimethylarsine oxide on induction of rat liver preneoplastic glutathione S-transferase placental form positive foci: a possible reactive oxygen species mechanism. *Int J Cancer* 100:136-9

404. Elshenawy OH, El-Kadi AO. 2015. Modulation of aryl hydrocarbon receptor-regulated enzymes by trimethylarsine oxide in C57BL/6 mice: In vivo and in vitro studies. *Toxicology letters* 238:17-31

405. Vineetha RC, Archana V, Binu P, Arathi P, Nair RH. 2018. L-Ascorbic Acid and α-Tocopherol Reduces Hepatotoxicity Associated with Arsenic Trioxide Chemotherapy by Modulating Nrf2 and Bcl2 Transcription Factors in Chang liver Cells. *Nutrition and cancer* 70:684-96

406. Yang D, Lv Z, Zhang H, Liu B, Jiang H, et al. 2017. Activation of the Nrf2 Signaling Pathway Involving KLF9 Plays a Critical Role in Allicin Resisting Against Arsenic Trioxide-Induced Hepatotoxicity in Rats. *Biological trace element research* 176:192-200

407. Sasaki A, Oshima Y, Fujimura A. 2007. An approach to elucidate potential mechanism of renal toxicity of arsenic trioxide. *Experimental hematology* 35:252-62

408. Vineetha VP, Raghu KG. 2019. An Overview on Arsenic Trioxide-Induced Cardiotoxicity. *Cardiovascular toxicology* 19:105-19
409. Guengerich FP. 2017. Intersection of the Roles of Cytochrome P450 Enzymes with Xenobiotic and Endogenous Substrates: Relevance to Toxicity and Drug Interactions. *Chem Res Toxicol* 30:2-12
410. Lu J, Shang X, Zhong W, Xu Y, Shi R, Wang X. 2020. New insights of CYP1A in endogenous metabolism: a focus on single nucleotide polymorphisms and diseases. *Acta pharmaceutica Sinica. B* 10:91-104
411. Pelkonen O, Turpeinen M, Hakkola J, Honkakoski P, Hukkanen J, Raunio H. 2008. Inhibition and induction of human cytochrome P450 enzymes: current status. *Archives of toxicology* 82:667-715
412. Zhou SF, Wang B, Yang LP, Liu JP. 2010. Structure, function, regulation and polymorphism and the clinical significance of human cytochrome P450 1A2. *Drug Metab Rev* 42:268-354
413. Lin D, Kostov R, Huang JT, Henderson CJ, Wolf CR. 2017. Novel Pathways of Ponatinib Disposition Catalyzed By CYP1A1 Involving Generation of Potentially Toxic Metabolites. *The Journal of pharmacology and experimental therapeutics* 363:12-9
414. Nakamura H, Ariyoshi N, Okada K, Nakasa H, Nakazawa K, Kitada M. 2005. CYP1A1 is a major enzyme responsible for the metabolism of granisetron in human liver microsomes. *Curr Drug Metab* 6:469-80
415. Klomp F, Wenzel C, Drozdzik M, Oswald S. 2020. Drug-Drug Interactions Involving Intestinal and Hepatic CYP1A Enzymes. *Pharmaceutics* 12
416. Baird WM, Hooven LA, Mahadevan B. 2005. Carcinogenic polycyclic aromatic hydrocarbon-DNA adducts and mechanism of action. *Environmental and molecular mutagenesis* 45:106-14
417. Rifkind AB. 2006. CYP1A in TCDD toxicity and in physiology-with particular reference to CYP dependent arachidonic acid metabolism and other endogenous substrates. *Drug Metab Rev* 38:291-335
418. Takiguchi M, Darwish WS, Ikenaka Y, Ohno M, Ishizuka M. 2010. Metabolic activation of heterocyclic amines and expression of CYP1A1 in the tongue. *Toxicological sciences : an official journal of the Society of Toxicology* 116:79-91

419. Guengerich FP, Shimada T. 1991. Oxidation of toxic and carcinogenic chemicals by human cytochrome P-450 enzymes. *Chem Res Toxicol* 4:391-407

420. Walsh AA, Szklarz GD, Scott EE. 2013. Human cytochrome P450 1A1 structure and utility in understanding drug and xenobiotic metabolism. *J Biol Chem* 288:12932-43

421. O'Malley M, King AN, Conte M, Ellingrod VL, Ramnath N. 2014. Effects of cigarette smoking on metabolism and effectiveness of systemic therapy for lung cancer. *Journal of thoracic oncology : official publication of the International Association for the Study of Lung Cancer* 9:917-26

422. Faber MS, Jetter A, Fuhr U. 2005. Assessment of CYP1A2 activity in clinical practice: why, how, and when? *Basic & clinical pharmacology & toxicology* 97:125-34

423. Barrangou-Poueys-Darlas M, Guerlais M, Laforgue EJ, Bellouard R, Istvan M, et al. 2021. CYP1A2 and tobacco interaction: a major pharmacokinetic challenge during smoking cessation. *Drug Metab Rev* 53:30-44

424. Ercal N, Gurer-Orhan H, Aykin-Burns N. 2001. Toxic metals and oxidative stress part I: mechanisms involved in metal-induced oxidative damage. *Current topics in medicinal chemistry* 1:529-39

425. Dehn PF, White CM, Conners DE, Shipkey G, Cumbo TA. 2004. Characterization of the human hepatocellular carcinoma (hepg2) cell line as an in vitro model for cadmium toxicity studies. *In vitro cellular & developmental biology. Animal* 40:172-82

426. Soldatow VY, Lecluyse EL, Griffith LG, Rusyn I. 2013. In vitro models for liver toxicity testing. *Toxicol Res (Camb)* 2:23-39

427. Grant MH, Duthie SJ, Gray AG, Burke MD. 1988. Mixed function oxidase and UDP-glucuronyltransferase activities in the human Hep G2 hepatoma cell line. *Biochem Pharmacol* 37:4111-6

428. Silkworth JB, Koganti A, Illouz K, Possolo A, Zhao M, Hamilton SB. 2005. Comparison of TCDD and PCB CYP1A induction sensitivities in fresh hepatocytes from human donors, sprague-dawley rats, and rhesus monkeys and HepG2 cells. *Toxicological sciences : an official journal of the Society of Toxicology* 87:508-19

429. Westerink WM, Schoonen WG. 2007. Cytochrome P450 enzyme levels in HepG2 cells and cryopreserved primary human hepatocytes and their induction in HepG2 cells. *Toxicology in vitro : an international journal published in association with BIBRA* 21:1581-91

430. Lipp HP, Schrenk D, Wiesmüller T, Hagenmaier H, Bock KW. 1992. Assessment of biological activities of mixtures of polychlorinated dibenzo-p-dioxins (PCDDs) and their constituents in human HepG2 cells. *Archives of toxicology* 66:220-3

431. Kikuchi H, Kato H, Mizuno M, Hossain A, Ikawa S, et al. 1996. Differences in inducibility of CYP1A1-mRNA by benzimidazole compounds between human and mouse cells: evidences of a human-specific signal transduction pathway for CYP1A1 induction. *Arch Biochem Biophys* 334:235-40

432. Krusekopf S, Kleeberg U, Hildebrandt AG, Ruckpaul K. 1997. Effects of benzimidazole derivatives on cytochrome P450 1A1 expression in a human hepatoma cell line. *Xenobiotica* 27:1-9

433. Kim WK, In YJ, Kim JH, Cho HJ, Kim JH, et al. 2006. Quantitative relationship of dioxin-responsive gene expression to dioxin response element in Hep3B and HepG2 human hepatocarcinoma cell lines. *Toxicology letters* 165:174-81

434. Bernhard HP, Darlington GJ, Ruddle FH. 1973. Expression of liver phenotypes in cultured mouse hepatoma cells: synthesis and secretion of serum albumin. *Developmental biology* 35:83-96

435. Benedict WF, Gielen JE, Owens IS, Niwa A, Bebert DW. 1973. Aryl hydrocarbon hydroxylase induction in mammalian liver cell culture. IV. Stimulation of the enzyme activity in established cell lines derived from rat or mouse hepatoma and from normal rat liver. *Biochem Pharmacol* 22:2766-9

436. Livak KJ, Schmittgen TD. 2001. Analysis of relative gene expression data using real-time quantitative PCR and the 2(-Delta Delta C(T)) Method. *Methods (San Diego, Calif.)* 25:402-8

437. Lowry OH, Rosebrough NJ, Farr AL, Randall RJ. 1951. Protein measurement with the Folin phenol reagent. *J Biol Chem* 193:265-75

438. Diaz GJ, Squires EJ. 2000. Metabolism of 3-methylindole by porcine liver microsomes: responsible cytochrome P450 enzymes. *Toxicological sciences : an official journal of the Society of Toxicology* 55:284-92

439. Zordoky BN, Anwar-Mohamed A, Aboutabl ME, El-Kadi AO. 2010. Acute doxorubicin cardiotoxicity alters cardiac cytochrome P450 expression and arachidonic acid metabolism in rats. *Toxicology and applied pharmacology* 242:38-46

440. Lorenzen A, Kennedy SW. 1993. A fluorescence-based protein assay for use with a microplate reader. *Anal Biochem* 214:346-8

441. He G, Tsutsumi T, Zhao B, Baston DS, Zhao J, et al. 2011. Third-generation Ah receptor-responsive luciferase reporter plasmids: amplification of dioxin-responsive elements dramatically increases CALUX bioassay sensitivity and responsiveness. *Toxicological sciences : an official journal of the Society of Toxicology* 123:511-22

442. Nair AB, Jacob S. 2016. A simple practice guide for dose conversion between animals and human. *Journal of basic and clinical pharmacy* 7:27-31

443. Lew YS, Brown SL, Griffin RJ, Song CW, Kim JH. 1999. Arsenic trioxide causes selective necrosis in solid murine tumors by vascular shutdown. *Cancer Res* 59:6033-7

444. Lew YS, Kolozsvary A, Brown SL, Kim JH. 2002. Synergistic interaction with arsenic trioxide and fractionated radiation in locally advanced murine tumor. *Cancer Res* 62:4202-5

445. Griffin RJ, Lee SH, Rood KL, Stewart MJ, Lyons JC, et al. 2000. Use of arsenic trioxide as an antivascular and thermosensitizing agent in solid tumors. *Neoplasia (New York, N.Y.)* 2:555-60

446. Griffin RJ, Williams BW, Park HJ, Song CW. 2005. Preferential action of arsenic trioxide in solid-tumor microenvironment enhances radiation therapy. *International journal of radiation oncology, biology, physics* 61:1516-22

447. Griffin RJ, Monzen H, Williams BW, Park H, Lee SH, Song CW. 2003. Arsenic trioxide induces selective tumour vascular damage via oxidative stress and increases thermosensitivity of tumours. *International journal of hyperthermia : the official journal of European Society for Hyperthermic Oncology, North American Hyperthermia Group* 19:575-89

448. Griffin RJ, Williams BW, Koonce NA, Bischof JC, Song CW, et al. 2012. Vascular disrupting agent arsenic trioxide enhances thermoradiotherapy of solid tumors. *Journal of oncology* 2012:934918

449. Albrecht W. 2020. Which concentrations are optimal for in vitro testing? *EXCLI journal* 19:1172-3

450. Shen ZX, Chen GQ, Ni JH, Li XS, Xiong SM, et al. 1997. Use of arsenic trioxide (As2O3) in the treatment of acute promyelocytic leukemia (APL): II. Clinical efficacy and pharmacokinetics in relapsed patients. *Blood* 89:3354-60

451. Shen Y, Shen ZX, Yan H, Chen J, Zeng XY, et al. 2001. Studies on the clinical efficacy and pharmacokinetics of low-dose arsenic trioxide in the treatment of relapsed acute promyelocytic leukemia: a comparison with conventional dosage. *Leukemia* 15:735-41

452. Zhang P. 2017. On arsenic trioxide in the clinical treatment of acute promyelocytic leukemia. *Leukemia research reports* 7:29-32

453. Gao C, Hu S, Guo M, Hai X, Zhou J. 2018. Clinical pharmacokinetics and safety profile of single agent arsenic trioxide by continuous slow-rate infusion in patients with newly diagnosed acute promyelocytic leukemia. *Cancer chemotherapy and pharmacology* 82:229-36

454. NRC(US). 1977. *National Research Council (US) Committee on Medical and Biological Effects of Environmental Pollutants: Arsenic*. Washington (DC): National Academies Press (US)

455. Greenwood NN, Earnshaw A. 1997. *Chemistry of the Elements (Second Edition)*. Oxford: Butterworth-Heinemann

456. EMEA. 2005. *Trisenox : EPAR - Scientific Discussion*. Amsterdam: European Medicines Evaluation Agency

457. Diaz Z, Laurenzana A, Mann KK, Bismar TA, Schipper HM, Miller WH, Jr. 2007. Trolox enhances the anti-lymphoma effects of arsenic trioxide, while protecting against liver toxicity. *Leukemia* 21:2117-27

458. Yue Z, Zhong L, Mou Y, Wang X, Zhang H, et al. 2015. Arsenic Trioxide Activate Transcription of Heme Oxygenase-1 by Promoting Nuclear Translocation of NFE2L2. *International journal of medical sciences* 12:674-9

459. Wu R, Wu X, Wang H, Fang X, Li Y, et al. 2017. Strain differences in arsenic-induced oxidative lesion via arsenic biomethylation between C57BL/6J and 129X1/SvJ mice. *Scientific reports* 7:44424

460. Liang Y, Zheng B, Li J, Shi J, Chu L, et al. 2020. Crocin ameliorates arsenic trioxide-induced cardiotoxicity via Keap1-Nrf2/HO-1 pathway: Reducing oxidative stress,

inflammation, and apoptosis. *Biomedicine & pharmacotherapy = Biomedecine & pharmacotherapie* 131:110713

461. O'Donnell EF, Saili KS, Koch DC, Kopparapu PR, Farrer D, et al. 2010. The anti-inflammatory drug leflunomide is an agonist of the aryl hydrocarbon receptor. *PLoS One* 5

462. Amigo-Jiménez I, Bailón E, Aguilera-Montilla N, García-Marco JA, García-Pardo A. 2016. Gene expression profile induced by arsenic trioxide in chronic lymphocytic leukemia cells reveals a central role for heme oxygenase-1 in apoptosis and regulation of matrix metalloproteinase-9. *Oncotarget* 7:83359-77

463. Wang L, Kou MC, Weng CY, Hu LW, Wang YJ, Wu MJ. 2012. Arsenic modulates heme oxygenase-1, interleukin-6, and vascular endothelial growth factor expression in endothelial cells: roles of ROS, NF-κB, and MAPK pathways. *Archives of toxicology* 86:879-96

464. Miller WH, Jr., Schipper HM, Lee JS, Singer J, Waxman S. 2002. Mechanisms of action of arsenic trioxide. *Cancer Res* 62:3893-903

465. Jansen T, Daiber A. 2012. Direct Antioxidant Properties of Bilirubin and Biliverdin. Is there a Role for Biliverdin Reductase? *Frontiers in pharmacology* 3:30

466. Correia MA, Sinclair PR, De Matteis F. 2011. Cytochrome P450 regulation: the interplay between its heme and apoprotein moieties in synthesis, assembly, repair, and disposal. *Drug Metab Rev* 43:1-26

467. Bissell DM, Hammaker LE. 1976. Cytochrome P-450 heme and the regulation of hepatic heme oxygenase activity. *Arch Biochem Biophys* 176:91-102

468. Elbekai RH, El-Kadi AO. 2005. The role of oxidative stress in the modulation of aryl hydrocarbon receptor-regulated genes by As3+, Cd2+, and Cr6+. *Free Radic Biol Med* 39:1499-511

469. Korashy HM, El-Kadi AO. 2008. The role of redox-sensitive transcription factors NF-kappaB and AP-1 in the modulation of the Cyp1a1 gene by mercury, lead, and copper. *Free Radic Biol Med* 44:795-806

470. Korashy HM, El-Kadi AO. 2005. Regulatory mechanisms modulating the expression of cytochrome P450 1A1 gene by heavy metals. *Toxicological sciences : an official journal of the Society of Toxicology* 88:39-51

471. Alarifi S, Ali D, Alkahtani S, Siddiqui MA, Ali BA. 2013. Arsenic trioxide-mediated oxidative stress and genotoxicity in human hepatocellular carcinoma cells. *OncoTargets and therapy* 6:75-84

472. Naranmandura H, Bu N, Suzuki KT, Lou Y, Ogra Y. 2010. Distribution and speciation of arsenic after intravenous administration of monomethylmonothioarsonic acid in rats. *Chemosphere* 81:206-13

473. Ahsan H, Perrin M, Rahman A, Parvez F, Stute M, et al. 2000. Associations between drinking water and urinary arsenic levels and skin lesions in Bangladesh. *Journal of occupational and environmental medicine* 42:1195-201

474. Chen Y, Wu F, Graziano JH, Parvez F, Liu M, et al. 2013. Arsenic exposure from drinking water, arsenic methylation capacity, and carotid intima-media thickness in Bangladesh. *Am J Epidemiol* 178:372-81

475. El-Ghiaty MA, Alqahtani MA, El-Kadi AOS. 2022. Down-regulation of hepatic cytochromes P450 1A1 and 1A2 by arsenic trioxide (ATO) in vivo and in vitro: A role of heme oxygenase 1. *Chemico-biological interactions* 364:110049

476. Denison MS, Nagy SR. 2003. Activation of the aryl hydrocarbon receptor by structurally diverse exogenous and endogenous chemicals. *Annu Rev Pharmacol Toxicol* 43:309-34

477. Roman RJ. 2002. P-450 metabolites of arachidonic acid in the control of cardiovascular function. *Physiological reviews* 82:131-85

478. Zhao Z, Li J, Zheng B, Liang Y, Shi J, et al. 2020. Ameliorative effects and mechanism of crocetin in arsenic trioxide-induced cardiotoxicity in rats. *Molecular medicine reports* 22:5271-81

479. Zhang M, Xue Y, Zheng B, Li L, Chu X, et al. 2021. Liquiritigenin protects against arsenic trioxide-induced liver injury by inhibiting oxidative stress and enhancing mTOR-mediated autophagy. *Biomedicine & pharmacotherapy = Biomedecine & pharmacotherapie* 143:112167

480. Piscaglia F, Knittel T, Kobold D, Barnikol-Watanabe S, Di Rocco P, Ramadori G. 1999. Cellular localization of hepatic cytochrome 1B1 expression and its regulation by aromatic hydrocarbons and inflammatory cytokines. *Biochem Pharmacol* 58:157-65

481. Umannová L, Zatloukalová J, Machala M, Krcmár P, Májková Z, et al. 2007. Tumor necrosis factor-alpha modulates effects of aryl hydrocarbon receptor ligands on cell

proliferation and expression of cytochrome P450 enzymes in rat liver "stem-like" cells. *Toxicological sciences : an official journal of the Society of Toxicology* 99:79-89

482. Malaplate-Armand C, Ferrari L, Masson C, Siest G, Batt AM. 2003. Astroglial CYP1B1 up-regulation in inflammatory/oxidative toxic conditions: IL-1beta effect and protection by N-acetylcysteine. *Toxicology letters* 138:243-51

483. Maglich JM, Stoltz CM, Goodwin B, Hawkins-Brown D, Moore JT, Kliewer SA. 2002. Nuclear pregnane x receptor and constitutive androstane receptor regulate overlapping but distinct sets of genes involved in xenobiotic detoxification. *Mol Pharmacol* 62:638-46

484. Köhle C, Bock KW. 2009. Coordinate regulation of human drug-metabolizing enzymes, and conjugate transporters by the Ah receptor, pregnane X receptor and constitutive androstane receptor. *Biochem Pharmacol* 77:689-99

485. Wang Y, Masuyama H, Nobumoto E, Zhang G, Hiramatsu Y. 2014. The inhibition of constitutive androstane receptor-mediated pathway enhances the effects of anticancer agents in ovarian cancer cells. *Biochem Pharmacol* 90:356-66

486. Cornejo M, Mieres-Castro D, Blanco EH, Beltrán AR, Araya JE, et al. 2021. Arsenic trioxide-increased MDCK cells proliferation requires activator protein 1-mediated increase of the sodium/proton exchanger 1 activity. *Biochimica et biophysica acta. Molecular basis of disease* 1867:165977

487. Anwar-mohamed A, Zordoky BN, Aboutabl ME, El-Kadi AO. 2010. Alteration of cardiac cytochrome P450-mediated arachidonic acid metabolism in response to lipopolysaccharide-induced acute systemic inflammation. *Pharmacological research* 61:410-8

488. Mitchell SR, Sewer MB, Kardar SS, Morgan ET. 2001. Characterization of CYP4A induction in rat liver by inflammatory stimuli: dependence on sex, strain, and inflammation-evoked hypophagia. *Drug Metab Dispos* 29:17-22

489. Theken KN, Deng Y, Kannon MA, Miller TM, Poloyac SM, Lee CR. 2011. Activation of the acute inflammatory response alters cytochrome P450 expression and eicosanoid metabolism. *Drug Metab Dispos* 39:22-9

490. Habib A, Hamade E, Mahfouz R, Nasrallah MS, de Thé H, Bazarbachi A. 2008. Arsenic trioxide inhibits ATRA-induced prostaglandin E2 and cyclooxygenase-1 in NB4 cells, a model of acute promyelocytic leukemia. *Leukemia* 22:1125-30

491. Borin TF, Angara K, Rashid MH, Achyut BR, Arbab AS. 2017. Arachidonic Acid Metabolite as a Novel Therapeutic Target in Breast Cancer Metastasis. *International journal of molecular sciences* 18

492. Huang H, Al-Shabrawey M, Wang MH. 2016. Cyclooxygenase- and cytochrome P450-derived eicosanoids in stroke. *Prostaglandins & other lipid mediators* 122:45-53

493. Muller DN, Schmidt C, Barbosa-Sicard E, Wellner M, Gross V, et al. 2007. Mouse Cyp4a isoforms: enzymatic properties, gender- and strain-specific expression, and role in renal 20-hydroxyeicosatetraenoic acid formation. *Biochem J* 403:109-18

494. Ziegler N, Awwad K, Fisslthaler B, Reis M, Devraj K, et al. 2016. β-Catenin Is Required for Endothelial Cyp1b1 Regulation Influencing Metabolic Barrier Function. *The Journal of neuroscience : the official journal of the Society for Neuroscience* 36:8921-35

495. Chen L, Joseph G, Zhang FF, Nguyen H, Jiang H, et al. 2016. 20-HETE contributes to ischemia-induced angiogenesis. *Vascular pharmacology* 83:57-65

496. Garcia V, Joseph G, Shkolnik B, Ding Y, Zhang FF, et al. 2015. Angiotensin II receptor blockade or deletion of vascular endothelial ACE does not prevent vascular dysfunction and remodeling in 20-HETE-dependent hypertension. *American journal of physiology. Regulatory, integrative and comparative physiology* 309:R71-8

497. Seki T, Wang MH, Miyata N, Laniado-Schwartzman M. 2005. Cytochrome P450 4A isoform inhibitory profile of N-hydroxy-N'-(4-butyl-2-methylphenyl)-formamidine (HET0016), a selective inhibitor of 20-HETE synthesis. *Biological & pharmaceutical bulletin* 28:1651-4

498. Garcia V, Shkolnik B, Milhau L, Falck JR, Schwartzman ML. 2016. 20-HETE Activates the Transcription of Angiotensin-Converting Enzyme via Nuclear Factor-κB Translocation and Promoter Binding. *The Journal of pharmacology and experimental therapeutics* 356:525-33

499. Moore GY, Pidgeon GP. 2017. Cross-Talk between Cancer Cells and the Tumour Microenvironment: The Role of the 5-Lipoxygenase Pathway. *International journal of molecular sciences* 18

500. Ding XZ, Hennig R, Adrian TE. 2003. Lipoxygenase and cyclooxygenase metabolism: new insights in treatment and chemoprevention of pancreatic cancer. *Molecular cancer* 2:10

501. Greene ER, Huang S, Serhan CN, Panigrahy D. 2011. Regulation of inflammation in cancer by eicosanoids. *Prostaglandins & other lipid mediators* 96:27-36
502. Tang K, Honn KV. 1999. 12(S)-HETE in cancer metastasis. *Advances in experimental medicine and biology* 447:181-91
503. Liu Z, Carbrey JM, Agre P, Rosen BP. 2004. Arsenic trioxide uptake by human and rat aquaglyceroporins. *Biochem Biophys Res Commun* 316:1178-85
504. Yao D, Liu S, Lian F, Xu X, Yang J, et al. 2022. AQP9 (Aquaporin 9) Determines Arsenic Uptake and Tolerance in Human Hepatocellular Carcinoma Cells In Vitro. *Cureus* 14:e26753
505. Yu S, Li LH, Lee CH, Jeyakannu P, Wang JJ, Hong CH. 2021. Arsenic leads to autophagy of keratinocytes by increasing aquaporin 3 expression. *Scientific reports* 11:17523
506. Huang D, Feng X, Liu Y, Deng Y, Chen H, et al. 2017. AQP9-induced cell cycle arrest is associated with RAS activation and improves chemotherapy treatment efficacy in colorectal cancer. *Cell death & disease* 8:e2894
507. Liu Z, Shen J, Carbrey JM, Mukhopadhyay R, Agre P, Rosen BP. 2002. Arsenite transport by mammalian aquaglyceroporins AQP7 and AQP9. *Proc Natl Acad Sci U S A* 99:6053-8
508. Bhattacharjee H, Carbrey J, Rosen BP, Mukhopadhyay R. 2004. Drug uptake and pharmacological modulation of drug sensitivity in leukemia by AQP9. *Biochem Biophys Res Commun* 322:836-41
509. Chau D, Ng K, Chan TS, Cheng YY, Fong B, et al. 2015. Azacytidine sensitizes acute myeloid leukemia cells to arsenic trioxide by up-regulating the arsenic transporter aquaglyceroporin 9. *Journal of hematology & oncology* 8:46
510. Garbinski LD, Rosen BP, Chen J. 2019. Pathways of arsenic uptake and efflux. *Environ Int* 126:585-97
511. Kala SV, Neely MW, Kala G, Prater CI, Atwood DW, et al. 2000. The MRP2/cMOAT transporter and arsenic-glutathione complex formation are required for biliary excretion of arsenic. *J Biol Chem* 275:33404-8
512. Klaassen CD, Aleksunes LM. 2010. Xenobiotic, bile acid, and cholesterol transporters: function and regulation. *Pharmacological reviews* 62:1-96

513. Leslie EM, Haimeur A, Waalkes MP. 2004. Arsenic transport by the human multidrug resistance protein 1 (MRP1/ABCC1). Evidence that a tri-glutathione conjugate is required. *J Biol Chem* 279:32700-8

514. Maher JM, Slitt AL, Cherrington NJ, Cheng X, Klaassen CD. 2005. Tissue distribution and hepatic and renal ontogeny of the multidrug resistance-associated protein (Mrp) family in mice. *Drug Metab Dispos* 33:947-55

515. Ros JE, Libbrecht L, Geuken M, Jansen PL, Roskams TA. 2003. High expression of MDR1, MRP1, and MRP3 in the hepatic progenitor cell compartment and hepatocytes in severe human liver disease. *The Journal of pathology* 200:553-60

516. Donner MG, Warskulat U, Saha N, Häussinger D. 2004. Enhanced expression of basolateral multidrug resistance protein isoforms Mrp3 and Mrp5 in rat liver by LPS. *Biological chemistry* 385:331-9

517. Leslie EM, Deeley RG, Cole SP. 2005. Multidrug resistance proteins: role of P-glycoprotein, MRP1, MRP2, and BCRP (ABCG2) in tissue defense. *Toxicology and applied pharmacology* 204:216-37

518. Juliano RL, Ling V. 1976. A surface glycoprotein modulating drug permeability in Chinese hamster ovary cell mutants. *Biochimica et biophysica acta* 455:152-62

519. Ma X, Idle JR, Gonzalez FJ. 2008. The pregnane X receptor: from bench to bedside. *Expert opinion on drug metabolism & toxicology* 4:895-908

520. Liu J, Liu Y, Powell DA, Waalkes MP, Klaassen CD. 2002. Multidrug-resistance mdr1a/1b double knockout mice are more sensitive than wild type mice to acute arsenic toxicity, with higher arsenic accumulation in tissues. *Toxicology* 170:55-62

521. Xie Y, Liu J, Liu Y, Klaassen CD, Waalkes MP. 2004. Toxicokinetic and genomic analysis of chronic arsenic exposure in multidrug-resistance mdr1a/1b(-/-) double knockout mice. *Molecular and cellular biochemistry* 255:11-8

522. Hayes JD, Dinkova-Kostova AT, McMahon M. 2009. Cross-talk between transcription factors AhR and Nrf2: lessons for cancer chemoprevention from dioxin. *Toxicological sciences : an official journal of the Society of Toxicology* 111:199-201

523. Damery E, Solimando DA, Jr., Waddell JA. 2016. Arsenic Trioxide and Tretinoin (AsO/ATRA) for Acute Promyelocytic Leukemia (APL). *Hospital pharmacy* 51:628-32

524. Gerges SH, El-Kadi AOS. 2023. Sexual Dimorphism in the Expression of Cytochrome P450 Enzymes in Rat Heart, Liver, Kidney, Lung, Brain, and Small Intestine. *Drug Metab Dispos* 51:81-94

525. Yang L, Li Y, Hong H, Chang CW, Guo LW, et al. 2012. Sex Differences in the Expression of Drug-Metabolizing and Transporter Genes in Human Liver. *Journal of drug metabolism & toxicology* 3:1000119

526. Gerges SH, Alammari AH, El-Ghiaty MA, Isse FA, El-Kadi AOS. 2023. Sex- and enantiospecific differences in the formation rate of hydroxyeicosatetraenoic acids in rat organs. *Can J Physiol Pharmacol* 101:425-36

527. Kato R, Yamazoe Y. 1992. Sex-specific cytochrome P450 as a cause of sex- and species-related differences in drug toxicity. *Toxicology letters* 64-65 Spec No:661-7

528. Huang Y, Shan Y, Zhang W, Lee AM, Li F, et al. 2023. Deciphering genetic causes for sex differences in human health through drug metabolism and transporter genes. *Nature communications* 14:175

529. Lee YS, Park SS, Kim ND. 1992. Sex-related differences in rat hepatic cytochromes P450 expression following treatment with phenobarbital or 3-methylcholanthrene. *Arch Pharm Res* 15:78-86

530. Augustine LM, Fisher CD, Lickteig AJ, Aleksunes LM, Slitt AL, Cherrington NJ. 2008. Gender divergent expression of Nqo1 in Sprague Dawley and August Copenhagen x Irish rats. *J Biochem Mol Toxicol* 22:93-100